GLOBAL DISSEMINATION AND EVOLUTION OF EPIDEMIC MULTIDRUG-RESISTANT GRAM-NEGATIVE BACTERIAL PATHOGENS: SURVEILLANCE, DIAGNOSIS AND TREATMENT

EDITED BY: Fang He, Ziad Daoud, Zhi Ruan, Guo-bao Tian and Fenni Zhang
PUBLISHED IN: Frontiers in Microbiology

frontiers Research Topics

frontiers

ISSN 1664-8714
ISBN 978-2-88976-955-1
DOI 10.3389/978-2-88976-955-1

About Frontiers

Frontiers is more than just an open-access publisher of scholarly articles: it is a pioneering approach to the world of academia, radically improving the way scholarly research is managed. The grand vision of Frontiers is a world where all people have an equal opportunity to seek, share and generate knowledge. Frontiers provides immediate and permanent online open access to all its publications, but this alone is not enough to realize our grand goals.

Frontiers Journal Series

The Frontiers Journal Series is a multi-tier and interdisciplinary set of open-access, online journals, promising a paradigm shift from the current review, selection and dissemination processes in academic publishing. All Frontiers journals are driven by researchers for researchers; therefore, they constitute a service to the scholarly community. At the same time, the Frontiers Journal Series operates on a revolutionary invention, the tiered publishing system, initially addressing specific communities of scholars, and gradually climbing up to broader public understanding, thus serving the interests of the lay society, too.

Dedication to Quality

Each Frontiers article is a landmark of the highest quality, thanks to genuinely collaborative interactions between authors and review editors, who include some of the world's best academicians. Research must be certified by peers before entering a stream of knowledge that may eventually reach the public - and shape society; therefore, Frontiers only applies the most rigorous and unbiased reviews.
Frontiers revolutionizes research publishing by freely delivering the most outstanding research, evaluated with no bias from both the academic and social point of view. By applying the most advanced information technologies, Frontiers is catapulting scholarly publishing into a new generation.

What are Frontiers Research Topics?

Frontiers Research Topics are very popular trademarks of the Frontiers Journals Series: they are collections of at least ten articles, all centered on a particular subject. With their unique mix of varied contributions from Original Research to Review Articles, Frontiers Research Topics unify the most influential researchers, the latest key findings and historical advances in a hot research area! Find out more on how to host your own Frontiers Research Topic or contribute to one as an author by contacting the Frontiers Editorial Office: frontiersin.org/about/contact

GLOBAL DISSEMINATION AND EVOLUTION OF EPIDEMIC MULTIDRUG-RESISTANT GRAM-NEGATIVE BACTERIAL PATHOGENS: SURVEILLANCE, DIAGNOSIS AND TREATMENT

Topic Editors:
Fang He, Zhejiang Provincial People's Hospital, China
Ziad Daoud, Central Michigan University Mount Pleasant, United States
Zhi Ruan, Zhejiang University, China
Guo-bao Tian, Sun Yat-sen University, China
Fenni Zhang, Zhejiang University, China

Citation: He, F., Daoud, Z., Ruan, Z., Tian, G.-b., Zhang, F., eds. (2022). Global Dissemination and Evolution of Epidemic Multidrug-Resistant Gram-Negative Bacterial Pathogens: Surveillance, Diagnosis and Treatment. Lausanne: Frontiers Media. doi: 10.3389/978-2-88976-955-1

Table of Contents

05 ***Editorial: Global Dissemination and Evolution of Epidemic Multidrug-Resistant Gram-Negative Bacterial Pathogens: Surveillance, Diagnosis, and Treatment***
Ziad Daoud

09 ***International High-Risk Clones Among Extended-Spectrum β-Lactamase–Producing* Escherichia coli *in Dhaka, Bangladesh***
Razib Mazumder, Arif Hussain, Ahmed Abdullah, Md. Nazrul Islam, Md. Tuhin Sadique, S. M. Muniruzzaman, Anika Tabassum, Farhana Halim, Nasrin Akter, Dilruba Ahmed and Dinesh Mondal

20 ***Transmission Dynamics of Carbapenem-Resistant* Klebsiella pneumoniae *Sequence Type 11 Strains Carrying Capsular Loci KL64 and* rmpA/rmpA2 *Genes***
Yingying Kong, Qingyang Sun, Hangfei Chen, Mohamed S. Draz, Xinyou Xie, Jun Zhang and Zhi Ruan

32 ***Genetic Diversity and Characteristics of* bla_{NDM}*-Positive Plasmids in* Escherichia coli**
Zhiren Zhang, Hengzhao Guo, Xiaodong Li, Wenting Li, Guang Yang, Wenjun Ni, Meixiao Zhan, Ligong Lu, Zhenlin Zhang, Xiaobin Li and Zhiling Zhou

44 ***Genomic Characterization of Extensively Drug-Resistant NDM-Producing* Acinetobacter baumannii *Clinical Isolates With the Emergence of Novel* $bla_{ADC-257}$**
Mai M. Zafer, Amira F. A. Hussein, Mohamed H. Al-Agamy, Hesham H. Radwan and Samira M. Hamed

57 ***Whole-Genome Sequencing-Based Antimicrobial Resistance Characterization and Phylogenomic Investigation of 19 Multidrug-Resistant and Extended-Spectrum Beta-Lactamase-Positive* Escherichia coli *Strains Collected From Hospital Patients in Benin in 2019***
Carine Laurence Yehouenou, Bert Bogaerts, Sigrid C. J. De Keersmaecker, Nancy H. C. Roosens, Kathleen Marchal, Edmond Tchiakpe, Dissou Affolabi, Anne Simon, Francis Moise Dossou, Kevin Vanneste and Olivia Dalleur

69 ***Clonal Dissemination of Clinical Carbapenem-Resistant* Klebsiella pneumoniae *Isolates Carrying* fosA3 *and* bla_{KPC-2} *Coharboring Plasmids in Shandong, China***
Yingying Hao, Xuguang Zhao, Cui Zhang, Yuanyuan Bai, Zhen Song, Xinglun Lu, Ran Chen, Yaoyao Zhu and Yueling Wang

82 ***Temperature-Regulated IncX3 Plasmid Characteristics and the Role of Plasmid-Encoded H-NS in Thermoregulation***
Liu Baomo, Shui Lili, Robert A. Moran, Willem van Schaik and Zhuo Chao

91 ***Clinical Impact of Colistin Banning in Food Animal on* mcr-1*-Positive Enterobacteriaceae in Patients From Beijing, China, 2009–2019: A Long-Term Longitudinal Observational Study***
Qian Zhao, Yiming Li, Yingxin Tian, Yueyun Shen, Shaolin Wang and Ying Zhang

101 ***Epidemiology and Drug Resistance of Neonatal Bloodstream Infection Pathogens in East China Children's Medical Center From 2016 to 2020***
Xin Zhang, Yang Li, Yunzhen Tao, Yu Ding, Xuejun Shao and Wei Li

112 ***Epidemiology of* bla$_{CTX-M}$*-Positive* Salmonella *Typhimurium From Diarrhoeal Outpatients in Guangdong, China, 2010–2017***
Qi Jiang, Bi-xia Ke, De-shu Wu, Dong Wang, Liang-xing Fang, Ruan-yang Sun, Min-ge Wang, Jing-er Lei, Zheng Shao and Xiao-ping Liao

frontiers | Frontiers in Microbiology

TYPE Editorial
PUBLISHED 04 October 2022
DOI 10.3389/fmicb.2022.1028288

OPEN ACCESS

EDITED AND REVIEWED BY
Rustam Aminov,
University of Aberdeen,
United Kingdom

*CORRESPONDENCE
Ziad Daoud
zdaoud@mihealthclinic.com

SPECIALTY SECTION
This article was submitted to Antimicrobials, Resistance and Chemotherapy, a section of the journal Frontiers in Microbiology

RECEIVED 25 August 2022
ACCEPTED 30 August 2022
PUBLISHED 04 October 2022

CITATION
Daoud Z (2022) Editorial: Global dissemination and evolution of epidemic multidrug-resistant gram-negative bacterial pathogens: Surveillance, diagnosis, and treatment. *Front. Microbiol.* 13:1028288. doi: 10.3389/fmicb.2022.1028288

Editorial: Global dissemination and evolution of epidemic multidrug-resistant gram-negative bacterial pathogens: Surveillance, diagnosis, and treatment

Ziad Daoud[1,2]*

[1]Department of Foundational Sciences, College of Medicine, Central Michigan University, Mount Pleasant, MI, United States, [2]Michigan Health Clinics, Saginaw, MI, United States

KEYWORDS

extended-spectrum β-lactamase (ESBL), CRE, Multi-Drug-Resistant (MDR), One Health (OH)—approach, epidemiology—descriptive

Editorial on the Research Topic
Global dissemination and evolution of epidemic multidrug-resistant gram-negative bacterial pathogens: Surveillance, diagnosis, and treatment

In January 2022, Murray et al. published in The Lancet a study based on statistical models to predict the spread of antimicrobial resistance. They reported 4,95 million (362–657) deaths associated with bacterial resistance to antimicrobial agents in 2019, "including 1,27 million (95% UI 0.911–1.71) deaths attributable to bacterial AMR" (Murray et al., 2022). In the same study, the total death rate related to resistance was estimated to be highest in western sub-Saharan Africa and lowest in Australasia. Unfortunately, the Covid-19 pandemic might have contributed to worsening the situation of bacterial resistance globally "through the non-rational use of antibiotics as part of preventive and therapeutic management of COVID-19" (Ansari et al., 2021).

The Research Topic of Frontiers in Microbiology, Antimicrobials, Resistance, and Chemotherapy, titled *Global dissemination and evolution of epidemic multi-drug-resistant gram-negative bacterial pathogens: Surveillance, diagnosis, and treatment*, deals with many aspects of the spread of antimicrobial resistance. Specifically, it explores the epidemiology of Multi-Drug-Resistance (MDR), the genes responsible for that resistance, and sheds some light on the importance of stewardship activities and the One Health concept as a means of curbing the spread of resistance.

In their study *Epidemiology and drug resistance of neonatal bloodstream infection pathogens in East China Children's Medical Center from 2016 to 2020*, Zhang X. et al. present an analysis of pathogens and related drug resistance in newborns with a bloodstream infection. The average rate of positivity of blood culture from neonates

was 2.50% (mean of 5 years). The most commonly isolated pathogens were coagulase-negative *Staphylococci*, *Escherichia coli*, *Klebsiella pneumoniae*, *Streptococcus agalactiae*, and *Staphylococcus aureus*. Gram-negative isolates manifested high resistance to a variety of antibacterial drugs, mainly cephalosporins. The authors conclude that while Gram-positive bacteria were the most common pathogens in these infections, Gram-negative bacilli predominated infections in preterm newborns.

With the aim of better understanding the spread of resistant organisms, this Research Topic is being investigated and researched all over the world. Unfortunately, some regions are still lacking baseline data about population structure, virulence, and mechanisms of resistance in important organisms. The study *International high-risk clones among extended-spectrum β-lactamase–producing Escherichia coli in Dhaka, Bangladesh* by Mazumder et al. uses whole-genome sequencing to study ESBL-producing *E. coli* isolated from patients at International Center for Diarrheal Disease Research, Bangladesh (icddr,b)-Dhaka. The data revealed the presence of ST131, ST405, ST648, ST410, ST38, ST73, and ST1193, with ST131 being the most common major high-risk clone. $bla_{\mathrm{CTX-M-15}}$ and FII-FIA-FIB were simultaneously found in different groups and subtypes. $bla_{\mathrm{NDM-5}}$ (9%) gene was mainly detected in *E. coli* Subtypes. Only 1 isolate (belonging to ST1011) was found to produce the *mcr*-1 gene in addition to the $bla_{\mathrm{CTX-M-55}}$ gene was detected. A major finding is that clones strongly associated with cephalosporin resistance and virulence genes are circulating and require close monitoring.

Another important intestinal pathogen, *Salmonella enterica*, is investigated by Jiang et al. in *Epidemiology of* bla_{CTX-M}*-positive Salmonella Typhimurium from diarrhoeal outpatients in Guangdong, China, 2010–2017*. The study reported a total of 221 $bla_{\mathrm{CTX-M}}$-producing isolates out of 1,263 *S.* Typhimurium isolated from the fecal material of patients with diarrhea. The gene $bla_{\mathrm{CTX-M-55}}$ was the most detected in the CTX-M-1 group with a rate of (39.6%), followed by $bla_{\mathrm{CTX-M-14}}$ and $bla_{\mathrm{CTX-M-65}}$. PFGE analysis confirmed the clonal transmission of $bla_{\mathrm{CTX-M-55}}$ isolates in different hospitals in the province. As shown by MLST studies, ST34 and ST19 were detected in *S.* Typhimurium. In addition, a close relationship of $bla_{\mathrm{CTX-M}}$-positive *S.* Typhimurium isolates was observed between outpatients and pork, as documented by phylogenomic analysis, highlighting the need for more emphasis on the resistance issue in a One Health context.

Another study, *Whole-genome sequencing-based antimicrobial resistance characterization and phylogenomic investigation of 19 multidrug-resistant and extended-spectrum beta-lactamase-positive Escherichia coli strains collected from hospital patients in Benin in 2019* by Yehouenou et al. assesses the antimicrobial resistance and phylogenetic relatedness of ESBL-producing *E. coli* from patients with post-surgery infections in Benin hospitals in 2019. The results show the presence of 13 different sequence types including ST131, ST38, ST410, ST405, ST617, and ST1193 at the same rate. The $bla_{\mathrm{CTX-M-15}}$ gene was found in 78.9% of the isolates. In addition, other genes of resistance to other antibiotics were also found [*aac-(6')-Ib-cr*, *qnrS1*, *tet(B)*, *sul2*, and *dfrA17*]. The chromosomal mutations in *parC* and *gyrA* are known to confer resistance to quinolones and were identified in many isolates as well. Such studies are important and highlight the significance and relevance of advanced technologies such as alert systems for the spread of potential antimicrobial resistance. In this same context, WGS is used to assess the epidemiological characteristics and transmission events of carbapenem-resistant *Klebsiella pneumoniae* (CRKP) isolates in two fetal outbreaks of nosocomial infection by Kong et al. (*Transmission dynamics of carbapenem-resistant Klebsiella pneumoniae sequence type 11 strains carrying capsular loci KL64 and rmpA/rmpA2 genes*). In this study, CRKP isolates fell into three clusters as separated by PFGE analysis. The most predominant PFGE cluster was associated with a significant resistance rate to most tested antibiotics and only susceptibility to colistin. Multiple Drug resistance was observed in all ST11 types members of ST11. Core genome single nucleotide polymorphism-based phylogenetic studies suggest that two independent transmission scenarios might have co-occurred. This study presents more evidence supporting the need for new strategies for the surveillance and treatment of CRKP.

NDMs are commonly found in *Escherichia coli* worldwide, and China is not an exception. Being a plasmid gene plays a major role in the dissemination of bla_{NDM}. With the objective of better understanding the conjugation and mobilization of plasmid-harboring bla_{NDM}, the study *Genetic diversity and characteristics of* bla_{NDM}*-positive plasmids in Escherichia coli* by Zhang Z. et al. was conducted. bla_{NDM} variants, types, phylogenetic patterns, conjugative transfers, STs, and epidemiologic distributions of related plasmids were subject to this study. Out of 114 bla_{NDM}-positive plasmids, eight variants were found, with $bla_{\mathrm{NDM-5}}$ and $bla_{\mathrm{NDM-1}}$ being the most dominant. In addition, three $bla_{\mathrm{NDM-4}}$-harboring plasmids with IncFIA(HI1) replicon from *E. coli* ST405 were found to be the potential mobilizable plasmids. A similar study by Zafer et al. (*Genomic characterization of extensively drug-resistant NDM-producing Acinetobacter baumannii clinical isolates with the emergence of novel* $bla_{ADC-257}$) investigates the determinants for antimicrobial resistance in extensive drug-resistant (XDR) *A. baumannii* producing NDM. Isolates were collected from one single hospital in Cairo, Egypt. Ut. Twenty clinical isolates including four NDM-producers were identified and selected for further testing. Three of the NDM producers were identified and selected for further testing. Three of these belonged to high-risk international clones IC2 and IC9. The authors of this study claim to be the first "to report blaNDM-1 gene on the chromosome of *A. baumannii* strain that belongs to sequence type $ST164^{Pas}$/$ST1418^{Oxf}$." In

addition, resistance to colistin was accompanied by missense mutations in the *lpxACD* and *pmrABC* genes. This study, as well as the previous one, confirms the need for advanced technologies, such as WGS, to reveal possible associations between resistance genes and diverse mobile genetic elements in the clinical setting. One of the major drawbacks of the spread of such resistance to carbapenems is the unavailability of efficient treatments and subsequently the use of older molecules such as fosfomycin which has attracted renewed interest in combination therapy to fight *K. pneumoniae* infections. In the study, *Clonal dissemination of clinical carbapenem-resistant Klebsiella pneumoniae isolates carrying fosA3 and* bla_{KPC-2} *coharboring plasmids in Shandong, China* by Hao et al., whole genome sequencing and bioinformatic analysis were conducted to reveal molecular characteristics of fosfomycin-resistant *K. pneumoniae*. Resistance to fosfomycin from *fosA3*-positive isolates was successfully passed to *Escherichia coli* J53Azi^R at a rate of 17.39%. It is important to mention, as recommended by the authors, "that ST11-KL64 and ST11-KL47 *K. pneumoniae*, with higher resistance and virulence should be critically monitored to prevent the future dissemination of resistance."

Focusing more on carbapenem-resistant Enterobacteriaceae, the paper, *Temperature-regulated IncX3 plasmid characteristics and the role of plasmid-encoded H-NS in thermoregulation* by Baomo et al. sheds some light on the temperature effects on the conjugation rates of pIncX3, as well as on its stability and fitness in *E. coli*. The authors provide evidence that temperature can affect plasmid phenotypes. The results suggest that tpGZIncX3 was correlated to a higher frequency transfer and lower fitness cost at 37°C than at other temperatures. These findings suggest that "bla_{NDM}-bearing IncX3 plasmids are adapted to carriage by enterobacteria that colonize mammalian hosts and could explain the rapid dissemination of these plasmids."

The colistin resistance gene *mcr*-1 is gaining a lot of attention given its spread and isolation in different areas of the world (Liu et al., 2016; Olaitan et al., 2021). In addition, it has been proposed that banning the use of colistin in farms and animal food is a good strategy to limit the spread of such resistance and contain Enterobacteriaceae resistance to colistin. In this Research Topic, the study *Clinical impact of colistin banning in food animal on mcr-1-positive Enterobacteriaceae in patients from Beijing, China, 2009–2019: A long-term longitudinal observational study* by Zhao et al. investigates colistin resistance in Gram-negative bacteria in patients in China over 10 years. A total of 26,080 isolates were tested including 15,742 *E. coli*, of which 171 (1.1%) turned out to be *mcr*-1 producers and 7 (0.1%) were *K. pneumoniae*, producing the same gene of resistance. The data shows an increase in the prevalence of *mcr*-1-producing *E. coli* between 2009 and 2016, after which a decreasing trend was observed. MLST analysis showed diverse genetic backgrounds of *mcr*-1-producing *E. coli*. The authors relate the decrease in resistance to colistin to the banning of this antibiotic in food animals. It is not surprising to find out that these genes or resistance are circulating in our surroundings, specifically between humans, animals, and the environment; thereby confirming the theory of One Health. Olaitan et al. (2021) conclude that "to slow or possibly stop the continued spread of plasmid-mediated colistin resistance, more countries need to adopt policies that ban the use of colistin as a feed additive for growth promotion." The concept of antimicrobial stewardship should be widened and made more global so stewardship activities can be designed and implemented in different contexts, specifically, in hospitals, farms, and the environment. This constitutes an efficiant step in moving towards a world with a more controlled, and lessened, multidrug resistance.

Author contributions

The author confirms being the sole contributor of this work and has approved it for publication.

Conflict of interest

The author declares that the research was conducted in the absence of any commercial or financial relationships that could be construed as a potential conflict of interest.

Publisher's note

References

Ansari, S., Hays, J. P., Kemp, A., Okechukwu, R., Murugaiyan, J., Ekwanzala, M. D., et al. (2021). The potential impact of the COVID-19 pandemic on global antimicrobial and biocide resistance: an AMR insights global perspective. *J. A. C. Antimicrob. Resist.* 3, dlab038. doi: 10.1093/jacamr/dlab038

Liu, Y-Y., Wang, Y., Walsh, T. R., Yi, L. X., Zhang, R., Spencer, J., et al. (2016). Emergence of plasmid-mediated colistin resistance mechanism MCR-1 in animals and human beings in China: a microbiological and molecular biological study. *Lancet Infect. Dis.* 16, 161–168. doi: 10.1016/S1473-3099(15)00424-7

Murray, C. J. L., Ikuta, K. S., Sharara, F., Swetschinski, L., Aguilar, G. R., Gray, A., et al. (2022). Global burden of bacterial antimicrobial resistance in 2019: a systematic analysis. *Lancet* 399, 629–655. doi: 10.1016/S0140-6736(21)02724-0

Olaitan, A. O., Dandachi, I., Baron, S. A., Daoud, Z., Morand, S., Rolain, J. M. (2021). Banning colistin in feed additives: a small step in the right direction. *Lancet Infect. Dis.* 21, 29–30. doi: 10.1016/S1473-3099(20)30915-4

frontiers in Microbiology

ORIGINAL RESEARCH
published: 04 October 2021
doi: 10.3389/fmicb.2021.736464

International High-Risk Clones Among Extended-Spectrum β-Lactamase–Producing *Escherichia coli* in Dhaka, Bangladesh

Razib Mazumder[1†], Arif Hussain[1†], Ahmed Abdullah[1], Md. Nazrul Islam[2], Md. Tuhin Sadique[2], S. M. Muniruzzaman[2], Anika Tabassum[2], Farhana Halim[2], Nasrin Akter[2], Dilruba Ahmed[2] and Dinesh Mondal[1]**

[1] Genomics Center, Laboratory Sciences and Services Division, International Centre for Diarrhoeal Disease Research, Bangladesh (icddr,b), Dhaka, Bangladesh, [2] Clinical Microbiology and Immunology Laboratory, Laboratory Sciences and Services Division, International Centre for Diarrhoeal Disease Research, Bangladesh (icddr,b), Dhaka, Bangladesh

OPEN ACCESS

Edited by:
Ziad Daoud,
Central Michigan University,
United States

Reviewed by:
Deepjyoti Paul,
Assam University, India
Aldert Zomer,
Utrecht University, Netherlands

***Correspondence:**
Dilruba Ahmed
dahmed@icddrb.org
Dinesh Mondal
din63d@icddrb.org

[†]These authors have contributed equally to this work and share first authorship

Specialty section:
This article was submitted to Antimicrobials, Resistance and Chemotherapy, a section of the journal Frontiers in Microbiology

Received: 05 July 2021
Accepted: 03 September 2021
Published: 04 October 2021

Citation:
Mazumder R, Hussain A, Abdullah A, Islam MN, Sadique MT, Muniruzzaman SM, Tabassum A, Halim F, Akter N, Ahmed D and Mondal D (2021) International High-Risk Clones Among Extended-Spectrum β-Lactamase–Producing Escherichia coli in Dhaka, Bangladesh. Front. Microbiol. 12:736464. doi: 10.3389/fmicb.2021.736464

Background: *Escherichia coli* is a major extended-spectrum β-lactamase (ESBL)–producing organism responsible for the rapid spread of antimicrobial resistance (AMR) that has compromised our ability to treat infections. Baseline data on population structure, virulence, and resistance mechanisms in *E. coli* lineages from developing countries such as Bangladesh are lacking.

Methods: Whole-genome sequencing was performed for 46 ESBL–*E. coli* isolates cultured from patient samples at the International Centre for Diarrhoeal Disease Research, Bangladesh (icddr,b)-Dhaka. Sequence data were analyzed to glean details of AMR, virulence, and phylogenetic and molecular markers of *E. coli* lineages.

Results: Genome comparison revealed presence of all major high-risk clones including sequence type 131 (ST131) (46%), ST405 (13%), ST648 (7%), ST410 (4.3%), ST38 (2%), ST73 (2%), and ST1193 (2%). The predominant ESBL gene and plasmid combination were $bla_{CTX-M-15}$ and FII-FIA-FIB detected in diverse *E. coli* phylogroups and STs. The bla_{NDM-5} (9%) gene was present in prominent *E. coli* STs. One (2%) *mcr-1*–positive ST1011 *E. coli*, coharboring $bla_{CTXM-55}$ gene, was detected. The extraintestinal pathogenic *E. coli* genotype was associated with specific *E. coli* lineages. The single nucleotide polymorphism (SNP)-based genome phylogeny largely showed correlation with phylogroups, serogroups, and *fimH* types. Majority of these isolates were susceptible to amikacin (93%), imipenem (93%), and nitrofurantoin (83%).

Conclusion: Our study reveals a high diversity of *E. coli* lineages among ESBL-producing *E. coli* from Dhaka. This study suggests ongoing circulation of ST131 and all major non-ST131 high-risk clones that are strongly associated with cephalosporin resistance and virulence genes. These findings warrant prospective monitoring of high-risk clones, which would otherwise worsen the AMR crises.

Keywords: CTX-M, NDM, MCR, extraintestinal pathogenic *E. coli* (ExPEC), carbapenem resistance, whole-genome sequencing, epidemiological successful clones, ST131 and non-ST131 lineages

INTRODUCTION

Infections with *Escherichia coli* that produce extended-spectrum β-lactamases (ESBLs) present an increasing clinical and public health threat (Mathers et al., 2015). These bacteria are resistant to several new-generation cephalosporin agents and render them ineffective for treating infections (Pitout and Laupland, 2008). Infections of ESBL *E. coli* causes increased morbidity, high mortality, longer hospital stays, and increased health care costs in comparison to infections caused by non-ESBL *E. coli* (Paterson and Bonomo, 2005). Treatment of such infections has been further complicated by the emergence of carbapenem resistance in ESBL–*E. coli*; these carbapenem-resistant isolates are often found resistant to all the available antibiotics (Doi, 2019).

Several strains of ESBL-producing *E. coli* are pathogenic; they commonly cause urinary tract infections (UTIs) in otherwise healthy people (Calbo et al., 2006; Franz et al., 2015). Moreover, when certain pathogenic bacterial clones horizontally acquire ESBL genes, they can emerge and reemerge rapidly within the population through clonal dissemination and thereby gain local or even global predominance as international high-risk clones (Price et al., 2013). Examples of such epidemiological successful extraintestinal pathogenic *E. coli* (ExPEC) lineages include sequence type 131 (ST131), ST410, ST38, ST73, ST405, and ST648, which are associated with both nosocomial and community-acquired infections and are being increasingly detected from multiple origins, worldwide (Baquero et al., 2013; Shaik et al., 2017; Manges et al., 2019). Since the last decade, CTX-M–type enzymes have become the most predominant ESBLs in *E. coli* and other Gram-negative bacteria of clinical significance (Cantón and Coque, 2006). Similarly, the transposable elements containing the New Delhi metallo-β-lactamase (NDM) gene have been identified to be responsible for the rapid dissemination of carbapenem resistance in *E. coli* (Kumarasamy et al., 2010).

Currently, a high number of ESBL-producing *E. coli* infections are linked to the pandemic *E. coli* lineage ST131 (Nicolas-Chanoine et al., 2008). Moreover, it is shown that *E. coli* ST131 strains are strongly associated with CTX-M-15–type ESBL and are predominantly responsible for causing bladder infections, kidney infections, and urosepsis worldwide including Southeast Asia (Nicolas-Chanoine et al., 2014; Chen et al., 2019). For instance, in India, it was reported that 93% of ST131 *E. coli* isolates carried CTX-M-15. Studies have also reported the presence of the *H30* subclone that is reportedly responsible for the clonal dissemination of ST131 *E. coli* (Hussain et al., 2012, 2014; Ranjan et al., 2015; Shaik et al., 2017). A study from Bangladesh reported that 71% of ESBL-producing *E. coli* was linked to the ST131 clone (Begum and Shamsuzzaman, 2016). Another study from Bangladesh identified a clonal cluster of clinical *E. coli* isolates belonging to serotype O25:H4, which indicates the widespread circulation of the ST131 *E. coli* lineage (Lina et al., 2014).

High-resolution studies on ESBL-producing *E. coli* strains from Bangladesh are lacking compared with the rest of the world, which limit our understanding of the population structure, emerging antimicrobial resistance (AMR) and their potential to spread. Herein, we report the findings of a genomic epidemiological investigation of the recent ESBL–*E. coli* isolates, especially the CTX-M–type ESBL producers associated with extraintestinal infections in Dhaka, Bangladesh. We analyzed their resistance genes, virulence genes, plasmid types, phylogenetic relatedness, and molecular features. Our study suggests ongoing circulation of ST131 and all major non-ST131 *E. coli* high-risk clones in Dhaka, Bangladesh. Studies such as these will provide important insights into the evolution of pathogens and will inform novel interventional strategies.

MATERIALS AND METHODS

Study Setting, Bacterial Isolates, and Antimicrobial Susceptibility

Bacterial isolates were collected randomly as part of routine (1%) surveillance (128 *E. coli* isolates) between March 2018 and July 2019 from the Clinical Microbiology and Immunology Laboratory of the International Center for Diarrheal Disease Research, Bangladesh (icddr,b) (Mazumder et al., 2020a). From this collection of 128 *E. coli* isolates, 46 randomly selected ESBL *E. coli* spanning over the entire 16-month period (representing 1–4 isolates per month) were whole genome sequenced. Of these 46 isolates, 34 were obtained from urine and 12 from pus specimen (**Table 1**). Identification of bacterial isolates was performed using standard biochemical methods. Antimicrobial susceptibility testing by disk diffusion was performed against the following antibiotics: gentamicin (10 μg), amikacin (30 μg), cotrimoxazole (25 μg), ciprofloxacin (5 μg), nitrofurantoin (200 μg), cefuroxime (30 μg), ceftriaxone (30 μg), cefixime (5 μg), cefepime (30 μg), and imipenem (10 μg). *E. coli* ATCC 25922 was used for quality control (Clinical and Laboratory Standards Institute, 2015).

Whole-Genome Sequencing, Genome Assembly, and Annotation

Genomic DNA from an overnight bacterial culture was extracted and purified using QIAamp DNA Mini kit (Qiagen, Germany). The purity of the genomic DNA was assessed using a NanoDrop spectrophotometer (Thermo Fisher Scientific, United States), and quantification was performed using a Qubit 2.0 fluorometer (Life Technologies). DNA libraries were prepared using the Nextera XT DNA library Prep kit (Illumina) (Mazumder et al., 2020b). The pooled library was sequenced at the genomic sequencing facility of icddr,b on an Illumina Nextseq500 system using the 150-base-paired-end Mid-output v2.5 sequencing kit. The sequence reads were trimmed and filtered using Trimmomatic 0.39 (Bolger et al., 2014), and *de novo* assemblies of the resulting reads were generated using SPAdes 3.11.1 (Bankevich et al., 2012), and the quality check was done using QUAST v5.02 (Mikheenko et al., 2018). The genomes of our study were annotated using Prokka *de novo* (Seemann, 2014). The program was run on fast mode, and the genus-specific BLAST database was used. The genome features and associated metadata are listed in **Table 1**.

In silico Molecular Analysis

Phylotyping was done using the ClermonTyping online tool (Beghain et al., 2018). Other molecular features were

TABLE 1 | Genome features and metadata of 46 ESBL *E. coli* isolates sequenced in this study.

Sl no.	Isolate ID	Date of isolation	Source	STs	Genome coverage	Accession no.	Contig no. (>200 bp)	Genome size (bp)	No. of Coding Sequences (CDS)
1	LMLEEc001	20-Apr-2018	Urine	131	83.9X	JACHQR000000000.1	104	*5,220,525*	4,897
2	LMLEEc002	3-May-2018	Urine	3,748	91.4X	JACHQQ000000000.1	160	5,079,033	4,793
3	LMLEEc003	3-May-2018	Pus	131	91.4X	JACHQP000000000.1	199	5,210,796	4,887
4	LMLEEc010	2-Jun-2018	Urine	131	95.4X	JACHQO000000000.1	112	5,299,824	5,029
5	LMLEEc018	28-Jun-2018	Pus	410	92.3X	JACHQN000000000.1	98	4,888,814	4,570
6	LMLEEc019	28-Jun-2018	Pus	410	97.8X	JACHQM000000000.1	99	4,888,382	4,566
7	LMLEEc020	5-Jul-2018	Urine	167	88.6X	JACHQL000000000.1	150	4,963,734	4,655
8	LMLEEc025	19-Jul-2018	Urine	131	113.5X	JACHQK000000000.1	119	5,076,042	4,785
9	LMLEEc027	26-Jul-2018	Urine	131	62.9X	JACHQJ000000000.1	123	5,211,152	4,905
10	LMLEEc029	2-Aug-2018	Urine	131	67X	JACHQI000000000.1	97	5,234,461	4,966
11	LMLEEc033	16-Aug-2018	Urine	162	71.4X	JACHQH000000000.1	113	5,004,684	4,677
12	LMLEEc034	24-Aug-2018	Urine	131	71.4X	JACHQG000000000.1	113	5,261,112	4,939
13	LMLEEc035	23-Aug-2018	Pus	648	65.4X	JACHQF000000000.1	188	5,376,792	5,053
14	LMLEEc036	31-Aug-2018	Urine	131	73.2X	JACHQE000000000.1	86	5,237,487	4,928
15	LMLEEc039	6-Sep-2018	Urine	648	83.2X	JACHQD000000000.1	118	5,119,774	4,741
16	LMLEEc040	13-Sep-2018	Urine	131	65.6X	JACHQC000000000.1	122	5,263,046	4,943
17	LMLEEc041	13-Sep-2018	Urine	1,193	73.7X	JACHQB000000000.1	82	5,023,339	4,696
18	LMLEEc043	20-Sep-2018	Urine	131	62.1X	JACHQA000000000.1	92	4,972,440	4,633
19	LMLEEc050	18-Oct-2018	Urine	131	54.6X	JACHPZ000000000.1	92	5,237,567	4,926
20	LMLEEc056	8-Nov-2018	Urine	405	62.2X	JACHPY000000000.1	149	5,278,053	4,880
21	LMLEEc059	15-Nov-2018	Urine	405	66.8X	JACHPX000000000.1	156	5,348,292	4,939
22	LMLEEc062	29-Nov-2018	Urine	405	67.4X	JACHPW000000000.1	129	5,228,791	4,886
23	LMLEEc063	29-Nov-2018	Urine	131	62.5X	JACHPV000000000.1	83	5,180,621	4,908
24	LMLEEc064	6-Dec-2018	Urine	2,851	53X	JACHPU000000000.1	156	5,180,445	4,969
25	LMLEEc070	29-Dec-2018	Pus	2,178	83.2X	JACHPT000000000.1	90	4,980,462	4,708
26	LMLEEc071	29-Dec-2018	Pus	131	73.1X	JACHPS000000000.1	65	5,110,507	4,817
27	LMLEEc072	3-Jan-2019	Urine	131	76.9X	JACHPR000000000.1	113	5,248,087	4,933
28	LMLEEc074	10-Jan-2019	Urine	131	89.8X	JACHPQ000000000.1	121	5,315,415	5,069
29	LMLEEc078	24-Jan-2019	Urine	421	143.1X	JACHPP000000000.1	106	5,087,660	4,788
30	LMLEEc082	14-Feb-2019	Urine	131	89.8X	JACHPO000000000.1	109	5,282,720	5,015
31	LMLEEc087	21-Feb-2019	Urine	131	67.9X	JACHPN000000000.1	115	5,197,822	4,882
32	LMLEEc088	28-Feb-2019	Urine	648	73.9X	JACHPM000000000.1	135	5,193,220	4,906
33	LMLEEc089	28-Feb-2019	Urine	405	62.7X	JACHPL000000000.1	166	5,359,628	5,003
34	LMLEEc091	6-Mar-2019	Urine	617	50.6X	JACHPK000000000.1	143	5,042,428	4,717
35	LMLEEc097	28-Mar-2019	Urine	131	68.2X	JACHPJ000000000.1	125	5,354,581	5,109
36	LMLEEc101	11-Apr-2019	Pus	48	77.9X	JACHPI000000000.1	121	4,535,056	4,220
37	LMLEEc103	18-Apr-2019	Pus	131	85X	JACHPH000000000.1	106	5,233,284	4,952
38	LMLEEc104	25-Apr-2019	Urine	131	69.4X	JACHPG000000000.1	100	5,277,281	5,004
39	LMLEEc108	9-May-2019	Urine	405	62.4X	JACHPF000000000.1	173	5,515,065	5,131
40	LMLEEc111	23-May-2019	Urine	38	63.4X	JACHPE000000000.1	93	4,982,213	4,587
41	LMLEEc115	13-Jun-2019	Pus	73	78.7X	JACHPD000000000.1	138	5,149,754	4,752
42	LMLEEc117	7-Jun-2019	Urine	354	56.4X	JACHPC000000000.1	93	5,346,716	5,078
43	LMLEEc120	27-Jun-2019	Urine	131	49.8X	JACHPB000000000.1	159	5,245,925	4,948
44	LMLEEc123	6-Jul-2019	Pus	1,011	79X	JACHPA000000000.1	140	5,218,770	4,823
45	LMLEEc125	11-Jul-2019	Pus	405	76.5X	JACHOZ000000000.1	216	5,514,459	5,180
46	LMLEEc127	20-Jul-2019	Pus	1,884	68.2X	JACHOY000000000.1	72	5,050,573	4,666

identified using the Center for Genomic Epidemiology's Bioinformatics tools using default parameters unless otherwise stated. Specifically, MLST 2.0 (Larsen et al., 2012) was used to identify STs, SerotypeFinder 1.1 (Joensen et al., 2015) for detecting serotypes, FimTyper 1.0 (Roer et al., 2017) to determine *fimH* types, and PlasmidFinder 2.1 (Carattoli et al., 2014) for identification of plasmid incompatibility groups. Comprehensive Antibiotic Resistance Database (McArthur et al., 2013) was used for screening the presence of acquired AMR genes; virulence genes were detected using a custom-made database of 50 genes from the Virulence Factors Database (Chen et al., 2005) belonging to different categories as described previously

(Stoesser et al., 2015), a threshold, ≥ 90% identity; minimum coverage, ≥ 70% was used for both. AMR-related chromosomal point mutations were identified in the draft genomes using PointFinder (Zankari et al., 2017). The genetic context of $bla_{\mathrm{CTX-M-15}}$, $bla_{\mathrm{NDM-5}}$, and *mcr-1* with respect to plasmid was determined by BLAST searching of particular contigs against the GenBank database. Genomes having three or more ExPEC-associated genes were classified as ExPEC according to Johnson's criteria (Johnson and Stell, 2000). From virulence and resistance gene presence and absence CSV files, heat plots were obtained, using the Python module seaborn and matplotlib.

Single Nucleotide Polymorphism-Based Core Genome Phylogeny

The reference (*E. coli* 0154:H7 Sakai strain) guided multi-fasta consensus alignment of 46 *E. coli* genomes was obtained using the Snippy v4.4.0 pipeline (Seemann, 2015). Putative recombination regions were detected and masked using Gubbins v2.3.4 (Croucher et al., 2015). Finally, the SNP- based phylogeny was inferred using RaxML v8.2.12 (Stamatakis, 2014) using GTR (Generalized Time Reversible) substitution model and GAMMA distribution as the model of rate heterogeneity.

Statistical Analysis

Using SPSS statistics software (version 25.0), continuous variables were compared with the non-parametric Mann–Whitney *U*-test, and proportions were analyzed using the χ^2-test; *p*-values with a threshold of < 0.05 were considered statistically significant. Accordingly, the *p*-values are indicated within text where appropriate.

RESULTS

Molecular Typing of Extended-Spectrum β-Lactamase *Escherichia coli* Isolates

The sequence diversity of the study isolates as analyzed by *in silico* MLST demonstrates that the 46 ESBL–*E. coli* isolates belonged to 19 different STs (**Figure 1**). The pandemic ST131 lineage was the most predominant ST identified, comprising 46% (21/46) of the isolates. Apart from ST131, the other significant STs included the presence of isolates belonging to the international high-risk clones, such as ST405 (13% 6/46), ST648 (7% 3/46), ST410 (4.3% 2/46) ST38 (2%), ST73 (2%), and ST1193 (2%). Phylogrouping identified a total of six phylogroups, namely, A, B1, B2, C, D, and F, in the ESBL–*E. coli* isolates (**Figure 1**). The phylogroup B2 (24/46) was the major phylogroup in our collection, which predominantly consisted of ST131 isolates (88%, 21/24). Phylogroup D was the second largest phylogroup with 20% isolates ($n = 9$, 6 ST405, 1 ST38, 1 ST1011, 1 ST1884), which was followed by group F ($n = 4$, 3 ST648, 1 ST354), B1 ($n = 3$, 1 ST3748, 1 ST162, 1 ST2178), C ($n = 3$, 2 ST410, 1 ST2851), and A ($n = 3$, 1 ST167, 1 ST617, 1 ST48). Serotyping revealed that out of the 21 ST131 *E. coli*, 19 had serotype O25:H4, and two had O16:H5 serogroup (**Figure 1**). All 19 ST131 *E. coli* with O25; H4 serogroup had *fimH* 30 alleles, whereas the two ST131 *E. coli* isolates with O16:H5 serogroup had *fimH*41 allele, whereas the non-ST131 isolates exhibited diverse serotypes that included 19 different serotypes. Among them, the six emerging urosepsis pathogenic isolates belonging to ST405 had O102:H6 serogroup with *fimH* 29 allele except for one strain, which had *fimH* 27. The two isolates of high-risk clone ST410 had O8:H21 serogroup with *fimH* 24 allele. However, the three isolates belonging to the emerging pandemic lineage ST648 were not associated with any distinct sero or *fimH* group. Similar to the results of serogroups, the non-ST131 isolates exhibited diverse *fimH* (10 different) types.

Phenotypic and Genotypic Antimicrobial Resistance

Majority of isolates were susceptible to amikacin (93%), imipenem (93%), and nitrofurantoin (83%) (**Figure 2**). On the other hand, a majority of isolates were resistant to the common, empirically used antibiotics such as cefixime (96%), cefuroxime (96%), ceftriaxone (98%), and ciprofloxacin (78%). Besides, a moderate number of isolates were also resistant to cotrimoxazole (70%), gentamicin (43%), and cefepime (67%). In contrast to the non-ST131 *E. coli*, isolates belonging to the ST131 lineage had higher resistance prevalence as the aggregate resistance score [median (range)] for ST131 isolates [6 (4–8)] was higher than that of non-ST131 isolates [5.5 (0–10)]. However, the difference was not statistically significant ($p > 0.5$ Mann–Whitney *U*-test).

Whole-genome sequencing (WGS) analysis identified 60 acquired AMR genes that are known to encode proteins conferring resistance to different classes of antibiotics including β-lactams, aminoglycosides, chloramphenicol, tetracycline, sulfonamides, trimethoprim, fluoroquinolone, and colistin (**Figure 2**).

β-Lactam and Extended-Spectrum β-Lactamase Resistance

We identified 24 genes associated with β-lactam resistance including 13 ESBL, 10 AmpC β-lactamase, and 1 carbapenemase gene. The 13 ESBL genes included $bla_{\mathrm{OXA-1}}$ (43%), $bla_{\mathrm{TEM-1B}}$ (28%), $bla_{\mathrm{CTX-M-27}}$ (7%), and $bla_{\mathrm{CTX-M-55}}$ (4%). Thirty-eight of 46 isolates (81%) carried the $bla_{\mathrm{CTX-M-15}}$ gene. Of 38 isolates carrying the $bla_{\mathrm{CTX-M-15}}$ gene, 36 were resistant to ceftriaxone and cefixime; therefore, this gene was strongly associated with third-generation cephalosporin resistance ($p < 0.001$). Moreover, the gene $bla_{\mathrm{CTX-M-15}}$ was detected in isolates of diverse genetic backgrounds affiliated to 6 different phylogroups and 13 different STs, including the high-risk clones—ST131 (18/21), ST405 (5/6), ST648 (3/3), ST410 (2/2), ST38 (1/1), ST73 (1/1), and ST1193 (1/1). The $bla_{\mathrm{CTX-M-15}}$ gene was located on a plasmid for 23 of 38 isolates. Isolates also harbored other ESBL genes that included $bla_{\mathrm{CTX-M-123}}$, $bla_{\mathrm{CTX-M-65}}$, $bla_{\mathrm{MIR-3}}$, $bla_{\mathrm{OXA-9}}$, $bla_{\mathrm{TEM-169}}$, $bla_{\mathrm{TEM-1A}}$, $bla_{\mathrm{TEM-1B}}$, $bla_{\mathrm{TEM-206}}$, and $bla_{\mathrm{TEM-214}}$ in lesser proportion. Similarly, a low prevalence of AmpC β-lactamase genes was detected (**Figure 2**).

Aminoglycoside Resistance

We identified 12 genes known to confer resistance to aminoglycosides (**Figure 2**). These included *aac(6′)-Ib-cr* (45%), *aadA5* (40%), *aac(3)-IIa* (30%), *aph(3′′)-Ib* (30%), *aph(6)-Id* (30%), and *aadA2* (17%). Of these six prominent

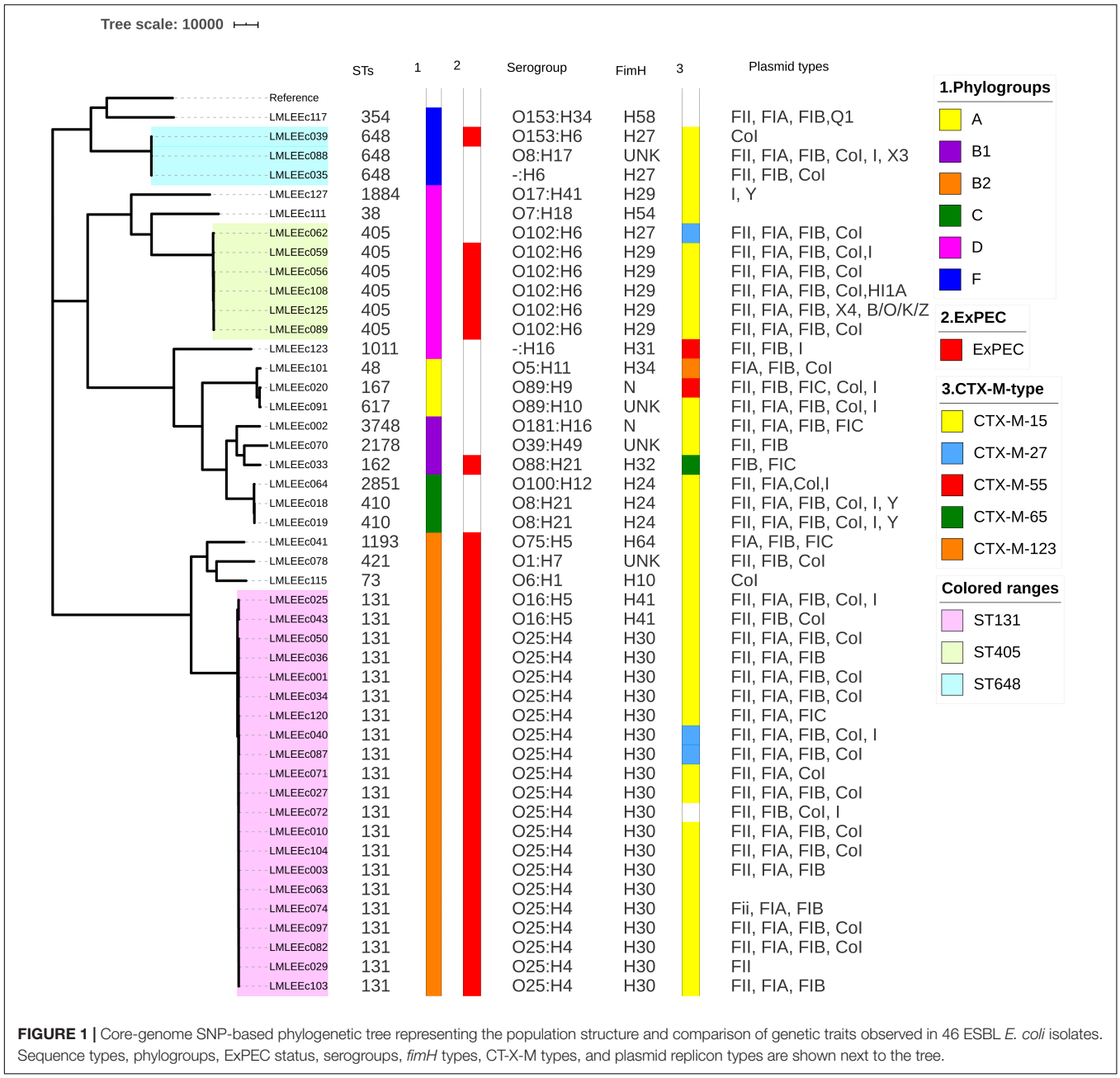

FIGURE 1 | Core-genome SNP-based phylogenetic tree representing the population structure and comparison of genetic traits observed in 46 ESBL *E. coli* isolates. Sequence types, phylogroups, ExPEC status, serogroups, *fimH* types, CT-X-M types, and plasmid replicon types are shown next to the tree.

aminoglycoside genes, only two, *aac(3)-IIa* (14/13) and *aac(6′)-Ib-cr* (21/14), were strongly associated with gentamicin resistance ($p < 0.001$). None of the aminoglycoside genes was associated with amikacin resistance. Approximately 4% of the isolates harbored *aac(3)-IId*, *aadA1*, and *aph(3′)-Ia*; other genes of this class included *aac(6′)-Ib* (one isolate), *aadA2b* (one isolate), and *armA* (one isolate).

Cotrimoxazole Resistance

Three genes known to encode sulfonamide resistance were identified: *sul1* in 26/46 (57%) isolates, *sul2* in 14/46 (30%) isolates, and *sul3* in 2/46 (4%) isolates. The presence of *sul1* was positively correlated with phenotypic resistance to cotrimoxazole (23/26) ($p < 0.001$). Similarly, of the four genes responsible for trimethoprim resistance [*dfrA17* (43%), *dfrA12* (19%), *dfrA14* (4%), *dfrA5* (4%)], the gene dfrA17 was strongly associated with cotrimoxazole resistance ($p < 0.001$).

Fluoroquinolone Resistance

Using PointFinder, we identified two mutations in *gyrA* including S83L (serine to leucine) and D87N (aspartic acid to asparagine). The mutation S83L was detected in 13% (6/46) of isolates. In contrast, 80% (37/46) of isolates had both the mutations (S83L and D87N); the dual *gyrA* mutants were all resistant to ciprofloxacin. However, isolates (4/46) having a single mutation (S83L) were all susceptible to ciprofloxacin. Similarly, in the *parC* amino acid product, we identified two substitutions at codon position 80 (serine to isoleucine) and codon 84 (glutamic acid to

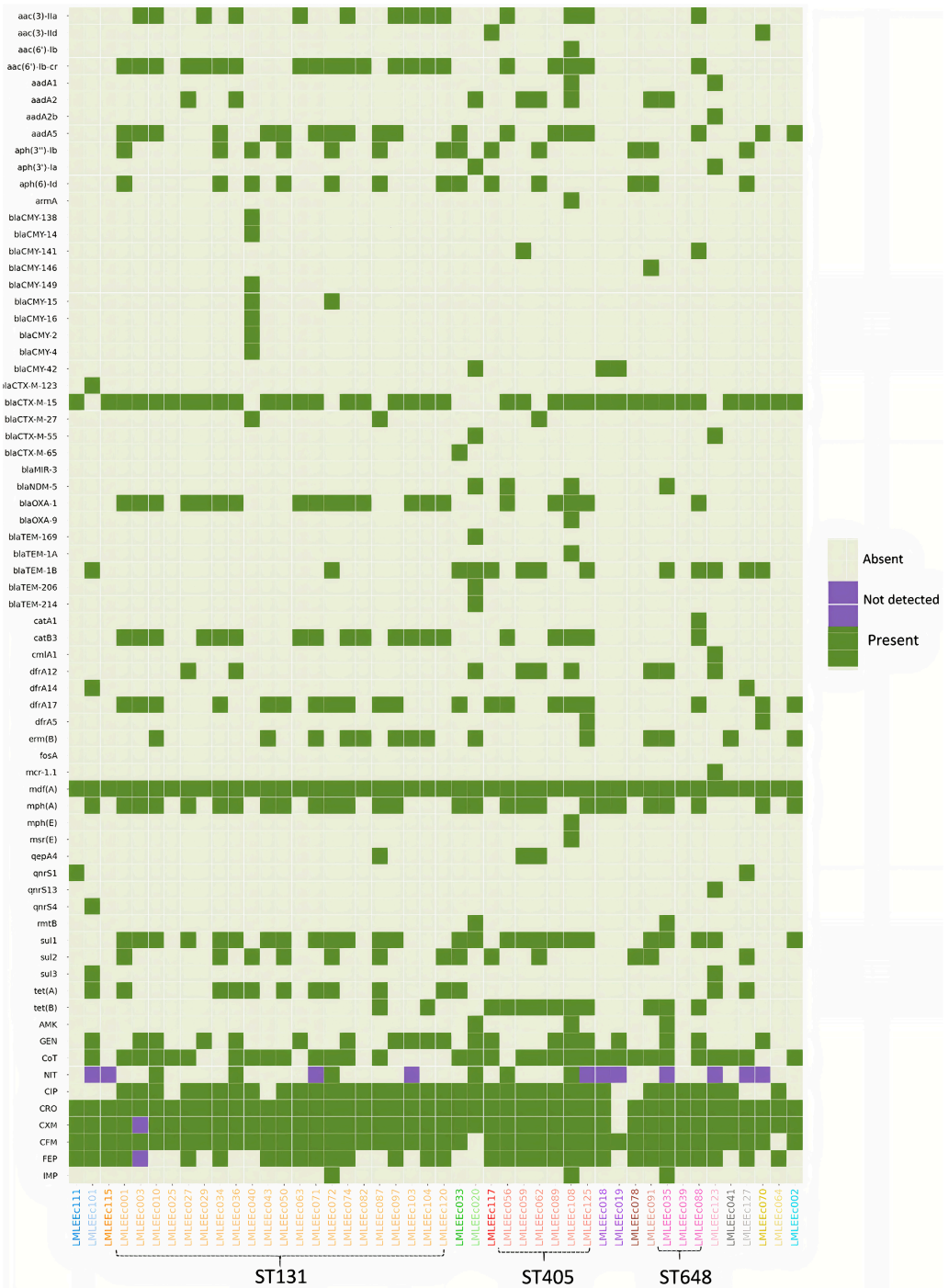

FIGURE 2 | Heatmap showing the distribution of acquired AMR genes and AMR phenotypic profiles within 46 *E. coli* isolates. Gene names are listed on the left, and strain names are listed below the image. The presence of gene is indicated by colored blocks, and the gene absence is indicated by gray blocks. CRO, ceftriaxone; CXM, cefuroxime; CFM, cefixime; FEP, cefepime; NIT, nitrofurantoin; AMK, amikacin; CIP, ciprofloxacin; CoT, cotrimoxazole; IMP, imipenem; GEN, gentamicin.

valine). The mutation S80I was present in 33% (15/46) of isolates, and the mutation E84V was detected in one isolate, whereas 22 of 46 isolates harbored both of these mutations, and they were all resistant to ciprofloxacin. Three substitutions were also detected in *parE* gene, with I529L being predominant (20/46) followed by S458A (11/46) and L416F (1/46). All isolates (20/46) carrying I529L mutation were ciprofloxacin-resistant, and this mutation was found in the majority of ST131 strains (18/21 ST131 strains). Additionally, the plasmid-mediated quinolone resistance gene *qnrs*1 was detected in two isolates followed by *qnrS*4 and *qnrS*13

in one isolate each. Except for *qnrs*13, isolates carrying *qnrS* genes were susceptible to ciprofloxacin.

Carbapenem and Colistin Resistance

NDM-5 carbapenemase was detected in four *E. coli* isolates (8.5%). All four isolates belonged to the prominent clonal groups: two ST405 (phylogroup D), one ST648 (phylogroup F), and one ST167 (phylogroup A). All four bla_{NDM-5} genes were found to be located on plasmids (4/4 isolates). Except for one (ST167), all three isolates coharbored a $bla_{\mathrm{CTX-M-15}}$ gene. Phenotypic resistance to imipenem was detected in only two of four $bla_{\mathrm{NDM-5}}$–positive isolates. Nonetheless, all four $bla_{\mathrm{NDM-5}}$–positive *E. coli* were pan–drug-resistant as resistance was detected to at least 7 of 10 antibiotics tested. We detected one *mcr-1*–positive *E. coli* belonging to ST1011; the *mcr-1* gene was detected on a plasmid. This strain was coharboring a $bla_{\mathrm{CTXM-55}}$ gene and showed phenotypic resistance to cotrimoxazole, ciprofloxacin, ceftriaxone, cefuroxime, and cefixime and was notably susceptible to imipenem, gentamicin, and amikacin.

Replicon Typing

Screening of plasmid replicons among 46 *E. coli* isolates using PlasmidFinder database detected a total of 12 plasmid replicons, which included FII, FIA, FIB, FIC, Col, I, X3, X4, Q1, B/O/K/Z, HI, and Y (**Figure 1**). FII was the predominant replicon identified in 83% (38/46) of isolates followed by FIB, Col, and FIA replicon types, with 80% (37/46), 72% (33/46), and 70% (32/46), respectively. The *mcr-1*–positive *E. coli* harbored FII and FIB plasmid replicon types.

Virulence Genes

Figure 3 shows the distribution of virulence genes among the 46 sequenced *E. coli* isolates. A total of 32 of the 46 *E. coli* isolates were classified as ExPEC, which comprised 21/21 ST131 isolates (100%) and 11/26 non-ST131 isolates (42%). The ExPEC isolates identified were enriched with virulence genes such as *pap*, *fim*, *sat*, *tia*, *hlyE*, *iutA*, *sitA*, and *fyuA*. Isolates belonging to the ST131 clone showed higher aggregate virulence scores [median (range)], 22 (18–27) compared with non-ST131 isolates 14.5 (6–33). The only isolate that carried the highest virulence genes (33) belonged to ST73.

Population Structure of Extended-Spectrum β-Lactamase *Escherichia coli* Isolates

To investigate the relatedness of 46 ESBL *E. coli* isolates, single nucleotide polymorphism (SNP)-based core genome phylogenetic tree was constructed (**Figure 1**). The 46 *E. coli* genomes clustered with a good concordance to their phylogroups. Particularly, strains belonging to phylogroups B2, D, and F formed distinct clades, whereas strains belonging to phylogroups A, B1, and C were clustered together under a large clade; 24 of these 46 *E. coli* isolates formed a large cluster of B2 phylogroup all qualified as ExPEC and had the most common plasmid combination of FII, FIA, and FIB; this clade mainly comprised (21/24) ST131 isolates. Further, it was identified that 16 of 21 ST131 *E. coli* belonged to the most virulent, widespread H30Rx subclone, three belonged to H30R, and two belonged to fluoroquinolone-susceptible *fimH 41*, CTX-M-15–positive ST131 *E. coli*. The 21 ST131 *E. coli* isolates showed little or no difference in the SNP analysis; these isolates were collected over 15 months, which indicates widespread dissemination of this particular lineage. The sister clade of ST131 clustered *E. coli* lineages that included ST1193, ST73, and ST421. When the branches of non-ST131 isolates were assessed closely, high clonality was observed between individual isolates in a few cases. For instance, six strains of ST405 formed an identical cluster; these were collected from November 2018 to July 2018, and five of six isolates carried $bla_{\mathrm{CTX-M-15}}$ and had identical serogroup and *fimH* types with almost common plasmid profile. However, two of these six isolates carried $bla_{\mathrm{NDM-5}}$ gene in addition to the shared profiles. Similarly, ST410 isolates formed identical clusters with shared molecular profiles. However, ST648 strains formed an identical cluster but demonstrated diverse molecular profiles.

DISCUSSION

ESBL-producing *E. coli* is responsible for a significant number of nosocomial and community-acquired infections (Pana and Zaoutis, 2018). In this study, we used a WGS approach to analyze 46 ESBL–*E. coli* isolates collected over a year (16 months) from a referral diagnostic center in Dhaka, Bangladesh, a Southeast Asian country from which data such as these are acutely lacking.

Our study revealed that the ST131 lineage is by far the most prevalent lineage (45%) represented particularly by H30Rx isolates (34%). This dominance of ST131 *E. coli* in our study isolates is possibly because of our focus on ESBL–*E. coli*. However, the non-ST131 (55%) *E. coli* isolates showed high diversity with respect to phylogroups, phylogenetic clustering, STs, serotypes, and *fimH* types, which is consistent with previous reports (Hussain et al., 2014; Musicha et al., 2017). Furthermore, we demonstrated that ESBLs, in particular, the CTX-M–type ESBLs, in Bangladesh have emerged across major high-risk international clones that comprise ST38, ST73, ST405, ST410, ST648, and ST1193 lineages, in addition to isolates of the pandemic *E. coli* ST131.

Molecular typing revealed that a majority of CTX-M–type ESBL producers belonged to the ST131 lineage, which constituted the most clonal group in the population structure of the studied isolates. The predominance of this lineage and its association with CTX-M-15 is in line with the reports from worldwide studies (Nicolas-Chanoine et al., 2014), including those from Asia (Hussain et al., 2012; Ranjan et al., 2015). Further, we documented a greater proportion (76%) of H30Rx subclones within the ST131 *E. coli* isolates, indicating a scenario of endemic circulation of H30Rx strains in the current setting, as these strains have been recovered between the span of April 2018 to June 2019. Clonal expansion of H30RX subclone might be the reason for the high prevalence and transmission of CTX-M-15–associated ST131 *E. coli* isolates in this setting. The H30Rx subclone is also reported in the neighboring country, India, in 2015 (Ranjan et al., 2015). The H30Rx isolates detected in this study were all qualified

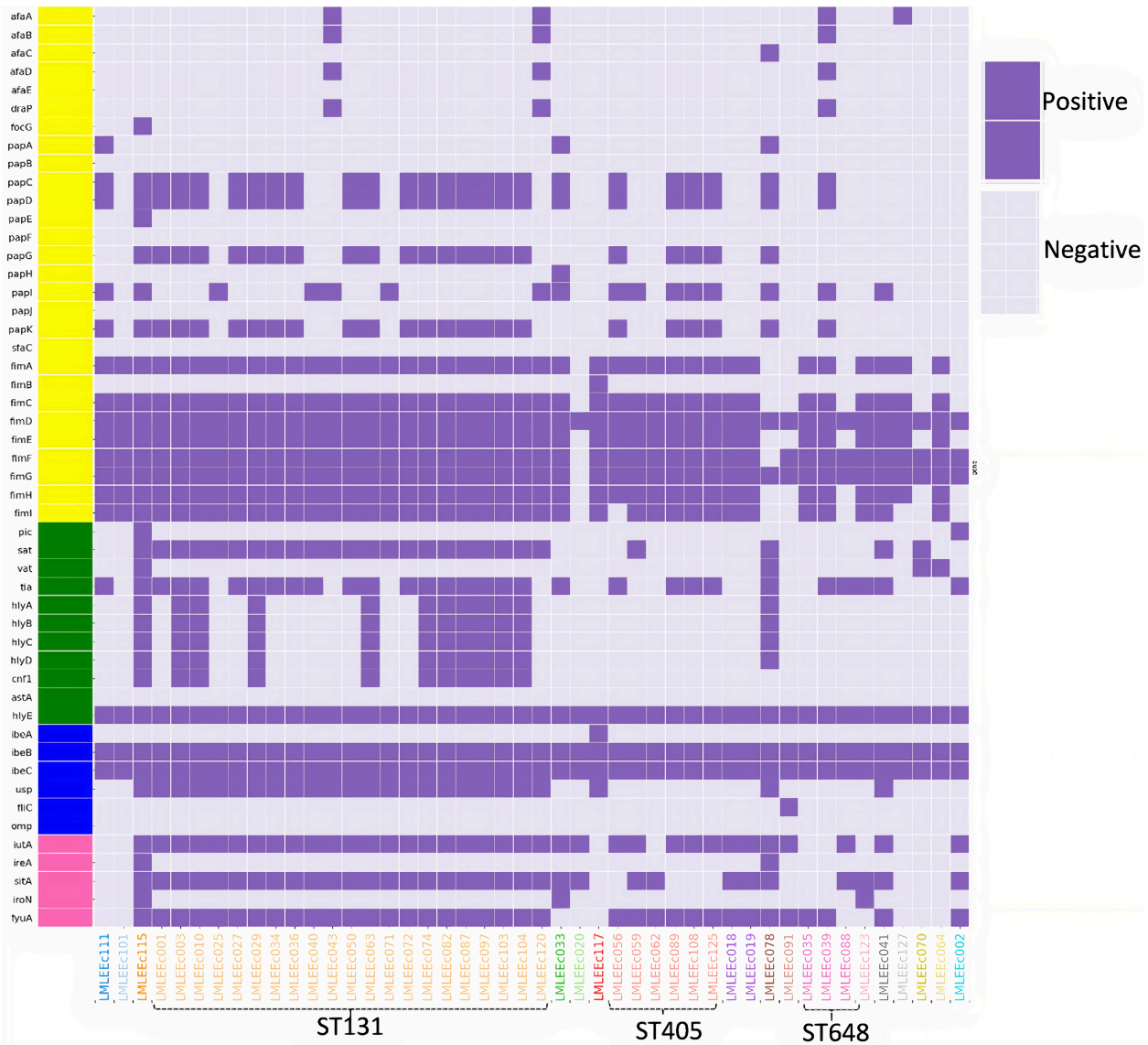

FIGURE 3 | Distribution of virulence gene profiles within 46 *E. coli* isolates are represented in the heatmap, with colored blocks indicating the gene presence and gray-colored blocks indicating the gene absence. Further, the virulence genes are vertically colored coded by functional categories (yellow, adhesins; blue, toxins; pink, miscellaneous; green, siderophores).

as ExPEC, which harbored a broad range of virulence genes with a relatively high virulence score, median (range): 27 (18–27). These isolates exhibited a high prevalence of a combination of IncFII, IncFIA, and IncFIB plasmid replicons, which is consistent with a recent WGS study from North Carolina (Kanamori et al., 2017). The gene *aac(6')-lb-cr* encoding the aminoglycoside and fluoroquinolone-modifying enzyme was strongly associated with H30Rx strains. In addition to the $bla_{\mathrm{CTX-M-15}}$ gene, they exhibited a high prevalence of $bla_{\mathrm{OXA-1}}$ and high resistance to third-generation cephalosporin antibiotics (ceftriaxone and cefixime). The association of H30Rx subclone with extended-spectrum cephalosporin and fluoroquinolone resistance might have contributed to their predominance and epidemiological success over other *E. coli* lineages.

In this study, we have further shown that the $bla_{\mathrm{CTX-M-15}}$ gene exists in genetically diverse strains including the prominent non-ST131 uropathogenic *E. coli* lineages such as ST38, ST73, ST405, ST410, ST648, and ST1193. Isolates of ST38 were reported to be evolving and is described to be increasingly detected in UTIs, which was previously considered to be a gut pathogen because they harbor genes for both EAEC and ExPEC (Chattaway et al., 2014). It is noticed that the ST38 isolate identified in this study was moderately lower in virulence and AMR gene content; particularly, it lacked the fluoroquinolone resistance and plasmids. Nonetheless, they were identified as ExPEC. ST73 is another frequently isolated ExPEC from UTI and bloodstream infections (Riley, 2014). The ST73 isolate in our study was found to carry an extensive array of virulence genes, whereas it was

susceptible to most of the antibiotics and carried only IncCoI plasmid type, in contrast to other studies, which detected FII, FIA, and FIB plasmids; the reason for this could be that the ST73 strains are not expanding clonally as also suggested by others (Bogema et al., 2020).

ST405 *E. coli* lineage has been implicated as drivers of $bla_{\mathrm{CTXM-15}}$ and is often associated with bla_{NDM} genes and extensive virulence repertoire similar to the ST131 (Devanga Ragupathi et al., 2020). All six ST405 isolates from our study demonstrated high AMR rates and specifically carried a set of common plasmid replicons, including IncFII, IncFIA, IncFIB, and IncCoI. Five of these six ST405 strains qualified as ExPEC with extensive virulence gene profiles, consistent with other reports (Zhang et al., 2018; Devanga Ragupathi et al., 2020). Two of these six ST405 isolates also harbored $bla_{\mathrm{NDM-5}}$ gene. ST410 is considered another emerging "high-risk" clone that is resistant to fluoroquinolones, cephalosporins, and sometimes carbapenems (Roer et al., 2018). The two ST410 isolates in our collection showed moderate virulence and resistance profiles; they harbored $bla_{\mathrm{CTX-M-15}}$ gene with a set of five plasmid replicon types and *fimH* 24 allele (**Figure 1**). The lineage ST648 has been predicted to become another internationally circulating clone that will worsen infection treatment possibilities because of its AMR (Schaufler et al., 2019). The three ST648 isolates detected in this study carried $bla_{\mathrm{CTX-M-15}}$ and demonstrated high AMR rates; all the three strains consistently carried IncCoI plasmids. One ST648 strain was also positive for the $bla_{\mathrm{NDM-5}}$ gene. ST1193 is the latest pandemic multidrug-resistant uropathogenic clonal group (Johnson et al., 2019), which is usually detected among non-lactose fermenters (Johnson et al., 2019). The ST1193 isolate in our collection was qualified as ExPEC; it showed high resistance rates, with particular resistance to fluoroquinolones, cephalosporins, and cotrimoxazole. It harbored IncFIA, IncFIB, and IncCoI plasmid types.

Several WGS studies have described the features of *E. coli* ST131. In contrast, not many have addressed the molecular epidemiology of non-ST131 *E. coli* worldwide. In this study, we have described that the ST131 *E. coli* is currently the most prevalent CTX-M–type ESBL producer in our community. However, we have also drawn attention to the emergence of significant clonal groups among non-ST131 *E. coli*. Further work is warranted in Bangladesh to accurately estimate the prevalence of these clonal groups and systematically analyze them in a global context, which is pertinent from public health and clinical standpoint.

Taken together, our study suggests that the CTX-M–type ESBLs and particularly the CTX-M-15 are prevalent among diverse *E. coli* STs circulating in Dhaka, Bangladesh. Further, our findings confirm the striking predominance of ST131 lineage and also revealed the presence of several major high-risk non-ST131 ExPEC clonal lineages, such as ST38, ST73, ST405, ST410, ST648, and ST1193, all associated with cephalosporin resistance and virulence. Further genomic epidemiological studies are needed to keep track of significant virulent/multiresistant *E. coli* clones in Bangladesh. Such studies are needed to inform us about the evolutionary dynamics of pathogenicity and resistance in emerging *E. coli* lineages of public health concern which will aid in evidence-based infection control and antibiotic-prescribing policies.

DATA AVAILABILITY STATEMENT

The datasets generated for this study can be found in the GenBank (Bioproject Accession: PRJNA654992). The GenBank accession numbers of 46 genomes sequenced in this study can be found in **Table 1**.

AUTHOR CONTRIBUTIONS

AH and RM designed the study, performed genome sequencing, and drafted the manuscript. AA, AH, and RM carried out the bioinformatics analyses and interpretation of results. MI, MS, SM, AT, FH, and NA were involved in the culture and AST of bacteria isolates. DA and DM supervised the study. All authors have read and approved the final manuscript.

ACKNOWLEDGMENTS

This research study was funded by core donors who provide unrestricted support to icddr,b for its operations and research. Current donors providing unrestricted support include the governments of Bangladesh, Canada, Sweden, and the United Kingdom. We gratefully acknowledge these donors for their support and commitment to icddr,b's research efforts.

REFERENCES

Bankevich, A., Nurk, S., Antipov, D., Gurevich, A. A., Dvorkin, M., Kulikov, A. S., et al. (2012). SPAdes: a new genome assembly algorithm and its applications to single-cell sequencing. *J. Comput. Biol.* 19, 455–477. doi: 10.1089/cmb.2012.0021

Baquero, F., Tedim, A. P., and Coque, T. M. (2013). Antibiotic resistance shaping multi-level population biology of bacteria. *Front. Microbiol.* 4:15. doi: 10.3389/fmicb.2013.00015

Beghain, J., Bridier-Nahmias, A., Le Nagard, H., Denamur, E., and Clermont, O. (2018). ClermonTyping: an easy-to-use and accurate *in silico* method for *Escherichia* genus strain phylotyping. *Microb. Genomics* 4:192. doi: 10.1099/mgen.0.000192

Begum, N., and Shamsuzzaman, S. M. (2016). Emergence of CTX-M-15 producing E. coli O25b-ST131 clone in a tertiary care hospital of Bangladesh. *Malays. J. Pathol.* 38, 241–249.

Bogema, D. R., McKinnon, J., Liu, M., Hitchick, N., Miller, N., Venturini, C., et al. (2020). Whole-genome analysis of extraintestinal *Escherichia coli* sequence type 73 from a single hospital over a 2 year period identified different circulating clonal groups. *Microb. Genom.* 6:e000255. doi: 10.1099/mgen.0.000255

Bolger, A. M., Lohse, M., and Usadel, B. (2014). Trimmomatic: a flexible trimmer for Illumina sequence data. *Bioinformatics* 30, 2114–2120. doi: 10.1093/bioinformatics/btu170

Calbo, E., Romaní, V., Xercavins, M., Gómez, L., Vidal, C. G., Quintana, S., et al. (2006). Risk factors for community-onset urinary tract infections due

to *Escherichia coli* harbouring extended-spectrum β-lactamases. *J. Antimicrob. Chemother.* 57, 780–783. doi: 10.1093/jac/dkl035

Cantón, R., and Coque, T. M. (2006). The CTX-M beta-lactamase pandemic. *Curr. Opin. Microbiol.* 9, 466–475.

Carattoli, A., Zankari, E., García-Fernández, A., Voldby Larsen, M., Lund, O., Villa, L., et al. (2014). *In silico* detection and typing of plasmids using plasmidfinder and plasmid multilocus sequence typing. *Antimicrob. Agents Chemother.* 58, 3895–3903. doi: 10.1128/AAC.02412-14

Chen, L., Yang, J., Yu, J., Yao, Z., Sun, L., Shen, Y., et al. (2005). VFDB: a reference database for bacterial virulence factors. *Nucleic Acids Res.* 33, D325–D328. doi: 10.1093/nar/gki008

Chen, S. L., Ding, Y., Apisarnthanarak, A., Kalimuddin, S., Archuleta, S., Omar, S. F. S., et al. (2019). The higher prevalence of extended spectrum beta-lactamases among *Escherichia coli* ST131 in Southeast Asia is driven by expansion of a single, locally prevalent subclone. *Sci. Rep.* 9:13245. doi: 10.1038/s41598-019-49467-5

Clinical and Laboratory Standards Institute (2015). *Performance Standards for Antimicrobial Susceptibility Testing; 20th Informational Supplement M100-S25*. Wayne, PA: Clinical and Laboratory Standards Institute.

Croucher, N. J., Page, A. J., Connor, T. R., Delaney, A. J., Keane, J. A., Bentley, S. D., et al. (2015). Rapid phylogenetic analysis of large samples of recombinant bacterial whole genome sequences using Gubbins. *Nucleic Acids Res.* 43:e15. doi: 10.1093/nar/gku1196

Doi, Y. (2019). Treatment options for carbapenem-resistant gram-negative bacterial infections. *Clin. Infect. Dis.* 69, S565–S575. doi: 10.1093/cid/ciz830

Franz, E., Veenman, C., van Hoek, A. H. A. M., Husman, A., de, R., Blaak, H., et al. (2015). Pathogenic *Escherichia coli* producing extended-spectrum β-lactamases isolated from surface water and wastewater. *Sci. Rep.* 5:14372. doi: 10.1038/srep14372

Hussain, A., Ewers, C., Nandanwar, N., Guenther, S., Jadhav, S., Wieler, L. H., et al. (2012). Multiresistant uropathogenic *Escherichia coli* from a region in India where urinary tract infections are endemic: genotypic and phenotypic characteristics of sequence type 131 isolates of the CTX-M-15 extended-spectrum-β-lactamase-producing lineage. *Antimicrob. Agents Chemother.* 56, 6358–6365. doi: 10.1128/AAC.01099-12

Hussain, A., Ranjan, A., Nandanwar, N., Babbar, A., Jadhav, S., and Ahmed, N. (2014). Genotypic and phenotypic profiles of *Escherichia coli* isolates belonging to clinical sequence type 131 (ST131), clinical non-ST131, and fecal non-ST131 lineages from India. *Antimicrob. Agents Chemother.* 58, 7240–7249. doi: 10.1128/AAC.03320-14

Joensen, K. G., Tetzschner, A. M. M., Iguchi, A., Aarestrup, F. M., and Scheutz, F. (2015). Rapid and easy *in silico* serotyping of *Escherichia coli* isolates by use of whole-genome sequencing data. *J. Clin. Microbiol.* 53, 2410–2426. doi: 10.1128/JCM.00008-15

Johnson, J. R., and Stell, A. L. (2000). Extended virulence genotypes of *Escherichia coli* strains from patients with urosepsis in relation to phylogeny and host compromise. *J. Infect. Dis.* 181, 261–272. doi: 10.1086/315217

Johnson, T. J., Elnekave, E., Miller, E. A., Munoz-Aguayo, J., Figueroa, C. F., Johnston, B., et al. (2019). Phylogenomic analysis of extraintestinal pathogenic *Escherichia coli* sequence type 1193, an emerging multidrug-resistant clonal group. *Antimicrob. Agents Chemother.* 63:e01913-18. doi: 10.1128/AAC.01913-18

Kanamori, H., Parobek, C. M., Juliano, J. J., Johnson, J. R., Johnston, B. D., Johnson, T. J., et al. (2017). Genomic analysis of multidrug-resistant *Escherichia coli* from north carolina community hospitals: ongoing circulation of CTX-M-producing ST131-H30Rx and ST131-H30R1 strains. *Antimicrob. Agents Chemother.* 61:e00912-17. doi: 10.1128/AAC.00912-17

Kumarasamy, K. K., Toleman, M. A., Walsh, T. R., Bagaria, J., Butt, F., Balakrishnan, R., et al. (2010). Emergence of a new antibiotic resistance mechanism in India, Pakistan, and the UK: a molecular, biological, and epidemiological study. *Lancet Infect. Dis.* 10, 597–602. doi: 10.1016/S1473-3099(10)70143-2

Larsen, M. V., Cosentino, S., Rasmussen, S., Friis, C., Hasman, H., Marvig, R. L., et al. (2012). Multilocus sequence typing of total-genome-sequenced bacteria. *J. Clin. Microbiol.* 50, 1355–1361. doi: 10.1128/JCM.06094-11

Lina, T. T., Khajanchi, B. K., Azmi, I. J., Islam, M. A., Mahmood, B., Akter, M., et al. (2014). Phenotypic and molecular characterization of extended-spectrum beta-lactamase-producing *Escherichia coli* in Bangladesh. *PLoS One* 9:e108735. doi: 10.1371/journal.pone.0108735

Chattaway, M. A., Jenkins, C., Ciesielczuk, H., Day, M., DoNascimento, V., Day, M., et al. (2014). Evidence of evolving extraintestinal enteroaggregative *Escherichia Coli* ST38 clone. *Emerg. Infect. Dis.* 20, 1935–1937. doi: 10.3201/EID2011.131845

Manges, A. R., Geum, H. M., Guo, A., Edens, T. J., Fibke, C. D., and Pitout, J. D. D. (2019). Global extraintestinal pathogenic *escherichia coli* (Expec) lineages. *Clin. Microbiol. Rev.* 32:e00135-18. doi: 10.1128/CMR.00135-18

Mathers, A. J., Peirano, G., and Pitout, J. D. D. (2015). The role of epidemic resistance plasmids and international high-risk clones in the spread of multidrug-resistant *Enterobacteriaceae*. *Clin. Microbiol. Rev.* 28, 565–591. doi: 10.1128/CMR.00116-14

Mazumder, R., Abdullah, A., Ahmed, D., and Hussain, A. (2020a). High prevalence of blactx-m-15 gene among extended-spectrum β-lactamase-producing *escherichia coli* isolates causing extraintestinal infections in bangladesh. *Antibiotics* 9:796. doi: 10.3390/antibiotics9110796

Mazumder, R., Abdullah, A., Hussain, A., Ahmed, D., and Mondal, D. (2020b). Draft genome sequence of chromobacterium violaceum RDN09, isolated from a patient with a wound infection in bangladesh. *Microbiol. Resour. Announc.* 9:e00957-20. doi: 10.1128/mra.00957-20

McArthur, A. G., Waglechner, N., Nizam, F., Yan, A., Azad, M. A., Baylay, A. J., et al. (2013). The comprehensive antibiotic resistance database. *Antimicrob. Agents Chemother* 57, 3348–3357. doi: 10.1128/AAC.00419-13

Mikheenko, A., Prjibelski, A., Saveliev, V., Antipov, D., and Gurevich, A. (2018). Versatile genome assembly evaluation with QUAST-LG. *Bioinformatics* 34, i142–i150. doi: 10.1093/bioinformatics/bty266

Musicha, P., Feasey, N. A., Cain, A. K., Kallonen, T., Chaguza, C., Peno, C., et al. (2017). Genomic landscape of extended-spectrum β-lactamase resistance in *Escherichia coli* from an urban African setting. *J. Antimicrob. Chemother.* 72, 1602–1609. doi: 10.1093/jac/dkx058

Nicolas-Chanoine, M.-H., Bertrand, X., and Madec, J.-Y. (2014). *Escherichia coli* ST131, an intriguing clonal group. *Clin. Microbiol. Rev.* 27, 543–574. doi: 10.1128/CMR.00125-13

Nicolas-Chanoine, M. H., Blanco, J., Leflon-Guibout, V., Demarty, R., Alonso, M. P., Caniça, M. M., et al. (2008). Intercontinental emergence of *Escherichia coli* clone O25:H4-ST131 producing CTX-M-15. *J. Antimicrob. Chemother.* 61, 273–281. doi: 10.1093/jac/dkm464

Ragupathi, N. K. D., Veeraraghavan, B., Sethuvel, D. P. M., Anandan, S., Vasudevan, K., Neerav, A. R., et al. (2020). First Indian report on genome-wide comparison of multidrug-resistant *Escherichia Coli* from blood stream infections. *PLoS One* 15:e0220428. doi: 10.1371/JOURNAL.PONE.0220428

Pana, Z. D., and Zaoutis, T. (2018). Treatment of extended-spectrum β-lactamase-producing *Enterobacteriaceae* (ESBLs) infections: what have we learned until now? *F1000 Res.* 7:F1000 Faculty Rev-1347. doi: 10.12688/F1000RESEARCH.14822.1

Paterson, D. L., and Bonomo, R. A. (2005). Extended-spectrum β-lactamases: a clinical update. *Clin. Microbiol. Rev.* 18, 657–686. doi: 10.1128/CMR.18.4.657-686.2005

Pitout, J. D., and Laupland, K. B. (2008). Extended-spectrum β-lactamase-producing *Enterobacteriaceae*: an emerging public-health concern. *Lancet Infect. Dis.* 8, 159–166. doi: 10.1016/S1473-3099(08)70041-0

Price, L. B., Johnson, J. R., and Aziz, M. (2013). The epidemic of extended-spectrum- β -lactamase-producing *Escherichia coli* ST131 is driven by a single highly pathogenic subclone. H 30-Rx. *MBio* 4:e00377-13. doi: 10.1128/mBio.00377-13.Editor

Ranjan, A., Shaik, S., Hussain, A., Nandanwar, N., Semmler, T., Jadhav, S., et al. (2015). Genomic and functional portrait of a highly virulent, CTX-M-15-producing H 30-Rx subclone of *Escherichia coli* sequence type 131. *Antimicrob. Agents Chemother.* 59, 6087–6095. doi: 10.1128/AAC.01447-15

Riley, L. W. (2014). Pandemic lineages of extraintestinal pathogenic *Escherichia coli*. *Clin. Microbiol. Infect.* 20, 380–390. doi: 10.1111/1469-0691.12646

Roer, L., Overballe-Petersen, S., Hansen, F., Schønning, K., Wang, M., Røder, B. L., et al. (2018). *Escherichia coli* sequence type 410 is causing new international high-risk clones. *mSphere* 3:e00337-18. doi: 10.1128/MSPHERE.00337-18

Roer, L., Tchesnokova, V., Allesoe, R., Muradova, M., Chattopadhyay, S., Ahrenfeldt, J., et al. (2017). Development of a web tool for *Escherichia coli*

subtyping based on fimh alleles. *J. Clin. Microbiol.* 55, 2538–2543. doi: 10.1128/JCM.00737-17

Schaufler, K., Semmler, T., Wieler, L. H., Trott, D. J., Pitout, J., Peirano, G., et al. (2019). Genomic and functional analysis of emerging virulent and multidrug-resistant *Escherichia coli* lineage sequence type 648. *Antimicrob. Agents Chemother.* 63:e00243-19. doi: 10.1128/AAC.00243-19

Seemann, T. (2014). Prokka: rapid prokaryotic genome annotation. *Bioinformatics* 30, 2068–2069. doi: 10.1093/bioinformatics/btu153

Seemann, T. (2015). *Snippy: Rapid Haploid Variant Calling and Core SNP Phylogeny*. San Francisco, CA: GitHub.

Shaik, S., Ranjan, A., Tiwari, S. K., Hussain, A., Nandanwar, N., Kumar, N., et al. (2017). Comparative genomic analysis of globally dominant ST131 clone with other epidemiologically successful extraintestinal pathogenic *Escherichia coli* (ExPEC) lineages. *MBio* 8:e01596-17. doi: 10.1128/mBio.01596-17

Stamatakis, A. (2014). *RAxML Version 8: A Tool for Phylogenetic Analysis and Post-Analysis of Large Phylogenies*.

Stoesser, N., Sheppard, A. E., Moore, C. E., Golubchik, T., Parry, C. M., Nget, P., et al. (2015). Extensive within-host diversity in fecally carried extended-spectrum-beta-lactamase-producing *Escherichia coli* Isolates: Implications for transmission analyses. *J. Clin. Microbiol.* 53, 2122–2131. doi: 10.1128/JCM.00378-15

Zankari, E., Allesøe, R., Joensen, K. G., Cavaco, L. M., Lund, O., and Aarestrup, F. M. (2017). PointFinder: a novel web tool for WGS-based detection of antimicrobial resistance associated with chromosomal point mutations in bacterial pathogens. *J. Antimicrob. Chemother.* 72, 2764–2768. doi: 10.1093/jac/dkx217

Zhang, X., Feng, Y., Zhou, W., McNally, A., and Zong, Z. (2018). Cryptic transmission of ST405 *Escherichia coli* carrying bla NDM-4 in hospital. *Sci. Rep.* 8:390. doi: 10.1038/s41598-017-18910-w

Conflict of Interest: The authors declare that the research was conducted in the absence of any commercial or financial relationships that could be construed as a potential conflict of interest.

Publisher's Note: All claims expressed in this article are solely those of the authors and do not necessarily represent those of their affiliated organizations, or those of the publisher, the editors and the reviewers. Any product that may be evaluated in this article, or claim that may be made by its manufacturer, is not guaranteed or endorsed by the publisher.

frontiers in Microbiology

ORIGINAL RESEARCH
published: 07 October 2021
doi: 10.3389/fmicb.2021.736896

Transmission Dynamics of Carbapenem-Resistant *Klebsiella pneumoniae* Sequence Type 11 Strains Carrying Capsular Loci KL64 and *rmpA/rmpA2* Genes

Yingying Kong[1], Qingyang Sun[2], Hangfei Chen[1], Mohamed S. Draz[3], Xinyou Xie[1], Jun Zhang[1]* and Zhi Ruan[1]**

[1]Department of Clinical Laboratory, Sir Run Run Shaw Hospital, Zhejiang University School of Medicine, Hangzhou, China, [2]Department of Clinical Laboratory, No. 903 Hospital of PLA Joint Logistic Support Force, Hangzhou, China, [3]Department of Medicine, Case Western Reserve University School of Medicine, Cleveland, OH, United States

OPEN ACCESS

Edited by:
Santi M. Mandal,
Indian Institute of Technology Kharagpur, India

Reviewed by:
Kai Zhou,
First Affiliated Hospital of Southern University of Science and Technology, China
Haiquan Kang,
Affiliated Hospital of Xuzhou Medical University, China
Dhiviya Prabaa MS,
Christian Medical College and Hospital, India

***Correspondence:**
Zhi Ruan
r_z@zju.edu.cn
Jun Zhang
jameszhang2000@zju.edu.cn
Xinyou Xie
scottxie@zju.edu.cn

Specialty section:
This article was submitted to Antimicrobials, Resistance and Chemotherapy, a section of the journal Frontiers in Microbiology

Received: 06 July 2021
Accepted: 10 September 2021
Published: 07 October 2021

Citation:
Kong Y, Sun Q, Chen H, Draz MS, Xie X, Zhang J and Ruan Z (2021) Transmission Dynamics of Carbapenem-Resistant Klebsiella pneumoniae Sequence Type 11 Strains Carrying Capsular Loci KL64 and rmpA/rmpA2 Genes. Front. Microbiol. 12:736896. doi: 10.3389/fmicb.2021.736896

The presence and dissemination of carbapenem-resistant *Klebsiella pneumoniae* (CRKP) often cause life-threatening infections worldwide, but the therapeutic option is limited. In this study, whole-genome sequencing (WGS) was applied to assess the epidemiological characteristics and transmission dynamics of CRKP isolates recovered from two fetal outbreaks of nosocomial infections. Between April 2016 and March 2018, a total of 70 isolates of *K. pneumoniae* were collected from sterile samples in a tertiary hospital in Hangzhou, China. The minimal inhibitory concentrations (MICs) of 21 antimicrobial agents were determined using the broth microdilution methods. Pulsed-field gel electrophoresis (PFGE) was performed on 47 CRKP isolates, and 16 clonally related isolates were further characterized by Illumina sequencing. In addition, the complete genome sequences of three representative isolates (KP12, KP36, and KP37) were determined by Oxford Nanopore sequencing. The *K. pneumoniae* isolates were recovered from patients diagnosed with pulmonary infection, cancer, or encephalopathy. For all CRKP isolates, PFGE separated three clusters among all strains. The most predominant PFGE cluster contained 16 isolates collected from patients who shared close hospital units and represented a potential outbreak. All 16 isolates showed an extremely high resistance level (≥87.5%) to 18 antimicrobials tested but remain susceptible to colistin (CST). Multiple antimicrobial resistance and virulence determinants, such as the carbapenem resistance gene bla_{KPC-2}, and genes encoding the virulence factor aerobactin and the regulator of the mucoid phenotype (*rmpA* and *rmpA2*), were observed in the 16 CRKP isolates. These isolates belonged to sequence type 11 (ST11) and capsular serotype KL64. A core genome single nucleotide polymorphism (cgSNP)-based phylogenetic analysis indicated that the 16 CRKP isolates could be partitioned into two separate clades (≤15 SNPs), suggesting the two independent transmission scenarios co-occurred. Moreover, a high prevalence

of IncFIB/IncHI1B type virulence plasmid with the *iroBCDN* locus deleted, and an IncFII/IncR type bla_{KPC-2}-bearing plasmid was co-harbored in ST11-KL64 CRKP isolates. In conclusion, our data indicated that the nosocomial dissemination of ST11-KL64 CRKP clone is a potential threat to anti-infective therapy. The development of novel strategies for surveillance, diagnosis, and treatment of this high-risk CRKP clone is urgently needed.

Keywords: *Klebsiella pneumoniae*, carbapenem resistance, outbreak, whole-genome sequencing, single-nucleotide polymorphisms, genomic surveillance, hypervirulence plasmid

INTRODUCTION

Klebsiella pneumoniae, as an increasingly important human pathogen, represents increasingly multidrug-resistance, particularly to carbapenems and the third-generation cephalosporins (Navon-Venezia et al., 2017). Carbapenem-resistant *K. pneumoniae* (CRKP) is widely reported as a multidrug-resistant bacteria and associated with high morbidity and mortality rates (Wyres et al., 2020a). CRKP can produce carbapenem-hydrolyzing enzymes to hydrolyze carbapenemase and eventually nullify the effectiveness of the last-resort antibiotics. In 1996, the first *K. pneumoniae* carbapenemase (KPC) enzyme, encoded by the bla_{KPC} gene, was found in *K. pneumoniae* (Yigit et al., 2001). Subsequently, other carbapenemase genes have emerged, such as bla_{NDM}, bla_{OXA-48}, bla_{VIM}, and bla_{IMP} (Fukigai et al., 2007; Perez-Vazquez et al., 2019; Lu et al., 2020; Nishida et al., 2020). The KPC-producing isolates are always reported to be associated with nosocomial outbreaks worldwide. In China, outbreaks of CRKP isolates mainly carried the bla_{KPC-2} or bla_{NDM-1} gene and can be classified as sequence type (ST)11 by multilocus sequence typing (MLST; Gu et al., 2018; Zhang et al., 2020a). Unfortunately, the KPC-producing isolates are resistant to almost all β-lactams and β-lactamase inhibitors, which significantly limits treatment options and eventually leads to high mortality rates, especially among inpatients with prolonged hospitalization (Jiang et al., 2015; Gu et al., 2018; Sui et al., 2018; Zhang et al., 2020a).

Compared with the classic *K. pneumoniae* (cKP), hypervirulent *K. pneumoniae* (hvKP) causes more severe infections, such as liver abscesses, endophthalmitis, meningitis, and pneumonia, and displays a higher level of susceptibility to the antimicrobial agents (Wang et al., 2018; Russo and Marr, 2019; Choby et al., 2020). The hvKP is undergoing global dissemination and has been confirmed to be highly associated with several virulence factors as the hallmarks, including the regulator of the mucoid phenotype (encoded by the *rmpA* gene), the regulator of mucoid phenotype 2 (*rmpA2*), aerobactin (*iucABCD*, *iutA*), salmochelin (*iroBCDN*), and metabolite transporter (*peg-344*), which were typically co-located on a classic pLVPK-like virulence plasmid (Wyres et al., 2020b). However, hvKP strains are becoming increasingly resistant to antimicrobials, including carbapenems (Feng et al., 2018; Gu et al., 2018). Moreover, the combination of carbapenem resistance and hypervirulence significantly reduces the efficacy of antimicrobial agents to treat the life-threatening infections caused by carbapenem-resistant hvKP (CR-hvKP). Therefore, they represent an extremely severe health challenge and public concern. Consequently, it is urgent to investigate the genomic characteristics of CRKP to prevent, diagnose, and treat *K. pneumoniae* infections.

Rapid advances in whole-genome sequencing (WGS) technology and bioinformatics tools can facilitate understanding the spread of *K. pneumoniae*, including the identification of transmission routes, evolutionary patterns, and antimicrobial resistance mechanisms (Klemm et al., 2018; Schurch et al., 2018). Due to the advances in next-generation sequencing platforms, the cost of WGS continues to decrease. Moreover, WGS can detect minor genomic differences between isolates for its high resolution, limited in traditional molecular typing techniques, such as pulsed-field gel electrophoresis (PFGE) and MLST.

In this study, a total of 70 *K. pneumoniae* isolates were collected from patients during their hospitalizations in a tertiary hospital in China. The 16 KPC-2-producing CRKP isolates, represented a hospital outbreak based on antimicrobial susceptibility testing and PFGE, were further subjected to WGS analysis. The genomic epidemiological characteristics, the transmission route of this outbreak, and the genetic features of the virulence plasmids and bla_{KPC-2}-bearing plasmids were investigated.

MATERIALS AND METHODS

Patients and Isolates

Seventy *K. pneumoniae* isolates, recovered from patients in severe conditions or long-term hospitalization, were collected from a tertiary hospital in Hangzhou, Zhejiang province, China, between April 2016 and March 2018. The quick Sequential Organ Failure Assessment (qSOFA) score and the Confusion, Urea, Respiratory rate, Blood pressure plus age ≥ 65 years (CURB-65) score were used to help determine patients with severe illness. An inpatient hospitalization lasting 14 days or more was considered a long hospital stay. All isolates were cultured from the sputum, urine, blood, excreta, catheters, feces, and cerebrospinal fluids specimens. Demographic data, such as gender, age, department of hospitalization, clinical diagnosis, outcome, time of admission, time of discharge, and length of hospital stay, were extracted from the patient administration system. This study was approved by the local Research Ethics Committee of Sir Run Run Shaw Hospital, Zhejiang University School of Medicine. All isolates were generated as part of routine clinical laboratory procedures, and no identifiable patient information was collected.

Bacterial Identification and Antimicrobial Susceptibility

Bacterial identification was performed using VITEK 2 (bioMérieux, Marcy-l'Étoile, France) and Matrix-assisted laser desorption/ionization–time-of-flight mass spectrometry (MALDI-TOF-MS, Bruker, Billerica, MA, United States). Antimicrobial susceptibility testing was carried out for all isolates using the broth microdilution methods. The susceptibility breakpoint was interpreted according to Clinical and Laboratory Standards Institute (CLSI) 2020 guidelines or European Committee on Antibiotic Susceptibility Testing (EUCAST) 10.0 guidelines. The list of tested antimicrobial agents includes the following: aztreonam (ATM), fosfomycin (FOF), ertapenem (ETP), ceftazidime (CAZ), cefepime (FEP), cefoperazone-sulbactam (SCF), cefoxitin (FOX), levofloxacin (LVX), ciprofloxacin (CIP), amikacin (AMK), tetracycline (TET), tigecycline (TGC), minocycline (MH), colistin (CST), cefotaxime (CTX), meropenem (MEM), imipenem (IPM), gentamicin (GEN), trimethoprim-sulfamethoxazole (SXT), piperacillin (PRL), and piperacillin-tazobactam (PRL/TZP). *Escherichia coli* ATCC 25922 was used as a quality control strain for antimicrobial susceptibility testing.

Pulsed-Field Gel Electrophoresis

All the 47 CRKP isolates were characterized by PFGE. Genomic DNA of isolates was digested overnight with XbaI restriction enzyme (Sangon, Shanghai, China), and the DNA fragments were subjected to electrophoresis in 1% agarose III (Sangon) with a CHEF apparatus (CHEF Mapper XA; Bio-Rad, Hercules, CA, United States). The electrophoresis conditions were 14°C and 6 V/cm with alternating pulses at a 120° angle with a 5–35 s pulse time gradient for 22 h. *Salmonella enterica* serotype Braenderup H9812 was used as a molecular size marker, covering the fragment ranges generated by *K. pneumoniae*. The PFGE patterns were analyzed by BioNumerics 7.0 software (Applied Maths, Sint-MartensLatem, Belgium) with the Dice similarity index. Interpretation is based on the criteria proposed by Tenover et al. (1995), that is, two isolates shared no more than three band differences of PFGE patterns are deemed as the same clone.

Whole-Genome Sequencing

Total DNA was extracted from the 16 CRKP isolates using a QIAamp DNA Mini Kit (Qiagen, Valencia, CA, United States) and fragmented by sonication using a Covaris M220 sonicator (Covaris, Woburn, MA, United States). Genomic libraries were prepared with an average insert size of 350 bp using a TruSeq DNA Sample Prep kit (Illumina, San Diego, CA, United Staets) and sequenced using the Illumina NovaSeq 6,000 platform (Illumina, San Diego, CA, United States) with the 150 bp paired-end protocol. Furthermore, the genomic DNA of three representative isolates (KP12, KP36, and KP37) out of the 16 CRKP isolates was also sequenced on the long-read Oxford Nanopore MinION platform (Nanopore Technologies, Oxford, United Kingdom). The derived short Illumina reads and long MinION reads were assembled using Unicycler v0.4.8 software (Wick et al., 2017).

The genome annotation was performed using the NCBI Prokaryotic Genome Annotation Pipeline (PGAP; Tatusova et al., 2016). Acquired antimicrobial resistance genes and virulence genes were identified using ResFinder 4.1 and VFDB 2019 databases, respectively, with a 90% threshold for gene identification and a 60% minimum length to respective database entries. *In silico* MLST analysis was performed by BacWGSTdb 2.0 server (Ruan and Feng, 2016; Ruan et al., 2020b; Feng et al., 2021). The type of capsule and lipopolysaccharide serotype of *K. pneumoniae* was conducted using Kaptive v0.6.1 (Wick et al., 2018).

Single-Nucleotide Polymorphisms and Phylogenetic Analysis

The ST11 *K. pneumoniae* strain KP58, another ST11 CRKP isolate recovered in Hangzhou, China, was used as a reference sequence to identify genomic variations between 16 CRKP isolates. Bacterial core genome single nucleotide polymorphism (cgSNP) was analyzed using the BacWGSTdb 2.0 server (Ruan and Feng, 2016; Feng et al., 2021). SNPs in the core genome and the removal of recombination regions from SNP alignments were predicted using Snippy v4.4.5. The output was used to construct a phylogenetic tree, with 1,000 bootstraps, under the general time-reversible (GTR) model with RAxML v8.2.12, and also used to identify the pairwise SNP distances using snp-dist v0.6.3 (Stamatakis, 2014). Isolates were considered the same outbreak if the threshold for SNPs distance ≤ 18 (Schurch et al., 2018). Visualization and annotation of the phylogenetic tree and the presence of antimicrobial resistance genes and plasmid-borne virulence genes were performed by the Interactive Tree Of Life (iTOL) v5 webserver (Letunic and Bork, 2021). Sequence comparison of virulence plasmids and bla_{KPC-2}-bearing plasmids was conducted using BLAST Ring Image Generator (BRIG) and Easyfig (Alikhan et al., 2011; Sullivan et al., 2011).

Accession Number

The genome sequences of the 16 CRKP isolates were deposited in the NCBI GenBank database under the BioProject accession numbers PRJNA553055.

RESULTS

Clinical Characteristics of *K. pneumoniae* Isolates

From April 2016 to March 2018, a total of 70 *K. pneumoniae* isolates were cultured from 68 inpatients in a tertiary hospital in Hangzhou. The mean age of the inpatients was 70.5 ± 17.3 years. Among the 68 inpatients, 47 (69.12%) inpatients were males, and 21 (30.88%) were females. These clinical isolates were cultured from sputum (28/70, 40.00%), urine (20/70, 28.57%), blood (12/70, 17.14%), excreta (7/70, 10.00%), catheters (1/70, 1.43%), feces (1/70, 1.43%), and cerebrospinal fluids (1/70, 1.43%). The inpatients were diagnosed as pulmonary infection (19/68, 27.94%), cancer (9/68, 13.24%), encephalopathy (23/68, 33.82%), upper gastrointestinal bleeding (2/68, 2.94%), abdominal

pain (1/68, 1.47%), hydronephrosis (1/68, 1.47%), cardiopulmonary arrest (1/68, 1.47%), chronic sinusitis (1/68, 1.47%), perianal abscess (1/68, 1.47%), diabetes (1/68, 1.47%), and nine (13.24%) inpatients suffered external injury or had a history of surgery. Among the 70 *K. pneumoniae* isolates, 47 isolates showed a carbapenem resistance phenotype, with a rate of 67.14%.

Comparison of Outbreak Isolates According to PFGE and WGS-Based SNPs

Based on the PFGE typing results of 47 CRKP isolates, three clusters were observed according to the similarity between PFGE banding patterns (**Figure 1**). The dominant PFGE cluster C contained 16 isolates and represented a putative outbreak in the hospital for similar PFGE patterns (differed by <three bands). The PFGE cluster A and B included two and three isolates, respectively. In contrast, the remaining 26 isolates showed sporadic PFGE patterns.

The draft genomes of the 16 CRKP isolates, presented in PFGE cluster C, were determined by whole-genome sequencing. All the isolates harbored bla_{KPC-2} gene. According to the MLST scheme of *K. pneumoniae*, all the 16 KPC-2-producing CRKP isolates were identified to be ST11 and shared the same capsular serotype KL64.

Phylogenetic analysis indicated that all the ST11-KL64 CRKP isolates were partitioned into two clades (**Figure 2A**). Clade 1 contained seven isolates (KP32, KP33, KP35, KP36, KP37, KP45, and KP38-2), and clade 2 comprised four isolates (KP12, KP15, KP18, and KP19), while the remaining five isolates (KP38-1, KP1-1, KP1-2, KP5, and KP65) were singletons. The number of SNPs separating ST11-KL64 CRKP isolates ranged from 0 to 41 after removing recombination regions (**Figure 2B**). Concerning the different variants among the 16 isolates, the internal members of each clade were closely related (≤18 SNPs), and a high diversity between the two clades was also observed. The differences in the internal isolates of clade 1 and 2 ranged from 0 to 18 SNPs and 1 to 6 SNPs, respectively, representing two independent outbreaks. It is noteworthy that only eight SNPs were detected between KP1-1 and KP1-2 (recovered from the same patient), suggesting they were the variants of the same clone. In comparison, 33 SNPs were observed between KP38-1 and KP38-2, implying that the patient Pa38 were infected with two different clones of CRKP. The detailed information for SNPs detected in 16 *K. pneumoniae* strains is shown in **Supplementary Table S1**.

Clinical and Microbiological Characteristics of the 16 ST11-KL64 CRKP Isolates

Demographic and clinical characteristics and the timeline of inpatients with 16 KPC-2-producing ST11-KL64 CRKP clinical cultures are shown in **Table 1** and **Figure 3**. The 16 strains were isolated from 14 separate patients admitted into the respiratory (KP1-1, KP1-2, KP5, KP12, KP15, KP18, KP19, and KP65), intensive care unit (ICU; KP32, KP33, KP35, KP36, and KP37), and neurosurgery (KP38-1, KP38-2, and KP45). Isolate KP32, isolated from patient 32 (Pa 32) on May 15, 2017, represented the first case of the first outbreak. In the next 34 days, another four CRKP isolates (KP33, KP35, KP36, and KP37) were cultured from the sputum and blood specimens of four patients in the ICU. About 22 days later, KP38-1 and KP38-2 were isolated from the blood and sputum of the same patient (Pa38) admitted into neurosurgery with a 112-day interval, respectively. KP45 was isolated from Pa45 in the same ward on the same day of KP38-2 isolated. Between November 2017 and January 2018, another seven inpatients were continuously confirmed to have CRKP infection in the respiratory ward. Finally, 10 patients gradually recovered among the 14 patients involved in this outbreak, and four died of CRKP infection.

Antimicrobial Susceptibility Testing

All 16 ST11-KL64 CRKP isolates were multidrug-resistant (**Table 2**). According to the antimicrobial susceptibility testing data, all the bla_{KPC}-carrying *K. pneumoniae* isolates displayed resistance to ATM (MIC ≥ 32 mg/L), ETP (MIC ≥ 256 mg/L), CAZ (MIC ≥ 128 mg/L), FEP (MIC ≥ 256 mg/L), SCF (MIC > 256 mg/L), FOX (MIC ≥ 128 mg/L), LVX (MIC ≥ 16 mg/L), CIP (MIC ≥ 16 mg/L), TET (MIC ≥ 256 mg/L), MH (MIC ≥ 16 mg/L), CTX (MIC ≥ 64 mg/L), MEM (MIC = 128 mg/L), IPM (MIC ≥ 64 mg/L), GEN (MIC ≥ 256 mg/L), PRL (MIC > 512 mg/L), and PRL/TZP (MIC ≥ 512 mg/L). Moreover, a high level of resistance (≥87.5%) was observed to AMK (MIC > 256 mg/L, except for KP5) and SXT (MIC = 16 mg/L, except for KP38-1 and KP38-2). Additionally, resistance to FOF and TGC was observed in 4 (25.00%) and 3 (18.75%) isolates, respectively, and colistin resistance was detected only in one isolate KP1-2 (6.25%). Compared to the 16 ST11-KL64 CRKP isolates, the remaining 31 CRKP isolates showed relatively more susceptibility to most antimicrobials, especially for tetracycline and minocycline, but higher resistant rates of fosfomycin and trimethoprim-sulfamethoxazole. Most of the remaining 31 CRKP isolates also maintained high resistance (resistance rate > 80.65%) to the aztreonam, ertapenem, ceftazidime, cefepime, cefoperazone-sulbactam, cefoxitin, levofloxacin, ciprofloxacin, amikacin, cefotaxime, meropenem, imipenem, gentamicin, trimethoprim-sulfamethoxazole, piperacillin, and piperacillin-tazobactam (**Supplementary Table S2**).

Identification of Antimicrobial Resistance Genes and Virulence Genes

According to the WGS data, antimicrobial resistance genes and virulence genes among the 16 ST11-KL64 CRKP isolates are determined and showed in **Figure 2A**. All the isolates harbored aminoglycosides (*rmtB*), chloramphenicol (*catA2*), fosfomycin (*fosA*), quinolones (*qnrS1*), sulfonamides (*sul2*), tetracyclines [*tet(A)*], and β-lactams ($bla_{CTX-M-65}$, bla_{KPC-2}, bla_{SHV-12}, and bla_{TEM-1B}) resistance genes. Aminoglycoside resistance gene *aadA2* was observed in 15 CRKP isolates but only absent in isolate KP5. Trimethoprim resistance gene *dfrA14* was also found in all CRKP isolates except for KP38-1. Moreover, the

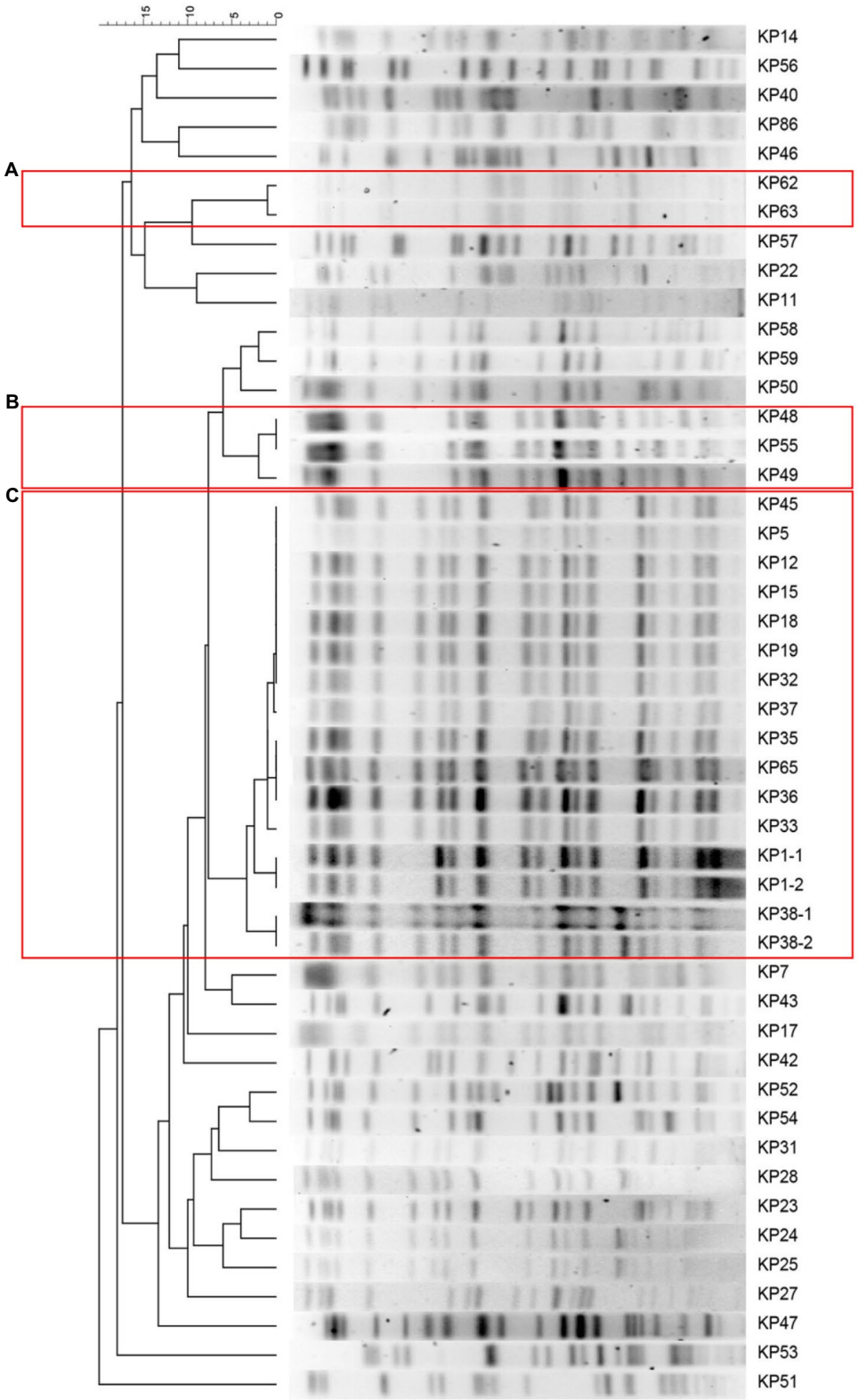

FIGURE 1 | Clustering of the 16 carbapenem-resistant *Klebsiella pneumoniae* (CRKP) isolates based on pulsed-field gel electrophoresis (PFGE) profiles. The information of strain ID is listed to the left of the patterns. The three predominant PFGE cluster **(A)**, **(B)**, and **(C)** are represented by red rectangles.

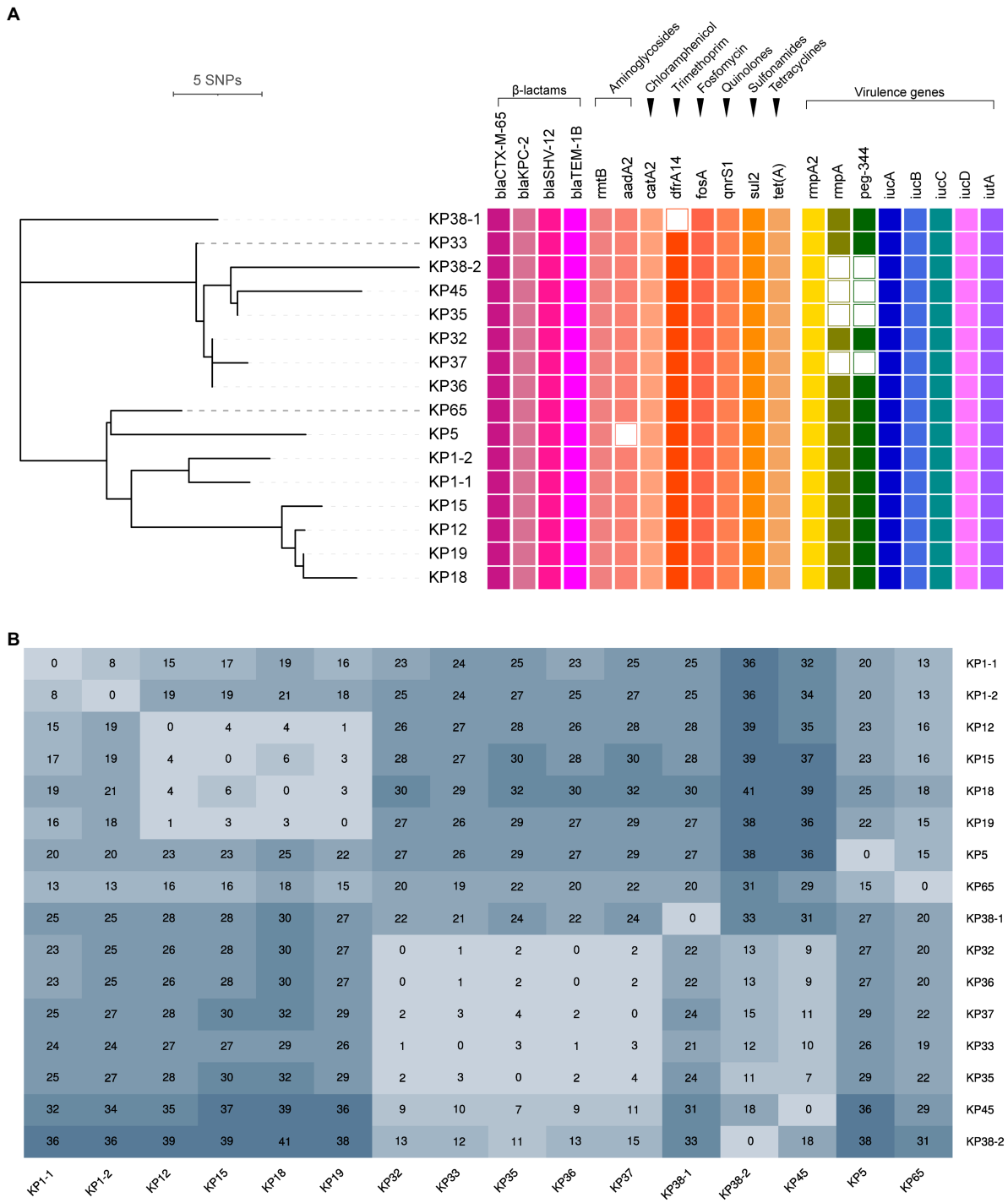

FIGURE 2 | Phylogenetic analysis of 16 *K. pneumoniae* carbapenemase (KPC)-2-producing ST11-KL64 CRKP isolates. **(A)** Recombination-filtered core genome phylogeny and the distribution of antimicrobial resistance genes and virulence genes in the CRKP isolates. The cell in different colors represents the presence of the gene, while the blank cell represents the absence of the gene. **(B)** The single nucleotide polymorphisms (SNPs) numbers between each isolate.

analysis of quinolone resistance-determining regions (QRDRs) revealed three amino acid mutations associated with fluoroquinolone resistance, including S83I and D87G in GyrA and S80I in ParC, in all the 16 CRKP isolates. Additionally, all the 16 ST11-KL64 CRKP isolates contained aerobactin (*iucABCD* and *iutA*) and hypermucoviscosity (*rmpA2*) virulence genes, representing a potential CR-hvKP phenotype. The regulator of mucoid phenotype gene (*rmpA*) and

TABLE 1 | Characteristics and outcomes of the 14 inpatients involved in the KPC-2-producing ST11-KL64 CRKP isolates outbreaks.

Patient	Isolate number	Age (years)	Gender	Department	Diagnosis	Outcome	Isolate date	Isolate type
Pa1	KP1-1	66	Female	Respiratory	History of pancreatic malignancy	Died	19/12/2017	Blood
	KP1-2	66	Female	Respiratory	History of pancreatic malignancy	Died	28/12/2017	Feces
Pa5	KP5	57	Male	Respiratory	Pulmonary malignancy	Discharged	20/11/2017	Blood
Pa12	KP12	53	Male	Respiratory	Pulmonary malignancy	Discharged	25/12/2017	Urine
Pa15	KP15	91	Male	Respiratory	Pulmonary infection	Discharged	13/1/2018	Urine
Pa18	KP18	73	Male	Respiratory	Pulmonary infection	Discharged	21/1/2018	Sputum
Pa19	KP19	93	Female	Respiratory	Pulmonary infection, heart failure	Discharged	29/1/2018	Urine
Pa32	KP32	61	Male	ICU	Severe craniocerebral injury	Discharged	15/5/2017	Sputum
Pa33	KP33	96	Male	ICU	Pulmonary malignancy, respiratory failure	Died	25/5/2017	Sputum
Pa35	KP35	60	Female	ICU	Pulmonary infection, intracranial space-occupied	Discharged	1/6/2017	Sputum
Pa36	KP36	96	Male	ICU	Pulmonary malignancy, respiratory failure	Died	7/6/2017	Blood
Pa37	KP37	36	Male	ICU	Cardiopulmonary arrest	Discharged	18/6/2017	Blood
Pa38	KP38-1	92	Female	Neurosurgery	Aspiration pneumonia, hypertension	Died	10/7/2017	Urine
	KP38-2	92	Female	Neurosurgery	Sequelae of cerebral infarction, Aspiration pneumonia	Died	30/10/2017	Blood
Pa45	KP45	83	Female	Neurosurgery	Post-traumatic syndrome, cerebral hemorrhage	Discharged	30/10/2017	Urine
Pa65	KP65	73	Male	Respiratory	Pulmonary infection	Discharged	14/3/2018	Excreta

ICU, intensive care unit.

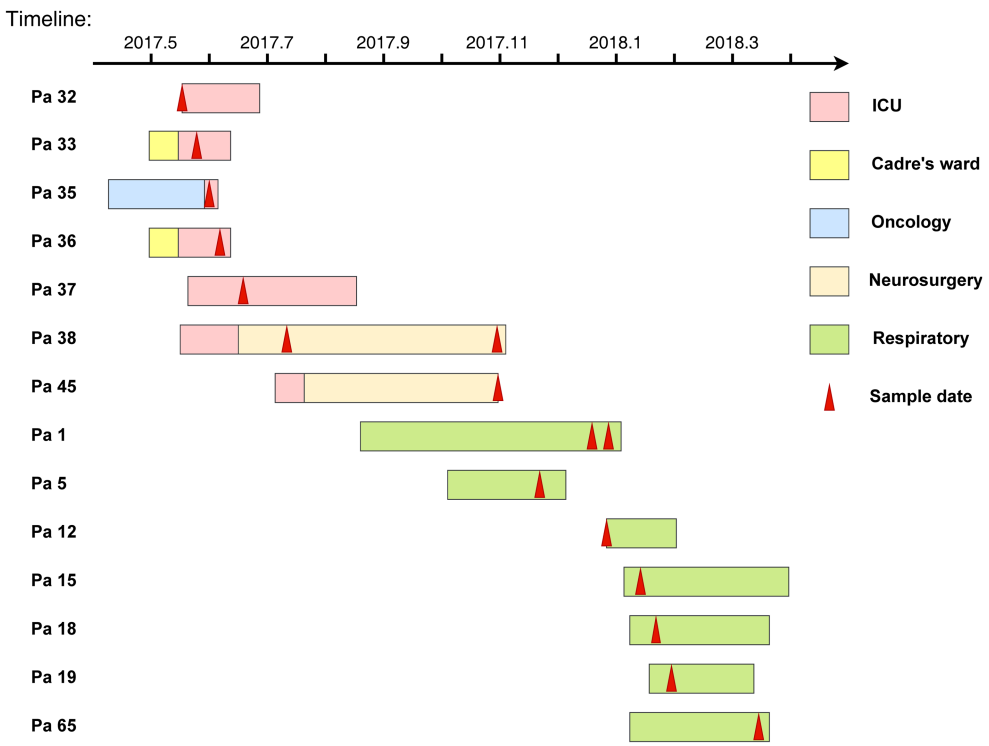

FIGURE 3 | The timelines of inpatients harboring KPC-2-producing ST11-KL64 CRKP isolates in the clinical setting. The rectangle on the timeline represents the admitting's duration of the patients. Different wards are shown in different colors, and the red arrows indicate sampling dates.

peg-344 were detected in all CRKP isolates except for KP35, KP37, KP38-2, and KP45.

Genetic Features of Virulence Plasmids and *bla*$_{KPC-2}$-Bearing Plasmids

To investigate the genetic features of virulence plasmids and *bla*$_{KPC-2}$-bearing plasmids, *K. pneumoniae* KP12, KP36, and KP37 were further subjected to whole-genome sequencing using the Oxford Nanopore MinION platform. Plasmid sequence analysis confirmed that all the three *K. pneumoniae* isolates harbored an IncFIB/IncHI1B type virulence plasmid and an IncFII/IncR type *bla*$_{KPC-2}$-bearing plasmid (**Figure 4**). Interestingly, *iroBCDN* with IS*110* transposase on the upstream, located in the same transposon IS*3* with *rmpA* and *peg-344* in pLVPK, were absent

TABLE 2 | Minimal inhibitory concentrations (MICs) of the 16 KPC-2-producing ST11-KL64 CRKP isolates to different antimicrobials.

Isolate	ATM[a]	FOF	ETP	CAZ	FEP	SCF	FOX	LVX	CIP	AMK	TET	TGC	MH	CST	CTX	MEM	IPM	GEN	SXT	PRL	PRL/TZP
KP1-1	32[b]	16	>256	>256	256	>256	256	64	128	>256	>256	8	64	0.03	64	128	128	>256	16	>512	>512
KP1-2	32	32	>256	256	256	>256	128	128	128	>256	>256	8	64	64	128	128	128	>256	16	>512	512
KP5	128	64	>256	>256	256	>256	>256	128	128	1	>256	4	64	0.03	>256	128	128	>256	16	>512	>512
KP12	128	128	256	>256	256	>256	256	32	64	>256	256	2	32	0.06	>256	128	128	256	16	>512	>512
KP15	128	32	>256	>256	256	>256	>256	64	128	>256	256	4	64	0.03	>256	128	32	>256	16	>512	>512
KP18	128	256	>256	>256	256	>256	>256	64	64	>256	256	4	32	0.06	>256	128	128	>256	16	>512	>512
KP19	128	256	>256	>256	256	>256	256	32	64	>256	>256	4	32	0.06	>256	128	128	>256	16	>512	>512
KP32	128	16	>256	>256	256	>256	>256	64	128	>256	>256	4	64	0.03	>256	128	128	>256	16	>512	>512
KP33	128	32	>256	>256	512	>256	>256	128	128	>256	>256	4	64	0.03	>256	128	128	>256	16	>512	>512
KP35	128	32	>256	>256	256	>256	>256	64	128	>256	>256	4	64	0.125	>256	128	128	>256	16	>512	>512
KP36	128	32	256	>256	256	>256	256	64	128	>256	>256	4	64	2	256	128	128	>256	16	>512	>512
KP37	128	32	>256	>256	256	>256	>256	128	128	>256	>256	4	32	0.03	>256	128	128	>256	16	>512	>512
KP45	128	32	256	256	256	>256	256	16	16	>256	256	4	16	0.03	256	128	128	>256	16	>512	512
KP65	128	64	>256	128	>256	>256	>256	128	128	>256	>256	8	64	0.03	>256	128	64	>256	16	>512	>512
KP38-1	128	>512	512	512	256	512	512	128	128	512	512	2	64	0.06	512	128	128	>256	1	>512	>512
KP38-2	128	>512	512	512	256	512	512	128	128	512	512	2	64	0.06	512	128	128	>256	1	>512	>512

[a]*ATM, aztreonam; FOF, fosfomycin; ETP, ertapenem; CAZ, ceftazidime; FEP, cefepime; SCF, cefoperazone-sulbactam; FOX, cefoxitin; LVX, levofloxacin; CIP, ciprofloxacin; AMK, amikacin; TET, tetracycline; TGC, tigecycline; MH, minocycline; CST, colistin; CTX, cefotaxime; MEM, meropenem; IPM, imipenem; GEN, gentamicin; SXT, trimethoprim-sulfamethoxazole; PRL, piperacillin; and PRL/TZP, piperacillin-tazobactam.*

[b]*mg/L.*

in KP12, KP36, and KP37 (**Figure 5A**). It is worth noting that *rmpA* and *peg-344* were located between two IS*Kpn26* transposons in pKP12-vir and pKP36-vir, but the two virulence genes were further missing in pKP37-vir. According to these results, we hypothesize that IS*110* might be responsible for the deletion of *iroBCDN*, and then forming a new transposon IS*Kpn26* carrying *rmpA* and *peg-344* from the classical virulence plasmid pLVPK after this losing event.

Plasmids pKP12-KPC, pKP36-KPC, and pKP37-KPC exhibited a high level of homology (99% coverage and 99% identity) with other bla_{KPC-2}-bearing plasmids, i.e., the 133,772-bp IncFII/IncR plasmid p3_L39 recovered from *K. pneumoniae* strain L39_2 in China. Plasmids pKP12-KPC, pKP36-KPC, and pKP37-KPC also harbored several antimicrobial resistance genes, i.e., $bla_{CTX-M-65}$, bla_{SHV-12}, bla_{TEM-1B}, and *rmtB* (**Figure 5B**). Comparison of genetic surroundings of bla_{KPC-2} gene indicated that it was flanked by a similar core structure, IS*Kpn27*-bla_{KPC-2}-IS*Kpn6*. Another multi-drug resistance region consisted of $bla_{CTX-M-65}$, bla_{TEM-1B}, and *rmtB* genes and five mobile genetic elements on these bla_{KPC-2}-bearing plasmids.

DISCUSSION

The worldwide spread of carbapenem-resistant *K. pneumoniae*, associated with considerable morbidity and mortality, poses a severe threat to public health. ST11 was found to be the most predominant epidemic clone of CRKP strains in China, which has aroused considerable attention recently due to the scenarios for convergence of resistance and hypervirulence determinants in a single strain (Wyres et al., 2020a). Therefore, surveillance and tracking of high-risk clones of CRKP and understanding their clinical importance are critical. PFGE and MLST, as well-known genotyping methods, can monitor and control the spread of nosocomial pathogens (Singh et al., 2006). However, traditional molecular typing techniques are limited in distinguishing minor genomic differences between closely related strains involved in an outbreak. With the extensive use of next-generation sequencing, WGS analysis easily distinguishes minor differences between clones and is widely used for pathogen identification and tracking the rules underlying pathogen spread (Klemm et al., 2018; Schurch et al., 2018). This study investigated the origin and transmission pattern of KPC-2-producing ST11-KL64 CRKP outbreaks. The genetic features of virulence plasmids and bla_{KPC-2}-bearing plasmids were further investigated by comparative genomic analysis.

During the study period, 47 *K. pneumoniae* isolates were identified as CRKP, and three dominant PFGE clusters were observed. Among them, 16 CRKP isolates harbored the bla_{KPC-2} gene, representing a potential clonal spread due to their similar PFGE patterns. *In silico* MLST analysis identified all the 16 KPC-2-producing CRKP isolates as ST11, which is the most predominant sequence type of KPC-2-producing CRKP in China and has been reported worldwide, including America, Europe, and Asia (Baraniak et al., 2011; Jiang et al., 2015; Zhan et al., 2017; Gu et al., 2018; Ko, 2019; Spencer et al., 2019; Zhou et al., 2020; Jin et al., 2021; Yang et al., 2021).

Moreover, all the 16 KPC-2-producing CRKP isolates belonged to the serotype KL64, which differs from those reported previously, such as KL1, KL2, and KL62 (Feng et al., 2018; Gu et al., 2018). However, an infection caused by KPC-2-producing ST11-KL64 CRKP was frequently reported recently (De Campos et al., 2018; Jia et al., 2019; Ruan et al., 2020a; Zhang et al., 2020b; Zhou et al., 2020; Jin et al., 2021; Yang et al., 2021). Zhou et al. (2020) reported that patients infected by ST11-KL64 CRKP had a significantly higher mortality rate than those infected by other CRKP. In this study, four out of 16 patients died of ST11-KL64 CRKP infection. These findings suggested that KL64 clone of CRKP was closely related to high pathogenicity and transmissibility, and continuous monitoring should be taken to prevent further dissemination.

Following cgSNP-based phylogenetic analysis, 16 KPC-2-producing ST11-KL64 CRKP isolates could be divided into two clades, suggesting two independent transmission events. Some patients in the two clades showed overlaps in time frames or hospital stay units that may have contributed to *K. pneumoniae* dissemination among patients. The index patient of transmission 1 was Pa 32, and the infection was transmitted to Pa 33, Pa 35, Pa 36, and Pa 37 represented in clade 1. Pa 33, Pa 35, Pa 36, and Pa 37 shared months of overlapping ICU stay with Pa 32, and the five isolates from these inpatients were sampled in ICU and displayed considerable genomic similarity. CRKP was detected in the urine and blood culture of Pa 38 and Pa 45 after they were transferred from ICU to neurosurgery. A separate transmission route of KPC-2-producing CRKP infection was identified in Pa 12, Pa 15, Pa 18, and Pa 19. The sampling time of the above four inpatients was close, suggesting that a transmission event occurred within a short period. The spread of ST11 CRKP among different departments or different wards of the same department in the hospital is relatively expected, which has been reported frequently (Jiang et al., 2015; Gu et al., 2018; Sui et al., 2018; Lu et al., 2020; Zhang et al., 2020b). Our data suggested two independent outbreaks of KPC-2-producing ST11-KL64 CRKP isolates in the ICU and the respiratory ward, respectively, between 2016 and 2018. These results confirmed the easy transfer of ST11 CRKP, and practical strategies must be implemented to control the outbreak and avoid nosocomial transmission.

In this study, all the isolates of 16 ST11-KL64 CRKP harbored bla_{KPC-2} and were multidrug-resistant. In addition to carbapenemases, several extended-spectrum β-lactamase (ESBL) resistance genes, including $bla_{CTX-M-65}$, bla_{SHV-12}, and bla_{TEM-1B}, were identified in the 16 ST11-KL64 CRKP isolates. This finding indicated that all isolates contained multiple ESBL genes, which is in agreement with the reports on the co-occurrence of bla_{CTX-M}, bla_{SHV}, and bla_{TEM} in *K. pneumoniae* strains (Baraniak et al., 2011; Jiang et al., 2015; Gu et al., 2018; Sui et al., 2018). Therefore, more attention should be paid to the *K. pneumoniae* isolates, identified as epidemic ST11 clone and co-harbored carbapenemases and ESBLs in China. Besides the β-lactams resistance genes, other resistance genes that were found to be present in the majority of 16 ST11-KL64 CRKP isolates included *rmtB*, *catA2*, *fosA*, *qnrS1*, *sul2*, *tet*(A), *aadA2*

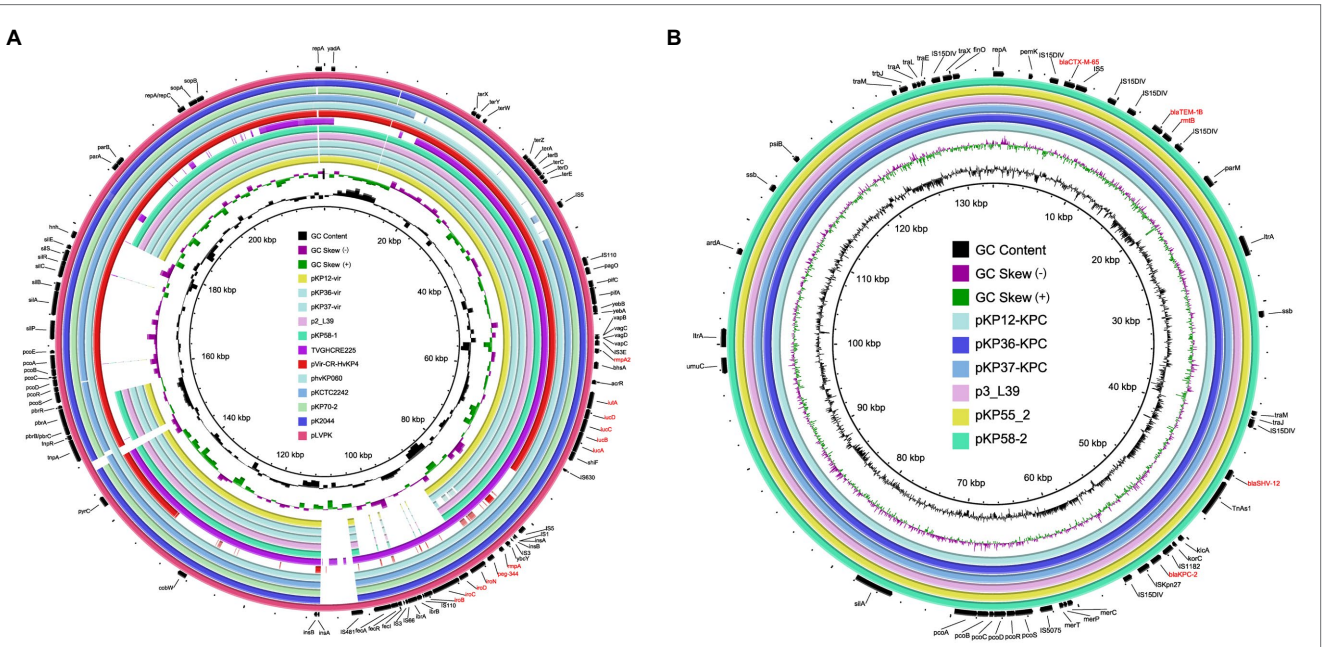

FIGURE 4 | Genetic comparison of virulence plasmids and bla_{KPC-2}-bearing plasmids recovered from *K. pneumoniae* KP12, KP36, and KP37 with similar plasmids in the NCBI database, respectively. **(A)** Alignment of virulence plasmids pKP12-vir, pKP36-vir, and pKP37-vir with p2_L39 (CP033955), pKP58-1 (CP041374), TVGHCRE225 (CP023723), pVir-CR-HvKP4 (MF437313), phvKP060 (CP034776), pKCTC2242 (CP002911), pKP70-2 (MF398271), pK2044 (AP006726), and pLVPK (AY378100). pLVPK was used as the reference plasmid. Virulence genes are highlighted in red. **(B)** Alignment of bla_{KPC-2}-bearing plasmid pKP12-KPC, pKP36-KPC, and pKP37-KPC with p3_L39 (CP033956), pKP55_2 (CP055296), and pKP58-2 (CP041375). p3_L39 was used as the reference plasmid. Antimicrobial resistance genes are highlighted in red.

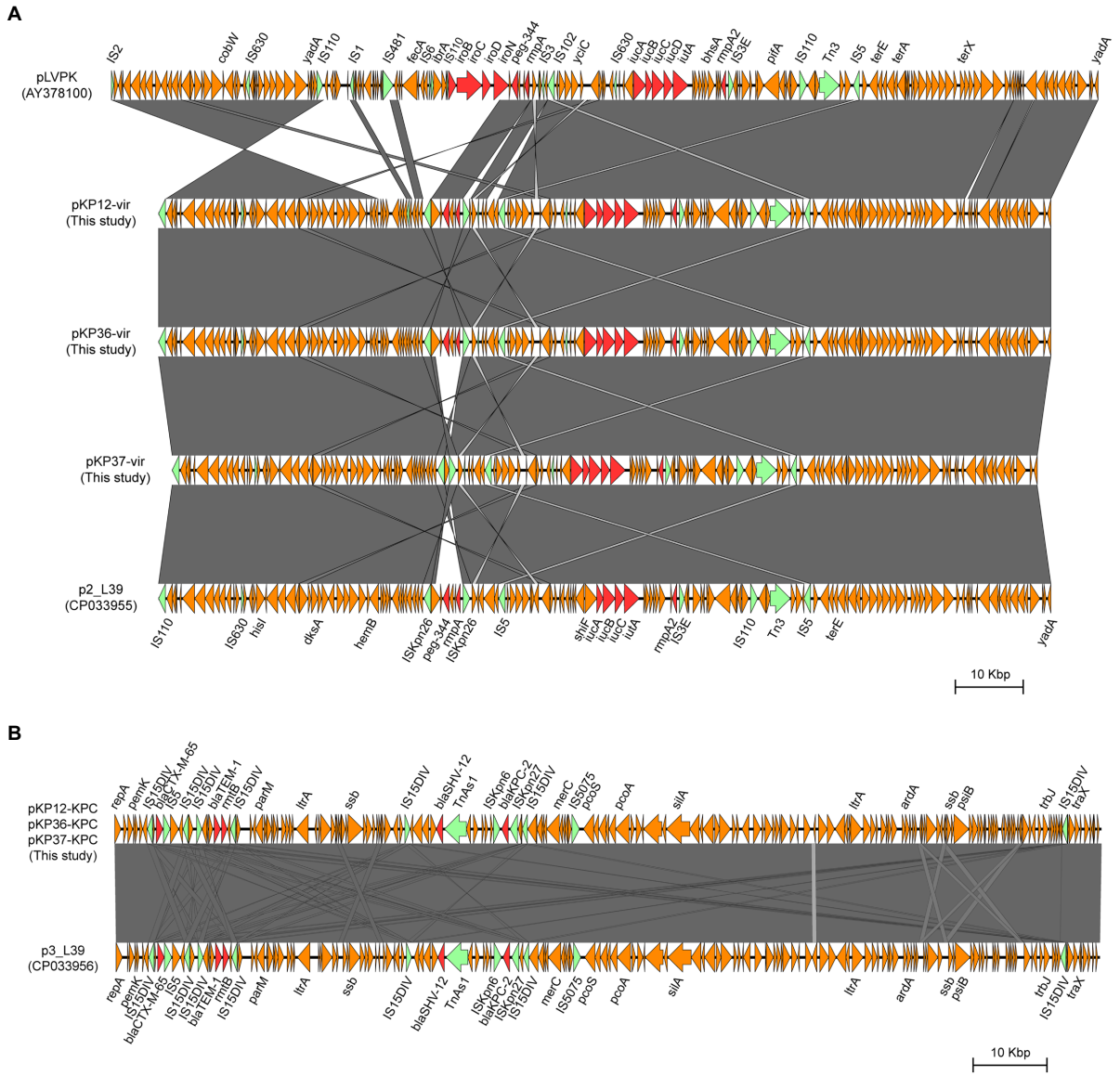

FIGURE 5 | Structural comparison of the genetic context of virulence genes **(A)** and bla_{KPC-2} gene **(B)** in representative plasmids. The arrows represent coding sequences (red arrows, antimicrobial resistance genes or virulence genes; green arrows, mobile elements). Shading denotes the regions with high homology (>95% nucleotide identity).

(detectable in 15 isolates), and *dfrA14* (detectable in 15 isolates), conferring resistance to aminoglycosides, chloramphenicol, fosfomycin, quinolone, sulphonamides, tetracycline, aminoglycoside, and trimethoprim, respectively. Undoubtedly, the presence of resistance genes allows the *K. pneumoniae* isolates to survive the barrage of antimicrobial agents used in treating infections. Fortunately, tigecycline and colistin were still effective *in vitro*, which suggested that the above two antimicrobials could be valuable treatment choices against ST11-KL64 CRKP infections.

Several virulence factors have been characterized as contributing to the hypervirulence phenotype of *K. pneumoniae*, but are not limited to the mucoid regulators *rmpA* and *rmpA2* and the aerobactin synthesis cluster *iucABCD/iutA* (Russo and Marr, 2019; Choby et al., 2020). The *rmpA* and *rmpA2* genes have both been considered determinants controlling the capsular polysaccharide (CPS) biosynthesis, representing the hypermucoviscous phenotype. The aerobactin has been appreciated as the predominant siderophore system in the hvKP. It has previously been common that ST11 *K. pneumoniae* is a widely disseminated multidrug-resistant clonal lineage, including carbapenems, but not hypervirulent. However, a fetal outbreak in five patients caused by an ST11 carbapenem-resistant *K. pneumoniae* strain, which turned into hvKP by acquiring a roughly 170 kb pLVPK-like plasmid, was reported in China (Gu et al., 2018). In this study, all the 16 KPC-2-producing

K64-ST11 CRKP isolates harbored hypermucoviscous phenotype regulators and aerobactin synthesis, showed not only resistance to antimicrobials but also hypervirulent phenotype. Alongside the plasmid-borne ESBL and carbapenemase genes, our data revealed a high prevalence of ST11-KL64 CR-hvKPs carrying the IncHI1B/IncFIB virulence plasmids with *iro* locus deletion. Clinically, the KPC-2-producing ST11-KL64 CRKP isolates carrying the *rmpA* and *rmpA2* genes exhibited enhanced environmental survival and caused more severe infection than classic ST11 KP strains, leading to high mortality (Zhou et al., 2020). This finding is consistent with our study, which showed that all the four dead patients (Pa 1, Pa 33, Pa36, and Pa38) harbored *rmpA* and *rmpA2* genes in ST11-KL64 CRKP isolates. These results revealed the hypervirulence nature of those isolates, and targeted surveillance is urgently needed. Further genomic epidemiology and evolutionary analysis at the national scale are warranted to understand the genetic basis and evolution characteristics of the wide dissemination of carbapenem-resistant hypervirulent ST11-KL64 *K. pneumoniae* in China.

During the two nosocomial CPKP outbreaks, we had implemented infection prevention and control measures to control the outbreaks in the ICU and respiratory. Several measures were implemented to eliminate the nosocomial CPKP infection. First, we implemented stringent isolation procedures for the CRKP-infected patients and limited the persons who came to contact with these patients. Second, we performed equipment disinfection and periodic environmental cleansing. Third, all the hospital staff contacted with patients carrying CRKP should wear medical gloves and contagion gowns and enforced hand hygiene once the operation was finished. Finally, the ST11-KL64 CRKP nosocomial infection was successfully eliminated and ended in April 2018.

In conclusion, our study identified the emergence of a high-risk clone of KPC-2-producing ST11-KL64 CRKP isolates in a clinical setting. Our results clearly showed that WGS could reveal the two transmission scenarios caused by these CRKP isolates. Due to the acquisition of multiple plasmid-borne antimicrobial resistance and virulence genes, these isolates have presented a significant challenge for public health. The placement of adequate infection control measures is necessary to prevent their further dissemination in nosocomial settings.

DATA AVAILABILITY STATEMENT

The datasets presented in this study can be found in online repositories. The names of the repository/repositories and accession number(s) can be found in the article/**Supplementary Material**.

AUTHOR CONTRIBUTIONS

ZR, JZ, and XX designed the experiments. YK, QS, and HC performed the experiments. ZR and YK analyzed the data. YK, ZR, and MD wrote the manuscript. All authors contributed to the article and approved the submitted version.

FUNDING

This study was supported by the National Natural Science Foundation of China (81871696 and 82072342) and the Zhejiang Provincial Medical and Health Science and Technology Plan (2021KY943).

SUPPLEMENTARY MATERIAL

The Supplementary Material for this article can be found online at: https://www.frontiersin.org/articles/10.3389/fmicb.2021.736896/full#supplementary-material

REFERENCES

Alikhan, N. F., Petty, N. K., Ben Zakour, N. L., and Beatson, S. A. (2011). BLAST ring image generator (BRIG): simple prokaryote genome comparisons. *BMC Genomics* 12:402. doi: 10.1186/1471-2164-12-402

Baraniak, A., Grabowska, A., Izdebski, R., Fiett, J., Herda, M., Bojarska, K., et al. (2011). Molecular characteristics of KPC-producing Enterobacteriaceae at the early stage of their dissemination in Poland, 2008-2009. *Antimicrob. Agents Chemother.* 55, 5493–5499. doi: 10.1128/AAC.05118-11

Choby, J. E., Howard-Anderson, J., and Weiss, D. S. (2020). Hypervirulent *Klebsiella pneumoniae*: clinical and molecular perspectives. *J. Intern. Med.* 287, 283–300. doi: 10.1111/joim.13007

De Campos, T. A., Goncalves, L. F., Magalhaes, K. G., De Paulo Martins, V., Pappas Junior, G. J., Peirano, G., et al. (2018). A fatal bacteremia caused by hypermucousviscous KPC-2 producing extensively drug-resistant K64-ST11 *Klebsiella pneumoniae* in Brazil. *Front. Med.* 5:265. doi: 10.3389/fmed.2018.00265

Feng, Y., Lu, Y., Yao, Z., and Zong, Z. (2018). Carbapenem-resistant hypervirulent *Klebsiella pneumoniae* of sequence type 36. *Antimicrob. Agents Chemother.* 62, e02644–e02717. doi: 10.1128/AAC.02644-17

Feng, Y., Zou, S., Chen, H., Yu, Y., and Ruan, Z. (2021). BacWGSTdb 2.0: a one-stop repository for bacterial whole-genome sequence typing and source tracking. *Nucleic Acids Res.* 49, D644–D650. doi: 10.1093/nar/gkaa821

Fukigai, S., Alba, J., Kimura, S., Iida, T., Nishikura, N., Ishii, Y., et al. (2007). Nosocomial outbreak of genetically related IMP-1 beta-lactamase-producing *Klebsiella pneumoniae* in a general hospital in Japan. *Int. J. Antimicrob. Agents* 29, 306–310. doi: 10.1016/j.ijantimicag.2006.10.011

Gu, D., Dong, N., Zheng, Z., Lin, D., Huang, M., Wang, L., et al. (2018). A fatal outbreak of ST11 carbapenem-resistant hypervirulent *Klebsiella pneumoniae* in a Chinese hospital: a molecular epidemiological study. *Lancet Infect. Dis.* 18, 37–46. doi: 10.1016/S1473-3099(17)30489-9

Jia, H., Chen, H., and Ruan, Z. (2019). Unravelling the genome sequence of a pandrug-resistant *Klebsiella pneumoniae* isolate with sequence type 11 and capsular serotype KL64 from China. *J. Glob. Antimicrob. Resist.* 19, 40–42. doi: 10.1016/j.jgar.2019.08.013

Jiang, Y., Wei, Z., Wang, Y., Hua, X., Feng, Y., and Yu, Y. (2015). Tracking a hospital outbreak of KPC-producing ST11 *Klebsiella pneumoniae* with whole genome sequencing. *Clin. Microbiol. Infect.* 21, 1001–1007. doi: 10.1016/j.cmi.2015.07.001

Jin, X., Chen, Q., Shen, F., Jiang, Y., Wu, X., Hua, X., et al. (2021). Resistance evolution of hypervirulent carbapenem-resistant *Klebsiella pneumoniae* ST11 during treatment with tigecycline and polymyxin. *Emerg. Microbes Infect.* 10, 1129–1136. doi: 10.1080/22221751.2021.1937327

Klemm, E. J., Wong, V. K., and Dougan, G. (2018). Emergence of dominant multidrug-resistant bacterial clades: lessons from history and whole-genome sequencing. *Proc. Natl. Acad. Sci. U. S. A.* 115, 12872–12877. doi: 10.1073/pnas.1717162115

Ko, K. S. (2019). Antibiotic-resistant clones in gram-negative pathogens: presence of global clones in Korea. *J. Microbiol.* 57, 195–202. doi: 10.1007/s12275-019-8491-2

Letunic, I., and Bork, P. (2021). Interactive tree Of life (iTOL) v5: an online tool for phylogenetic tree display and annotation. *Nucleic Acids Res.* 49, W293–W296. doi: 10.1093/nar/gkab301

Lu, M. C., Chen, Y. T., Tang, H. L., Liu, Y. Y., Chen, B. H., Wang, Y. W., et al. (2020). Transmission and evolution of OXA-48-producing *Klebsiella pneumoniae* ST11 in a single hospital in Taiwan. *J. Antimicrob. Chemother.* 75, 318–326. doi: 10.1093/jac/dkz431

Navon-Venezia, S., Kondratyeva, K., and Carattoli, A. (2017). *Klebsiella pneumoniae*: a major worldwide source and shuttle for antibiotic resistance. *FEMS Microbiol. Rev.* 41, 252–275. doi: 10.1093/femsre/fux013

Nishida, S., Matsunaga, N., Kamimura, Y., Ishigaki, S., Furukawa, T., and Ono, Y. (2020). Emergence of enterobacter cloacae complex co-producing IMP-10 and CTX-M, and *Klebsiella pneumoniae* producing VIM-1 in clinical isolates in Japan. *Microorganisms* 8:1816. doi: 10.3390/microorganisms8111816

Perez-Vazquez, M., Sola Campoy, P. J., Ortega, A., Bautista, V., Monzon, S., Ruiz-Carrascoso, G., et al. (2019). Emergence of NDM-producing *Klebsiella pneumoniae* and *Escherichia coli* in Spain: phylogeny, resistome, virulence and plasmids encoding blaNDM-like genes as determined by WGS. *J. Antimicrob. Chemother.* 74, 3489–3496. doi: 10.1093/jac/dkz366

Ruan, Z., and Feng, Y. (2016). BacWGSTdb, a database for genotyping and source tracking bacterial pathogens. *Nucleic Acids Res.* 44, D682–D687. doi: 10.1093/nar/gkv1004

Ruan, Z., Wu, J., Chen, H., Draz, M. S., Xu, J., and He, F. (2020a). Hybrid genome assembly and annotation of a pandrug-resistant *Klebsiella pneumoniae* strain using nanopore and illumina sequencing. *Infect. Drug Resist.* 13, 199–206. doi: 10.2147/IDR.S240404

Ruan, Z., Yu, Y., and Feng, Y. (2020b). The global dissemination of bacterial infections necessitates the study of reverse genomic epidemiology. *Brief Bioinform.* 21, 741–750. doi: 10.1093/bib/bbz010

Russo, T. A., and Marr, C. M. (2019). Hypervirulent *Klebsiella pneumoniae*. *Clin. Microbiol. Rev.* 32, e00001–e00019. doi: 10.1128/CMR.00001-19

Schurch, A. C., Arredondo-Alonso, S., Willems, R. J. L., and Goering, R. V. (2018). Whole genome sequencing options for bacterial strain typing and epidemiologic analysis based on single nucleotide polymorphism versus gene-by-gene-based approaches. *Clin. Microbiol. Infect.* 24, 350–354. doi: 10.1016/j.cmi.2017.12.016

Singh, A., Goering, R. V., Simjee, S., Foley, S. L., and Zervos, M. J. (2006). Application of molecular techniques to the study of hospital infection. *Clin. Microbiol. Rev.* 19, 512–530. doi: 10.1128/CMR.00025-05

Spencer, M. D., Winglee, K., Passaretti, C., Earl, A. M., Manson, A. L., Mulder, H. P., et al. (2019). Whole genome sequencing detects inter-facility transmission of carbapenem-resistant *Klebsiella pneumoniae*. *J. Infect.* 78, 187–199. doi: 10.1016/j.jinf.2018.11.003

Stamatakis, A. (2014). RAxML version 8: a tool for phylogenetic analysis and post-analysis of large phylogenies. *Bioinformatics* 30, 1312–1313. doi: 10.1093/bioinformatics/btu033

Sui, W., Zhou, H., Du, P., Wang, L., Qin, T., Wang, M., et al. (2018). Whole genome sequence revealed the fine transmission map of carbapenem-resistant *Klebsiella pneumonia* isolates within a nosocomial outbreak. *Antimicrob. Resist. Infect. Control* 7:70. doi: 10.1186/s13756-018-0363-8

Sullivan, M. J., Petty, N. K., and Beatson, S. A. (2011). Easyfig: a genome comparison visualizer. *Bioinformatics* 27, 1009–1010. doi: 10.1093/bioinformatics/btr039

Tatusova, T., Dicuccio, M., Badretdin, A., Chetvernin, V., Nawrocki, E. P., Zaslavsky, L., et al. (2016). NCBI prokaryotic genome annotation pipeline. *Nucleic Acids Res.* 44, 6614–6624. doi: 10.1093/nar/gkw569

Tenover, F. C., Arbeit, R. D., Goering, R. V., Mickelsen, P. A., Murray, B. E., Persing, D. H., et al. (1995). Interpreting chromosomal DNA restriction patterns produced by pulsed-field gel electrophoresis: criteria for bacterial strain typing. *J. Clin. Microbiol.* 33, 2233–2239. doi: 10.1128/jcm.33.9.2233-2239.1995

Wang, X., Xie, Y., Li, G., Liu, J., Li, X., Tian, L., et al. (2018). Whole-genome-sequencing characterization of bloodstream infection-causing hypervirulent *Klebsiella pneumoniae* of capsular serotype K2 and ST374. *Virulence* 9, 510–521. doi: 10.1080/21505594.2017.1421894

Wick, R. R., Heinz, E., Holt, K. E., and Wyres, K. L. (2018). Kaptive web: user-friendly capsule and lipopolysaccharide serotype prediction for *Klebsiella* genomes. *J. Clin. Microbiol.* 56, e00197–e00218. doi: 10.1128/JCM.00197-18

Wick, R. R., Judd, L. M., Gorrie, C. L., and Holt, K. E. (2017). Unicycler: resolving bacterial genome assemblies from short and long sequencing reads. *PLoS Comput. Biol.* 13:e1005595. doi: 10.1371/journal.pcbi.1005595

Wyres, K. L., Lam, M. M. C., and Holt, K. E. (2020a). Population genomics of *Klebsiella pneumoniae*. *Nat. Rev. Microbiol.* 18, 344–359. doi: 10.1038/s41579-019-0315-1

Wyres, K. L., Nguyen, T. N. T., Lam, M. M. C., Judd, L. M., Van Vinh Chau, N., Dance, D. A. B., et al. (2020b). Genomic surveillance for hypervirulence and multi-drug resistance in invasive *Klebsiella pneumoniae* from south and Southeast Asia. *Genome Med.* 12:11. doi: 10.1186/s13073-019-0706-y

Yang, Y., Yang, Y., Chen, G., Lin, M., Chen, Y., He, R., et al. (2021). Molecular characterization of carbapenem-resistant and virulent plasmids in *Klebsiella pneumoniae* from patients with bloodstream infections in China. *Emerg. Microbes Infect.* 10, 700–709. doi: 10.1080/22221751.2021.1906163

Yigit, H., Queenan, A. M., Anderson, G. J., Domenech-Sanchez, A., Biddle, J. W., Steward, C. D., et al. (2001). Novel carbapenem-hydrolyzing beta-lactamase, KPC-1, from a carbapenem-resistant strain of *Klebsiella pneumoniae*. *Antimicrob. Agents Chemother.* 45, 1151–1161. doi: 10.1128/AAC.45.4.1151-1161.2001

Zhan, L., Wang, S., Guo, Y., Jin, Y., Duan, J., Hao, Z., et al. (2017). Outbreak by hypermucoviscous *Klebsiella pneumoniae* ST11 isolates with carbapenem resistance in a tertiary hospital in China. *Front. Cell. Infect. Microbiol.* 7:182. doi: 10.3389/fcimb.2017.00182

Zhang, Y., Jin, L., Ouyang, P., Wang, Q., Wang, R., Wang, J., et al. (2020b). Evolution of hypervirulence in carbapenem-resistant *Klebsiella pneumoniae* in China: a multicentre, molecular epidemiological analysis. *J. Antimicrob. Chemother.* 75, 327–336. doi: 10.1093/jac/dkz446

Zhang, P., Shi, Q., Hu, H., Hong, B., Wu, X., Du, X., et al. (2020a). Emergence of ceftazidime/avibactam resistance in carbapenem-resistant *Klebsiella pneumoniae* in China. *Clin. Microbiol. Infect.* 26, 124.e1–124.e4. doi: 10.1016/j.cmi.2019.08.020

Zhou, K., Xiao, T., David, S., Wang, Q., Zhou, Y., Guo, L., et al. (2020). Novel subclone of carbapenem-resistant *Klebsiella pneumoniae* sequence type 11 with enhanced virulence and transmissibility, China. *Emerg. Infect. Dis.* 26, 289–297. doi: 10.3201/eid2602.190594

Conflict of Interest: The authors declare that the research was conducted in the absence of any commercial or financial relationships that could be construed as a potential conflict of interest.

Publisher's Note: All claims expressed in this article are solely those of the authors and do not necessarily represent those of their affiliated organizations, or those of the publisher, the editors and the reviewers. Any product that may be evaluated in this article, or claim that may be made by its manufacturer, is not guaranteed or endorsed by the publisher.

frontiers in Microbiology

ORIGINAL RESEARCH
published: 16 November 2021
doi: 10.3389/fmicb.2021.729952

Genetic Diversity and Characteristics of *bla*$_{NDM}$-Positive Plasmids in *Escherichia coli*

Zhiren Zhang[1†], Hengzhao Guo[2†], Xiaodong Li[3†], Wenting Li[1], Guang Yang[1], Wenjun Ni[4], Meixiao Zhan[1,5], Ligong Lu[1,5], Zhenlin Zhang[6], Xiaobin Li[1*] and Zhiling Zhou[7*]*

[1] Zhuhai Precision Medical Center, Zhuhai People's Hospital (Zhuhai Hospital Affiliated With Jinan University), Zhuhai, China, [2] Department of Radiation Oncology, Zhuhai People's Hospital (Zhuhai Hospital Affiliated With Jinan University), Zhuhai, China, [3] Department of Spine and Osteology, Zhuhai People's Hospital (Zhuhai Hospital Affiliated With Jinan University), Zhuhai, China, [4] Department of Urology, Zhuhai People's Hospital (Zhuhai Hospital Affiliated With Jinan University), Zhuhai, China, [5] Zhuhai Interventional Medical Center, Zhuhai People's Hospital (Zhuhai Hospital Affiliated With Jinan University), Zhuhai, China, [6] Department of Clinical Laboratory, Zhuhai People's Hospital (Zhuhai Hospital Affiliated With Jinan University), Zhuhai, China, [7] Department of Pharmacy, Zhuhai People's Hospital (Zhuhai Hospital Affiliated With Jinan University), Zhuhai, China

New Delhi metallo-β-lactamases (NDMs), including at least 28 variants, are a rapidly emerging family of β-lactamases worldwide, with a variety of infections caused by NDM-positive strains usually associated with very poor prognosis and high mortality. NDMs are the most prevalent carbapenemases in *Escherichia coli* (*E. coli*) worldwide, especially in China. The vast majority of *bla*$_{NDM}$ cases occur on plasmids, which play a vital role in the dissemination of *bla*$_{NDM}$. To systematically explore the relationships between plasmids and *bla*$_{NDM}$ genes in *E. coli* and obtain an overall picture of the conjugative and mobilizable *bla*$_{NDM}$-positive plasmids, we analyzed the variants of *bla*$_{NDM}$, replicon types, phylogenetic patterns, conjugative transfer modules, host STs, and geographical distributions of 114 *bla*$_{NDM}$-positive plasmids, which were selected from 3786 plasmids from 1346 complete whole genomes of *E. coli* from the GenBank database. We also established links among the characteristics of *bla*$_{NDM}$-positive plasmids in *E. coli*. Eight variants of *bla*$_{NDM}$ were found among the 114 *bla*$_{NDM}$-positive plasmids, with *bla*$_{NDM-5}$ (74 *bla*$_{NDM-5}$ genes in 73 plasmids), and *bla*$_{NDM-1}$ (31 *bla*$_{NDM-1}$ genes in 28 plasmids) being the most dominant. The variant *bla*$_{NDM-5}$ was mainly carried by the IncX3 plasmids and IncF plasmids in *E. coli*, the former were mainly geographically distributed in East Asia (especially in China) and the United States, and the latter were widely distributed worldwide. IncC plasmids were observed to be the predominant carriers of *bla*$_{NDM-1}$ genes in *E. coli*, which were mainly geographically distributed in the United States and China. Other *bla*$_{NDM-1}$-carrying plasmids also included IncM2, IncN2, and IncHI1. Moreover, the overall picture of the conjugative and mobilizable *bla*$_{NDM}$-positive plasmids in *E. coli* was described in our study. Our findings enhance our understanding of the genetic diversity and characteristics of *bla*$_{NDM}$-positive plasmids in in *E. coli*.

Keywords: *Escherichia coli*, New Delhi metallo-β-lactamase, plasmid, conjugative, mobilizable

OPEN ACCESS

Edited by:
Ziad Daoud,
Central Michigan University,
United States

Reviewed by:
Haiquan Kang,
Affiliated Hospital of Xuzhou Medical University, China
Hua Zhou,
Zhejiang University, China
Jun Sung Hong,
Yonsei University College of Medicine, South Korea
Zhihai Liu,
Qingdao Agricultural University, China
Bahareh Hajikhani,
Shahid Beheshti University of Medical Sciences, Iran

***Correspondence:**
Zhenlin Zhang
jnudoctor@163.com
Xiaobin Li
xiaobinli@sjtu.edu.cn
Zhiling Zhou
zhouzl@aliyun.com

† These authors have contributed equally to this work

Specialty section:
This article was submitted to Antimicrobials, Resistance and Chemotherapy, a section of the journal Frontiers in Microbiology

Received: *24 June 2021*
Accepted: *11 October 2021*
Published: *16 November 2021*

Citation:
Zhang Z, Guo H, Li X, Li W, Yang G, Ni W, Zhan M, Lu L, Zhang Z, Li X and Zhou Z (2021) Genetic Diversity and Characteristics of bla$_{NDM}$-Positive Plasmids in Escherichia coli. Front. Microbiol. 12:729952. doi: 10.3389/fmicb.2021.729952

INTRODUCTION

New Delhi metallo-β-lactamase (NDM) is a metallo-β-lactamase that can hydrolyze almost all β-lactam antibiotics, including carbapenems (Nordmann et al., 2011). NDM-1 was first identified in a *Klebsiella pneumoniae* strain isolated from a Swedish patient who had been hospitalized in New Delhi, India in 2008 (Yong et al., 2009). So far, 28 variants of NDM have been reported (Farhat and Khan, 2020). A variety of infections caused by NDM-positive strains are reportedly associated with very poor prognosis and high mortality, especially in neonates and high-risk immunocompromised patients (Guducuoglu et al., 2018). NDM-positive strains have been found worldwide, with the highest prevalence in the Indian subcontinent, the Middle East, and the Balkans (Albiger et al., 2015; Wu and Feng, 2019). According to the Study for Monitoring Antimicrobial Resistance Trends (SMART) global surveillance program, bla_{NDM} is the third most common carbapenemase-encoding gene and accounts for 19.42% of carbapenemase positivity after bla_{KPC} (53.18%) and the bla_{OXA-48}-like gene (20.09%) (Karlowsky et al., 2017). In China, the presence of bla_{KPC} (51.6%) and bla_{NDM} (35.7%) is responsible for phenotypic resistance in most carbapenem-resistant Enterobacteriaceae (CRE) strains (Han et al., 2020), according to data from the China Antimicrobial Surveillance Network (CHINET) in 2018. Furthermore, data from SMART and CHINET2018 demonstrated that NDM was the most prevalent carbapenemase in *E. coli*, especially in China; bla_{NDM} accounted for 93.0 and 97.2% of carbapenem-resistant *E. coli* isolates from adults and children, respectively (Han et al., 2020).

Antimicrobial resistance (AMR) in CRE isolates is frequently mediated by plasmid-borne genes, in addition to chromosomal determinants (Rozwandowicz et al., 2018). Plasmids remain important microbial components that mediate horizontal gene transfer (HGT) and play a vital role in the dissemination of AMR (Jiang et al., 2020). bla_{NDM} has been reported to be carried on plasmids with a variety of replicon types, most of which belong to limited replicon types (IncX3, IncFII, or IncC) (Wu and Feng, 2019). For CRE isolates, conjugative plasmids have been highlighted as important vehicles for the dissemination of AMR (Smillie et al., 2010; Ravi et al., 2018). The conjugative transfer regions of the conjugative plasmids typically consist of four modules: an origin of transfer (*oriT*) region, relaxase gene, type IV coupling protein (T4CP) gene, and gene cluster for the bacterial type IV secretion system (T4SS) apparatus (de la Cruz et al., 2010). In addition, mobilizable plasmids are also contributors to AMR, typically carrying the indispensable *oriT* sites and a limited number of *mob* genes for their own DNA processing in conjugation, which can be mobilized by conjugative elements (Ramsay and Firth, 2017). Currently, studies on the distribution of conjugative and mobilizable bla_{NDM}-positive carbapenem-resistant plasmids in *E. coli* are rare. With the increase in the amount of whole-genome/plasmid sequencing data, there is a need for large-scale plasmid analysis of bla_{NDM}-positive plasmids of *E. coli*.

In this study, we performed *in silico* typing and comparative analysis of bla_{NDM}-positive plasmids of *E. coli* using the bacterial genome and plasmid sequences available in the NCBI database. We analyzed the geographical distribution of bla_{NDM}-positive plasmids and compared the replicon types, conjugative transfer modules, and profiles of resistance determinants among bla_{NDM}-positive plasmids of *E. coli*. This study provides important insights into the phylogeny and evolution of bla_{NDM}-positive *E. coli* plasmids and further addresses their role in the acquisition and spread of resistance genes.

MATERIALS AND METHODS

For this study, the data collection and analysis are shown in **Supplementary Figure 1**.

Plasmid Genomic Sequences

A total of 1346 complete whole genomes of *E. coli*, including the genomes marked by "Chromosome" and "Complete" in assembly level, were downloaded from the GenBank (Benson et al., 2018) Genome database.[1] The download date was April 15, 2021. We extracted 3786 plasmid genomic sequences without duplicates (**Supplementary Table 1**) from the 1346 complete whole genomes of *E. coli*. In addition, a total of 35150 bacterial plasmid genomic sequences were downloaded from the NCBI RefSeq database (O'Leary et al., 2016),[2] including 6054 plasmids from *E. coli* (**Supplementary Table 2**), with the download date as July 14, 2021. The genome data (FASTA DNA format) were downloaded in bulk into a DELL PowerEdge R930 server with a Linux-CentOS7 operating system, using two Bioperl modules (Bio:DB:GenBank and Bio:SeqIO). Perl v5.16.3 was installed in the Linux platform.

Determination of bla_{NDM}-Positive Plasmids of *E. coli*

The potential β-lactamase genes of plasmids in FASTA DNA format were determined using the ResFinder software version 4.1[3] (Bortolaia et al., 2020) installed in our server, with a minimum coverage of 60%, minimum identity of 90%, and species of "*Escherichia coli*." The term "bla_{NDM}" was used to search in the "Resistance gene" list within the ResFinder results to determine the bla_{NDM}-positive plasmids of *E. coli*.

Replicon Sequence Analysis of the bla_{NDM}-Positive Plasmids of *E. coli*

Plasmid replicon typing was performed using the PlasmidFinder software[4] (Carattoli and Hasman, 2020). Selecting the database "Enterobacteriaceae," the DNA files in FASTA format were analyzed in bulk using the PlasmidFinder software version 2.0.1 installed in the Linux platform, with the minimum coverage of 60% and minimum identity of 95%.

[1] https://www.ncbi.nlm.nih.gov/genome/browse/#!/prokaryotes/167/

[2] https://ftp.ncbi.nih.gov/refseq/release/plasmid/

[3] https://cge.cbs.dtu.dk/services/ResFinder/

[4] https://cge.cbs.dtu.dk/services/PlasmidFinder/

Phylogenetic Analyses of the *bla*$_{NDM}$-Positive Plasmids of *E. coli*

The files in GenBank format of the *bla*$_{NDM}$-positive plasmids of *E. coli* were downloaded in bulk using the Bio:DB:GenBank and Bio:SeqIO modules. Files containing protein sequences were extracted from the files in GenBank format using the Bioperl/Bio:SeqIO module. Phylogenetic patterns based on the presence/absence of orthologous gene families of all *bla*$_{NDM}$-positive plasmids of *E. coli* were analyzed in this study. A binary protein presence/absence matrix was created using OrthoFinder[5] (Emms and Kelly, 2019) with DIAMOND for sequence similarity searches, and then a hierarchical cluster result was shown by iTOL[6] (Letunic and Bork, 2016).

Characterization of the Conjugative Modules of *bla*$_{NDM}$-Positive Plasmids

The files in GenBank format of the *bla*$_{NDM}$-positive plasmids of *E. coli* were analyzed in bulk using the software oriTfinder[7] (Li et al., 2018) (local version) to determine the presence/absence of *oriT*s, relaxase genes, T4CP genes, and gene cluster for T4SS. Furthermore, the types of *oriT*s, relaxase genes, T4CP genes, and gene cluster for T4SS toward the plasmids were identified based on the exhibition of oriTDB database[8] (Li et al., 2018).

Multilocus Sequence Typing of *E. coli* Strains Bearing *bla*$_{NDM}$-Positive Plasmids

The *bla*$_{NDM}$-positive plasmid-matched host *E. coli* strains were collected, and their DNA fasta sequences were downloaded in bulk using the Bio:DB:GenBank and Bio:SeqIO modules. The MLST software (Larsen et al., 2012) version 2.0.4 was downloaded from the website[9] and installed on the Linux platform. The genomes of *E. coli* strains were analyzed in bulk using MLST software. The "*Escherichia_coli#1*" dataset containing the seven housekeeping genes (*adk*, *fumC*, *gyrB*, *icd*, *mdh*, *purA*, and *recA*) (Wirth et al., 2006) was selected.

RESULTS

General Characteristics of *bla*$_{NDM}$-Positive Plasmids of *E. coli*

Using ResFinder, 1001 (26.4%) plasmids bearing β-lactamase genes were identified from the 3786 plasmids, which were included in the 1346 complete whole genomes of *E. coli*. Among the 1001 plasmids containing β-lactamase genes, 114 (11.6%) were further identified as *bla*$_{NDM}$-positive plasmids, which were distributed in 113 strains of *E. coli*.

We analyzed and compared the genome sizes of the *bla*$_{NDM}$-positive plasmids, plasmids containing β-lactamase genes, and all 3786 plasmids of *E. coli*. Among the 113 fully sequenced *E. coli* strains, the genome sizes of 114 *bla*$_{NDM}$-positive plasmids varied from 10.49 to 248.8 kb, with the 25% percentile, median, and 75% percentile were 46.16, 75.6, and 128.8 kb, respectively (**Figure 1A**). For the β-lactamase gene-positive plasmids and all 3786 plasmids of *E. coli*, their genome sizes varied greatly. Genome sizes of the former ranged from 4.49 to 369.3 kb and those of the latter ranged from 0.3 to 404.2 kb (**Figure 1A**).

We calculated the GC contents of the *bla*$_{NDM}$-positive plasmids, plasmids containing β-lactamase genes, and all 3786 plasmids of *E. coli*. The GC content of the 114 *bla*$_{NDM}$-positive plasmids ranged from 46.5 to 56.4%, with a median GC content of 50.8% (25% percentile = 46.7%; 75% percentile = 52.2%) (**Figure 1B**). For the plasmids containing β-lactamase genes and all 3786 plasmids of *E. coli*, the range of GC contents varied greatly. The GC content of the former ranged from 9.6 to 59.3%, and those of the latter ranged from 9.6 to 63.5% (**Figure 1B**).

Variants of *bla*$_{NDM}$ Genes in the *bla*$_{NDM}$-Positive Plasmids of *E. coli*

Among the 114 *bla*$_{NDM}$-positive plasmids, 124 *bla*$_{NDM}$ genes belonging to eight kinds of variants of *bla*$_{NDM}$, including *bla*$_{NDM-1}$, *bla*$_{NDM-4}$, *bla*$_{NDM-5}$, *bla*$_{NDM-6}$, *bla*$_{NDM-7}$, *bla*$_{NDM-9}$, *bla*$_{NDM-15}$, and *bla*$_{NDM-21}$, were identified. Among the eight variants of *bla*$_{NDM}$, *bla*$_{NDM-5}$ was found to be the most dominant variant (74 *bla*$_{NDM-5}$ genes in 73 plasmids), followed by *bla*$_{NDM-1}$ (31 *bla*$_{NDM-1}$ genes in 28 plasmids), and *bla*$_{NDM-7}$ (7 *bla*$_{NDM-7}$ genes in seven plasmids) (**Figure 1C**).

Replicon Types of Plasmids Carrying *bla*$_{NDM}$ of *E. coli*

Replicon typing of the 114 *bla*$_{NDM}$-positive plasmids was performed using PlasmidFinder. Among the 114 plasmids, 112 successfully identified their replicon types, including 83 single-replicon plasmids and 29 multi-replicon plasmids (13 plasmids with two replicons, 3 plasmids with three replicons, and 13 plasmids with four replicons) (**Figure 1D**). For the 83 single-replicon plasmids, plasmids with an IncX3 replicon were found to be the most dominant single-replicon plasmids (47 plasmids), followed by plasmids with an IncFII replicon (13 plasmids) and those with an IncC replicon (12 plasmids) (**Figure 1E**). Interestingly, the multi-replicon plasmids were mainly classified into IncF plasmids (**Figure 1E**). In summary, all 114 *bla*$_{NDM}$-positive plasmids were mainly classified into IncX3, IncF, and IncC plasmids (**Supplementary Figure 2**).

Genetic Diversity of the *bla*$_{NDM}$-Positive Plasmids of *E. coli*

To obtain a comprehensive overview of *bla*$_{NDM}$-positive plasmids, we constructed phylogenetic trees of all 114 *bla*$_{NDM}$-positive plasmids (**Figure 2**). Based on the phylogenetic patterns of plasmids, combined with the plasmid types and conjugative transfer modules, 109 of the 114 *bla*$_{NDM}$-positive plasmids were classified into eight main clades (Clade I—Clade VIII), representing eight representative plasmid patterns carrying *bla*$_{NDM}$ genes in *E. coli*. We also investigated the

[5]http://www.stevekellylab.com/software/orthofinder
[6]https://itol.embl.de/
[7]https://bioinfo-mml.sjtu.edu.cn/oriTfinder/
[8]https://bioinfo-mml.sjtu.edu.cn/oriTDB/index.php
[9]https://cge.cbs.dtu.dk/services/MLST/

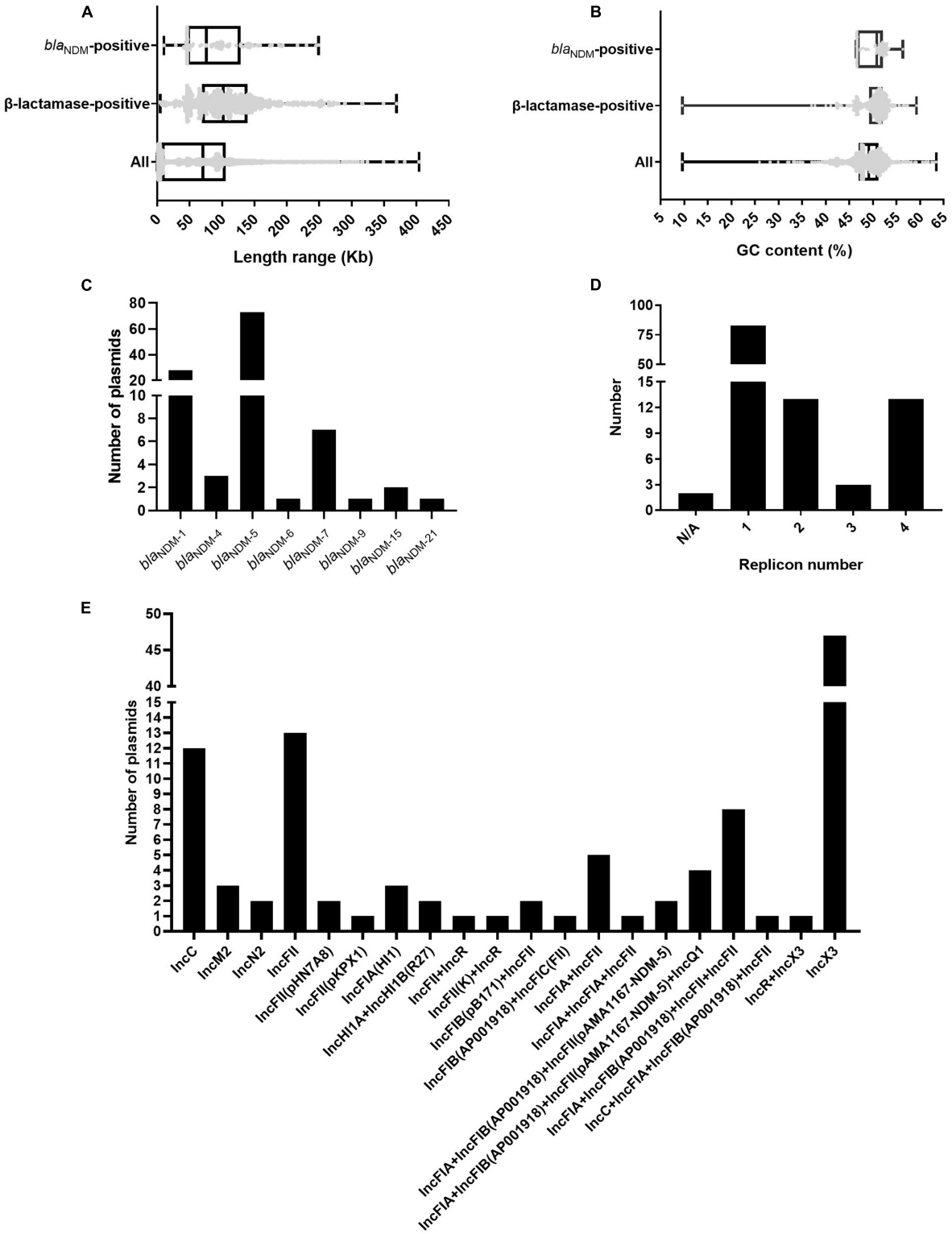

FIGURE 1 | Characteristics of the 114 *bla*$_{NDM}$-positive plasmids from 113 completely sequenced *E. coli* genomes. **(A)** Box plot of the length distribution of the 114 *bla*$_{NDM}$-positive plasmids, the 1001 plasmids carrying β-lactamase genes, and all 3786 plasmids of *E. coli*. **(B)** Box plot of the GC content distribution of the 114 *bla*$_{NDM}$-positive plasmids, the 1001 plasmids carrying β-lactamase genes, and all 3786 plasmids of *E. coli*. **(C)** Histogram of number of variants of *bla*$_{NDM}$ genes among the 114 *bla*$_{NDM}$-positive plasmids. **(D)** Histogram of number of replicons per plasmid for the 114 *bla*$_{NDM}$-positive plasmids. **(E)** Histogram of number of combination modes of different replicons among the 114 *bla*$_{NDM}$-positive plasmids.

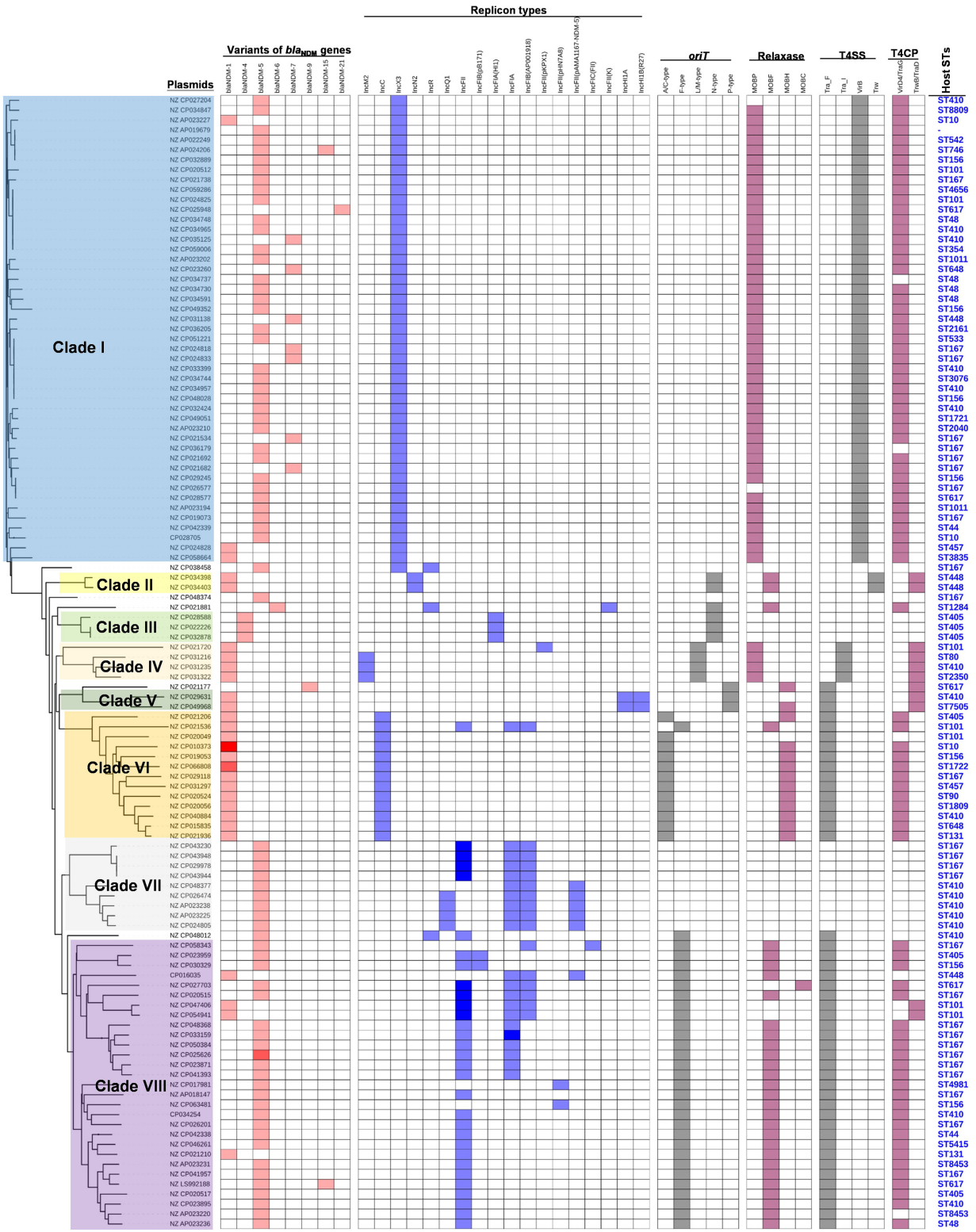

FIGURE 2 | Details of variants of *bla*$_{NDM}$ genes, replicon types of plasmids, and the conjugative transfer modules of the 114 *bla*$_{NDM}$-positive plasmids in *E. coli*. The five categories of information present in this figure include the phylogenetic tree of 114 *bla*$_{NDM}$-positive plasmids, variants of *bla*$_{NDM}$ genes, replicon types, conjugative transfer modules, and STs of host strains. The gradient of color of each heatmap (variants of *bla*$_{NDM}$ genes, replicon types, phylogenetic patterns, conjugative transfer modules including *oriT*, relaxase, T4CP, and T4SS) represents the variable numbers of genes or gene clusters.

geographical distribution of the eight clades from *bla*$_{NDM}$-positive *E. coli* plasmids.

Clade I: A total of 47 plasmids were identified in the Clade I cluster, accounting for approximately 41.2% of all 114 *bla*$_{NDM}$-positive plasmids, which is the clade with the largest number among all the eights clades (**Figure 2**). Most (76.6%) of the plasmids classified into Clade I carried *bla*$_{NDM-5}$ gene. All plasmids below Clade I were single-replicon plasmids with an IncX3 replicon, and most were 46-kb plasmids. For the conjugative transfer modules, almost all the plasmids belonging to Clade I carried relaxases of the MOB$_P$ family and T4CPs of the VirD4/TraG subfamily. All 47 Clade I plasmids carrying *bla*$_{NDM}$ were found to contain VirB-type T4SS gene clusters (**Figure 3A**). The current version of oriTfinder could not identify the *oriT* sites of the Clade I plasmids, while 354-bp intergenic sequences flanking the relaxase genes were *oriT*–like regions, with the inverted repeat (IR) sequence (TAACTA.TAGTTA) (**Figures 2**, **3A**). The STs of *E. coli* host strains containing all Clade I plasmids were distributed in ST167, ST410, ST48, etc. For the clade with the largest number, Clade I, its plasmids were mainly distributed in East Asia (especially in China) and the United States (**Figure 4**). Most of the Clade I plasmids were the human origin, some were animal origin (mainly in China) and environment origin (both in Japan and China) (**Supplementary Table 3**).

Clade II: Two *bla*$_{NDM-1}$-positive IncN2 plasmids of *E. coli* ST448 were clustered into Clade II (**Figure 2**). They both carried the N-type *oriT*s, relaxases of MOB$_F$ family, T4CPs of TrwB/TraD subfamily, and Trw type of T4SS gene clusters (**Figure 2** and **Supplementary Figure 3**). Clade II, containing two *bla*$_{NDM-1}$-positive IncN2 plasmids, was found to be distributed only in Thailand (human origin) (**Figure 4** and **Supplementary Table 3**).

Clade III: Three *bla*$_{NDM-4}$-positive IncF plasmids with IncFIA(HI1) replicon of *E. coli* ST405 were clustered into Clade III (**Figure 2**). They were all found to carry only one conjugative transfer module: N-type *oriT*s, but no relaxases, T4CPs, or T4SS gene clusters were found, indicating that they should be mobilizable plasmids (**Supplementary Figure 4**). All three members of Clade III, inferred as mobilizable plasmids, were only found to be geographically distributed in China (all human origin) (**Figure 4** and **Supplementary Table 3**).

Clade IV: Four *bla*$_{NDM-1}$-positive single-replicon plasmids were classified into Clade IV, including three IncM2 plasmids and one IncFII(pKPX1) plasmid (**Figure 2**). For the conjugative transfer modules of the four Clade IV plasmids, they all carry the L/M-type *oriT*s, relaxases of MOB$_P$ family, T4CPs of TrwB/TraD subfamily, and Tra_I type of T4SS gene clusters (**Figure 2** and **Supplementary Figure 5**). *E. coli* host strains containing all four Clade IV plasmids were distributed into four different STs. Members of Clade IV were mainly geographically distributed in the United Kingdom (three plasmids, all human origin) (**Figure 4** and **Supplementary Table 3**).

Clade V: Two *bla*$_{NDM-1}$-positive multi-replicon plasmids, both containing IncHI1A and IncHI1B(R27) replicons, were grouped into the clade V cluster (**Figure 2**). They both carried the P-type *oriT*s, T4CPs of the TrwB/TraD subfamily, and Tra_F type of T4SS gene clusters (**Figure 2** and **Supplementary Figure 6**). One plasmid of *E. coli* ST7505 was found to carry a relaxase of the MOB$_H$ family; the other plasmid of *E. coli* ST410 was not able to identify the relaxase gene in the genome of the plasmid. The two members of Clade V were geographically distributed in Ghana and New Zealand, respectively (both human origin) (**Figure 4** and **Supplementary Table 3**).

Clade VI: All 13 plasmids grouped into the clade VI cluster of the phylogenetic tree were found to carry *bla*$_{NDM-1}$ gene (**Figure 2**). All plasmids belonging to Clade VI were identified as IncC plasmids, including 12 single-replicon plasmids with IncC replicon and one multi-replicon plasmid with four replicons (IncC, IncFIA, IncFIB(AP001918), and IncFII). For the conjugative transfer modules, most of the plasmids belonging to Clade VI carry the A/C-type *oriT*s, relaxases of MOB$_H$ family and T4CPs of VirD4/TraG subfamily. All 13 clade VI plasmids carrying *bla*$_{NDM-1}$ were found to have Tra_F type T4SS gene clusters (**Figures 2**, **5**). No prevalent STs of *E. coli* host strains containing all Clade VI plasmids were found. The members of Clade VI were mainly geographically distributed in the United States and China (human origin) (**Figure 4** and **Supplementary Table 3**).

Clade VII: Nine *bla*$_{NDM-5}$-positive IncF plasmids were classified into clade VII (**Figure 2**). All the plasmids belonging to Clade VII were found to contain both replicon IncFIA and replicon IncFIB(AP001918), including two main kinds of replication combination modes: four plasmids with replicons IncFIA + IncFIB(AP001918) + IncFII + IncFII and four plasmids with replicons IncFIA + IncFIB(AP001918) + IncFII(pAMA1167-NDM-5) + IncQ1. Moreover, no conjugative transfer modules were found in the nine plasmids belonging to Clade VII, indicating that the nine plasmids should be non-transferable plasmids. The STs of *E. coli* host strains containing Clade VII plasmids were distributed into ST167 and ST410. The members of clade VII were mainly geographically distributed in Switzerland (**Figure 4**). In addition, clade VII members were also sporadically discovered in Myanmar, Korea, and Denmark. Clade VII plasmids included the human and animal origin (**Supplementary Table 3**).

Clade VIII: A total of 29 plasmids were identified in the Clade VIII cluster, accounting for approximately 25.4% of all 114 *bla*$_{NDM}$-positive plasmids, which is the clade with the second largest number among all eights clades (**Figure 2**). Most (86.2%) of the plasmids grouped into clade VIII were found to carry *bla*$_{NDM-5}$ gene. All plasmids below Clade VIII were IncF plasmids, with replicon IncFII as the most common replicons. For the conjugative transfer modules, all the plasmids belonging to Clade VIII carry the F-type *oriT*s and Tra_F type of T4SS gene clusters (**Figures 2**, **3B**). Almost all the plasmids of Clade VIII had relaxases of the MOB$_F$ family and T4CPs of the VirD4/TraG subfamily. The STs of *E. coli* host strains containing all Clade VIII plasmids were distributed in ST167, ST101, ST44, ST410 etc. For the clade with the second largest number, Clade VIII, its members were widely distributed all over the world, including East Asia, India, the United States, and some European countries (e.g., Germany, Switzerland, and the Czech Republic) (**Figure 4**). Most of the Clade VIII plasmids

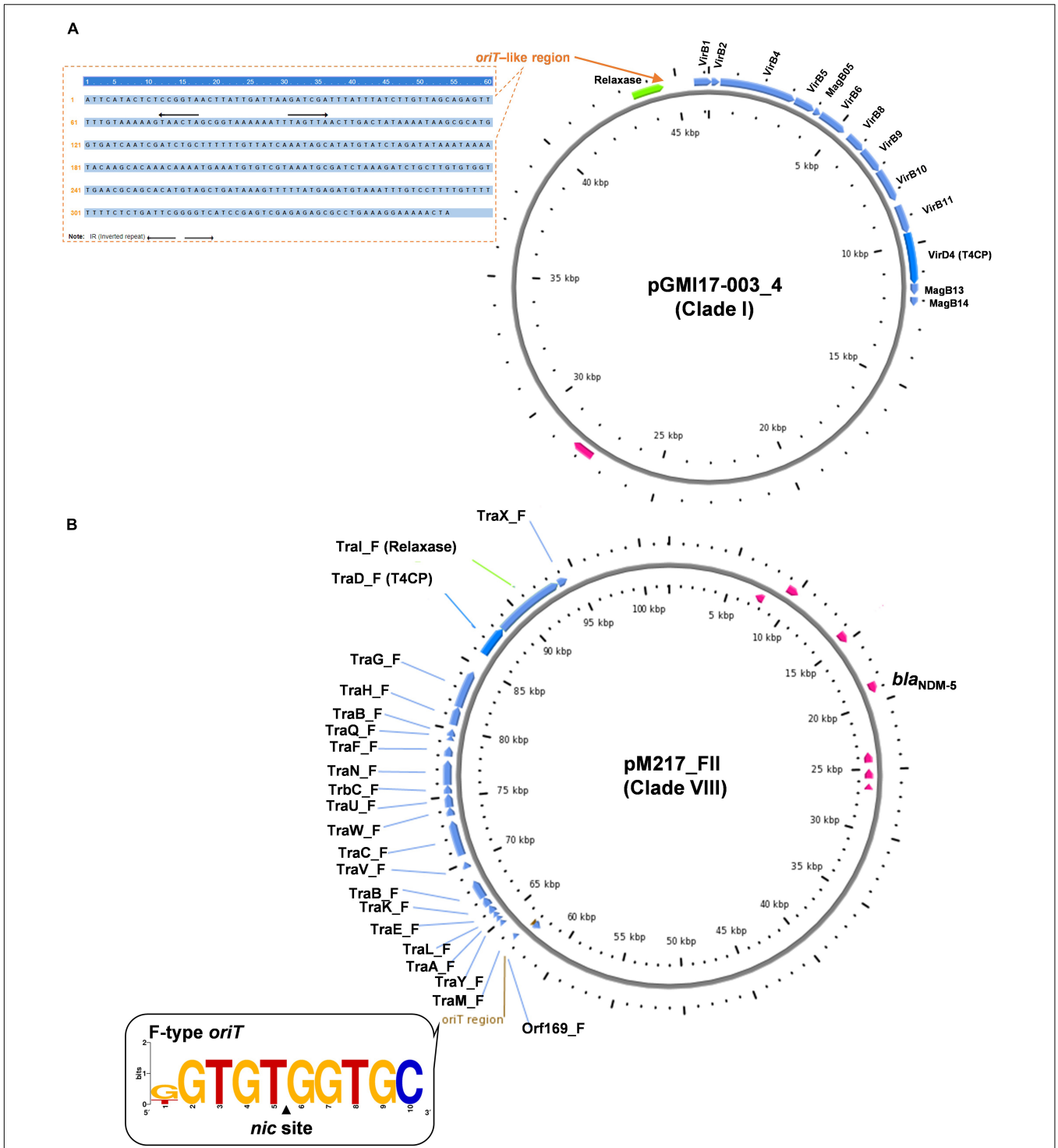

FIGURE 3 | Conjugative transfer modules including *oriT*, relaxase, T4CP, and T4SS of the representative plasmids from Clade I **(A)** and Clade VIII **(B)**, respectively.

were the human origin, few were animal and environment origin (**Supplementary Table 3**).

We also analyzed the 6054 plasmids of *E. coli* downloaded from the NCBI RefSeq database, both with and without host strains. The results indicated that 301 *bla*$_{NDM}$-positive plasmids were identified from the 6054 plasmids of *E. coli* (**Supplementary Figure 7**). We explored the distribution of the above eight representative plasmid patterns carrying *bla*$_{NDM}$ genes of *E. coli* in the 301 *bla*$_{NDM}$-positive plasmids. For the *bla*$_{NDM-5}$ gene, it was mainly carried by the IncX3 plasmids (Clade I pattern) and

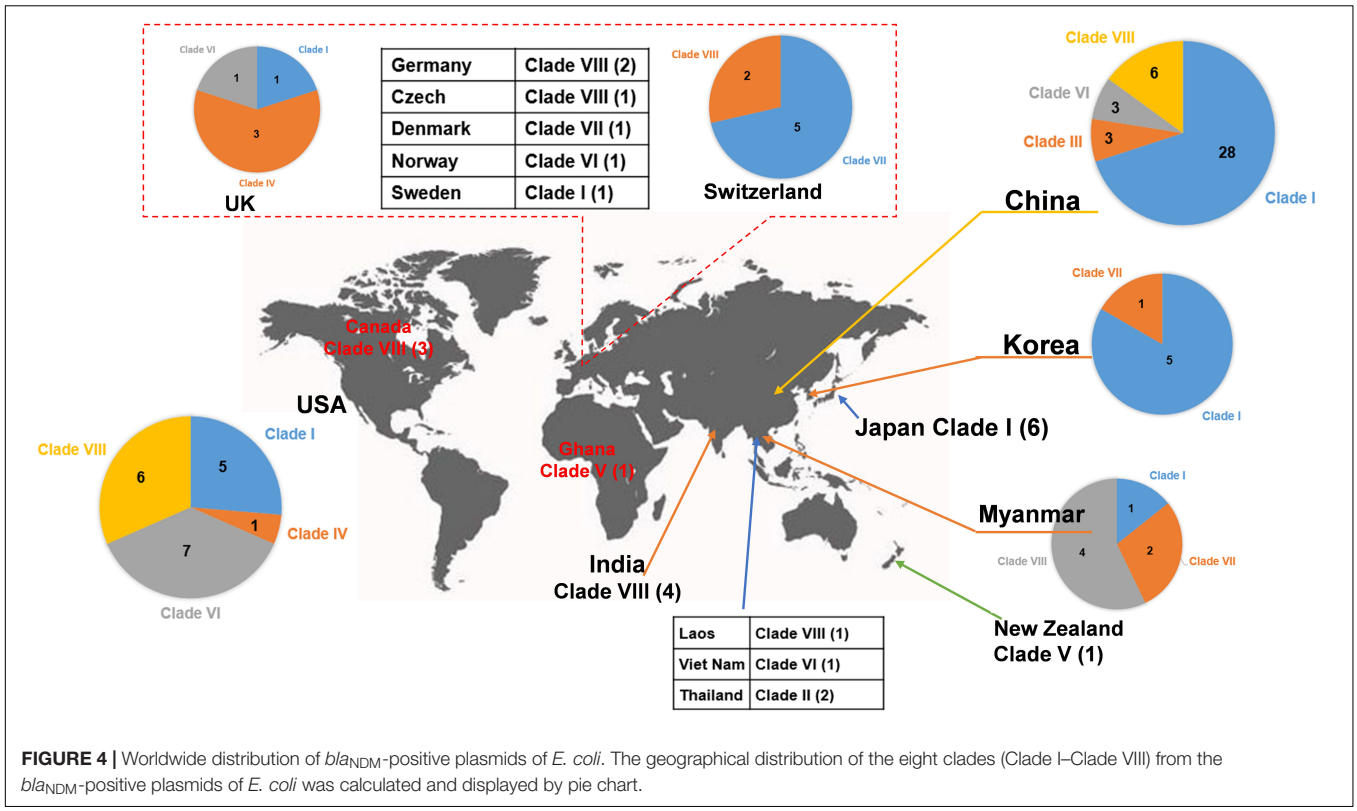

FIGURE 4 | Worldwide distribution of *bla*$_{NDM}$-positive plasmids of *E. coli*. The geographical distribution of the eight clades (Clade I–Clade VIII) from the *bla*$_{NDM}$-positive plasmids of *E. coli* was calculated and displayed by pie chart.

IncF plasmids (Clade VII and Clade VIII patterns), consistent with the results based on the 114 *bla*$_{NDM}$-positive plasmids with hosts. The IncN plasmids (including IncN2 and IncN replicons) were found to mainly carry the *bla*$_{NDM-1}$ gene (Clade II pattern) in the 301 *bla*$_{NDM}$-positive plasmids, consistent with the results from the 114 *bla*$_{NDM}$-positive plasmids with hosts. The *bla*$_{NDM-4}$ gene was carried sporadically by IncF, IncX, and IncR plasmids, not limited to the Clade III pattern from the 114 *bla*$_{NDM}$-positive plasmids with hosts. The IncM2 plasmids were found to carry the *bla*$_{NDM-1}$ gene (Clade IV pattern) in the 301 *bla*$_{NDM}$-positive plasmids, consistent with the results of *bla*$_{NDM}$-positive plasmids with hosts. For the IncHI1 and IncHI2 from the 301 *bla*$_{NDM}$-positive plasmids, they were found to carry not only the *bla*$_{NDM-1}$ (Clade V pattern) but also the *bla*$_{NDM-5}$ gene. The IncC plasmids were found to carry the *bla*$_{NDM-1}$ gene (Clade VI pattern) in the 301 *bla*$_{NDM}$-positive plasmids, consistent with the conclusion from *bla*$_{NDM}$-positive plasmids with hosts.

DISCUSSION

NDM carbapenemases are a rapidly emerging and troublesome family of β-lactamases (Pérez-Vázquez et al., 2019; Sugawara et al., 2019; Han et al., 2020). To explore the relationships among plasmids, *bla*$_{NDM}$ genes, and hosts in *E. coli*, we systematically analyzed the profiles of resistance determinants, replicon typing, and comparative analysis of 3786 plasmids from 1346 complete whole genomes of *E. coli* from the GenBank database. Overall, 114 *bla*$_{NDM}$-positive plasmids from 113 *E. coli* strains were identified.

Variants of *bla*$_{NDM}$ included in the 114 *bla*$_{NDM}$-positive plasmids in our study were classified into eight types. The *bla*$_{NDM-5}$-carrying plasmids were the most common *bla*$_{NDM}$-positive plasmids and accounted for 64.0% of the 114 *bla*$_{NDM}$-positive plasmids, followed by *bla*$_{NDM-1}$-positive plasmids (24.6%) and *bla*$_{NDM-7}$-positive plasmids (6.1%). *bla*$_{NDM-1}$ was first identified on a 180-kb plasmid of *K. pneumoniae* strain 05-506 and on a 140-kb plasmid carried by *E. coli* strain NF-NDM-1, both isolated from a Swedish patient who had been hospitalized in New Delhi, India, in 2008 (Yong et al., 2009). The variant NDM-5 was first detected in a strain of *E. coli* EC405 belonging to ST648, isolated from a 41-year-old patient in the United Kingdom with a history of travel to the Indian subcontinent, and *bla*$_{NDM-5}$ was localized to an IncF plasmid with a length > 100 kb (Hornsey et al., 2011). The variant NDM-7 was first detected in a strain of *E. coli* ST599, isolated from the rectum, throat, and infected wounds of a Yemeni patient admitted to the Frankfurt University Hospital of Germany, and *bla*$_{NDM-7}$ was localized on a self-transferable IncX3 plasmid of 60 kb (Göttig et al., 2013).

Among the 114 *bla*$_{NDM}$-positive plasmids in *E. coli*, 112 were successfully identified by their replicon types, and mainly classified into IncX3, IncF, and IncC plasmids. Our results also indicated that the 112 *bla*$_{NDM}$-positive plasmids contained 83 single-replicon plasmids and 29 multi-replicon plasmids.

IncX3 plasmids have been reported to carry various carbapenemase genes in CRE worldwide (Mouftah et al., 2019).

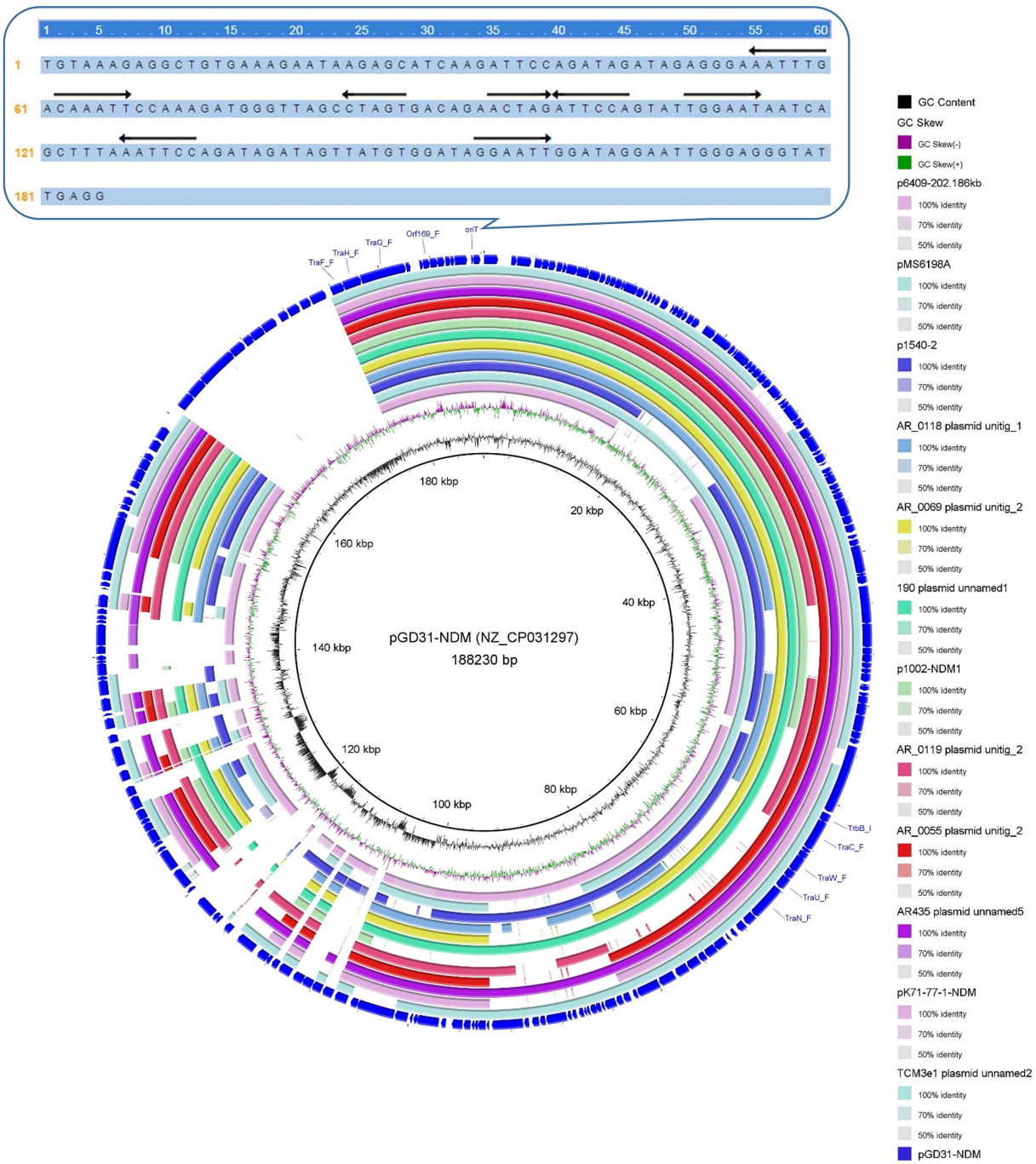

FIGURE 5 | Conjugative transfer modules of 13 *bla*$_{NDM-1}$-positive IncC plasmids grouped into the clade VI and the sequence logos of the flanking conserved regions of the *nic* sites of A/C-type *oriT* regions.

Herein, our work indicated that the IncX3 plasmids were the most prevalent single-replicon plasmids among the 114 *bla*$_{NDM}$-positive plasmids in *E. coli*, which were observed to be the predominant carriers of *bla*$_{NDM-5}$ genes, distributed in Clade I of the phylogenetic profiles constructed by the 114 *bla*$_{NDM}$-positive plasmids of *E. coli*. Common types of *E. coli* strains containing *bla*$_{NDM-5}$-positive IncX3 plasmids were ST167, ST410, and ST48, located in East Asia (especially China) and the United States.

In our study, multi-replicon IncF plasmids, especially the plasmids with IncFII replicon, were another common carrier of *bla*$_{NDM-5}$ genes, which were distributed in Clade VII and Clade VIII of the phylogenetic profiles of the 114 *bla*$_{NDM}$-positive plasmids of *E. coli*, members of the former were

identified as the non-transferable plasmids and those of the latter were identified as the conjugative plasmids. The IncF plasmids, widely distributed in Enterobacteriaceae, are known as conjugative plasmids that contribute to the carriage and spread of AMR genes (Carattoli, 2011), similar to Clade VIII of the phylogenetic profiles of the 114 *bla*$_{NDM}$-positive plasmids of *E. coli* in our own study. However, in our study, we also found nine *bla*$_{NDM-5}$-positive IncF plasmids without any classical conjugative transfer modules, classified into Clade VII of the phylogenetic patterns of the 114 *bla*$_{NDM}$-positive plasmids of *E. coli*, which were identified as non-transferable plasmids. The nine non-transferable IncF plasmids of Clade VII were distributed in the *E. coli* strains of ST167 (four plasmids) and ST410 (five plasmids), mainly located in Switzerland. The *bla*$_{NDM}$-positive IncF plasmids in *E. coli* grouped into Clade VIII, which were the classical conjugative plasmids, mainly distributed in the *E. coli* strains of ST167 and geographically distributed worldwide (East Asia, India, the United States, and some European countries).

IncC plasmids, almost all single-replicon plasmids, were observed to be the predominant carriers of *bla*$_{NDM-1}$ genes in *E. coli*, which were grouped into Clade VI of the phylogenetic profiles constructed by the 114 *bla*$_{NDM}$-positive plasmids of *E. coli* in this study. *E. coli* strains containing *bla*$_{NDM-1}$-positive IncC plasmids belonged to a variety of STs, and no predominant STs were found, which were mainly geographically distributed in the United States and China. Other types of *bla*$_{NDM-1}$-carrying plasmids included IncM2, IncN2, IncHI1, IncX3, and IncF. The large, broad host range IncC plasmids are important contributors to the spread of key antibiotic resistance genes, and over 200 complete sequences of IncC plasmids have been reported (Ambrose et al., 2018).

Bacterial mobile genetic elements, such as conjugative plasmids and transposons, have been highlighted as important vehicles for the dissemination of AMR, which play a central role in facilitating horizontal genetic exchange and therefore promoting the acquisition and spread of resistance genes (Partridge et al., 2018; Jiang et al., 2020). Currently, the genetic context of *bla*$_{NDM}$ is mainly focused on the insertion sequences and transposons, for example, IS*Aba125*, IS*26*, and the composite transposon Tn*125* (Yong et al., 2009; Göttig et al., 2013; Partridge et al., 2018; Wu and Feng, 2019). In fact, conjugation is a dominant mechanism of HGT, and bacterial genome comparisons highlight conjugative and mobilizable elements as vehicles for dissemination of pathogenesis and AMR determinants (Ramsay and Firth, 2017). Reports on the distribution of various conjugative and mobilizable *bla*$_{NDM}$-positive carbapenem-resistant plasmids in *E. coli* and their conjugative transfer modules are currently scarce. Herein, we performed a comprehensive analysis and comparison of the conjugative transfer modules located on the 114 *bla*$_{NDM}$-positive plasmids using the software oriTfinder (Li et al., 2018), the database oriTDB (Li et al., 2018) and the database SecReT4 (Bi et al., 2013). The oriTDB database recorded nine types of plasmid-borne *oriT*[10] (Li et al., 2018). In our study, five types of *oriT* regions were identified, including A/C-type *oriT*s in conjugative IncC plasmids carrying *bla*$_{NDM-1}$ genes, F-type *oriT*s in conjugative IncF plasmids bearing *bla*$_{NDM-5}$ genes, L/M-type *oriT*s in mostly *bla*$_{NDM-1}$-positive conjugative IncM2 plasmids, N-type *oriT*s in both *bla*$_{NDM-1}$-positive conjugative IncN2 plasmids and *bla*$_{NDM-4}$-positive mobilizable plasmids with IncFIA(HI1) replicon, as well as P-type *oriT*s in *bla*$_{NDM-1}$-positive conjugative IncHI1 plasmids. The oriTDB database recorded eight main relaxase families[11] (Li et al., 2018), and four relaxase families were found in our study. Relaxases belonging to the MOB$_P$ family were found in conjugative IncX3 plasmids and most of the conjugative IncM2 plasmids; Relaxases of MOB$_F$ family were found in conjugative IncF plasmids and IncN2 conjugative plasmids; MOB$_F$ relaxases were mostly found in conjugative IncC plasmids; the only one relaxase belonging to MOB$_C$ was found in one conjugative IncF plasmid. The oriTDB database recorded two main subfamilies of T4CPs[12] (Li et al., 2018). In our study, most T4CPs of conjugative IncX3, IncC, and IncF plasmids belong to the VirD4/TraG subfamily, while the T4CPs of conjugative IncN2, IncM2, and IncHI1 plasmids belong to the TrwB/TraD subfamily. The database SecReT4 collected the five main types of T4SS gene clusters, including 18 kinds of systems[13] (Bi et al., 2013). Our study demonstrated that four kinds of T4SS gene clusters were found in the *bla*$_{NDM}$-positive plasmids of *E. coli*, including the Tra_F-type of T4SS distributed in the conjugative IncF, IncC, and IncHI1 plasmids, VirB-type T4SS distributed in the conjugative IncX3 plasmids, Tra_I-type of T4SS mostly in conjugative IncM2 plasmids, Trw-type of T4SS in conjugative IncN2 plasmids.

CONCLUSION

In this study, we analyzed the variants of *bla*$_{NDM}$, replicon types, phylogenetic patterns, conjugative transfer modules, host STs, and geographical distributions of the 114 *bla*$_{NDM}$-positive plasmids, from 3786 plasmids within 1346 complete whole genomes of *E. coli* from the GenBank database. Eight variants of *bla*$_{NDM}$ were found among the 114 *bla*$_{NDM}$-positive plasmids, with *bla*$_{NDM-5}$ and *bla*$_{NDM-1}$ as the most dominant. The variant *bla*$_{NDM-5}$ was mainly carried by the IncX3 plasmids and IncF plasmids in *E. coli*, the former were mainly geographically distributed in East Asia (especially in China) and the United States, and the latter were widely distributed all over the world, including East Asia, Southeast Asia, India, the United States, and some European countries. IncC plasmids were observed to be the predominant carriers of *bla*$_{NDM-1}$ genes in *E. coli*, which were mainly geographically distributed in the United States and China. Other *bla*$_{NDM-1}$-carrying plasmids also included IncM2 (mainly geographically distributed in the United Kingdom), IncN2 (distributed in Thailand), and IncHI1 (in Ghana and New Zealand). In addition,

[10]https://bioinfo-mml.sjtu.edu.cn/oriTDB/browse_oriT_type_p.php

[11]https://bioinfo-mml.sjtu.edu.cn/oriTDB/browse_relaxase.php

[12]https://bioinfo-mml.sjtu.edu.cn/oriTDB/browse_t4cp.php

[13]https://db-mml.sjtu.edu.cn/SecReT4/browse_type.php

the overall picture of the conjugative and mobilizable bla_{NDM}-positive plasmids in *E. coli* was described in our study. The eight representative plasmid patterns carrying bla_{NDM} genes of *E. coli* was also validated with a larger data set (6054 plasmids of *E. coli* downloaded from the NCBI RefSeq database). This study provides important insights into the phylogeny and evolution of bla_{NDM}-positive *E. coli* plasmids and further addresses their role in the acquisition and spread of resistance genes. However, the genetic diversity and characteristics of bla_{NDM} -positive plasmids in other Enterobacteriaceae species need further study in the future.

DATA AVAILABILITY STATEMENT

The original contributions presented in the study are included in the article/**Supplementary Material**, further inquiries can be directed to the corresponding author/s.

AUTHOR CONTRIBUTIONS

ZLZ and ZLZ conceived the project. ZRZ and XBL analyzed all the data and wrote the manuscript. WL, GY, and WN performed data acquisition. MZ and LL provided some suggestions for manuscript writing. HG and XDL reviewed and edited the manuscript. All authors read and approved the final manuscript.

FUNDING

This work was supported financially by the grants from the State Key Development Program for Basic Research of China (Grant No. 2017YFA0205200), the National Natural Science Foundation of China (Grant Nos. 81901857 and 82002170), the Xiangshan Talent Project of Zhuhai People's Hospital (Grant No. 2020XSYC-02), and the Natural Science Foundation of Guangdong Province of China (Grant No. 2021A1515010697).

SUPPLEMENTARY MATERIAL

The Supplementary Material for this article can be found online at: https://www.frontiersin.org/articles/10.3389/fmicb.2021.729952/full#supplementary-material

REFERENCES

Albiger, B., Glasner, C., Struelens, M. J., Grundmann, H., and Monnet, D. L. (2015). Carbapenemase-producing *Enterobacteriaceae* in Europe: assessment by national experts from 38 countries, May 2015. *Euro. Surveill.* 20:pii=30062. doi: 10.2807/1560-7917.es.2015.20.45.30062

Ambrose, S. J., Harmer, C. J., and Hall, R. M. (2018). Evolution and typing of IncC plasmids contributing to antibiotic resistance in Gram-negative bacteria. *Plasmid* 99, 40–55. doi: 10.1016/j.plasmid.2018.08.001

Benson, D. A., Cavanaugh, M., Clark, K., Karsch-Mizrachi, I., Ostell, J., Pruitt, K. D., et al. (2018). GenBank. *Nucleic Acids Res.* 46, D41–D47. doi: 10.1093/nar/gkx1094

Bi, D., Liu, L., Tai, C., Deng, Z., Rajakumar, K., and Ou, H. Y. (2013). SecReT4: a web-based bacterial type IV secretion system resource. *Nucleic Acids Res.* 41, D660–D665. doi: 10.1093/nar/gks1248

Bortolaia, V., Kaas, R. S., Ruppe, E., Roberts, M. C., Schwarz, S., Cattoir, V., et al. (2020). ResFinder 4.0 for predictions of phenotypes from genotypes. *J. Antimicrob. Chemother.* 75, 3491–3500. doi: 10.1093/jac/dkaa345

Carattoli, A. (2011). Plasmids in Gram negatives: molecular typing of resistance plasmids. *Int. J. Med. Microbiol.* 301, 654–658. doi: 10.1016/j.ijmm.2011.09.003

Carattoli, A., and Hasman, H. (2020). PlasmidFinder and in silico pMLST: identification and typing of plasmid replicons in whole-genome sequencing (WGS). *Methods Mol. Biol.* 2075, 285–294. doi: 10.1007/978-1-4939-9877-7_20

de la Cruz, F., Frost, L. S., Meyer, R. J., and Zechner, E. L. (2010). Conjugative DNA metabolism in Gram-negative bacteria. *FEMS Microbiol. Rev.* 34, 18–40. doi: 10.1111/j.1574-6976.2009.00195.x

Emms, D. M., and Kelly, S. (2019). OrthoFinder: phylogenetic orthology inference for comparative genomics. *Genome Biol.* 20:238. doi: 10.1186/s13059-019-1832-y

Farhat, N., and Khan, A. U. (2020). Evolving trends of New Delhi Metallo-betalactamse (NDM) variants: a threat to antimicrobial resistance. *Infect. Genet. Evol.* 86:104588. doi: 10.1016/j.meegid.2020.104588

Göttig, S., Hamprecht, A. G., Christ, S., Kempf, V. A., and Wichelhaus, T. A. (2013). Detection of NDM-7 in Germany, a new variant of the New Delhi metallo-β-lactamase with increased carbapenemase activity. *J. Antimicrob. Chemother.* 68, 1737–1740. doi: 10.1093/jac/dkt088

Guducuoglu, H., Gursoy, N. C., Yakupogullari, Y., Parlak, M., Karasin, G., Sunnetcioglu, M., et al. (2018). Hospital outbreak of a colistin-resistant, NDM-1- and OXA-48-producing *Klebsiella pneumoniae*: high mortality from pandrug resistance. *Microb. Drug Resist.* 24, 966–972. doi: 10.1089/mdr.2017.0173

Han, R., Shi, Q., Wu, S., Yin, D., Peng, M., Dong, D., et al. (2020). Dissemination of carbapenemases (KPC, NDM, OXA-48, IMP, and VIM) among carbapenem-resistant *Enterobacteriaceae* isolated from adult and children patients in China. *Front. Cell. Infect. Microbiol.* 10:314. doi: 10.3389/fcimb.2020.00314

Hornsey, M., Phee, L., and Wareham, D. W. (2011). A novel variant, NDM-5, of the New Delhi metallo-β-lactamase in a multidrug-resistant *Escherichia coli* ST648 isolate recovered from a patient in the United Kingdom. *Antimicrob. Agents Chemother.* 55, 5952–5954. doi: 10.1128/aac.05108-11

Jiang, Y., Wang, Y., Hua, X., Qu, Y., Peleg, A. Y., and Yu, Y. (2020). Pooled plasmid sequencing reveals the relationship between mobile genetic elements and antimicrobial resistance genes in clinically isolated *Klebsiella pneumoniae*. *Genomics Proteomics Bioinformatics* 18, 539–548. doi: 10.1016/j.gpb.2020.12.002

Karlowsky, J. A., Lob, S. H., Kazmierczak, K. M., Badal, R. E., Young, K., Motyl, M. R., et al. (2017). In vitro activity of imipenem against carbapenemase-positive *Enterobacteriaceae* isolates collected by the SMART Global Surveillance Program from 2008 to 2014. *J. Clin. Microbiol.* 55, 1638–1649. doi: 10.1128/jcm.02316-16

Larsen, M. V., Cosentino, S., Rasmussen, S., Friis, C., Hasman, H., Marvig, R. L., et al. (2012). Multilocus sequence typing of total-genome-sequenced bacteria. *J. Clin. Microbiol.* 50, 1355–1361. doi: 10.1128/jcm.06094-11

Letunic, I., and Bork, P. (2016). Interactive tree of life (iTOL) v3: an online tool for the display and annotation of phylogenetic and other trees. *Nucleic Acids Res.* 44, W242–W245. doi: 10.1093/nar/gkw290

Li, X., Xie, Y., Liu, M., Tai, C., Sun, J., Deng, Z., et al. (2018). oriTfinder: a web-based tool for the identification of origin of transfers in DNA sequences of bacterial mobile genetic elements. *Nucleic Acids Res.* 46, W229–W234. doi: 10.1093/nar/gky352

Mouftah, S. F., Pál, T., Darwish, D., Ghazawi, A., Villa, L., Carattoli, A., et al. (2019). Epidemic IncX3 plasmids spreading carbapenemase genes in the United Arab Emirates and worldwide. *Infect. Drug Resist.* 12, 1729–1742. doi: 10.2147/idr.s210554

Nordmann, P., Poirel, L., Walsh, T. R., and Livermore, D. M. (2011). The emerging NDM carbapenemases. *Trends Microbiol.* 19, 588–595. doi: 10.1016/j.tim.2011.09.005

O'Leary, N. A., Wright, M. W., Brister, J. R., Ciufo, S., Haddad, D., McVeigh, R., et al. (2016). Reference sequence (RefSeq) database at NCBI: current status, taxonomic expansion, and functional annotation. *Nucleic Acids Res.* 44, D733–D745. doi: 10.1093/nar/gkv1189

Partridge, S. R., Kwong, S. M., Firth, N., and Jensen, S. O. (2018). Mobile genetic elements associated with antimicrobial resistance. *Clin. Microbiol. Rev.* 31, e00088–17. doi: 10.1128/cmr.00088-17

Pérez-Vázquez, M., Sola Campoy, P. J., Ortega, A., Bautista, V., Monzón, S., Ruiz-Carrascoso, G., et al. (2019). Emergence of NDM-producing *Klebsiella pneumoniae* and *Escherichia coli* in Spain: phylogeny, resistome, virulence and plasmids encoding bla_{NDM}-like genes as determined by WGS. *J. Antimicrob. Chemother.* 74, 3489–3496. doi: 10.1093/jac/dkz366

Ramsay, J. P., and Firth, N. (2017). Diverse mobilization strategies facilitate transfer of non-conjugative mobile genetic elements. *Curr. Opin. Microbiol.* 38, 1–9.

Ravi, A., Valdés-Varela, L., Gueimonde, M., and Rudi, K. (2018). Transmission and persistence of IncF conjugative plasmids in the gut microbiota of full-term infants. *FEMS Microbiol. Ecol.* 94:fix158. doi: 10.1093/femsec/fix158

Rozwandowicz, M., Brouwer, M. S. M., Fischer, J., Wagenaar, J. A., Gonzalez-Zorn, B., Guerra, B., et al. (2018). Plasmids carrying antimicrobial resistance genes in *Enterobacteriaceae*. *J. Antimicrob. Chemother.* 73, 1121–1137. doi: 10.1093/jac/dkx488

Smillie, C., Garcillán-Barcia, M. P., Francia, M. V., Rocha, E. P., and de la Cruz, F. (2010). Mobility of plasmids. *Microbiol. Mol. Biol. Rev.* 74, 434–452. doi: 10.1128/mmbr.00020-10

Sugawara, Y., Akeda, Y., Hagiya, H., Sakamoto, N., Takeuchi, D., Shanmugakani, R. K., et al. (2019). Spreading patterns of NDM-producing *Enterobacteriaceae* in clinical and environmental settings in Yangon, Myanmar. *Antimicrob. Agents Chemother.* 63, e01924–18. doi: 10.1128/aac.01924-18

Wirth, T., Falush, D., Lan, R., Colles, F., Mensa, P., Wieler, L. H., et al. (2006). Sex and virulence in *Escherichia coli*: an evolutionary perspective. *Mol. Microbiol.* 60, 1136–1151. doi: 10.1111/j.1365-2958.2006.05172.x

Wu, W., and Feng, Y. (2019). NDM metallo-β-lactamases and their bacterial producers in health care settings. *Clin. Microbiol. Rev.* 32, e00115–18. doi: 10.1128/cmr.00115-18

Yong, D., Toleman, M. A., Giske, C. G., Cho, H. S., Sundman, K., Lee, K., et al. (2009). Characterization of a new metallo-beta-lactamase gene, bla_{NDM-1}, and a novel erythromycin esterase gene carried on a unique genetic structure in *Klebsiella pneumoniae* sequence type 14 from India. *Antimicrob. Agents Chemother.* 53, 5046–5054. doi: 10.1128/aac.00774-09

Conflict of Interest: The authors declare that the research was conducted in the absence of any commercial or financial relationships that could be construed as a potential conflict of interest.

Publisher's Note: All claims expressed in this article are solely those of the authors and do not necessarily represent those of their affiliated organizations, or those of the publisher, the editors and the reviewers. Any product that may be evaluated in this article, or claim that may be made by its manufacturer, is not guaranteed or endorsed by the publisher.

frontiers in Microbiology

ORIGINAL RESEARCH
published: 22 November 2021
doi: 10.3389/fmicb.2021.736982

Genomic Characterization of Extensively Drug-Resistant NDM-Producing *Acinetobacter baumannii* Clinical Isolates With the Emergence of Novel $bla_{ADC-257}$

Mai M. Zafer[1†], Amira F. A. Hussein[2], Mohamed H. Al-Agamy[3,4], Hesham H. Radwan[3] and Samira M. Hamed[5†]*

[1]Department of Microbiology and Immunology, Faculty of Pharmacy, Ahram Canadian University, Cairo, Egypt, [2]Clinical and Chemical Pathology Department, Faculty of Medicine, Cairo University, Cairo, Egypt, [3]Department of Pharmaceutics, College of Pharmacy, King Saud University, Riyadh, Saudi Arabia, [4]Department of Microbiology and Immunology, Faculty of Pharmacy, Al-Azhar University, Cairo, Egypt, [5]Department of Microbiology and Immunology, Faculty of Pharmacy, October University for Modern Sciences and Arts (MSA), Giza, Egypt

OPEN ACCESS

Edited by:
Ziad Daoud,
Central Michigan University,
United States

Reviewed by:
Dana Marshall,
Meharry Medical College,
United States
Gamal Wareth,
Friedrich-Loeffler-Institute, Germany

***Correspondence:**
Samira M. Hamed
satwa@msa.edu.eg

[†]These authors have contributed equally to this work

Specialty section:
This article was submitted to Antimicrobials, Resistance and Chemotherapy, a section of the journal Frontiers in Microbiology

Received: 06 July 2021
Accepted: 28 October 2021
Published: 22 November 2021

Citation:
Zafer MM, Hussein AFA, Al-Agamy MH, Radwan HH and Hamed SM (2021) Genomic Characterization of Extensively Drug-Resistant NDM-Producing Acinetobacter baumannii Clinical Isolates With the Emergence of Novel $bla_{ADC-257}$. Front. Microbiol. 12:736982. doi: 10.3389/fmicb.2021.736982

Acinetobacter baumannii has become a major challenge to clinicians worldwide due to its high epidemic potential and acquisition of antimicrobial resistance. This work aimed at investigating antimicrobial resistance determinants and their context in four extensively drug-resistant (XDR) NDM-producing *A. baumannii* clinical isolates collected between July and October 2020 from Kasr Al-Ainy Hospital, Cairo, Egypt. A total of 20 *A. baumannii* were collected and screened for acquired carbapenemases (bla_{NDM}, bla_{VIM} and bla_{IMP}) using PCR. Four NDM producer *A. baumannii* isolates were identified and selected for whole-genome sequencing, *in silico* multilocus sequence typing, and resistome analysis. Antimicrobial susceptibility profiles were determined using disk diffusion and broth microdilution tests. All bla_{NDM}-positive *A. baumannii* isolates were XDR. Three isolates belonged to high-risk international clones (IC), namely, IC2 corresponding to $ST570^{Pas}/1701^{Oxf}$ (M20) and IC9 corresponding to $ST85^{Pas}/ST1089^{Oxf}$ (M02 and M11). For the first time, we report bla_{NDM-1} gene on the chromosome of an *A. baumannii* strain that belongs to sequence type $ST164^{Pas}/ST1418^{Oxf}$. Together with *AphA6*, bla_{NDM-1} was bracketed by two copies of IS*Aba14* in $ST85^{Pas}$ isolates possibly facilitating co-transfer of amikacin and carbapenem resistance. A novel bla_{ADC} allele ($bla_{ADC-257}$) with an upstream IS*Aba1* element was identified in M19 (ST/CC164[Pas] and $ST1418^{Oxf}$/CC234[Oxf]). bla_{ADC} genes harbored by M02 and M11 were uniquely interrupted by IS1008. Tn*2006*-associated bla_{OXA-23} was carried by M20. bla_{OXA-94} genes were preceded by IS*Aba1* element in M02 and M11. AbGRI3 was carried by M20 hosting the resistance genes *aph*(*3`*)-*Ia*, *aac*(*6`*)-*Ib`*, *catB8*, ant(3``)-*Ia*, *sul1*, *armA*, *msr*(*E*), and *mph*(*E*). Nonsynonymous mutations were identified in the quinolone resistance determining regions (*gyrA* and *parC*) of all isolates. Resistance to colistin in M19 was accompanied by missense mutations in *lpxACD* and *pmrABC* genes. The current study provided an insight into the genomic background of XDR

phenotype in *A. baumannii* recovered from patients in Egypt. WGS revealed strong association between resistance genes and diverse mobile genetic elements with novel insertion sites and genetic organizations.

Keywords: healthcare-associated infections, *Acinetobacter baumannii*, extensive drug resistance, bla_{NDM}, whole-genome sequencing, multilocus sequence typing

INTRODUCTION

Hospital-associated infections (HAIs) present an elevated healthcare burden in both developed and developing countries (Chng et al., 2020). *Acinetobacter baumannii* is implicated in a considerable fraction of difficult to treat HAIs (Ayobami et al., 2019). Antimicrobial resistance, biofilm formation, and resistance to desiccation are among the competencies contributing to the environmental persistence and the epidemic potential of this species (Antunes et al., 2014). In addition to its intrinsic resistance to multiple antimicrobial classes, effective therapeutic options are being gradually depleted by the extraordinary ability of *A. baumannii* to acquire and upregulate resistance genes (Di Nocera et al., 2011). The emergence of multidrug-resistant (MDR) and extensively drug-resistant (XDR) *A. baumannii* has been increasing worldwide as well as in Egypt (Tal-Jasper et al., 2016; Elsayed et al., 2020). This forced the WHO to declare carbapenem-resistant *A. baumannii* as a category 1 (critical) priority pathogen for which novel therapeutic antimicrobials are urgently required (Tacconelli et al., 2018).

The New Delhi Metallo-β-lactamase-1 (NDM-1) is a carbapenemase that has been frequently linked to the XDR phenotype owing to its association with mobile elements loaded with other resistance genes (Wailan and Paterson, 2014). *A. baumannii* has been long recognized as an intermediate reservoir for bla_{NDM-1} genes in which the harboring transposon (Tn*125*) was built and subsequently transmitted to other Gram-negative species (Toleman et al., 2012; Bontron et al., 2016).

Genome studies contribute significantly to better comprehend the molecular basis and evolution dynamics of antimicrobial resistance in nosocomial infectious pathogens (Hendriksen et al., 2019). Despite the large number of studies from Egypt that have discussed the epidemiology of healthcare-associated *A. baumannii* (Al-Hassan et al., 2019; Benmahmod et al., 2019; Wasfi et al., 2021), few studies have explored the whole-genome sequence of those circulating in Egyptian hospitals (Fam et al., 2020).

The objective of the current study was to explore the genomic features of four XDR bla_{NDM}-positive *A. baumannii* clinical isolates recovered from hospitalized patients at a large tertiary hospital in Egypt by whole-genome sequencing (WGS).

MATERIALS AND METHODS

Bacterial Strains and Antimicrobial Susceptibility Testing

A total of 54 nonduplicate nonfermentative Gram-negative bacterial isolates were collected from Kasr Al-Ainy University Hospital, Cairo, Egypt, between July and October 2020. Of these, 20 isolates were identified as *A. baumannii* using VITEK 2 (bioMérieux, Marcy l'Etoile, France). The identity of *A. baumannii* isolates was further confirmed using PCR amplification of the $bla_{OXA-51-like}$ genes (Turton et al., 2006). Bacterial isolates were recovered at the clinical pathology laboratory as part of routine clinical care of hospitalized patients. Antimicrobial resistance profiles were identified using disk diffusion test according to the recommendations of the CLSI (2018). Tigecycline susceptibility test results were interpreted according to susceptibility breakpoints recommended by the EUCAST (2021) v11.0 for *Enterobacterales*. For disk diffusion test, 14 antimicrobial disks (Oxoid, United Kingdom) were used including the following: ampicillin (10 μg), amoxicillin/clavulanic acid (20/10 μg), piperacillin/tazobactam (10/100 μg), ceftriaxone (30 μg), cefoxitin (30 μg), cefepime (30 μg), cefotaxime (30 μg), levofloxacin (5 μg), imipenem (10 μg), meropenem (10 μg), amikacin (30 μg), tigecycline (15 μg), and trimethoprim/sulfamethoxazole (1.25/23.75 μg). The broth microdilution method was used to detect the minimum inhibitory concentration (MIC) of colistin according to CLSI guidelines. Amplification of MBL genes (bla_{NDM}, $bla_{VIM,}$ and bla_{IMP}) using polymerase chain reaction (PCR) was done for all *A. baumannii* isolates as previously described (Ghazawi et al., 2012). Individual *A. baumannii* isolates (M02, M11, M19, and M20) that harbored bla_{NDM} were selected for WGS analysis.

Whole-Genome Sequencing, Assembly, and Annotation

DNA was extracted from all bla_{NDM}-positive *A. baumannii* isolates using QIAGEN DNA purification kit (Qiagen, Valencia, CA). This was further manipulated by Nextera DNA Sample Preparation kit (Nextera, United States) for preparation of the DNA library according to the manufacturer's recommended protocol. Sequencing was performed using the paired end 2 × 150 bp reads sequencing technology on an Illumina MiSeq platform (Illumina Inc., San Diego, CA, United States). Reads quality was assessed using FastQC v0.11.9 (Brown et al., 2017) before trimming with Trimmomatic v0.35 to cut away remaining adaptors and low-quality reads (Bolger et al., 2014). Trimmed reads were *de novo* assembled using SPAdes 3.14.1 (Bankevich et al., 2012) with default parameters. The quality of genomes assembly was evaluated using QUAST v5.0.2 (Gurevich et al., 2013). Functional annotations of the draft genomes were generated during submission to the National Center for Biotechnology Information (NCBI) genome database using the NCBI Prokaryotic Genome Annotation Pipeline (PGAP; Tatusova et al., 2016). Plasmid sequences were identified using plasmidSPAdes (Antipov et al., 2016) and Unicycler (Wick et al., 2017) for raw reads assembly and Bandage (Wick et al., 2015) for visualization of circular contigs.

Multilocus Sequence Typing

Whole-genome sequencing data were used for *in silico* analysis of multilocus sequence types (MLSTs) of the isolates harboring bla_{NDM} gene based on both Pasteur and Oxford schemes. Allele numbers and sequence types (STs) were assigned using PubMLST server.[1] The global optimal eBURST (goeBURST) algorithm executed by PHYLOViZ V2.0 (Francisco et al., 2012) was used for constructing a complete minimum spanning tree (MST) of the sequence types of the bla_{NDM}-positive isolates together with other STs in MLST database (accessed on March 10, 2021), and clonal complexes (CCs) were assigned accordingly.

Phylogeny Analysis

A single nucleotide polymorphism (SNP)-based phylogeny analysis of the four bla_{NDM}-positive isolates was performed using the CSI-Phylogeny tool hosted by the CGE server (Center for Genomic Epidemiology, Lyngby, Denmark) available at http://www.genomicepidemiology.org/ (Kaas et al., 2014). The draft genomes of the isolates were compared to complete genomes of *A. baumannii* strains carrying bla_{NDM-1} gene and some *A. baumannii* strains that belong to high-risk international clones retrieved from the GenBank database (accessed in: October 12, 2021). In addition, draft genomes of *A. baumannii* strains that belong to $ST1418^{Oxf}$ and $ST164^{Pas}$ were also downloaded from PubMLST genome collection[2] and included in the analysis. A. *baumannii* ATCC 17978 was used as a reference genome. The phylogenetic tree was visualized and edited using the interactive tree of life v3 software (Letunic and Bork, 2016) available at: https://itol.embl.de/.

Analysis of Antimicrobial Resistance Determinants and Insertion Sequences

Acquired antimicrobial resistance genes were identified using the ResFinder 4.1 webtool on the CGE server (Center for Genomic Epidemiology, Lyngby, Denmark[3]; Bortolaia et al., 2020) using raw reads as an input. Assembled contigs were further analyzed using the Comprehensive Antibiotic Resistance Database server[4] (Alcock et al., 2020) with coverage and identity thresholds of 80 and 95%, respectively. Genomic resistance islands were predicted using IslandViewer4 webtool[5] (Bertelli et al., 2017). Gene mutations relevant to antimicrobial resistance were manually analyzed by extracting the genes of interest from genome assemblies and blasting against respective genes of the reference strain *A. baumannii* ATCC 19606 (Accession Number: CP045110.1). This involved analysis of *gyrA* and *parC* regions whose mutations are associated with quinolones resistance. In addition, other genes reported to affect the susceptibility of *A. baumannii* to colistin including those involved in lipid A biosynthesis pathway (*lpxA*, *lpxC*, and *lpxD*) and *pmrABC* operon were also analyzed in case of colistin nonsusceptibility. Insertion sequences (ISs) were identified using the online tool ISfinder[6] (Siguier et al., 2006).

[1]https://pubmlst.org/organisms/acinetobacter-baumannii/
[2]https://pubmlst.org/organisms/acinetobacter-baumannii/
[3]http://www.genomicepidemiology.org/
[4]https://card.mcmaster.ca/analyze/rgi
[5]http://www.pathogenomics.sfu.ca/islandviewer/
[6]http://www-is.biotoul.fr

Characterization of the Genetic Context of Resistance Genes

Contigs containing resistance genes were extracted from the assemblies. Genetic features were obtained from PGAP annotation data. Unannotated regions were manually reannotated after blasting against the GenBank nucleotide collection. Genetic environments of resistance gene cassettes located on more than one contig were identified by mapping of raw reads to the best hits of the contigs' blast analyses using BWA (Li and Durbin, 2009). Consensus sequences were obtained using SAMtools and bcftools v0.1.10 (Li, 2011). Finally, annotated genetic environments of resistance genes were visualized using SnapGene viewer v5.1.3.1 (from Insightful Science; available at snapgene.com) and compared to reference sequences using Easyfig v2.2.5 (Sullivan et al., 2011).

Nucleotide Sequence Accession Numbers

Raw reads obtained by WGS of the bla_{NDM}-positive isolates were submitted to the Sequencing Read Archive[7] of the NCBI. Draft genomes were submitted to the NCBI Genome database.[8] Together with their BioSamples, they were submitted under the BioProject number PRJNA690827. Raw reads and draft genomes accession numbers are shown in **Supplementary Table 1**. The nucleotide sequence of the novel $bla_{ADC-257}$ gene was deposited in the NCBI GenBank database under the accession number (MZ224611.1).

RESULTS

During the study period, a total of 20 *A. baumannii* isolates were recovered from 20 different hospitalized patients with age ranging between newborn (5 days) and 65 years old. Of these, 12 (60%) were females and 8 (40%) were males. More than half of the patients were hospitalized in intensive care units. Specimens were collected from different clinical sites (**Table 1**). Results are shown for the four bla_{NDM}-positive *A. baumannii* isolates.

Acinetobacter baumannii Strains Harboring bla_{NDM} Gene

To determine the prevalence of acquired carbapenemases in the recovered *A. baumannii* isolates, the presence of bla_{NDM}, $bla_{VIM,}$ and bla_{IMP} genes were assessed using PCR assay. Neither VIM- nor IMP-type carbapenemase-coding genes could be identified in the isolates. Out of 20 *A. baumannii* isolates, four (20%) showed amplification of 371 bp PCR product corresponding to bla_{NDM} gene.

Genome Assembly

Whole-genome sequencing of the bla_{NDM}-positive isolates yielded total assembly lengths ranging from 3,773,846 bp to 3,919,334 bp with a GC content ranging from 39.19 to 39.55%. The mean number of contigs was 633. The number of coding sequences predicted by PGAP annotation of the assembled contigs ranged

[7]https://www.ncbi.nlm.nih.gov/sra/
[8]https://submit.ncbi.nlm.nih.gov/subs/genome/

TABLE 1 | Clinical data of the four NDM-producing *Acinetobacter baumannii*.

Isolate	Site	Age	Sex	Diagnosis	Date of isolation	Hospital ward
M02	Wound	28 years	Female	Subovarian abscess removal	2020-07-10	ICU
M11	Pleural	20 days	Female	Pneumonia	2020-07-15	NICU
M19	Blood	20 years	Female	Fever of unknown origin	2020-10-20	ICU
M20	Blood	65 years	Male	Splenectomy and feverish	2020-08-2	ICU

ICU, intensive care unit; NICU, neonatal intensive care unit.

from 3,761 to 3,996. Post-assembly and annotation metrics of the bla_{NDM}-positive isolates are shown in **Supplementary Table 2**.

MLST and Phylogenetic Analysis

In silico MLST analysis of the bla_{NDM}-positive isolates and goeBURST analysis of their STs together with ST data from MLST database revealed that isolate M20 ($ST570^{Pas}/1701^{Oxf}$) belongs to clonal complex ($CC2^{Pas}/546^{Oxf}$) representing international (IC) 2. Two isolates M02 and M11 had the same sequence type ($ST85^{Pas}/ST1089^{Oxf}$) that was found to belong to $CC464^{Pas}/CC1078^{Oxf}$ classified within IC9. The allele profile of M19 matched ST/CC164 and ST1418/CC234, according to Pasteur and Oxford schemes, respectively. MST diagram of bla_{NDM}-positive isolates STs together with other STs in MLST database (Pasteur scheme) is shown in **Supplementary Figure 1**. A SNP-based phylogenetic tree depicting the genetic relatedness of our bla_{NDM}-positive isolates to other *A. baumannii* strains is shown in **Figure 1**.

Antimicrobial Susceptibility Testing and Resistance Determinants

Antimicrobial susceptibility testing revealed that all isolates were extensively drug resistant (XDR) with retained susceptibility to only two antimicrobial classes (Magiorakos et al., 2012; **Figure 2**). All isolates were susceptible to tigecycline. MIC values of ≤0.125, 0.25, ≥128, and 0.5 μg/ml were determined for colistin in M02, M11, M19, and M20, respectively. Resistance to colistin was shown by one isolate (M19) that also retained susceptibility to amikacin.

Investigating the genetic background of the XDR phenotype using WGS revealed that the isolates carried multiple acquired antimicrobial resistance determinants besides the intrinsic resistance genes (**Table 2**). Genes conferring resistance to β-lactams included class A β-lactamases ($bla_{CARB-16}$ and bla_{TEM-1}), one metallo-β-lactamase (bla_{NDM-1}), class C β-lactamases (bla_{ADC-73} and $bla_{ADC-257}$), and carbapenem-hydrolyzing Ambler class D β-lactamases, (bla_{OXA-23}, bla_{OXA-66}, bla_{OXA-91}, and bla_{OXA-94}). $bla_{ADC-257}$ is a novel allele of bla_{ADC-52} (GenBank accession: WP_001211232.1) detected in isolate M19 with two amino acid substitutions (R2Q and G24D). Resistance to other antimicrobial agents was conferred by *ant*(2″)-*Ia*, *ant*(3″)-*Ia*, *ant*(3″)-*IIc*, *aph*(3′)-*Ia*, *aph*(3″)-*Ia*, *aph*(3′)-*VI*, *aac*(6′)-*Ib*', and *ArmA* (aminoglycoside resistance), *mphE* and *msrE* (macrolide resistance), *catB8* (chloramphenicol resistance), and *sul1* and *sul2* (sulfonamide resistance).

Analysis of the nucleotide sequence of *pmrABC* and *IpxACD* genes of the colistin-resistant isolate (M19) and comparison to their wild-type alleles in *A. baumannii* ATCC 19606 revealed the existence of multiple mutations. These included point mutations in the histidine kinase gene *pmrB* (H89L) and mutations in *pmrC* (I42V, I212V, R323K, A354S, and V470I). Only silent mutations were identified in *pmrA*. Within *IpxACD* genes, point mutations were identified in *IpxA* (Y131H and Y231H), *IpxC* (C120R, N287D, and K130T), and *lpxD* (V631 and E117K). Further analysis of genomic mutations revealed that levofloxacin resistance in all isolates was promoted by amino acid substitutions in quinolone resistance determining regions (QRDRs) of both DNA gyrase (S83L) and topoisomerase (S80L) enzymes.

Multidrug efflux pumps, including members of the major facilitator superfamily (MFS) and resistance-nodulation-division (RND) family and additional multidrug efflux pumps, were identified in the isolates. Susceptibility profiles of the bla_{NDM}-positive isolates and resistance determinants carried by each are shown in **Figure 2**.

Insertion Sequences

Investigating the insertion sequences using ISfinder revealed the existence of at least 24 IS elements distributed throughout the genomes. Most of them originated from *A. baumannii* and other *Acinetobacter* species. Only four IS elements were acquired from other bacterial species, such as *Escherichia coli*, *Vibrio salmonicida*, and *Salmonella panama*. Six types of ISs were conserved in all isolates, including IS*Aba*1, IS*Aba*8, IS*Aba*10, IS*Aba*14, IS*Aba*33, and IS*Aba*125. The diversity of IS content of the four genomes and their microbial origins are depicted in **Figure 3**.

Genetic Context of Resistance Genes

Whole-genome sequencing results revealed that bla_{NDM-1} genes were carried on the chromosomes of all sequenced isolates. Analysis of the immediate genetic environment of the bla_{NDM-1} gene revealed the existence of IS*Aba14* upstream to the divalent cation tolerance protein (CutA)-coding gene in the isolates M2, M11, and M20 in addition to the IS*Aba125* element upstream to bla_{NDM-1}. This genetic organization is similar to that of Tn*125*-like transposon previously reported by Bonnin et al. (2013). BLAST analysis of the contigs harboring bla_{NDM-1} showed highest similarity to the chromosome of *A. baumannii* strain ACN21

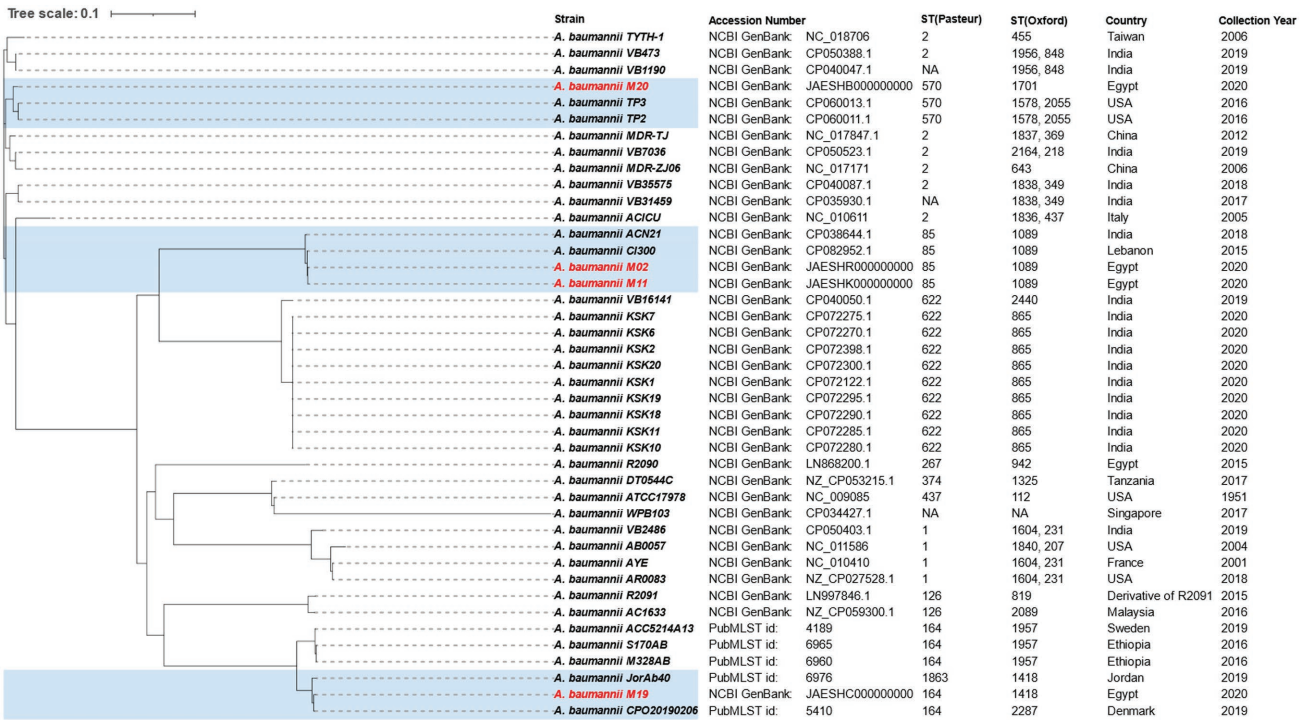

Strain	Accession Number		ST(Pasteur)	ST(Oxford)	Country	Collection Year
A. baumannii TYTH-1	NCBI GenBank:	NC_018706	2	455	Taiwan	2006
A. baumannii VB473	NCBI GenBank:	CP050388.1	2	1956, 848	India	2019
A. baumannii VB1190	NCBI GenBank:	CP040047.1	NA	1956, 848	India	2019
A. baumannii M20	NCBI GenBank:	JAESHB000000000	570	1701	Egypt	2020
A. baumannii TP3	NCBI GenBank:	CP060013.1	570	1578, 2055	USA	2016
A. baumannii TP2	NCBI GenBank:	CP060011.1	570	1578, 2055	USA	2016
A. baumannii MDR-TJ	NCBI GenBank:	NC_017847.1	2	1837, 369	China	2012
A. baumannii VB7036	NCBI GenBank:	CP050523.1	2	2164, 218	India	2019
A. baumannii MDR-ZJ06	NCBI GenBank:	NC_017171	2	643	China	2006
A. baumannii VB35575	NCBI GenBank:	CP040087.1	2	1838, 349	India	2018
A. baumannii VB31459	NCBI GenBank:	CP035930.1	NA	1838, 349	India	2017
A. baumannii ACICU	NCBI GenBank:	NC_010611	2	1836, 437	Italy	2005
A. baumannii ACN21	NCBI GenBank:	CP038644.1	85	1089	India	2018
A. baumannii CI300	NCBI GenBank:	CP082952.1	85	1089	Lebanon	2015
A. baumannii M02	NCBI GenBank:	JAESHR000000000	85	1089	Egypt	2020
A. baumannii M11	NCBI GenBank:	JAESHK000000000	85	1089	Egypt	2020
A. baumannii VB16141	NCBI GenBank:	CP040050.1	622	2440	India	2019
A. baumannii KSK7	NCBI GenBank:	CP072275.1	622	865	India	2020
A. baumannii KSK6	NCBI GenBank:	CP072270.1	622	865	India	2020
A. baumannii KSK2	NCBI GenBank:	CP072398.1	622	865	India	2020
A. baumannii KSK20	NCBI GenBank:	CP072300.1	622	865	India	2020
A. baumannii KSK1	NCBI GenBank:	CP072122.1	622	865	India	2020
A. baumannii KSK19	NCBI GenBank:	CP072295.1	622	865	India	2020
A. baumannii KSK18	NCBI GenBank:	CP072290.1	622	865	India	2020
A. baumannii KSK11	NCBI GenBank:	CP072285.1	622	865	India	2020
A. baumannii KSK10	NCBI GenBank:	CP072280.1	622	865	India	2020
A. baumannii R2090	NCBI GenBank:	LN868200.1	267	942	Egypt	2015
A. baumannii DT0544C	NCBI GenBank:	NZ_CP053215.1	374	1325	Tanzania	2017
A. baumannii ATCC17978	NCBI GenBank:	NC_009085	437	112	USA	1951
A. baumannii WPB103	NCBI GenBank:	CP034427.1	NA	NA	Singapore	2017
A. baumannii VB2486	NCBI GenBank:	CP050403.1	1	1604, 231	India	2019
A. baumannii AB0057	NCBI GenBank:	NC_011586	1	1840, 207	USA	2004
A. baumannii AYE	NCBI GenBank:	NC_010410	1	1604, 231	France	2001
A. baumannii AR0083	NCBI GenBank:	NZ_CP027528.1	1	1604, 231	USA	2018
A. baumannii R2091	NCBI GenBank:	LN997846.1	126	819	Derivative of R2091	2015
A. baumannii AC1633	NCBI GenBank:	NZ_CP059300.1	126	2089	Malaysia	2016
A. baumannii ACC5214A13	PubMLST id:	4189	164	1957	Sweden	2019
A. baumannii S170AB	PubMLST id:	6965	164	1957	Ethiopia	2016
A. baumannii M328AB	PubMLST id:	6960	164	1957	Ethiopia	2016
A. baumannii JorAb40	PubMLST id:	6976	1863	1418	Jordan	2019
A. baumannii M19	NCBI GenBank:	JAESHC000000000	164	1418	Egypt	2020
A. baumannii CPO20190206	PubMLST id:	5410	164	2287	Denmark	2019

FIGURE 1 | A single nucleotide polymorphism-based phylogenetic tree depicting the genetic relatedness of $bla_{\text{NDM-1}}$-positive isolates sequenced in the current study to other *Acinetobacter baumannii* strains. *A. baumannii* strains sequenced in the current study together with their genetically related strains are highlighted by blue color.

(GenBank accession: CP038644.1; Vijayakumar et al., 2020). Using this genome as a reference for Islandviewer analysis showed an upstream amikacin resistance gene (*AphA6*) and another copy of IS*Aba14* in ST85$^{\text{Pas}}$ isolates (M02 and M11). This was further confirmed by mapping raw sequencing reads of such isolates against a larger segment of *A. baumannii* strain ACN21 chromosome. This genetic organization was shown in **Figure 4** together with a comparative genetic analysis of Tn*125*-like transposon and Tn*125* (GenBank accession: KF702386.1). Similar analysis failed to localize *AphA6*-IS*Aba14* in the upstream region of the $bla_{\text{NDM-1}}$-harboring transposon in M20. Different genetic environment was noted for $bla_{\text{NDM-1}}$ carried by M19 in which the upstream IS*Aba125* element was immediately preceded by IS1 family transposase in an organization with no similarity in the NCBI nucleotide database. Furthermore, interruption of the right hand of the transposon by IS*Aba14* could not be concluded.

Analysis of the intrinsic bla_{ADC} genes and their association with upstream insertion elements revealed that the novel allele $bla_{\text{ADC-257}}$ carried by M19 was preceded by IS*Aba1*. In the isolates M02 and M11, bla_{ADC} genes were interrupted by IS1008 family transposase leading to missing N-terminus. Hence, the *Acinetobacter*-derived cephalosporinase variant could not be identified. The IS1008-interrupted gene had no similarity in the NCBI nucleotide database. The context of the interrupted gene compared to the closest match sequence (*A. baumannii* strain ACN21 chromosome) is shown in **Figure 5**. Similarly, $bla_{\text{ADC-73}}$ with missing N-terminus was harbored by M20, while the disrupting sequence could not be identified.

$bla_{\text{OXA-23}}$ carried by M20 was found to be embedded within Tn*2006* in which it was bracketed by IS*Aba1*, while $bla_{\text{OXA-94}}$ in M02 and M11 was preceded by IS*Aba1* element in a reverse orientation. On the other hand, $bla_{\text{OXA-91}}$ and $bla_{\text{OXA-66}}$ carried by the isolates M19 and M20 had no upstream insertion sequences.

Using *A. baumannii strain* MS14413 chromosome (GenBank: CP054302.1) as a reference for Islandviewer analysis, a 20,844 bp genomic resistance island that showed 99.62% identity to *A. baumannii* genomic resistance island 3 (AbGRI3, accession number: KX011025.2) was identified in M20. The resistance island hosted the resistance genes: *aph*(3`)-*Ia*, *aac*(6`)-*Ib*`, *catB8*, ant(3``)-*Ia*, *sul1*, *ArmA*, *msr*(*E*), and *mph*(*E*) bracketed by IS26 family transposases.

In all isolates carrying *ant*(2``)-*Ia* (*aadB*), the gene was found on pRAY plasmid (6,076 bp) derivatives. A plasmid sequence identical to pRAY*-v1 (GenBank accession: JF343536) was identified in M19, while those carried by M02 and M11 showed 100% identity to pRay* (GenBank accession: JQ904627). No other resistance plasmids were identified in our isolates.

The chloramphenicol resistance gene, *floR* harbored by the isolates M02 and M11, was linked to a genetic structure containing *sul2*. Both were flanked by insertion elements with the order IS4, *Sul2*, hypothetical protein-coding gene, IS*Vsa3*, IS1006, *LysR*, *floR*, and IS3. The closest match to this region was shown by *Acinetobacter indicus* chromosome (GenBank accession: CP071319.1). The genetic structure containing *floR*

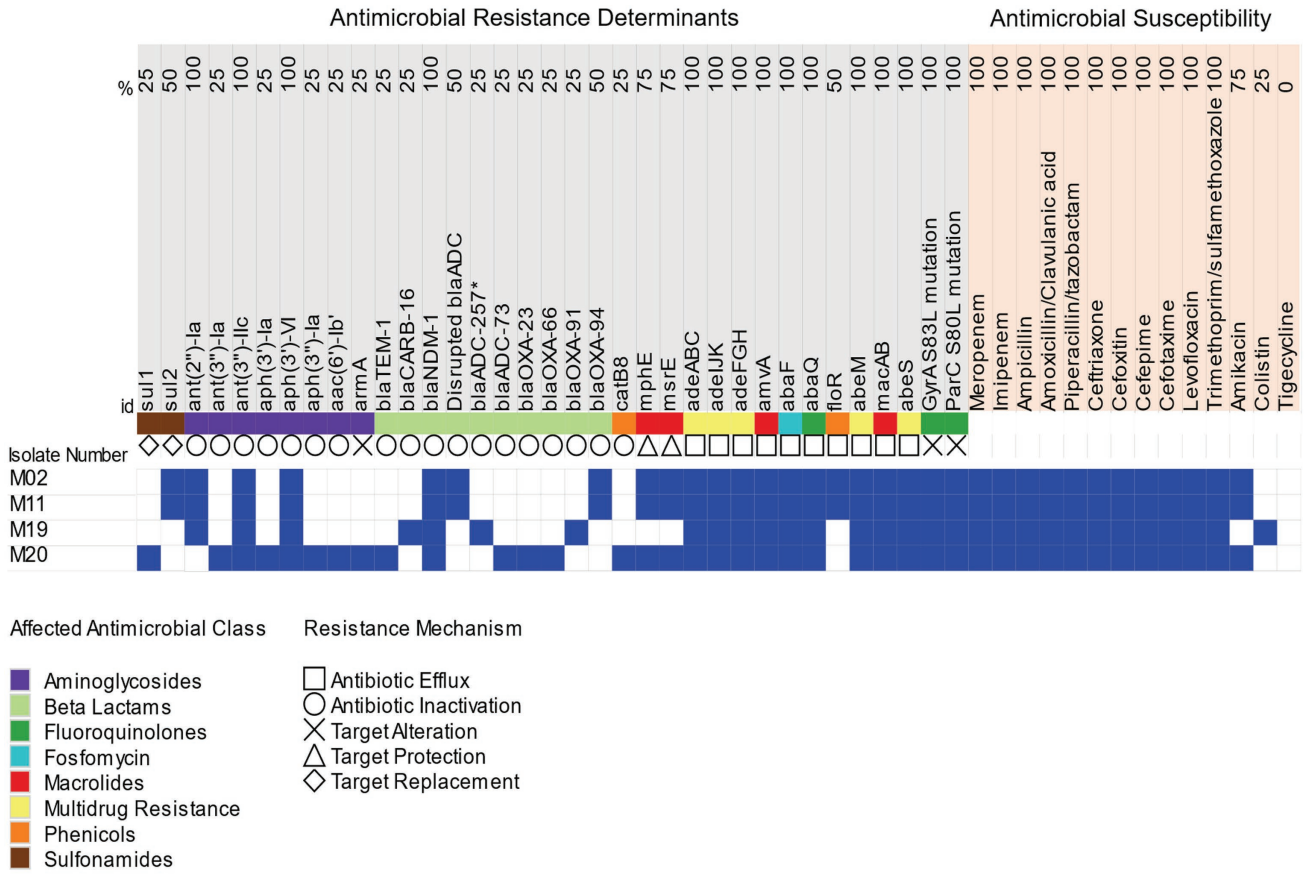

FIGURE 2 | Antimicrobial resistance profiles and distribution of antimicrobial resistance determinants in the *bla*$_{NDM}$-positive isolates. Blue colors denote antimicrobial resistance and harbored antimicrobial determinants, while susceptibility to antimicrobials and lack of resistance determinants are denoted by white colors; *bla*$_{ADC-257}$*, novel *bla*$_{ADC}$ allele identified in M19.

and *sul2* genes compared to the closest match sequence is depicted in **Figure 6**.

Macrolide resistance genes *msr*(*E*) and *mph*(*E*) were flanked by an upstream ISNCY family transposase and a downstream IS*Aba1* element. A genetic organization that is identical to that carried by *A. baumannii* strain ACN21 chromosome (GenBank accession: CP038644.1).

DISCUSSION

A threatening rise in the incidence of carbapenem-resistant *A. baumannii* has been increasingly reported worldwide (Levy-Blitchtein et al., 2018; Moghnieh et al., 2018; Alcantar-Curiel et al., 2019) and in Egypt as well (Al-Hassan et al., 2019; Benmahmod et al., 2019; Mabrouk et al., 2020), leaving behind a substantial number of difficult to treat infections. For a deeper insight into the molecular mechanisms underlying carbapenem resistance in this highly problematic pathogen, a collection of 20 *A. baumannii* clinical isolates was screened for carbapenemase-coding genes by PCR. Four NDM producers were identified in clinical specimens recovered from ICU patients with severe infections. XDR phenotype was identified in all *bla*$_{NDM}$-positive *A. baumannii* with few reserved therapeutic options. These included tigecycline, colistin (for M02, M11, and M20), and amikacin (for M19) frequently associated with unfavorable pharmacokinetics and/or adverse effects particularly in critically ill patients (Spapen et al., 2011).

Draft genomes of the *bla*$_{NDM}$-positive isolates were obtained by Illumina sequencing for subsequent MLST and resistome analysis. *In silico* MLST and goeBURST analysis revealed that three out of four NDM producer *A. baumannii* belonged to the high-risk international clones (ICs), known for outbreak potential, worldwide dissemination (Karah et al., 2012), and multidrug resistance (Diancourt et al., 2010). M02 and M11 were assigned ST85^{Pas}/1089^{Oxf} that belong to IC9, recently described by Müller et al. (2019). Abundance of studies reporting *bla*$_{NDM-1}$-positive *A. baumannii* of ST85^{Pas} from Middle East countries (Bonnin et al., 2013; Decousser et al., 2013; Rafei et al., 2014; Salloum et al., 2018) has drawn attention on its probable endemicity in this region. IC2 was represented only by M20 (ST570^{Pas}/1701^{Oxf}), whose genome was loaded by the highest share of resistance genes. The abundance of IC2 *A. baumannii* in Egypt was also reported by others (Al-Hassan

TABLE 2 | STs and antimicrobial resistance genes carried by the four bla_{NDM}-positive isolates.

Isolate number	MLST				Intrinsic bla_{OXA} gene	Antimicrobial resistance genes	Efflux pumps genes	QRDR[b]	
	Pasteur		Oxford					*gyrA*	*parC*
	ST	CC	ST	CC					
M02	85	464	1089	1078	bla_{OXA-94}	*aph(3′)-VI*, bla_{NDM-1}, bla_{ADC} (disrupted by IS6), *mphE*, *msrE*, *sul2*, *ant(2″)-Ia*, *ant(3″)-IIc*	*adeABC*, *adeIJK*, *adeFGH*, *abeM*, *amvA*, *abeS*, *abaF*, *abaQ*, *floR*, *macAB*	S83L	S80L
M11	85	464	1089	1078	bla_{OXA-94}	*aph(3′)-VI*, bla_{NDM-1}, bla_{ADC} (disrupted by IS6), *mphE*, *msrE*, *sul2*, *ant(2″)-Ia*, *ant(3″)-IIc*	*adeABC*, *adeIJK*, *adeFGH*, *abeM*, *amvA*, *abeS*, *abaF*, *abaQ*, *floR*, *macAB*	S83L	S80L
M19	164	164	1418	234	bla_{OXA-91}	*aph(3′)-VI*, bla_{NDM-1}, $bla_{ADC-257}$[a], $bla_{CARB-16}$, *ant(2″)-Ia*, *ant(3″)-IIc*	*adeABC*, *adeIJK*, *adeFGH*, *abeM*, *amvA*, *abeS*, *abaF*, *abaQ*, *macAB*	S83L	S80L
M20	570	2	1701	546	bla_{OXA-66}	bla_{OXA-23}, *aph(3′)-VI*, bla_{NDM-1}, bla_{ADC-73}, *aph(3′)-Ia*, bla_{TEM-1}, *aph(3″)-I*, *aac(6′)-Ib′*, *catB8*, *ant(3″)-Ia*, *sul1*, *ArmA*, *msr(E)*, *mph(E)*, *ant(3″)-IIc*	*adeABC*, *adeIJK*, *adeFGH*, *abeM*, *amvA*, *abeS*, *abaF*, *abaQ*, *macAB*	S83L	S80L

[a]*Novel ADC allele.*
[b]*QRDR, quinolone resistance determining regions.*

et al., 2019; Wasfi et al., 2021). To the best of our knowledge, this is the first report of bla_{NDM}-positive *A. baumannii* strain that belongs to ST164[Pas]/ST1418[Oxf]. Although MDR-resistant *A. baumannii* isolates that belong to ST164[Pas] have been increasingly reported from different parts of the world (Coelho-Souza et al., 2013; Loraine et al., 2020; Tada et al., 2020), none was reported to carry a bla_{NDM} gene.

The SNP-based phylogeny analysis (**Figure 1**) showed that the isolates M02 and M11 were genetically related to two bla_{NDM}-positive *A. baumannii* strains of the same sequence type (1089[Oxf]/85[Pas]). These included *A. baumannii* strain Cl300 isolated in Lebanon in 2015 and strain ACN21 isolated in India in 2018. M20 was found to be genetically related to two NDM producer *A. baumannii* strains isolated in United States in 2016 (TP2 and TP3). Both TP2 and TP3 had the Oxford ST1578 a double locus variant of ST1701 to which M20 belongs. On the other hand, M19 showed no genetic relatedness to any of the NDM producer *A. baumannii* strains for which complete genomes were available in the NCBI. Inclusion of four draft genomes that belong to ST164[Pas] and ST1418[Oxf] retrieved from PubMLST genome collection revealed that M19 was most genetically related to *A. baumannii* strain CPO20190206 isolated from Denmark (ST164[Pas]) and *A. baumannii* strain JorAb40 isolated from Jordan (ST1418[Oxf]). Both strains were isolated in 2019 and, interestingly, none was found to carry a bla_{NDM} gene.

Resistome analysis disclosed a wide arsenal of resistance genes presented in **Table 2** and correlated with the susceptibility profiles in **Figure 2**. Both intrinsic and acquired resistance mechanisms contributed to β-lactams resistance. The carbapenem-hydrolyzing class D β-lactamases (oxacillinases) provide both intrinsic ($bla_{OXA51\text{-}like}$ genes) and acquired ($bla_{OXA\text{-}23,\ 40,\ 58,\ 143,235}$-like genes) resistance to β-lactams including carabapenems (Poirel and Nordmann, 2006; Ghaith et al., 2017). Overexpression of OXA-type β-lactamases has been linked to an upstream IS element, most frequently IS*Aba1*, through which an additional promotor is provided (Evans and Amyes, 2014). bla_{OXA-94} preceded by IS*Aba1* element was identified in M02 and M11 while no IS elements could be identified upstream to bla_{OXA-91} or bla_{OXA-66} carried by M19 and M20, respectively.

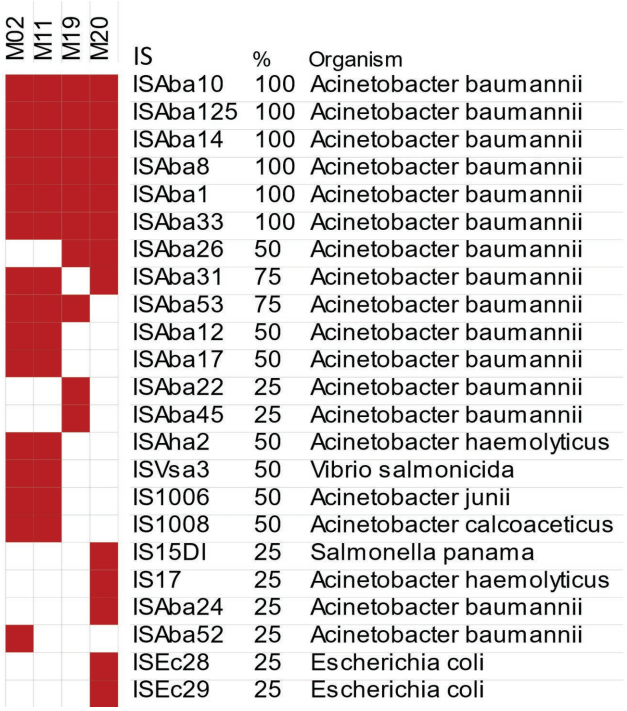

FIGURE 3 | Genome-wide distribution of different IS elements in the *bla*$_{NDM}$-positive isolates predicted by ISfinder. Red and white colors denote the presence and absence of each IS element, respectively.

In addition to intrinsic OXA-type β-lactamases, the IC2 isolate (M20) also carried *bla*$_{OXA-23}$ the most widely disseminated oxacillinase acquired by carbapenem-resistant *A. baumannii* (Mugnier et al., 2010). Association of *bla*$_{OXA-23}$ with IC2 *A. baumannii* has been reported worldwide (Hamidian and Nigro, 2019). As with other IC2 isolates, *bla*$_{OXA-23}$ carried by M20 was found to reside in Tn*2006* in which the gene is bracketed by two inversely oriented IS*Aba1* elements. Tn*2006* is the most common structure harboring *bla*$_{OXA-23}$ either alone or incorporated into AbGRIs (Hamidian and Nigro, 2019).

Although the association of *bla*$_{OXA-91}$ and *bla*$_{NDM-1}$ in *A. baumannii* was not previously described in Egypt, co-existence of *bla*$_{OXA-51}$-like, *bla*$_{OXA-23}$ and *bla*$_{NDM-1}$ was reported by Wasfi et al. (2021).

Analysis of the genetic environment of *bla*$_{NDM-1}$ in the sequenced isolates showed different environments in different sequence types. IS*Aba14* element was inserted upstream to the *cutA* gene in M02, M11, and M20. This was previously documented by Bonnin et al. (2013) who failed to identify a downstream second copy of IS*Aba125* by PCR and suggested loss of functionality of this truncated transposon (ΔTn*125*). WGS of *bla*$_{NDM}$-positive isolates by a later study (Vijayakumar et al., 2020) uncovered the existence of a second copy of IS*Aba125* downstream to the IS*Aba14*-interrupted transposon. Interestingly, analysis of the upstream region to the truncated transposon revealed the existence of the amikacin resistance gene *AphA6* preceded by another copy of IS*Aba14* in ST85^{Pas}

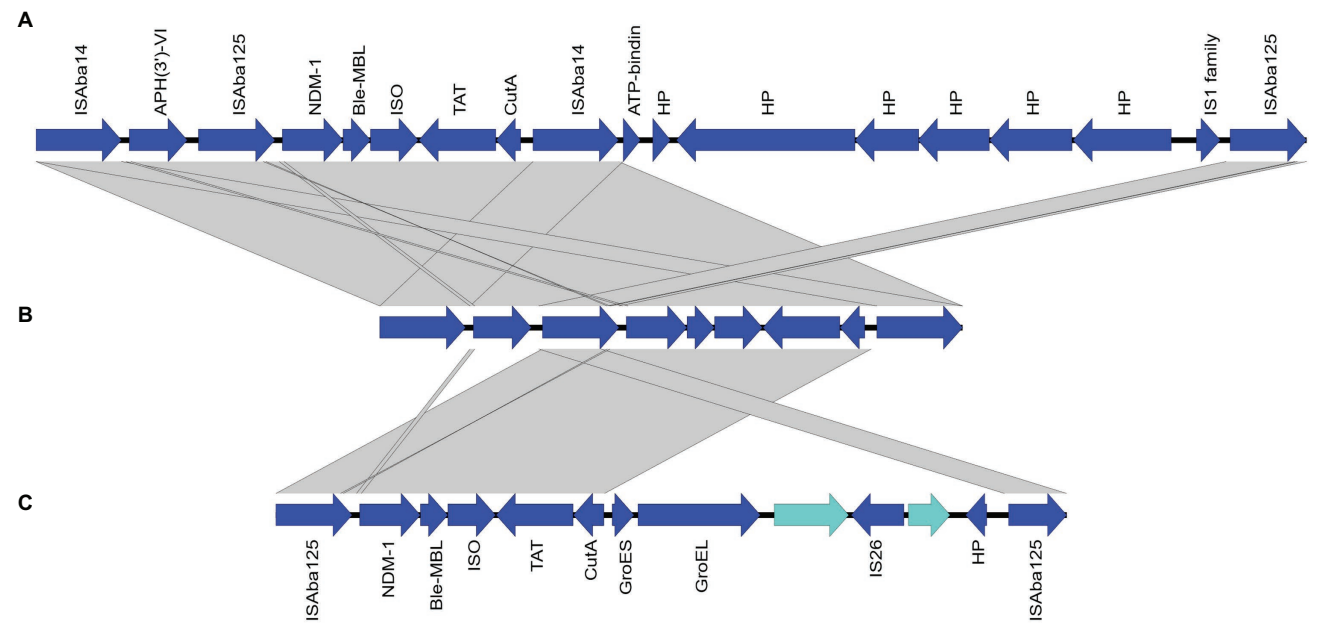

FIGURE 4 | Graphical representation of *bla*$_{NDM-1}$ genetic environment in isolates M02 and M11 **(B)** compared to the closest match sequence *Tn*125-like transposon of *A. baumannii* strain ACN21 (GenBank accession: CP038644.1) **(A)** and *Tn*125 (GenBank accession: KF702386.1) **(C)**. ORFs orientation is indicated by arrows. Grey bands between panels indicate more than 98% sequence similarity. Genes are labelled by their protein products; NDM-1, New Delhi metal-beta-lactamase enzyme; ble-MBL, bleomycin resistance protein; ISO, phosphoribosylanthranilate isomerase; TAT, twin-arginine translocation pathway signal sequence protein; CutA, divalent cation tolerance protein; HP, hypothetical protein; GroES, co-chaperonin protein; GroEL, type I chaperonin.

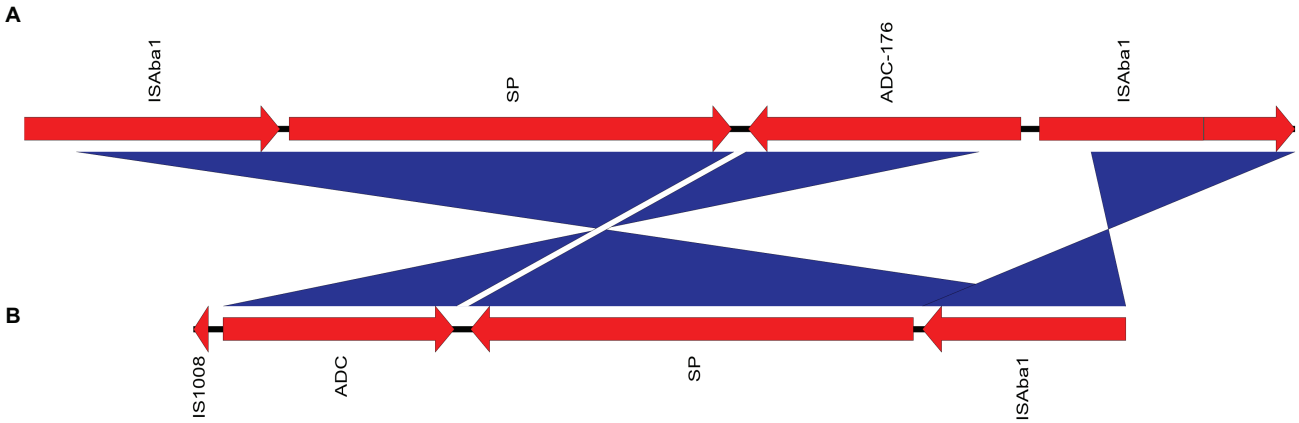

FIGURE 5 | Gene maps showing the genetic environment of *IS1008*-interrupted bla_{ADC} carried by M11 **(A)** compared to *A. baumannii* ACN21 chromosome (GenBank accession: CP038644.1) **(B)**. ORFs orientation is indicated by arrows. Blue bands between panels indicate inverted sequences with more than 98% sequence similarity. Genes are labelled by their protein products; ADC, bla_{ADC} gene disrupted by IS6; SP, signal peptide.

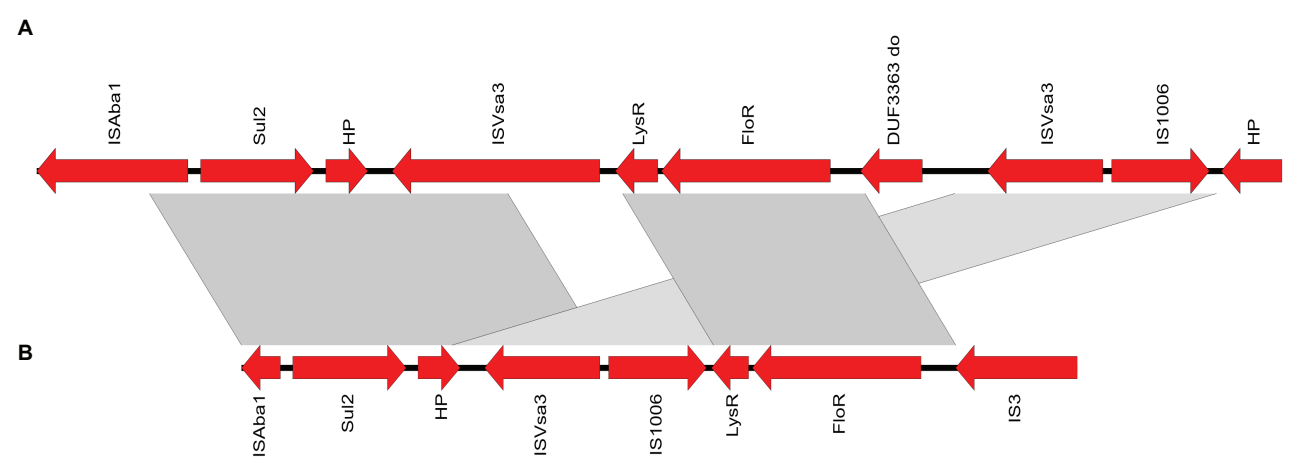

FIGURE 6 | Depiction of the genetic structure containing the genes *sul2* and *floR* identified in strain M11 **(A)** compared to *Acinetobacter indicus* strain GXNN62X4 chromosome, GenBank accession: CP071319 **(B)**. ORFs orientation is indicated by arrows. Grey bands between panels indicate more than 98% sequence similarity. Genes are labelled by their protein products; LysR, LysR family transcriptional regulator.

isolates (**Figure 4**). The two IS*Aba14* elements were thus thought to form an alternative composite transposon in which two resistance genes were enclosed for transposition (bla_{NDM-1} and *AphA6*) rather than the widely known Tn*125* in which bla_{NDM-1} was hosted as the sole antimicrobial resistance gene. Transposition of this composite transposon might, therefore, favor the co-transfer of resistance to two of the last-line antimicrobial treatment options for MDR and XDR *A. baumannii*. Nevertheless, experimental analysis is required to examine the transposition potential of this transposon. In M19, IS1 family transposase was identified immediately upstream to IS*Aba125* that precedes the bla_{NDM-1} gene. Insertion of IS1 element in this location was not identified in the nucleotide database of the NCBI.

Intrinsic to all *A. baumannii*, cephalosporin resistance is mediated by ADC (formerly known as bla_{AmpC}). In addition to the incomplete bla_{ADC-73} carried by M20, a novel bla_{ADC} allele ($bla_{ADC-257}$) with an upstream *ISAba1* element was identified in M19 recovered from a blood culture of a female patient admitted to the ICU with fever of unknown origin. With no similarity in the NCBI nucleotide database, bla_{ADC} genes carried by M02 and M11 were interrupted by an IS1008 element (**Figure 5**). No alternative intact copies of bla_{ADC} were identified in M02, M11, or M20. Other β-lactamases identified here included class A β-lactamases, more efficiently capable of hydrolyzing penicillins and cephalosporins than carbapenems (Jeon et al., 2015). These were coded by bla_{Tem-1} carried by M20 and $bla_{CARB-16}$ in M19. However, their association with mobile elements could not be clearly determined.

In addition to the intrinsic aminoglycoside resistance gene *ant*(3``)-*IIc* (Zhang et al., 2017), the amikacin-modifying

enzyme-coding gene *aph*(3`)-*VIa* (*aphA6*) was found in all isolates. The predominance of *aph*(3`)-*VIa* among the aminoglycoside modifying enzymes-coding genes was also reported by others (Aghazadeh et al., 2013; Sheikhalizadeh et al., 2017). Notably, the gene was also identified in the amikacin-sensitive isolate M19. Identification of *aph*(3`)-*VIa* in amikacin-susceptible isolates was also reported before (Aghazadeh et al., 2013; Sheikhalizadeh et al., 2017). In *ant*(2``)-*Ia*-positive isolates, the gene was found in pRAY plasmid variants. pRAY is a 6 Kb plasmid widely distributed in *Acinetobacter* species comprising the most common resistance mechanism to gentamicin and tobramycin (Hamidian et al., 2012).

Acquired 16S rRNA methyltransferases constitute the most important aminoglycoside resistance mechanism conferring resistance to most of the clinically important aminoglycosides (Galimand et al., 2003). Of them, *armA* has been widely reported from *A. baumannii* particularly those of the IC2 (Blackwell et al., 2017). Within a 20,844 bp genomic resistance island closely similar to *A. baumannii* genomic resistance island 3 (AbGRI3; Blackwell et al., 2017), *armA* gene was identified in M20 (IC2). Other resistance genes hosted by the genomic island include *aph*(3`)-*Ia*, *aac*(6`)-*Ib*`, *catB8*, ant(3``)-*Ia*, *sul1*, *msr*(*E*), and *mph*(*E*). Another unique genetic structure in which genes coding resistance to two different antimicrobial classes was identified in M02 and M11 (**Figure 6**). This included the chloramphenicol efflux pump (FloR)-coding gene and *sul2*, conferring resistance to sulfamethoxazole/trimethoprim, enclosed by insertion elements. The closest match to this region was shown by *Acinetobacter indicus* chromosome (GenBank accession: CP071319.1) from which it may have been acquired with some genetic rearrangement.

In the absence of plasmid-mediated quinolones resistance genes, nonsusceptibility to levofloxacin in all NDM producers investigated here was mediated by target site mutations. These affected the QRDRs within GyrA (S83L) and ParC (S80L) enzymes. The mutation pattern identified in our isolates was commonly reported as the predominant mechanism responsible for fluoroquinolones resistance in *A. baumannii* (Hamed et al., 2018; Nodari et al., 2020; Roy et al., 2021).

Resistance to colistin, the last line of defense against XDR *A. baumannii*, was evident in only one isolate (M19) that, fortunately, retained susceptibility to amikacin and tigecycline. Colistin resistance in M19 was accompanied by multiple nonsynonymous mutations affecting *pmrABC* and *IpxACD* genes. Missense mutations identified in *pmrB* (H89L) and *pmrC* (I42V) genes carried by M19 were also reported in colistin-resistant *A. baumannii* studied by Nurtop et al. (2019) in Turkey. It is worth mentioning that the amino acid affected by *pmrB* mutation identified here is located outside the histidine kinase domain, the main determinant of colistin resistance in *A. baumannii* (Arroyo et al., 2011; Beceiro et al., 2011; Lesho et al., 2013). Moreover, all *lpxACD* mutations identified here were previously reported in both colistin-susceptible and colistin-resistant isolates (Oikonomou et al., 2015; Haeili et al., 2018; Nurtop et al., 2019). Accordingly, novel unidentified resistance mechanisms might stand behind the high-level resistance (MIC ≥ 128 μg/ml) of M19 to colistin. Further investigations including gene expression analysis are therefore required to confirm or role out the impact of such mutations on colistin susceptibility.

Diverse efflux pumps, whose overexpression has been linked to multidrug resistance, were identified in the sequenced isolates. RND efflux pumps known by their broad substrate profiles (Coyne et al., 2011), including AdeABC, AdeIJK, and AdeFGH. were identified in all isolates. RND efflux pumps contribute to intrinsic resistance of *A. baumannii* to several classes of antimicrobials. Other multidrug efflux pumps carried by all isolates included AbeM, a member of the multidrug and toxic compound extrusion family efflux pumps and the small multidrug resistance efflux pump AbeS (Coyne et al., 2011). Except for FloR conferring resistance to phenicols in M02 and M11 only, efflux pumps of the MFS were disseminated in all sequenced genomes. With narrow substrate profiles, AmvA, AbaF, and AbaQ are known to extrude erythromycin, fosfomycin, and quinolones, respectively (Coyne et al., 2011; Perez-Varela et al., 2018). The macrolide-specific ABC pump MacAB was also found in all isolates.

It is worth mentioning that the current study suffers from some limitations, most importantly is using short-read sequencing technology instead of a hybrid long- and short-read sequencing approach known to produce more accurate genome organization. Consistent with other studies (Leal et al., 2020), resistance to some antimicrobials could not be correlated to known resistance genes highlighting the need for further investigations including gene expression analysis or identification of novel resistance determinants. Finally, only four genomes were sequenced here thus correlating resistance genes with particular STs could not be fully achieved.

CONCLUSION

The current study is one of the few studies reporting WGS of *A. baumannii* clinical isolates from Egypt. The isolates showed XDR phenotype and were recovered from ICU patients. High-risk international clones were identified, predominantly IC9 ($ST85^{Pas}$) widely reported from Middle East countries. Diverse mobile elements were associated with resistance genes with novel insertion sites and genetic organizations. Co-existence of amikacin and carbapenem resistance genes on an *ISAba14*-bracketed transposon was uniquely identified in $ST85^{Pas}$/$ST1089^{Oxf}$. bla_{NDM-1} gene was identified, for the first time, on the chromosome of an *A. baumannii* strain that belongs to sequence type $ST164^{Pas}$/$S1418^{Oxf}$. WGS of the highly problematic MDR and XDR pathogens may aid in the identification of emerging resistance genes and their dissemination dynamics. Co-existence of resistance genes within mobile genetic elements could also be identified. This may aid in optimizing treatment guidelines to avoid selection of resistance to last-line antimicrobials. WGS also permits monitoring the emergence of novel global MDR clones and facilitates comparative genomic analysis and developing cheaper molecular techniques for routine screening.

ETHICAL APPROVAL

The study was performed in accordance with relevant guidelines and regulations, and no experiments were performed on humans and/or human tissue samples. The study was approved by the local Ethical Committee of clinical and chemical pathology department, Kasr Al-Aini Hospital, Cairo university. Only bacterial isolates were collected for the routine laboratory work to ensure patient care and informed consents were not required.

DATA AVAILABILITY STATEMENT

The datasets presented in this study can be found in online repositories. The names of the repository/repositories and accession number(s) can be found in the article/**Supplementary Material**.

AUTHOR CONTRIBUTIONS

MZ, AH, MA, HR, and SH contributed to the study design, performance of experiments, and data analysis. SH performed the genomes assembly and bioinformatic analysis. MZ wrote the first draft of the manuscript. All authors read and approved the final version of manuscript.

FUNDING

The authors thank the Deanship of Scientific Research at King Saud University for funding this work through Project No. RGP-038.

ACKNOWLEDGMENTS

The authors extend their appreciation to Genomic unit at The Children's Cancer Hospital Egypt 57357 (CCHE) for performing part of the experiments.

SUPPLEMENTARY MATERIAL

The Supplementary Material for this article can be found online at: https://www.frontiersin.org/articles/10.3389/fmicb.2021.736982/full#supplementary-material

REFERENCES

Aghazadeh, M., Rezaee, M. A., Nahaei, M. R., Mahdian, R., Pajand, O., Saffari, F., et al. (2013). Dissemination of aminoglycoside-modifying enzymes and 16S rRNA methylases among *acinetobacter baumannii* and Pseudomonas aeruginosa isolates. *Microb. Drug Resist.* 19, 282–288. doi: 10.1089/mdr.2012.0223

Alcantar-Curiel, M. D., Rosales-Reyes, R., Jarillo-Quijada, M. D., Gayosso-Vazquez, C., Fernandez-Vazquez, J. L., Toledano-Tableros, J. E., et al. (2019). Carbapenem-resistant *Acinetobacter baumannii* in three tertiary care hospitals in Mexico: virulence profiles, innate immune response and clonal dissemination. *Front. Microbiol.* 10:2116. doi: 10.3389/fmicb.2019.02116

Alcock, B. P., Raphenya, A. R., Lau, T. T. Y., Tsang, K. K., Bouchard, M., Edalatmand, A., et al. (2020). CARD 2020: antibiotic resistome surveillance with the comprehensive antibiotic resistance database. *Nucleic Acids Res.* 48, D517–D525. doi: 10.1093/nar/gkz935

Al-Hassan, L., Zafer, M. M., and El-Mahallawy, H. (2019). Multiple sequence types responsible for healthcare-associated *Acinetobacter baumannii* dissemination in a single Centre in Egypt. *BMC Infect. Dis.* 19:829. doi: 10.1186/s12879-019-4433-1

Antipov, D., Hartwick, N., Shen, M., Raiko, M., Lapidus, A., and Pevzner, P. A. (2016). plasmidSPAdes: assembling plasmids from whole genome sequencing data. *Bioinformatics* 32, 3380–3387. doi: 10.1093/bioinformatics/btw493

Antunes, L. C., Visca, P., and Towner, K. J. (2014). *Acinetobacter baumannii*: evolution of a global pathogen. *Pathog Dis.* 71, 292–301. doi: 10.1111/2049-632X.12125

Arroyo, L. A., Herrera, C. M., Fernandez, L., Hankins, J. V., Trent, M. S., and Hancock, R. E. (2011). The pmrCAB operon mediates polymyxin resistance in *Acinetobacter baumannii* ATCC 17978 and clinical isolates through phosphoethanolamine modification of lipid A. *Antimicrob. Agents Chemother.* 55, 3743–3751. doi: 10.1128/AAC.00256-11

Ayobami, O., Willrich, N., Harder, T., Okeke, I. N., Eckmanns, T., and Markwart, R. (2019). The incidence and prevalence of hospital-acquired (carbapenem-resistant) *Acinetobacter baumannii* in Europe, eastern Mediterranean and Africa: a systematic review and meta-analysis. *Emerg. Microbes. Infect.* 8, 1747–1759. doi: 10.1080/22221751.2019.1698273

Bankevich, A., Nurk, S., Antipov, D., Gurevich, A. A., Dvorkin, M., Kulikov, A. S., et al. (2012). SPAdes: a new genome assembly algorithm and its applications to single-cell sequencing. *J. Comput. Biol.* 19, 455–477. doi: 10.1089/cmb.2012.0021

Beceiro, A., Llobet, E., Aranda, J., Bengoechea, J. A., Doumith, M., Hornsey, M., et al. (2011). Phosphoethanolamine modification of lipid A in colistin-resistant variants of *Acinetobacter baumannii* mediated by the pmrAB two-component regulatory system. *Antimicrob. Agents Chemother.* 55, 3370–3379. doi: 10.1128/AAC.00079-11

Benmahmod, A. B., Said, H. S., and Ibrahim, R. H. (2019). Prevalence and mechanisms of Carbapenem resistance Among *Acinetobacter baumannii* clinical isolates in Egypt. *Microb. Drug Resist.* 25, 480–488. doi: 10.1089/mdr.2018.0141

Bertelli, C., Laird, M. R., Williams, K. P., Simon Fraser University Research Computing GroupLau, B. Y., Hoad, G., et al. (2017). IslandViewer 4: expanded prediction of genomic islands for larger-scale datasets. *Nucleic Acids Res.* 45, W30–W35. doi: 10.1093/nar/gkx343

Blackwell, G. A., Holt, K. E., Bentley, S. D., Hsu, L. Y., and Hall, R. M. (2017). Variants of AbGRI3 carrying the armA gene in extensively antibiotic-resistant *Acinetobacter baumannii* from Singapore. *J. Antimicrob. Chemother.* 72, 1031–1039. doi: 10.1093/jac/dkw542

Bolger, A. M., Lohse, M., and Usadel, B. (2014). Trimmomatic: a flexible trimmer for Illumina sequence data. *Bioinformatics* 30, 2114–2120. doi: 10.1093/bioinformatics/btu170

Bonnin, R. A., Cuzon, G., Poirel, L., and Nordmann, P. (2013). Multidrug-resistant *Acinetobacter baumannii* clone, France. *Emerg. Infect. Dis.* 19, 822–823. doi: 10.3201/eid1905.121618

Bontron, S., Nordmann, P., and Poirel, L. (2016). Transposition of Tn125 encoding the NDM-1 Carbapenemase in *Acinetobacter baumannii*. *Antimicrob. Agents Chemother.* 60, 7245–7251. doi: 10.1128/AAC.01755-16

Bortolaia, V., Kaas, R. S., Ruppe, E., Roberts, M. C., Schwarz, S., Cattoir, V., et al. (2020). ResFinder 4.0 for predictions of phenotypes from genotypes. *J. Antimicrob. Chemother.* 75, 3491–3500. doi: 10.1093/jac/dkaa345

Brown, J., Pirrung, M., and Mccue, L. A. (2017). FQC dashboard: integrates FastQC results into a web-based, interactive, and extensible FASTQ quality control tool. *Bioinformatics* 33, 3137–3139. doi: 10.1093/bioinformatics/btx373

Chng, K. R., Li, C., Bertrand, D., Ng, A. H. Q., Kwah, J. S., Low, H. M., et al. (2020). Cartography of opportunistic pathogens and antibiotic resistance genes in a tertiary hospital environment. *Nat. Med.* 26, 941–951. doi: 10.1038/s41591-020-0894-4

CLSI (2018). *Performance Standards for Antimicrobial Susceptibility Testing: Twenty-Second Informational Supplement. CLSI Supplement M100*. Wayne, PA: Clinical and Laboratory Standards Institute.

Coelho-Souza, T., Reis, J. N., Martins, N., Martins, I. S., Menezes, A. O., Reis, M. G., et al. (2013). Longitudinal surveillance for meningitis by Acinetobacter in a large urban setting in Brazil. *Clin. Microbiol. Infect.* 19, E241–E244. doi: 10.1111/1469-0691.12145

Coyne, S., Courvalin, P., and Perichon, B. (2011). Efflux-mediated antibiotic resistance in Acinetobacter spp. *Antimicrob. Agents Chemother.* 55, 947–953. doi: 10.1128/AAC.01388-10

Decousser, J. W., Jansen, C., Nordmann, P., Emirian, A., Bonnin, R. A., Anais, L., et al. (2013). Outbreak of NDM-1-producing *Acinetobacter baumannii* in France, January to may 2013. *Euro Surveill.* 18:20547. doi: 10.2807/1560-7917.ES2013.18.31.20547

Di Nocera, P. P., Rocco, F., Giannouli, M., Triassi, M., and Zarrilli, R. (2011). Genome organization of epidemic *Acinetobacter baumannii* strains. *BMC Microbiol.* 11:224. doi: 10.1186/1471-2180-11-224

Diancourt, L., Passet, V., Nemec, A., Dijkshoorn, L., and Brisse, S. (2010). The population structure of *Acinetobacter baumannii*: expanding multiresistant clones from an ancestral susceptible genetic pool. *PLoS One* 5:e10034. doi: 10.1371/journal.pone.0010034

Elsayed, E., Elarabi, M. A., Sherif, D. A., Elmorshedi, M., and El-Mashad, N. (2020). Extensive drug resistant *Acinetobacter baumannii*: a comparative study between non-colistin based combinations. *Int. J. Clin. Pharm.* 42, 80–88. doi: 10.1007/s11096-019-00940-1

EUCAST (2021). Breakpoint tables for interpretation of MICs and zone diameters, version 11.0. Available at: http://www.eucast.org (Accessed May 1, 2021).

Evans, B. A., and Amyes, S. G. (2014). OXA beta-lactamases. *Clin. Microbiol. Rev.* 27, 241–263. doi: 10.1128/CMR.00117-13

Fam, N. S., Gamal, D., Mohamed, S. H., Wasfy, R. M., Soliman, M. S., El-Kholy, A. A., et al. (2020). Molecular characterization of Carbapenem/Colistin-resistant *Acinetobacter baumannii* clinical isolates from Egypt by whole-genome sequencing. *Infect. Drug Resist.* Volume 13, 4487–4493. doi: 10.2147/IDR.S288865

Francisco, A. P., Vaz, C., Monteiro, P. T., Melo-Cristino, J., Ramirez, M., and Carrico, J. A. (2012). PHYLOViZ: phylogenetic inference and data visualization for sequence based typing methods. *BMC Bioinformatics* 13:87. doi: 10.1186/1471-2105-13-87

Galimand, M., Courvalin, P., and Lambert, T. (2003). Plasmid-mediated high-level resistance to aminoglycosides in Enterobacteriaceae due to 16S rRNA methylation. *Antimicrob. Agents Chemother.* 47, 2565–2571. doi: 10.1128/AAC.47.8.2565-2571.2003

Ghaith, D. M., Zafer, M. M., Al-Agamy, M. H., Alyamani, E. J., Booq, R. Y., and Almoazzamy, O. (2017). The emergence of a novel sequence type of MDR *Acinetobacter baumannii* from the intensive care unit of an Egyptian tertiary care hospital. *Ann. Clin. Microbiol. Antimicrob.* 16:34. doi: 10.1186/s12941-017-0208-y

Ghazawi, A., Sonnevend, A., Bonnin, R. A., Poirel, L., Nordmann, P., Hashmey, R., et al. (2012). NDM-2 carbapenemase-producing *Acinetobacter baumannii* in the United Arab Emirates. *Clin. Microbiol. Infect.* 18, E34–E36. doi: 10.1111/j.1469-0691.2011.03726.x

Gurevich, A., Saveliev, V., Vyahhi, N., and Tesler, G. (2013). QUAST: quality assessment tool for genome assemblies. *Bioinformatics* 29, 1072–1075. doi: 10.1093/bioinformatics/btt086

Haeili, M., Kafshdouz, M., and Feizabadi, M. M. (2018). Molecular mechanisms of Colistin resistance Among Pandrug-resistant isolates of *Acinetobacter baumannii* with high case-fatality rate in intensive care unit patients. *Microb. Drug Resist.* 24, 1271–1276. doi: 10.1089/mdr.2017.0397

Hamed, S. M., Elkhatib, W. F., El-Mahallawy, H. A., Helmy, M. M., Ashour, M. S., and Aboshanab, K. M. A. (2018). Multiple mechanisms contributing to ciprofloxacin resistance among gram negative bacteria causing infections to cancer patients. *Sci. Rep.* 8:12268. doi: 10.1038/s41598-018-30756-4

Hamidian, M., and Nigro, S. J. (2019). Emergence, molecular mechanisms and global spread of carbapenem-resistant *Acinetobacter baumannii*. *Microb. Genom.* 5:306. doi: 10.1099/mgen.0.000306

Hamidian, M., Nigro, S. J., and Hall, R. M. (2012). Variants of the gentamicin and tobramycin resistance plasmid pRAY are widely distributed in Acinetobacter. *J. Antimicrob. Chemother.* 67, 2833–2836. doi: 10.1093/jac/dks318

Hendriksen, R. S., Bortolaia, V., Tate, H., Tyson, G. H., Aarestrup, F. M., and Mcdermott, P. F. (2019). Using genomics to track global antimicrobial resistance. *Front. Public Health* 7:242. doi: 10.3389/fpubh.2019.00242

Jeon, J. H., Lee, J. H., Lee, J. J., Park, K. S., Karim, A. M., Lee, C. R., et al. (2015). Structural basis for carbapenem-hydrolyzing mechanisms of carbapenemases conferring antibiotic resistance. *Int. J. Mol. Sci.* 16, 9654–9692. doi: 10.3390/ijms16059654

Kaas, R. S., Leekitcharoenphon, P., Aarestrup, F. M., and Lund, O. (2014). Solving the problem of comparing whole bacterial genomes across different sequencing platforms. *PLoS One* 9:e104984. doi: 10.1371/journal.pone.0104984

Karah, N., Sundsfjord, A., Towner, K., and Samuelsen, O. (2012). Insights into the global molecular epidemiology of carbapenem non-susceptible clones of *Acinetobacter baumannii*. *Drug Resist. Updat.* 15, 237–247. doi: 10.1016/j.drup.2012.06.001

Leal, N. C., Campos, T. L., Rezende, A. M., Docena, C., Mendes-Marques, C. L., De Sa Cavalcanti, F. L., et al. (2020). Comparative genomics of *Acinetobacter baumannii* clinical strains From Brazil reveals polyclonal dissemination and selective exchange of Mobile genetic elements associated With resistance genes. *Front. Microbiol.* 11:1176. doi: 10.3389/fmicb.2020.01176

Lesho, E., Yoon, E. J., Mcgann, P., Snesrud, E., Kwak, Y., Milillo, M., et al. (2013). Emergence of colistin-resistance in extremely drug-resistant *Acinetobacter baumannii* containing a novel pmrCAB operon during colistin therapy of wound infections. *J. Infect. Dis.* 208, 1142–1151. doi: 10.1093/infdis/jit293

Letunic, I., and Bork, P. (2016). Interactive tree of life (iTOL) v3: an online tool for the display and annotation of phylogenetic and other trees. *Nucleic Acids Res.* 44, W242–W245. doi: 10.1093/nar/gkw290

Levy-Blitchtein, S., Roca, I., Plasencia-Rebata, S., Vicente-Taboada, W., Velasquez-Pomar, J., Munoz, L., et al. (2018). Emergence and spread of carbapenem-resistant *Acinetobacter baumannii* international clones II and III in Lima, Peru. *Emerg. Microbes Infect.* 7:119. doi: 10.1038/s41426-018-0127-9

Li, H. (2011). A statistical framework for SNP calling, mutation discovery, association mapping and population genetical parameter estimation from sequencing data. *Bioinformatics* 27, 2987–2993. doi: 10.1093/bioinformatics/btr509

Li, H., and Durbin, R. (2009). Fast and accurate short read alignment with burrows-wheeler transform. *Bioinformatics* 25, 1754–1760. doi: 10.1093/bioinformatics/btp324

Loraine, J., Heinz, E., Soontarach, R., Blackwell, G. A., Stabler, R. A., Voravuthikunchai, S. P., et al. (2020). Genomic and phenotypic analyses of *Acinetobacter baumannii* isolates From three tertiary care hospitals in Thailand. *Front. Microbiol.* 11:548. doi: 10.3389/fmicb.2020.00548

Mabrouk, S. S., Abdellatif, G. R., El-Ansary, M. R., Aboshanab, K. M., and Ragab, Y. M. (2020). Carbapenemase producers Among extensive drug-resistant gram-negative pathogens recovered from febrile neutrophilic patients in Egypt. *Infect. Drug Resist.* 13, 3113–3124. doi: 10.2147/IDR.S269971

Magiorakos, A. P., Srinivasan, A., Carey, R. B., Carmeli, Y., Falagas, M. E., Giske, C. G., et al. (2012). Multidrug-resistant, extensively drug-resistant and pandrug-resistant bacteria: an international expert proposal for interim standard definitions for acquired resistance. *Clin. Microbiol. Infect.* 18, 268–281. doi: 10.1111/j.1469-0691.2011.03570.x

Moghnieh, R. A., Kanafani, Z. A., Tabaja, H. Z., Sharara, S. L., Awad, L. S., and Kanj, S. S. (2018). Epidemiology of common resistant bacterial pathogens in the countries of the Arab league. *Lancet Infect. Dis.* 18, e379–e394. doi: 10.1016/S1473-3099(18)30414-6

Mugnier, P. D., Poirel, L., Naas, T., and Nordmann, P. (2010). Worldwide dissemination of the bla_{OXA-23} carbapenemase gene of *Acinetobacter baumannii*. *Emerg. Infect. Dis.* 16, 35–40. doi: 10.3201/eid1601.090852

Müller, C., Stefanik, D., Wille, J., Hackel, M., Higgins, P. G., and Siefert, H. (2019). "Molecular epidemiology of carbapenem-resistant *Acinetobacter baumannii* clinical isolates and identification of the novel international clone IC9: results from a worldwide surveillance study (2012–2016)", in *Paper Presented at the ECCMID 2019: Proceeding of the 29th European Congress of Clinical Microbiology & Infectious Diseases*. (Amsterdam, Netherlands) April 13–16, 2019.

Nodari, C. S., Cayo, R., Streling, A. P., Lei, F., Wille, J., Almeida, M. S., et al. (2020). Genomic analysis of Carbapenem-resistant *Acinetobacter baumannii* isolates belonging to major endemic clones in South America. *Front. Microbiol.* 11:584603. doi: 10.3389/fmicb.2020.584603

Nurtop, E., Bayindir Bilman, F., Menekse, S., Kurt Azap, O., Gonen, M., Ergonul, O., et al. (2019). Promoters of Colistin resistance in *Acinetobacter*

baumannii infections. *Microb. Drug Resist.* 25, 997–1002. doi: 10.1089/mdr.2018.0396

Oikonomou, O., Sarrou, S., Papagiannitsis, C. C., Georgiadou, S., Mantzarlis, K., Zakynthinos, E., et al. (2015). Rapid dissemination of colistin and carbapenem resistant *Acinetobacter baumannii* in Central Greece: mechanisms of resistance, molecular identification and epidemiological data. *BMC Infect. Dis.* 15:559. doi: 10.1186/s12879-015-1297-x

Perez-Varela, M., Corral, J., Aranda, J., and Barbe, J. (2018). Functional characterization of AbaQ, a novel efflux pump mediating quinolone resistance in *Acinetobacter baumannii*. *Antimicrob. Agents Chemother.* 62:e00906-18. doi: 10.1128/AAC.00906-18

Poirel, L., and Nordmann, P. (2006). Carbapenem resistance in *Acinetobacter baumannii*: mechanisms and epidemiology. *Clin. Microbiol. Infect.* 12, 826–836. doi: 10.1111/j.1469-0691.2006.01456.x

Rafei, R., Dabboussi, F., Hamze, M., Eveillard, M., Lemarie, C., Mallat, H., et al. (2014). First report of blaNDM-1-producing *Acinetobacter baumannii* isolated in Lebanon from civilians wounded during the Syrian war. *Int. J. Infect. Dis.* 21, 21–23. doi: 10.1016/j.ijid.2014.01.004

Roy, S., Chatterjee, S., Bhattacharjee, A., Chattopadhyay, P., Saha, B., Dutta, S., et al. (2021). Overexpression of efflux pumps, mutations in the Pumps' regulators, chromosomal mutations, and AAC(6′)-Ib-cr are associated With fluoroquinolone resistance in diverse sequence types of neonatal Septicaemic *Acinetobacter baumannii*: A 7-year single center study. *Front. Microbiol.* 12:602724. doi: 10.3389/fmicb.2021.602724

Salloum, T., Tannous, E., Alousi, S., Arabaghian, H., Rafei, R., Hamze, M., et al. (2018). Genomic mapping of ST85 blaNDM-1 and blaOXA-94 producing *Acinetobacter baumannii* isolates from Syrian civil war victims. *Int. J. Infect. Dis.* 74, 100–108. doi: 10.1016/j.ijid.2018.07.017

Sheikhalizadeh, V., Hasani, A., Ahangarzadeh Rezaee, M., Rahmati-Yamchi, M., Hasani, A., Ghotaslou, R., et al. (2017). Comprehensive study to investigate the role of various aminoglycoside resistance mechanisms in clinical isolates of *Acinetobacter baumannii*. *J. Infect. Chemother.* 23, 74–79. doi: 10.1016/j.jiac.2016.09.012

Siguier, P., Perochon, J., Lestrade, L., Mahillon, J., and Chandler, M. (2006). ISfinder: the reference Centre for bacterial insertion sequences. *Nucleic Acids Res.* 34, D32–D36. doi: 10.1093/nar/gkj014

Spapen, H., Jacobs, R., Van Gorp, V., Troubleyn, J., and Honore, P. M. (2011). Renal and neurological side effects of colistin in critically ill patients. *Ann. Intensive Care* 1:14. doi: 10.1186/2110-5820-1-14

Sullivan, M. J., Petty, N. K., and Beatson, S. A. (2011). Easyfig: a genome comparison visualizer. *Bioinformatics* 27, 1009–1010. doi: 10.1093/bioinformatics/btr039

Tacconelli, E., Carrara, E., Savoldi, A., Harbarth, S., Mendelson, M., Monnet, D. L., et al. (2018). Discovery, research, and development of new antibiotics: the WHO priority list of antibiotic-resistant bacteria and tuberculosis. *Lancet Infect. Dis.* 18, 318–327. doi: 10.1016/S1473-3099(17)30753-3

Tada, T., Uchida, H., Hishinuma, T., Watanabe, S., Tohya, M., Kuwahara-Arai, K., et al. (2020). Molecular epidemiology of multidrug-resistant *Acinetobacter baumannii* isolates from hospitals in Myanmar. *J. Glob. Antimicrob. Resist.* 22, 122–125. doi: 10.1016/j.jgar.2020.02.011

Tal-Jasper, R., Katz, D. E., Amrami, N., Ravid, D., Avivi, D., Zaidenstein, R., et al. (2016). Clinical and epidemiological significance of Carbapenem resistance in *Acinetobacter baumannii* infections. *Antimicrob. Agents Chemother.* 60, 3127–3131. doi: 10.1128/AAC.02656-15

Tatusova, T., Dicuccio, M., Badretdin, A., Chetvernin, V., Nawrocki, E. P., Zaslavsky, L., et al. (2016). NCBI prokaryotic genome annotation pipeline. *Nucleic Acids Res.* 44, 6614–6624. doi: 10.1093/nar/gkw569

Toleman, M. A., Spencer, J., Jones, L., and Walsh, T. R. (2012). blaNDM-1 is a chimera likely constructed in *Acinetobacter baumannii*. *Antimicrob. Agents Chemother.* 56, 2773–2776. doi: 10.1128/AAC.06297-11

Turton, J. F., Woodford, N., Glover, J., Yarde, S., Kaufmann, M. E., and Pitt, T. L. (2006). Identification of *Acinetobacter baumannii* by detection of the blaOXA-51-like carbapenemase gene intrinsic to this species. *J. Clin. Microbiol.* 44, 2974–2976. doi: 10.1128/JCM.01021-06

Vijayakumar, S., Wattal, C., J, K. O., Bhattacharya, S., Vasudevan, K., Anandan, S., et al. (2020). Insights into the complete genomes of carbapenem-resistant *Acinetobacter baumannii* harbouring Bla OXA-23, Bla OXA-420 and Bla NDM-1 genes using a hybrid-assembly approach. *Access Microbiol.* 2:acmi000140. doi: 10.1099/acmi.0.000140

Wailan, A. M., and Paterson, D. L. (2014). The spread and acquisition of NDM-1: a multifactorial problem. *Expert Rev. Anti-Infect. Ther.* 12, 91–115. doi: 10.1586/14787210.2014.856756

Wasfi, R., Rasslan, F., Hassan, S. S., Ashour, H. M., and Abd El-Rahman, O. A. (2021). Co-existence of Carbapenemase-encoding genes in *Acinetobacter baumannii* from cancer patients. *Infect. Dis. Ther.* 10, 291–305. doi: 10.1007/s40121-020-00369-4

Wick, R. R., Judd, L. M., Gorrie, C. L., and Holt, K. E. (2017). Unicycler: resolving bacterial genome assemblies from short and long sequencing reads. *PLoS Comput. Biol.* 13:e1005595. doi: 10.1371/journal.pcbi.1005595

Wick, R. R., Schultz, M. B., Zobel, J., and Holt, K. E. (2015). Bandage: interactive visualization of de novo genome assemblies. *Bioinformatics* 31, 3350–3352. doi: 10.1093/bioinformatics/btv383

Zhang, G., Leclercq, S. O., Tian, J., Wang, C., Yahara, K., Ai, G., et al. (2017). A new subclass of intrinsic aminoglycoside nucleotidyltransferases, ANT(3″)-II, is horizontally transferred among Acinetobacter spp. by homologous recombination. *PLoS Genet.* 13:e1006602. doi: 10.1371/journal.pgen.1006602

Conflict of Interest: The authors declare that the research was conducted in the absence of any commercial or financial relationships that could be construed as a potential conflict of interest.

Publisher's Note: All claims expressed in this article are solely those of the authors and do not necessarily represent those of their affiliated organizations, or those of the publisher, the editors and the reviewers. Any product that may be evaluated in this article, or claim that may be made by its manufacturer, is not guaranteed or endorsed by the publisher.

frontiers in Microbiology

ORIGINAL RESEARCH
published: 09 December 2021
doi: 10.3389/fmicb.2021.752883

Whole-Genome Sequencing-Based Antimicrobial Resistance Characterization and Phylogenomic Investigation of 19 Multidrug-Resistant and Extended-Spectrum Beta-Lactamase-Positive *Escherichia coli* Strains Collected From Hospital Patients in Benin in 2019

Carine Laurence Yehouenou[1,2,3]†, Bert Bogaerts[4,5†], Sigrid C. J. De Keersmaecker[4], Nancy H. C. Roosens[4], Kathleen Marchal[5,6,7], Edmond Tchiakpe[8,9], Dissou Affolabi[2,3,10], Anne Simon[11], Francis Moise Dossou[12], Kevin Vanneste[4‡] and Olivia Dalleur[1,13‡]*

[1]Clinical Pharmacy Research Group (CLIP), Louvain Drug Research Institute (LDRI), Université Catholique de Louvain UCLouvain, Brussels, Belgium, [2]Laboratoire de Référence des Mycobactéries (LRM), Cotonou, Benin, [3]Faculté des Sciences de la Santé (FSS), Université d'Abomey Calavi (UAC), Cotonou, Benin, [4]Transversal activities in Applied Genomics, Sciensano, Brussels, Belgium, [5]Department of Plant Biotechnology and Bioinformatics, Ghent University, Ghent, Belgium, [6]Department of Information Technology, IDLab, Ghent University, IMEC, Ghent, Belgium, [7]Department of Genetics, University of Pretoria, Pretoria, South Africa, [8]Laboratory of Cell Biology and Physiology, Department of Biochemistry and Cellular Biology Faculty of Sciences and Technology and Institute of Applied Biomedical Sciences (ISBA), University of Abomey-Calavi, Cotonou, Benin, [9]National Reference Laboratory of Health Program Fighting Against AIDS in Benin, Health Ministry, Cotonou, Benin, [10]Centre National Hospitalier et Universitaire Hubert Koutoukou Maga (CNHU-HKM), Cotonou, Benin, [11]Centres hospitaliers Jolimont, prevention et contrôle des infections, Haine-Saint-Paul, Belgium, [12]Department of Surgery and Surgical Specialties, Faculty of Health Sciences, Campus universitaire champ de foire, Cotonou, Benin, [13]Pharmacy, Clinique universitaire Saint-Luc, Université catholique de Louvain, UCLouvain, Brussels, Belgium

The increasing worldwide prevalence of extended-spectrum beta-lactamase (ESBL) producing *Escherichia coli* constitutes a serious threat to global public health. Surgical site infections are associated with high morbidity and mortality rates in developing countries, fueled by the limited availability of effective antibiotics. We used whole-genome sequencing (WGS) to evaluate antimicrobial resistance and the phylogenomic relationships of 19 ESBL-positive *E. coli* isolates collected from surgical site infections in patients across public hospitals in Benin in 2019. Isolates were identified by MALDI-TOF mass spectrometry and phenotypically tested for susceptibility to 16 antibiotics. Core-genome multi-locus sequence typing and single-nucleotide polymorphism-based phylogenomic methods were used to investigate the relatedness between samples. The broader phylogenetic context was characterized through the inclusion of publicly available genome data. Among the 19 isolates, 13 different sequence types (STs) were observed, including ST131 ($n = 2$),

OPEN ACCESS

Edited by:
Guo-bao Tian,
Sun Yat-sen University, China

Reviewed by:
Phil Giffard,
Charles Darwin University, Australia
Bruno Gabriel Nascimento Andrade,
Munster Technological University, Ireland

***Correspondence:**
Carine Laurence Yehouenou
yehcarine@yahoo.fr;
carine.yehouenou@uclouvain.be

†These authors have contributed equally to this work
‡These authors share senior authorship

Specialty section:
This article was submitted to Antimicrobials, Resistance and Chemotherapy, a section of the journal Frontiers in Microbiology

Received: *03 August 2021*
Accepted: *08 November 2021*
Published: *09 December 2021*

Citation:
Yehouenou CL, Bogaerts B, De Keersmaecker SCJ, Roosens NHC, Marchal K, Tchiakpe E, Affolabi D, Simon A, Dossou FM, Vanneste K and Dalleur O (2021) Whole-Genome Sequencing-Based Antimicrobial Resistance Characterization and Phylogenomic Investigation of 19 Multidrug-Resistant and Extended-Spectrum Beta-Lactamase-Positive Escherichia coli Strains Collected From Hospital Patients in Benin in 2019. Front. Microbiol. 12:752883. doi: 10.3389/fmicb.2021.752883

ST38 ($n = 2$), ST410 ($n = 2$), ST405 ($n = 2$), ST617 ($n = 2$), and ST1193 ($n = 2$). The $bla_{CTX\text{-}M\text{-}15}$ gene encoding ESBL resistance was found in 15 isolates (78.9%), as well as other genes associated with ESBL, such as $bla_{OXA\text{-}1}$ ($n = 14$) and $bla_{TEM\text{-}1}$ ($n = 9$). Additionally, we frequently observed genes encoding resistance against aminoglycosides [*aac-(6')-Ib-cr*, $n = 14$], quinolones (*qnrS1*, $n = 4$), tetracyclines [*tet*(*B*), $n = 14$], sulfonamides (*sul2*, $n = 14$), and trimethoprim (*dfrA17*, $n = 13$). Nonsynonymous chromosomal mutations in the housekeeping genes *parC* and *gyrA* associated with resistance to fluoroquinolones were also detected in multiple isolates. Although the phylogenomic investigation did not reveal evidence of hospital-acquired transmissions, we observed two very similar strains collected from patients in different hospitals. By characterizing a set of multidrug-resistant isolates collected from a largely unexplored environment, this study highlights the added value for WGS as an effective early warning system for emerging pathogens and antimicrobial resistance.

Keywords: *Escherichia coli*, whole-genome sequencing, extended-spectrum beta-lactamases, antimicrobial resistance, Benin

INTRODUCTION

Multidrug-resistant (MDR) and extended-spectrum beta-lactamase (ESBL) producing bacteria pose a growing clinical and public health risk (Pitout and Laupland, 2008). In 2017, the World Health Organization (WHO) listed ESBL-producing *Enterobacterales*, including *E. coli*, as pathogens of critical priority for research and development of antibiotics (Asokan et al., 2019). ESBLs confer resistance to penicillins; to first-, second-, third-, and fourth-generation cephalosporins; and to aztreonam (but not to the cephamycins or carbapenems; Brolund, 2014). ESBL genes are commonly observed in association with genes that confer resistance to other classes of antibiotics, resulting in multidrug resistance (Harbarth et al., 2015). Additionally, they are easily transferred between bacteria through horizontal gene transfer (Brolund, 2014).

Two classification systems for beta-lactamases are currently in use. The most widely used is the Ambler molecular classification (Hall and Barlow, 2005), which defines four molecular classes of beta-lactamases based on amino-acid homology (A, B, C, and D). The most prevalent ESBLs belong to class A, which includes the Cefotaximase-Munich (CTX-M), Temoneria (TEM), and Sulfhydryl Variable (SHV) families.

Hospital-acquired infections of ESBL-producing *Enterobacterales* were first described in 1983 (Bradford, 2001), where resistance arose from point mutations in plasmid-mediated genes encoding beta-lactamase enzymes. These enzymes include TEM-1, TEM-2, and SHV-1, as well as CTX-M, which later became predominant worldwide (Hall and Barlow, 2005). Studies have shown that CTX-M-15-producing *E. coli* comprises one of the most prevalent ESBL-producing *Enterobacterales* (Cantón et al., 2012; Harbarth et al., 2015; Nwafia et al., 2019) and that the global dissemination of ESBL-producing *E. coli* is associated with specific clones mainly assigned to sequence types 131 (ST131) and 405 (ST405; Naseer and Sundsfjord, 2011). As these resistant strains are associated with higher mortality rates, extended hospital stays, and higher health costs, the burden of these infections is enormous.

Since only a few molecular typing studies have examined *E. coli* related infections in hospitals in low- and middle-income countries (LMICs), such as Benin, limited information is available on the subtypes that cause infections and their transmission dynamics in LMICs. Genotypic antimicrobial resistance evaluation has been performed mainly by polymerase chain reaction (PCR), which often fails to capture the full complexity of antimicrobial genetic structures (Anago et al., 2015; Koudokpon et al., 2018). In recent years, whole-genome sequencing (WGS) has increasingly been used to examine drug-resistant commensal and pathogenic *E. coli*, providing more complete insight into the genetic structures associated with the evolution of multidrug resistance (MDR) and transmission dynamics (Punina et al., 2015). In Benin, this information is currently lacking, as WGS-based studies are rarely performed. Therefore, we performed WGS on 19 ESBL-positive strains of clinical *E. coli* isolated from surgical site infections from patients in four public hospitals and characterized their phenotypic and genotypic AMR profiles, and phylogenomic diversity.

MATERIALS AND METHODS

Study Overview and Ethics Consent

This study was part of a larger project (Multidisciplinary Strategy for Prevention and Infection Control: MUSTPIC) conducted from April 2018 to January 2020 to explore etiological bacteria involved in surgical site infections in six public hospitals in Benin. Overall, 229 isolates were collected in the context of this project. This study was approved by the Ethics Committee of the Faculty of Health Sciences (FSS, Benin) under reference number: 012-19/UAC/FSS/CER-SS. Written informed consent was obtained from each participant before enrolment into the study.

Sample Collection and Species Identification

Samples were originally collected as wound swabs between January 2019 and January 2020 from patients that had consented to participate. We included the obstetric (particularly caesarean sections) and gastrointestinal wards at four of these six public hospitals in Benin. To maintain confidentiality, each of these hospitals was randomly assigned a letter A-D. These wards were chosen because caesarean sections are one of the most common surgical procedures, and gastrointestinal wards were present in all the hospitals. All participating hospitals are located in the south of Benin, thereby allowing daily transport from each hospital to the CNHU-HKM laboratory, where all wound swabs were initially collected and analyzed. All identifications were confirmed in Belgium using Matrix-Assisted Laser Desorption Ionization-Time of Flight (MALDI-TOF) mass spectrometry (Brucker daltonics, Bremen, Germany) employing a threshold of ≥2.0. Out of 229 samples, 49 were identified as *Staphylococcus aureus* and 180 as belonging to the *Enterobacterales*, of which 62 samples were identified as *E. coli*.

Antimicrobial Susceptibility Testing

The 62 isolates identified as *E. coli* were tested for susceptibility toward 16 antimicrobials using the modified Kirby-Bauer disk diffusion method according to the EUCAST guidelines (EUCAST, 2015). *Escherichia coli* strain ATCC 25922 was used for quality control. The following antimicrobial disks (Bio-Rad, Marnes-la-coquette, France) were used amikacin (30 µg), amoxicillin-clavulanic acid (20/10 µg), ampicillin (10 µg), cefepime (30 µg), cefotaxime (30 µg), cefoxitin (30 µg), ceftriaxone (30 µg), chloramphenicol (30 µg), ciprofloxacin (5 µg), gentamycin (10 µg), imipenem (10 µg), levofloxacin (5 µg), meropenem (10 µg), piperacillin (100 µg), tobramycin (10 µg), and trimethoprim + sulfamethoxazole (25 µg). Isolates that were resistant to at least three different classes of antimicrobials were considered as MDR (Magiorakos et al., 2012). Antimicrobial classes for 15 of the 16 tested antibiotics were assigned based on the ResFinder classification.[1] Levofloxacin was missing from the aforementioned classification and manually assigned to fluoroquinolones. The ESBL phenotype was identified by the double-disk synergy method on Mueller Hinton agar using ceftazidime and ceftriaxone placed at 20 mm apart from a disk containing amoxicillin and clavulanic acid. A clear-cut enhancement of the inhibition in front of either ceftazidime and/or ceftriaxone disks toward the clavulanic acid-containing disk (also called "champagne-cork" or "keyhole") was interpreted as positive for ESBL production. Additionally, isolates were tested for the presence of the beta-lactamase *ampC* phenotype using the cefoxitin-cloxacillin disk diffusion test, as described previously (Thean et al., 2009). Out of the 62 *E. coli* isolates, 43 exhibited ESBL-positive phenotypes. A subset of 19 isolates was then selected for WGS analysis based on their phenotypic resistance out of these ESBL-positive phenotypes in order to increase the chance of inferring transmission dynamics for this subset of strains, while also trying to retain samples highly resistant to different antibiotics and originating from the four different hospitals. An overview of the selected isolates is provided in **Table 1**.

[1]https://bitbucket.org/genomicepidemiology/resfinder_db/src/master/antibiotic_classes.txt

Whole-Genome Sequencing

DNA extraction for selected isolates was done by using the Qiagen universal Biorobot (Limburg, Netherlands) according to the manufacturer's instructions. Isolate sequencing libraries were created using Nextera XT DNA library preparation (Illumina, San Diego, CA) according to the manufacturer's instructions, and subsequently underwent Illumina sequencing using the MiSeq V3 chemistry (Illumina, San Diego, CA) for production of 2 × 250 bp paired-end reads. All sequencing data have been submitted to SRA (Leinonen et al., 2011) under BioProject PRJNA701417, and individual accession numbers are provided in **Supplementary Table S1**.

WGS-Based Isolate Characterization

All WGS reads were trimmed and *de novo* assembled using SPAdes (Bankevich et al., 2012) as described in Bogaerts et al. (2021). Detection of AMR genes was performed as described in Bogaerts et al. (2019) using the sequences from the NCBI NDARO database (downloaded on March 27, 2020; Feldgarden et al., 2019). Hits with less than 90% sequence identity or less than 90% target coverage were filtered out. A local installation of PointFinder (checked out from BitBucket on February 27, 2019; Zankari et al., 2017) was used to detect mutations associated with AMR. Phenotypic resistance was predicted when at least one gene or mutation was detected with resistance to the corresponding antibiotic(s). Isolates were then typed using the methodology described in Bogaerts et al. (2019) using the classic MLST and cgMLST schemes from EnteroBase (Zhou et al., 2020), downloaded on the September 6, 2020. The putative genetic origin (i.e., chromosomal or plasmidic) of the detected resistance genes was evaluated by classifying the corresponding contigs using the "mob-recon" command from MOB-suite 3.0.0 with default settings (Robertson and Nash, 2018).

The samples were screened for contaminants using Kraken 2 2.0.7 (Wood and Salzberg, 2014) with default parameters and an in-house database containing all NCBI RefSeq Genome entries with the "Complete Genome" assembly level (database accessed February 18, 2019; O'Leary et al., 2016) accession prefixes NC, NW, AC, NG, NT, NS, and NZ of the following taxonomic groups: archaea, bacteria, fungi, human, protozoa, and viruses. Samples for which Kraken 2 classified more than 5% of reads to a species other than *E. coli* were considered contaminated. For these samples, reads classified as the contaminant species (up to the genus level) were removed before the *de novo* assembly. All subsequent analyses were performed on these cleaned assemblies.

Comparison of Phenotypic and Genotypic Predicted AMR Susceptibility

Correspondence with observed phenotypic resistance was evaluated using the following definitions: true positive (TP)

TABLE 1 | Overview of the 19 samples sequenced in this study.

Sample name	Hospital	Ward	Collection date	Surgical intervention	Patient age	Patient sex
s_12116	D	GI	October 15, 2019	Peritonitis	18	Female
s_12117	D	GI	October 15, 2019	Peritonitis	18	Male
s_12155	C	M	October 16, 2019	Caesarean	26	Female
s_12301	C	M	October 20, 2019	Caesarean	35	Female
s_12414	B	GI	October 22, 2019	NA	36	Male
s_12479	C	M	October 23, 2019	Caesarean	22	Female
s_12480	D	M	October 23, 2019	Caesarean	34	Female
s_12845	D	GI	October 31, 2019	Appendicitis	18	Male
s_12849	D	GI	October 31, 2019	Appendicitis	21	Male
s_13022	D	GI	November 08, 2019	Evisceration	55	Female
s_13150	A	GI	November 08, 2019	Peritonitis	40	Female
s_13959	A	GI	November 26, 2019	Appendicitis	52	Female
s_13987	B	GI	November 26, 2019	Appendicitis	23	Female
s_3117	A	M	November 12, 2019	Caesarean	32	Female
s_316	D	GI	November 28, 2019	Appendicitis	23	Male
s_317	D	GI	June 06, 2019	Appendicitis	33	Male
s_4294	D	GI	June 04, 2019	NA	36	Male
s_6558	D	GI	May 30, 2019	NA	35	Male
s_90	A	M	November 28, 2019	Caesarean	28	Female

M, maternal; GI, gastro-internal; and NA, Not available.

and false negative (FN) as cases with phenotypic resistance to an antibiotic where the WGS-based workflow predicted resistance and susceptibility, respectively, and true negative (TN) and false positive (FP) as cases with phenotypic susceptibility to an antibiotic where the WGS-based workflow predicted susceptibility and resistance, respectively. This comparison was limited to six of the tested antibiotics for which the NDARO database or PointFinder databases contained at least one entry. For the remaining 10 antibiotics, the WGS workflow could only perform predictions at the level of the parent class since the database only contains information up to this level. For example, the NDARO database contains genes annotated as associated with resistance to cephalosporins, but it does not provide information on resistance to specific members of this class, such as cefepime or cefotaxime.

Phylogenomic Analysis

The relatedness between samples from this study was first determined by constructing phylogenies based on cgMLST results. Allele matrices were filtered by removing samples with less than 90% of loci detected and afterward removing loci detected in less than 90% of samples. Minimum spanning trees (MSTs) were then constructed from the filtered allele matrices using GrapeTree 2.2 (Zhou et al., 2017) with the "method" option set to "MSTreeV2." The phylogeny was visualized and annotated in the web-based iTOL platform (Letunic and Bork, 2019). The broader phylogenomic context of samples was also investigated by including all assemblies assigned to any of the STs detected in our samples collected after 2018 in Africa or Europe, retrieved from EnteroBase on January 19, 2021. Initially, only samples from Africa were collected, but since only very few samples matched these criteria, the dataset was extended with samples from Europe. Separate MSTs were then constructed for the six STs with at least two samples from this study (ST38, ST131, ST405, ST410, ST617, and ST1193) using the same methodology as described above. Additionally, Single-nucleotide polymorphism (SNP) addresses were determined using SnapperDB 1.0.6 (Ashton et al., 2015) and PHEnix v1.4.1,[2] as described previously (Nouws et al., 2020), for all newly sequenced samples and genomes retrieved from EnteroBase with available WGS Illumina data. An additional filtering step was introduced to remove SNPs located in regions of the reference genomes flagged as prophages by PHAST (Zhou et al., 2011) with default settings. The SNP address is a strain level 7-digit nomenclature based on the number of pairwise SNP differences. Each digit represents the cluster membership for the given number of SNP differences, starting (right to left) with 0 (i.e., no SNP differences) to 5, 10, 25, 50, 100, and 250. Isolates sharing the same cluster digit differ by fewer than the corresponding number of SNPs (Ashton et al., 2015). An example of the SNP address methodology is provided in **Supplementary Figures S2–S3**. The minimum required average mapping depth was lowered to 25x to ensure all samples from this study could be analyzed. Reference genomes from the corresponding ST were selected randomly from all genomes available in EnteroBase (**Supplementary Table S2**) for the respective STs but only considering complete genomes. Sequences with a "plasmid" annotation in the header were removed from the reference genomes before running the SNP typing analysis. AMR prediction for public genomes was performed as described above (phenotypic AMR susceptibility information was not available for these genomes).

[2]https://github.com/phe-bioinformatics/PHEnix

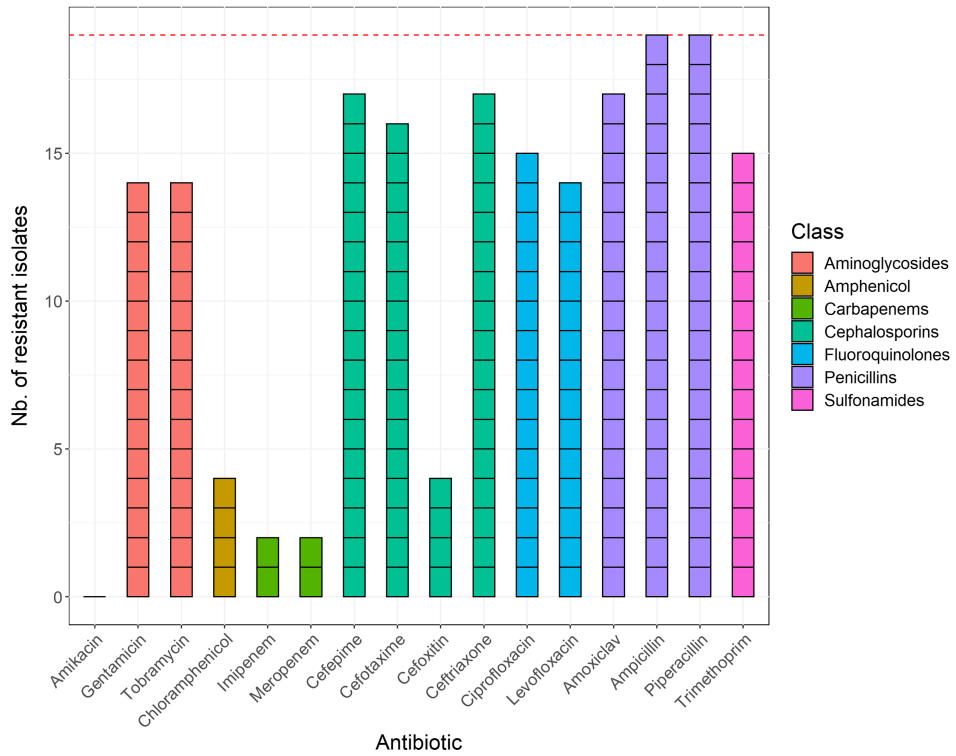

FIGURE 1 | Results of phenotypic antimicrobial susceptibility testing of the 19 sequenced *E. coli* isolates. Bars are colored according to the corresponding class of antibiotics. The red horizontal line corresponds to the total number of isolates ($n = 19$). Trimethoprim + sulfamethoxazole was abbreviated to trimethoprim and amoxicillin + clavulanic acid to amoxiclav.

RESULTS

Phenotypic Antimicrobial Susceptibility Testing

An overview of AMR susceptibility testing results of the 19 selected ESBL-positive isolates is provided in **Figure 1**. All 19 isolates exhibited resistance to ampicillin and piperacillin. Most samples also displayed low susceptibility to amoxicillin-clavulanic acid, cefepime, cefotaxime, ceftriaxone, ciprofloxacin, gentamycin, levofloxacin, tobramycin, and trimethoprim + sulfamethoxazole. Four isolates showed resistance to cefoxitin and chloramphenicol, while two isolates showed resistance to imipenem and meropenem. None of the tested isolates exhibited resistance to amikacin.

Isolate Characterization Based on WGS Data

Overviews of read trimming and *de novo* assembly statistics for the sequenced isolates are provided in **Supplementary Tables S3** and **S4**, respectively. Assembly statistics indicated generally high quality, with a median total assembly length of 5,064,374 bp and N50 of 168,657 bp. Samples s_316 and s_4294 were outliers with a larger total assembly length (9,568,828 bp and 8,564,805 bp, respectively) and smaller N50 (40,329 bp and 69,875 bp, respectively). Kraken 2 analysis indicated that these samples also contained reads from *Acinetobacter* besides *E. coli*, likely explaining their increased cumulative assembly lengths and lower N50. Notwithstanding, only a minor fraction of the total reads was identified as *Acinetobacter*, indicating that enough *E. coli* reads were present in both samples to be retained for further analysis. Reads classified as *Acinetobacter* were therefore removed before performing a new *de novo* assembly, which was used for further analysis for these two samples. We performed additional analysis to confirm that the contamination indicated by Kraken 2 in these two samples was not due to a plasmid, but rather due to the presence of an *Acinetobacter baumannii* strain, for which results are provided in the **Supplementary Material**. The 19 samples were classified into 13 different STs: ST10 (n: 1), ST38 (n: 2), ST127 (n: 1), ST131 (n: 2), ST167 (n: 1), ST354 (n: 1), ST405 (n: 2), ST410 (n: 2), ST569 (n: 1), ST617 (n: 2), ST648 (n: 1), ST1193 (n: 2), and ST2659 (n: 1), as indicated in **Supplementary Table S5**.

Genotypic WGS-Based AMR Characterization

We detected several beta-lactam resistance genes across our samples, including $bla_{\text{CTX-M-15}}$, $bla_{\text{CMY-42}}$, bla_{EC}, $bla_{\text{OXA-1}}$, $bla_{\text{OXA-181}}$, and $bla_{\text{TEM-1}}$. We also detected the *aph(3″)-Ib* (68.4%, n = 13) and *aph(6)-Id* (73.7%, n = 14) genes associated with resistance

to streptomycin, in the large majority of samples, as well as the *aac(6′)-Ib-cr* gene (73.7%, n = 14), responsible for a reduction in ciprofloxacin activity. Four different fluoroquinolone resistance determinants were observed [*qnrS1*, *qepA8*, *qepA4*, and *aac*(*6′*)-*Ib-cr*]. Other AMR genes that were detected were associated with trimethoprim resistance (*dfrA8*, *dfrA12*, *dfrA14*, and *dfrA17*), macrolide resistance *mph(A)*, sulphonamide resistance (*sul1*, *sul2*), tetracycline resistance *tet(A)* and *tet(B)*, and phenicol resistance (*catA1*). Additionally, 16 isolates carried at least one nonsynonymous mutation in the housekeeping genes *parC* S80I, *gyrA* S83L, *gyrA* D87N, and *parE* S458A, which are associated with resistance to fluoroquinolones.

A complete overview of the detected AMR genes, point mutations, and predicted phenotypes with WGS is provided in **Supplementary Table S6**. The majority of resistance genes was located on contigs with a plasmid origin predicted by MOB-suite, as indicated in **Supplementary Table S7**. Resistance was most commonly predicted for cephalosporins (all 19 samples), tetracycline ($n = 18$), and quinolones ($n = 17$).

Comparison of Phenotypic and Genotypically Predicted AMR Susceptibility

Full results for comparing genotypically predicted and observed phenotypic AMR profiles are provided in **Supplementary Table S8**. Out of 62 resistant phenotypes, 60 were predicted correctly (i.e., TP). Sample s_12117 was incorrectly predicted as sensitive to gentamicin, and sample s_4294 to tobramycin. While sample s_4294 was flagged as contaminated by our Kraken 2 analysis, we confirmed that these mismatches were not caused by the additional filtering step because no associated genes were presented in unfiltered assemblies (results not shown). Out of 52 susceptible phenotypes, 34 were predicted correctly (i.e., TN). The large majority of the 18 FP was limited to amikacin ($n = 14$) and caused by the detection of the *aac*(*6′*)-*Ib* gene in susceptible samples. The presence of this gene likely does not suffice for phenotypic resistance at the tested dosage (see also section "Discussion"). Similarly, for resistance to ciprofloxacin, the two FP samples, s_13022 and s_90, only carried the *gyrA* S83L mutation, while TP samples also carried multiple other mutations, including *gyrA* D87N, *parC* S80I, and *parE* L416F. Combining the predictions across all samples resulted in WGS-based prediction accuracy of 82.5%, precision of 76.9%, sensitivity of 96.8%, and specificity of 65.4%. When discarding the results for amikacin, the accuracy increased to 93.6%, precision to 93.8%, sensitivity to 96.8%, and specificity to 87.5%.

Phylogenomic Analysis

More than 90% of cgMLST loci were detected in all samples from this study. The resulting MST is shown in **Figure 2**. Generally, considerable phylogenetic differences were observed, with large branch lengths between isolates assigned to different STs. Six groups of two isolates with the same sequence type were found, i.e., ST38, ST131, ST405, ST410, ST617, and ST1193. Samples assigned to ST38 and ST617 differed by 190 and 34 cgMLST alleles, respectively. These relatively large genetic differences indicate that epidemiological links between these cases are unlikely, and the corresponding phylogenies are therefore not discussed in the main manuscript, but a description of the phylogenomic context for these samples can be found in the **Supplementary Material**. Results for the isolates assigned to the other four STs are described in detail below, in order of decreasing phylogenomic similarity based on cgMLST distance (i.e., cluster with most closely related samples from Benin first). SNP distance matrices for the isolates included in the SNP analysis are provided in **Supplementary Tables S9–S12**.

ST405 Cluster

The phylogeny for this ST was constructed using 24 additional genomes retrieved from EnteroBase that matched the criteria listed in the Material and Methods. No additional samples from Africa were available. The MST based on cgMLST for this ST is shown in **Figure 3A**, along with their corresponding SNP addresses. The two samples from this study in this cluster, s_317 and s_3117, were identical based on both cgMLST and SNP typing and exhibited identical phenotypic and genotypic AMR profiles. These results indicate that both isolates are identical, despite being obtained from different patients at different hospitals with 16 days in between. Phenotypic testing of these samples revealed resistance to 8 of the 16 tested antibiotics. The most similar isolate from EnteroBase was ESC_RB8807_AS, collected in Switzerland in 2019, which differed by three cgMLST loci, but WGS read data were not available for this sample rendering it impossible to investigate relatedness based on SNPs.

ST131 Cluster

The phylogeny for this ST was constructed using an additional 74 genomes retrieved from EnteroBase, which only contained two additional samples from Africa. The MST based on cgMLST and SNP addresses for this ST are shown in **Figure 3B**. The two samples from this study, s_13987 and s_13959, differed by only three cgMLST loci and had identical phenotypic and similar genotypic AMR profiles (the beta-lactamase gene bla_{TEM} was present in only s_13959) but still differed with between 100 and 250 SNPs according to their SNP address. A point source outbreak is therefore unlikely with this amount of observed variation, despite their close time of isolation (both samples were obtained on the same day). Additionally, both samples were obtained in different hospitals. Compared to the samples retrieved from EnteroBase, ESC_JB0483AA_AS isolated in Spain in 2018 was the most closely related isolate but still differed by 47 cgMLST loci. Predicted AMR susceptibility to different antibiotics was widespread in this cluster but did not correlate to the typology of the tree.

ST1193 Cluster

The phylogeny for this ST was constructed using six additional samples retrieved from EnteroBase. No additional samples from Africa were available. The MST based on cgMLST and SNP addresses for this ST are shown in **Figure 3C**. The two samples

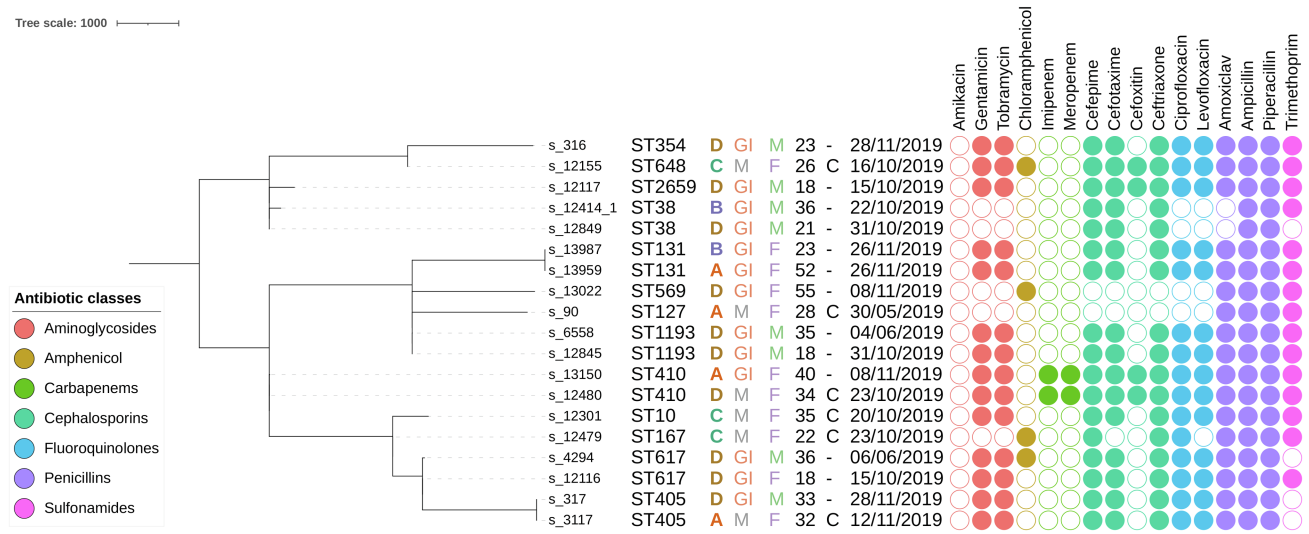

FIGURE 2 | Minimum spanning tree containing all *E. coli* samples sequenced in this study based on cgMLST results. The scale bar expresses the number of allele differences. Annotations are (from left to right) sample name, sequence type (based on classical MLST), hospital letter code, hospital ward, patient gender, patient age, surgical intervention, isolation date, and phenotypically determined AMR susceptibility (a filled circle indicates phenotypic resistance to the corresponding antibiotic). Circles are colored according to the class of the antibiotic as indicated in the legend in the bottom left corner. Abbreviations: maternal (M), gastrointestinal (GI), male (M), female (F), and caesarian (C).

from this study, s_6558 and s_12845, differed by five cgMLST alleles and between 50 and 100 SNPs and exhibited identical phenotypic and genotypic AMR profiles. Both samples were obtained from the same hospital with several months in between (as seen in ST617, described in the **Supplementary Results**). Similar to the two samples from the ST131 cluster, a point source outbreak appears therefore unlikely.

ST410 Cluster

The phylogeny for this ST was constructed using 23 additional samples retrieved from EnteroBase. Only one additional sample from Africa was available. The MST based on cgMLST and SNP addresses for this ST are shown in **Figure 3D**. The two samples from this study, s_12480 and s_13150, differed by 15 cgMLST alleles and between 50 and 100 SNPs. Compared to the samples from this study assigned to other STs, the number of allele differences was quite large compared to the number of SNP differences. Additional screening against inter- and intraspecies contamination did not reveal issues with either sample (results not shown). Both samples exhibited identical phenotypic and genotypic AMR profiles, which both indicated very high rates of resistance. Given the sizable genomic distance between both samples, and the fact they were collected in different hospitals, an epidemiological link between both samples appears unlikely. The only publicly available sample from Africa for this cluster, ESC_FB9431AA_AS, was collected in Nigeria (a neighboring country of Benin) in 2018 but was quite distant from the samples from Benin. The most similar sample from EnteroBase was ESC_FB0885AA_AS, which differed 13 alleles to s_12480 and 12 alleles to s_13150. Since no read data were available for this sample, the SNP address could not be determined.

DISCUSSION

To the best of our knowledge, this is the first study that employs WGS to investigate AMR profiles and phylogenomic relatedness among clinical *E. coli* isolated in Benin.

All of the 19 selected *E. coli* isolates showed phenotypic resistance to at least four of the 16 phenotypically tested antibiotics, and 14 samples showed resistance to 10 or more. These observations are in line with our previous study conducted in 2019 in the same hospitals, in which we reported 208 MDR-positive samples on a total of 229 aerobic bacteria (90.8%; Yehouenou et al., 2020). High resistance rates were observed in all isolates, especially to aminoglycosides, cephalosporins, penicillins, quinolones, and trimethoprim + sulfamethoxazole. Two isolates were also resistant to carbapenems, which was also observed recently in Nigeria (Aworh et al., 2021), and four were resistant to amphenicol. The high degree of AMR in our study is not surprising, as these antibiotics (ceftriaxone, ciprofloxacin, and beta-lactamases) are easily accessible and commonly used in Benin for therapeutic purposes and very few antimicrobial stewardship programs are in place.

The $bla_{\text{CTX-M-15}}$ gene is the most frequently reported gene that encodes for CTX-M enzymes in ESBLs (Zhao and Hu, 2013) and was observed in 15 isolates (78.9%) in this study. Four of those isolates also harbored *ampC* genes (bla_{CMY}) and other beta-lactamase genes ($bla_{\text{TEM-1}}$). AmpC beta-lactamases are cephalosporinases that are poorly inhibited by clavulanic acid. The co-occurrence of multiple AmpC beta-lactamases was previously reported in *E. coli* in Tunisia (Chérif et al., 2016) and various other studies, especially in isolates collected in African countries (Ribeiro et al., 2016; Sonda et al., 2018; Irenge et al., 2019; Jesumirhewe et al., 2020). These findings suggest that genes

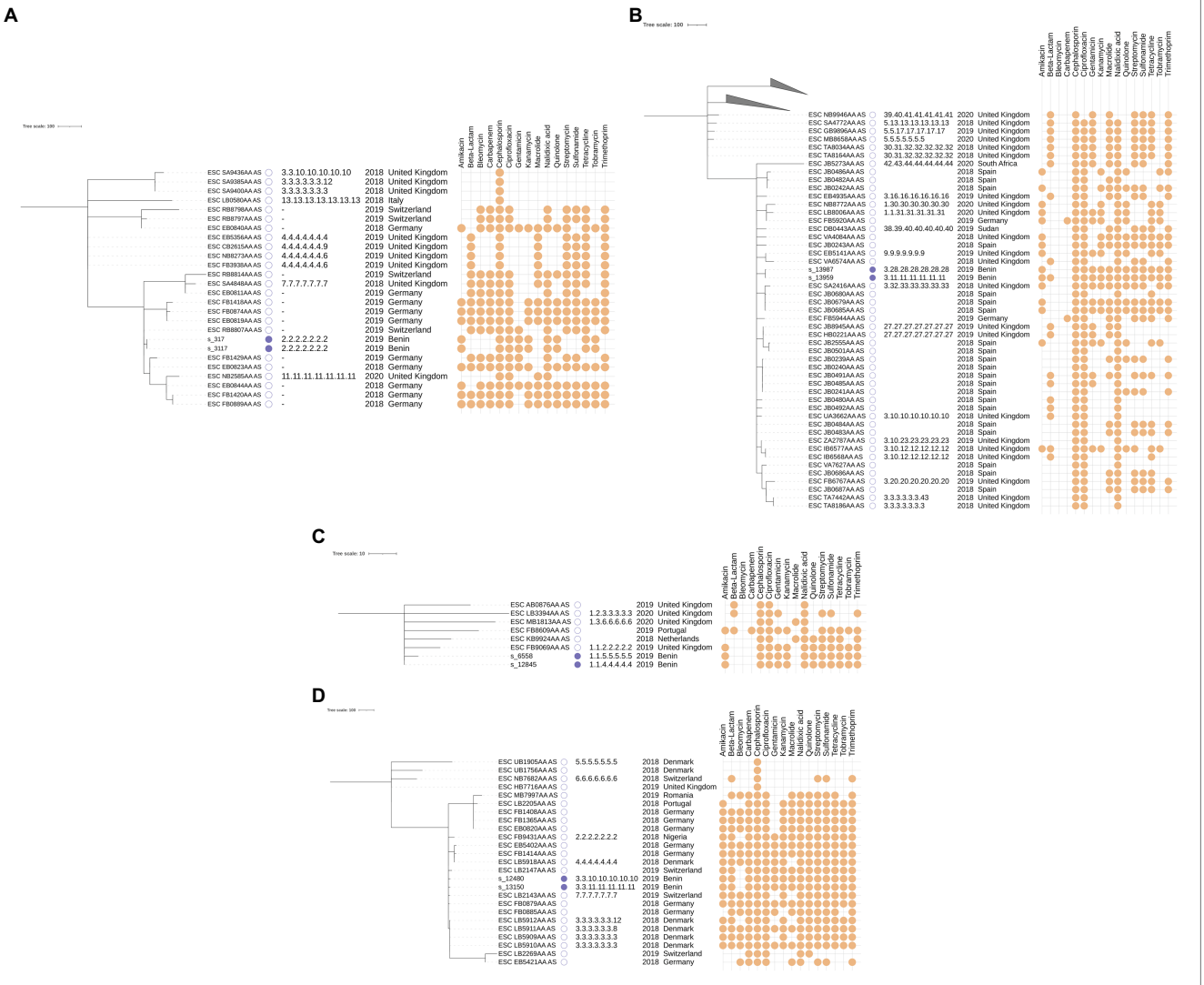

FIGURE 3 | cgMLST-based minimum spanning trees annotated with SNP typing results for samples classified as ST405 **(A)**, ST131 **(B)**, ST1193 **(C)**, and ST410 **(D)**. The scale bar and branch lengths are expressed as the number of allele differences. Annotations are (from left to right) as: sample name, sample origin (this study with a filled blue box or EnteroBase with an empty box), SNP address, isolation year, isolation country, and predicted AMR susceptibility based on genotypic AMR prediction. Samples with missing SNP addresses did not have publicly available Illumina paired-end data or were filtered out because their coverage was too low. Predicted AMR susceptibility is shown for the 16 antibiotics that were most often predicted (full results are provided in **Supplementary Table S5**). The top two clades in subfigure **B** were collapsed for visual clarity and contain 18 and 9 isolates, respectively.

from the CTX-M family are currently replacing SHV and TEM in *Enterobacterales*, as reported previously (Camacho et al., 2009).

In our study, 78.9% of ESBL-producing strains ($n = 15/19$) exhibited phenotypic resistance to quinolones, consistent with the previously reported association between ESBL production and quinolone resistance in *Enterobacterales* (Robicsek et al., 2006). This association might be explained by co-selection between ESBL and other AMR genes when exposed to various antimicrobials (Robicsek et al., 2006; Crémet et al., 2011). The *aac*(6′)-*Ib-cr* was observed frequently and was present in 14 strains. This gene has spread rapidly among *Enterobacterales*, and although conferring only low-level resistance, it may create an environment that facilitates the selection of highly resistant determinants, especially in organisms harboring other quinolone resistance determinants (Roy et al., 2021).

Out of 62 resistant phenotypes, 60 were correctly genotypically predicted, leading to an accuracy of 82.5%, which is considerably lower than other studies (Kozyreva et al., 2017; Bogaerts et al., 2021). Performance was mainly impacted by lower specificity due to predicted resistances supported only by a single genomic feature, which might not have been sufficient for resistance at the tested dosage. For example, samples s_13022 and s_90 carried the *gyrA* p.S83L mutation, associated with fluoroquinolone resistance, but still were susceptible to the antibiotic. Other samples,

such as s_12116 or s_12117, did exhibit phenotypic resistance but also carried three additional mutations associated with resistance to ciprofloxacin. We assume that a similar effect caused the FP predictions for amikacin. This hypothesis is also supported by the fact that our predictions for this antibiotic matched with the results of the NCBI AMRFinderPlus (Feldgarden et al., 2019) and online ResFinder (Zankari et al., 2012) tools (unpublished results). Accuracy increased to 93.6% when the results for amikacin were removed, in line with the performance obtained in the aforementioned studies.

We used MOB-suite to determine the genetic origin of the detected resistance genes as they are known to be frequently or almost exclusively plasmid-encoded (Brolund, 2014), associated with a higher risk of spreading. This analysis confirmed that most of the detected AMR genes were found on contigs predicted to be plasmid-encoded. However, this analysis might have suffered from lower accuracy since only short-read data were available. In future investigations, employing long-read sequencing might therefore be a promising alternative because longs reads can substantially facilitate predicting the genomic origin of detected AMR genes (Lemon et al., 2017; Berbers et al., 2020).

We observed 13 different sequence types with six STs (ST131, ST617, ST38, ST1193, ST410, and ST405) occurring twice, consistent with earlier observations in Tanzania where the same six STs were observed in a collection of 38 *E. coli* samples (Sonda et al., 2018). Resistance to cephalosporins and ciprofloxacin has often been reported in strains classified as ST131 (Cagnacci et al., 2008; Aibinu et al., 2012). The presence of other genetic lineages different from ST131 shows the potential for genetic diversification and emergence of new epidemic strains (Xu et al., 2011). In particular, the association of these clones with quinolone resistance, by carrying the often plasmid-encoded *qnr*, or, *aac-(6′)-Ib-cr* genes, is very worrisome due to its potential for further dissemination.

Although some STs (e.g., ST410) were found to contain more AMR determinants than other STs (e.g., ST38), AMR profiles were generally not correlated with the phylogeny (see **Figure 3**), suggesting that horizontal transfer of AMR genes is common, as also shown in numerous other studies on *E. coli* (Rodriguez-Villalobos et al., 2005; Upreti et al., 2018; Nwafia et al., 2019). Nevertheless, some genes have been reported to be associated with particular STs, such as the $bla_{\text{CTX-M-15}}$ gene, which is often present in the ST131 and ST410 isolates (Tegha et al., 2021), as also observed in this study (**Supplementary Table S6**).

We observed a generally large diversity among the analyzed *E. coli* strains circulating in the hospitals in Benin. The large phylogenomic differences between the isolates suggest that the infections were caused by multiple generally not very closely related *E. coli* strains, the notable exceptions being samples s_317 and s_3117, which were completely identical. Within individual hospitals, the two most closely related samples differed by at least five cgMLST alleles, i.e., samples s_12845 and s_6558 that were both isolated in hospital D. This diversity was also reflected in the number of observed STs with most samples belonging to different STs and only six STs that contained two isolates. Investigation of the samples assigned to the same STs indicated at least one ST in which both samples were identical (ST405); two STs with samples that were relatively closely related based on cgMLST, with 15 and 5 cgMLST alleles difference, but still differed by between 50 and 100 SNPs (ST410 and ST1193, respectively); and one ST with samples that were closely related based on cgMLST but still differed by between 100 and 250 SNPs (ST131). The sequenced isolates did therefore not indicate a pattern of hospital-acquired and transmitted infections, since they were either identical but isolated in different hospitals (ST405); relatively related but isolated in different hospitals (ST410); or their overall number of SNPs differed by at least 100 (ST38, ST131, ST617, and ST1193). It should be highlighted that these observations do not imply that no hospital-acquired infections and transmissions took place in Benin in 2019, which would be highly unlikely, given that multiple studies have shown that such transmissions constitute a major problem for nosocomial *E. coli* (Peleg and Hooper, 2010; Matta et al., 2018). Most likely, we did not observe such infections and transmissions because not enough samples were isolated and sequenced. More WGS-based screening is required to fully capture the transmission dynamics of the circulating strains. Nevertheless, we did observe a pattern suggestive of sporadic introductions of diverse strains into hospitals from the community, which corroborates results obtained in Tanzania by Sonda et al. in 2018, who observed 21 different sequence types in a collection of 38 clinical *E. coli*, the most common of which were ST131 and ST10 (Sonda et al., 2018). Jesumirhewe et al. observed ST131, ST405, and ST410 in a collection of 17 clinical *E. coli* isolated in Nigeria (Jesumirhewe et al., 2020). ST131 is the dominant international clinical clone, and ST405 was previously associated with the carriage of ESBLs (Aibinu et al., 2012). ST410 has been reported worldwide in extra-intestinal strains associated with resistance to fluoroquinolones, third-generation cephalosporins, and carbapenems (Roer et al., 2018).

Although a few samples in our study were related to isolates sampled in Europe in the background collection retrieved from EnteroBase, only distant phylogenetic relationships could be observed for most of them. This indicates that the background collection is missing isolates to provide the proper phylogenomic context for the samples in our study. This can be explained by the lack of available WGS data from Africa, which accounted for only a very minor fraction of the total dataset (with only two isolates for ST131 and one for ST410 being available). Consequently, the gap in available data and surveillance for Benin and Africa renders it impossible to study the history of the transmission and spread of these *E. coli* isolates within Benin and in a broader African context, and to investigate the relatively close relationship of some samples with European samples. To better understand the spread and dispersion of AMR and pathogenic *E. coli* in Africa, more extensive monitoring in this region, including by WGS, is required.

CONCLUSION

We report the first WGS-based analysis of AMR and phylogenomics relatedness of 19 clinical ESBL-positive samples collected from Benin in 2019. Although our study was limited by the relatively low number of sequenced samples, this provides a first genomic resource for Benin. In particular, the observed high levels of *E. coli* diversity regarding their antimicrobial resistance genes and sequence types underline the necessity for concerted efforts to routinely screen more bacterial isolates of clinical importance, even in resource-limited settings, such as Benin. Increased WGS-based surveillance will aid to fill the gaps in observed genotypes and help improve our understanding of the transmission dynamics and the prevalence of AMR genes in *E. coli* within Benin, and by extension, Africa. The information generated in this study not only provides updates on AMR at the hospital level but can also serve as a basis in formulating pragmatic antimicrobial stewardship programs and infection control initiatives, and accentuates the need for the competent authorities to provide more resources to study drug-resistant infections circulating in Benin by means of WGS.

DATA AVAILABILITY STATEMENT

The datasets supporting the conclusions of this study have been deposited in the NCBI SRA under BioProject PRJNA633966. Metadata and individual accession numbers are available in the **Supplementary Material**.

AUTHOR CONTRIBUTIONS

CY, OD, FD, DA, and AS conceived and designed the study. BB, KV, NR, SK, and KM designed and performed the WGS and bioinformatics analysis. CY, ET, BB, and KV wrote the original draft of the manuscript. All authors contributed to the article and approved the submitted version.

FUNDING

This study received financial support from the ARES (Académie de la Recherche pour l'Enseignement Supérieur; Grant number: COOP-CONV-18-108), Belgium.

ACKNOWLEDGMENTS

We acknowledge the team of the bacteriology laboratory of CNHU for their assistance with recruitment and data collection from study participants. We thank the technicians of the service Transversal activities in Applied Genomics at Sciensano, Belgium, for performing the Next-Generation Sequencing runs.

SUPPLEMENTARY MATERIAL

The Supplementary Material for this article can be found online at: https://www.frontiersin.org/articles/10.3389/fmicb.2021.752883/full#supplementary-material

REFERENCES

Aibinu, I., Odugbemi, T., Koenig, W., and Ghebremedhin, B. (2012). Sequence type ST131 and ST10 complex (ST617) predominant among CTX-M-15-producing Escherichia coli isolates from Nigeria. *Clin. Microbiol. Infect.* 18, E49–E51. doi: 10.1111/j.1469-0691.2011.03730.x

Anago, E., Ayi-Fanou, L., Akpovi, C. D., Hounkpe, W. B., Agassounon-Djikpo Tchibozo, M., Bankole, H. S., et al. (2015). Antibiotic resistance and genotype of beta-lactamase producing Escherichia coli in nosocomial infections in Cotonou, Benin. *Ann. Clin. Microbiol. Antimicrob.* 14, 1–6. doi: 10.1186/s12941-014-0061-1

Ashton, P., Nair, S., Peters, T., Tewolde, R., Day, M., Doumith, M., et al. (2015). Revolutionising public health reference microbiology using whole genome sequencing: Salmonella as an exemplar bioRxiv:033225. doi: 10.1101/033225,

Asokan, G. V., Ramadhan, T., Ahmed, E., and Sanad, H. (2019). WHO global priority pathogens list: A bibliometric analysis of medline-pubmed for knowledge mobilization to infection prevention and control practices in Bahrain. *Oman Med. J.* 34, 184–193. doi: 10.5001/omj.2019.37

Aworh, M. K., Kwaga, J. K. P., Hendriksen, R. S., Okolocha, E. C., and Thakur, S. (2021). Genetic relatedness of multidrug resistant Escherichia coli isolated from humans, chickens and poultry environments. *Antimicrob. Resist. Infect. Control* 10, 58–13. doi: 10.1186/s13756-021-00930-x

Bankevich, A., Nurk, S., Antipov, D., Gurevich, A. A., Dvorkin, M., Kulikov, A. S., et al. (2012). SPAdes: A new genome assembly algorithm and its applications to single-cell sequencing. *J. Comput. Biol.* 19, 455–477. doi: 10.1089/cmb.2012.0021

Berbers, B., Saltykova, A., Garcia-Graells, C., Philipp, P., Arella, F., Marchal, K., et al. (2020). Combining short and long read sequencing to characterize antimicrobial resistance genes on plasmids applied to an unauthorized genetically modified bacillus. *Sci. Rep.* 10, 4310. doi: 10.1038/s41598-020-61158-0

Bogaerts, B., Nouws, S., Verhaegen, B., Denayer, S., Van Braekel, J., Winand, R., et al. (2021). Validation strategy of a bioinformatics whole genome sequencing workflow for Shiga toxin-producing Escherichia coli using a reference collection extensively characterized with conventional methods. *Microb. Genomics* 7:000531. doi: 10.1099/mgen.0.000531

Bogaerts, B., Winand, R., Fu, Q., Van Braekel, J., Ceyssens, P. J., Mattheus, W., et al. (2019). Validation of a bioinformatics workflow for routine analysis of whole-genome sequencing data and related challenges for pathogen typing in a European national reference center: Neisseria meningitidis as a proof-of-concept. *Front. Microbiol.* 10:362. doi: 10.3389/fmicb.2019.00362

Bradford, P. A. (2001). Extended-spectrum β-lactamases in the 21st century: characterization, epidemiology, and detection of this important resistance threat. *Clin. Microbiol. Rev.* 14, 933–951. doi: 10.1128/CMR.14.4.933-951.2001

Brolund, A. (2014). Overview of ESBL-producing Enterobacterales from a nordic perspective. *Infect. Ecol. Epidemiol.* 4, 4. doi: 10.3402/iee.v4.24555

Cagnacci, S., Gualco, L., Debbia, E., Schito, G. C., and Marchese, A. (2008). European emergence of ciprofloxacin-resistant Escherichia coli clonal groups O25:H4-ST 131 and O15:K52:H1 causing community-acquired uncomplicated cystitis. *J. Clin. Microbiol.* 46, 2605–2612. doi: 10.1128/JCM.00640-08

Camacho, C., Coulouris, G., Avagyan, V., Ma, N., Papadopoulos, J., Bealer, K., et al. (2009). BLAST+: architecture and applications. *BMC Bioinformatics* 10, 421. doi: 10.1186/1471-2105-10-421

Cantón, R., González-Alba, J. M., and Galán, J. C. (2012). CTX-M enzymes: origin and diffusion. *Front. Microbiol.* 3. doi: 10.3389/fmicb.2012.00110

Chérif, T., Saidani, M., Decré, D., Boutiba-Ben Boubaker, I., and Arlet, G. (2016). Cooccurrence of multiple AmpC β-lactamases in Escherichia coli, Klebsiella pneumoniae, and Proteus mirabilis in Tunisia. *Antimicrob. Agents Chemother.* 60, 44–51. doi: 10.1128/AAC.00828-15

Crémet, L., Caroff, N., Dauvergne, S., Reynaud, A., Lepelletier, D., and Corvec, S. (2011). Prevalence of plasmid-mediated quinolone resistance determinants in ESBL Enterobacteriaceae clinical isolates over a 1-year period in a French hospital. *Pathol. Biol.* 59, 151–156. doi: 10.1016/j.patbio.2009.04.003

EUCAST (2015). The European Committee on Antimicrobial Susceptibility Testing. Breakpoint tables for interpretation of MICs and zone diameters, version 5.0. Available at: http://www.eucast.org/clinical_breakpoints/

Feldgarden, M., Brover, V., Haft, D. H., Prasad, A. B., Slotta, D. J., Tolstoy, I., et al. (2019). Validating the AMRFINder tool and resistance gene database by using antimicrobial resistance genotype-phenotype correlations in a collection of isolates. *Antimicrob. Agents Chemother.* 63, 1–19. doi: 10.1128/AAC.00483-19

Hall, B. G., and Barlow, M. (2005). Revised ambler classification of β-lactamases [1]. *J. Antimicrob. Chemother.* 55, 1050–1051. doi: 10.1093/jac/dki130

Harbarth, S., Balkhy, H. H., Goossens, H., Jarlier, V., Kluytmans, J., Laxminarayan, R., et al. (2015). Antimicrobial resistance: one world, one fight! *Antimicrob. Resist. Infect. Control* 4, 1–15. doi: 10.1186/s13756-015-0091-2

Irenge, L. M., Ambroise, J., Bearzatto, B., Durant, J. F., Chirimwami, R. B., and Gala, J. L. (2019). Whole-genome sequences of multidrug-resistant Escherichia coli in south-Kivu Province, Democratic Republic of Congo: characterization of phylogenomic changes, virulence and resistance genes. *BMC Infect. Dis.* 19, 1–10. doi: 10.1186/s12879-019-3763-3

Jesumirhewe, C., Springer, B., Allerberger, F., and Ruppitsch, W. (2020). Whole genome sequencing of extendedspectrum β-lactamase genes in Enterobacteriaceae isolates from Nigeria. *PLoS One* 15, 1–11. doi: 10.1371/journal.pone.0231146

Koudokpon, H., Dougnon, V., Hadjadj, L., Kissira, I., Fanou, B., Loko, F., et al. (2018). First sequence analysis of genes mediating extended-spectrum beta-lactamase (ESBL) bla-TEM, SHV- and CTX-M production in isolates of Enterobacteriaceae in Southern Benin. *Int. J. Infect.* doi: 10.5812/iji.83194, (in press)

Kozyreva, V. K., Truong, C. L., Greninger, A. L., Crandall, J., Mukhopadhyay, R., and Chaturvedi, V. (2017). Validation and Implementation of Clinical Laboratory Improvements Act-Compliant Whole-Genome Sequencing in the Public Health Microbiology Laboratory. *J. Clin. Microbiol.* 55, 2502–2520. doi: 10.1128/JCM.00361-17

Lemon, J. K., Khil, P. P., Frank, K. M., and Dekker, J. P. (2017). Rapid nanopore sequencing of plasmids and resistance gene detection in clinical isolates. *J. Clin. Microbiol.* 55, 3530–3543. doi: 10.1128/JCM.01069-17

Leinonen, R., Sugawara, H., and Shumway, M. (2011). International Nucleotide Sequence Database Collaboration. The sequence read archive. *Nucleic Acids Res.* 39, 19–21. doi: 10.1093/nar/gkq1019

Letunic, I., and Bork, P. (2019). Interactive tree of life (iTOL) v4: recent updates and new developments. *Nucleic Acids Res.* 47, W256–W259. doi: 10.1093/nar/gkz239

Magiorakos, A. P., Srinivasan, A., Carey, R. B., Carmeli, Y., Falagas, M. E., Giske, C. G., et al. (2012). Multidrug-resistant, extensively drug-resistant and pandrug-resistant bacteria: an international expert proposal for interim standard definitions for acquired resistance. *Clin. Microbiol. Infect* 18, 268–281. doi: 10.1111/j.1469-0691.2011.03570.x

Matta, R., Hallit, S., Hallit, R., Bawab, W., Rogues, A. M., and Salameh, P. (2018). Epidemiology and microbiological profile comparison between community and hospital acquired infections: A multicenter retrospective study in Lebanon. *J. Infect. Public Health* 11, 405–411. doi: 10.1016/j.jiph.2017.09.005

Naseer, U., and Sundsfjord, A. (2011). The CTX-M conundrum: dissemination of plasmids and Escherichia coli clones. *Microb. Drug Resist.* 17, 83–97. doi: 10.1089/mdr.2010.0132

Nouws, S., Bogaerts, B., Verhaegen, B., Denayer, S., Piérard, D., Marchal, K., et al. (2020). Impact of DNA extraction on whole genome sequencing analysis for characterization and relatedness of Shiga toxin-producing Escherichia coli isolates. *Sci. Rep.* 10, 14649–14616. doi: 10.1038/s41598-020-71207-3

Nwafia, I. N., Ohanu, M. E., Ebede, S. O., and Ozumba, U. C. (2019). Molecular detection and antibiotic resistance pattern of extended-spectrum beta-lactamase producing Escherichia coli in a tertiary Hospital in Enugu, Nigeria. *Ann. Clin. Microbiol. Antimicrob.* 18, 41. doi: 10.1186/s12941-019-0342-9

O'Leary, N. A., Wright, M. W., Brister, J. R., Ciufo, S., Haddad, D., McVeigh, R., et al. (2016). Reference sequence (RefSeq) database at NCBI: current status, taxonomic expansion, and functional annotation. *Nucleic Acids Res.* 44, D733–D745. doi: 10.1093/nar/gkv1189

Peleg, A. Y., and Hooper, D. C. (2010). Hospital-acquired infections due to Gram-negative bacteria. *N. Engl. J. Med.* 362, 1804–1813. doi: 10.1056/NEJMra0904124

Pitout, J. D. D., and Laupland, K. B. (2008). Extended-spectrum beta-lactamase-producing Enterobacteriaceae: an emerging public-health concern.. *Lancet Infect. Dis.* 8, 159–166. doi: 10.1016/S1473-3099(08)70041-0

Punina, N. V., Makridakis, N. M., Remnev, M. A., and Topunov, A. F. (2015). Whole-genome sequencing targets drug-resistant bacterial infections. *Hum. Genomics* 9, 19. doi: 10.1186/s40246-015-0037-z

Ribeiro, T. G., Novais, P., and L., and Machado, E., (2016). Atypical epidemiology of CTX-M-15 among Enterobacteriaceae from a high diversity of non-clinical niches in Angola. *J. Antimicrob. Chemother.* 71, 1169–1173. doi: 10.1093/jac/dkv489

Robertson, J., and Nash, J. H. E. (2018). MOB-suite: software tools for clustering, reconstruction and typing of plasmids from draft assemblies. *Microb. Genom.* 4:e000206. doi: 10.1099/mgen.0.000206

Robicsek, A., Jacoby, G. A., and Hooper, D. C. (2006). The worldwide emergence of plasmid-mediated quinolone resistance. *Lancet Infect. Dis.* 6, 629–640. doi: 10.1016/S1473-3099(06)70599-0

Rodriguez-Villalobos, H., Malaviolle, V., Frankard, J., De Mendonca, R., Nonhoff, C., Deplano, A., et al. (2005). Emergence of CTX-M extended spectrum beta-lactamase-producing Escherichia coli in Belgium. *Euro Surveill.* 10, E050224.3–E050224.15. doi: 10.2807/esw.10.08.02650-en

Roer, L., Overballe-Petersen, S., Hansen, F., Schønning, K., Wang, M., Røder, B. L., et al. (2018). *Escherichia coli* sequence type 410 is causing new international high-risk clones. *mSphere* 3, e00337–e00318. doi: 10.1128/msphere.00337-18

Roy, S., Chatterjee, S., Bhattacharjee, A., Chattopadhyay, P., Saha, B., Dutta, S., et al. (2021). Overexpression of efflux pumps, mutations in the pumps' regulators, chromosomal mutations, and AAC(6′)-Ib-cr are associated With Fluoroquinolone resistance in diverse sequence types of neonatal Septicaemic Acinetobacter baumannii: A 7-year single center S. *Front. Microbiol.* 12:602724. doi: 10.3389/fmicb.2021.602724

Sonda, T., Kumburu, H., van Zwetselaar, M., Alifrangis, M., Mmbaga, B. T., Aarestrup, F. M., et al. (2018). Whole genome sequencing reveals high clonal diversity of *Escherichia coli* isolated from patients in a tertiary care hospital in Moshi, Tanzania. *Antimicrob. Resist. Infect. Control* 7, 1–12. doi: 10.1186/s13756-018-0361-x

Tegha, G., Ciccone, E. J., Krysiak, R., Kaphatika, J., Chikaonda, T., Ndhlovu, I., et al. (2021). Genomic epidemiology of *Escherichia coli* isolates from a tertiary referral Center in Lilongwe, Malawi. *Microb. Genom.* 7:mgen000490. doi: 10.1099/mgen.0.000490

Thean, Y. T., Ng, L. S. Y., He, J., Tse, H. K., and Li, Y. H. (2009). Evaluation of screening methods to detect plasmid-mediated AmpC in Escherichia coli, Klebsiella pneumoniae, and Proteus mirabilis. *Antimicrob. Agents Chemother.* 53, 146–149. doi: 10.1128/AAC.00862-08

Upreti, N., Rayamajhee, B., Sherchan, S. P., Choudhari, M. K., and Banjara, M. R. (2018). Prevalence of methicillin resistant Staphylococcus aureus, multidrug resistant and extended spectrum β-lactamase producing gram negative bacilli causing wound infections at a tertiary care hospital of Nepal 11 medical and health sciences 1103 clinical Sci. *Antimicrob. Resist. Infect. Control* 7, 1–10. doi: 10.1186/s13756-018-0408-z

Wood, D. E., and Salzberg, S. L. (2014). Kraken: ultrafast metagenomic sequence classification using exact alignments. *Genome Biol.* 15, R46. doi: 10.1186/gb-2014-15-3-r46

Xu, L., Shabir, S., Bodah, T., McMurray, C., Hardy, K., Hawkey, P., et al. (2011). Regional survey of CTX-M-type extended-spectrum β-lactamases among Enterobacteriaceae reveals marked heterogeneity in the distribution of the ST131 clone. *J. Antimicrob. Chemother.* 66, 505–511. doi: 10.1093/jac/dkq482

Yehouenou, C. L., Kpangon, A. A., Affolabi, D., Rodriguez-Villalobos, H., Van Bambeke, F., Dalleur, O., et al. (2020). Antimicrobial resistance in hospitalized surgical patients: a silently emerging public health concern in Benin. *Ann. Clin. Microbiol. Antimicrob.* 19, 54–10. doi: 10.1186/s12941-020-00398-4

Zankari, E., Allesøe, R., Joensen, K. G., Cavaco, L. M., Lund, O., and Aarestrup, F. M. (2017). PointFinder: A novel web tool for WGS-based detection of antimicrobial resistance associated with chromosomal point

mutations in bacterial pathogens. *J. Antimicrob. Chemother.* 72, 2764–2768. doi: 10.1093/jac/dkx217

Zankari, E., Hasman, H., Cosentino, S., Vestergaard, M., Rasmussen, S., Lund, O., et al. (2012). Identification of acquired antimicrobial resistance genes. *J. Antimicrob. Chemother.* 67, 2640–2644. doi: 10.1093/jac/dks261

Zhao, W. H., and Hu, Z. Q. (2013). Epidemiology and genetics of CTX-M extended-spectrum β-lactamases in gram-negative bacteria. *Crit. Rev. Microbiol.* 39, 79–101. doi: 10.3109/1040841X.2012.691460

Zhou, Z., Alikhan, N. F., Mohamed, K., Fan, Y., and Achtman, M. (2020). The EnteroBase user's guide, with case studies on salmonella transmissions, Yersinia pestis phylogeny, and Escherichia core genomic diversity. *Genome Res.* 30, 138–152. doi: 10.1101/gr.251678.119

Zhou, Z., Alikhan, N. F., Sergeant, M. J., Luhmann, N., Vaz, C., Francisco, A. P., et al. (2017). GrapeTree: Visualization of core genomic relationships among 100,000 bacterial pathogens. *bioRxiv*, 1395–1404. doi: 10.1101/216788

Zhou, Y., Liang, Y., Lynch, K. H., Dennis, J. J., and Wishart, D. S. (2011). PHAST: A fast phage search tool. *Nucleic Acids Res.* 39, W347–W352. doi: 10.1093/nar/gkr485

Conflict of Interest: The authors declare that the research was conducted in the absence of any commercial or financial relationships that could be construed as a potential conflict of interest.

Publisher's Note: All claims expressed in this article are solely those of the authors and do not necessarily represent those of their affiliated organizations, or those of the publisher, the editors and the reviewers. Any product that may be evaluated in this article, or claim that may be made by its manufacturer, is not guaranteed or endorsed by the publisher.

frontiers in Microbiology

ORIGINAL RESEARCH
published: 17 December 2021
doi: 10.3389/fmicb.2021.771170

Clonal Dissemination of Clinical Carbapenem-Resistant *Klebsiella pneumoniae* Isolates Carrying *fosA3* and bla_{KPC-2} Coharboring Plasmids in Shandong, China

*Yingying Hao[1,2], Xuguang Zhao[3], Cui Zhang[4], Yuanyuan Bai[2], Zhen Song[2], Xinglun Lu[2], Ran Chen[1], Yaoyao Zhu[2] and Yueling Wang[2]**

[1] Department of Clinical Laboratory, Shandong Provincial Hospital, Cheeloo College of Medicine, Shandong University, Jinan, China, [2] Department of Clinical Laboratory, Shandong Provincial Hospital Affiliated to Shandong First Medical University, Jinan, China, [3] Department of Clinical Laboratory, The People's Hospital of Shouguang City, Shouguang, China, [4] Department of Clinical Laboratory, Feicheng Hospital of Shandong Guoxin Yiyang Group, Feicheng, China

OPEN ACCESS

Edited by:
Ziad Daoud, Central Michigan University, United States

Reviewed by:
Valentine Usongo, Health Canada, Canada
Anelise Ballaben, University of São Paulo, Brazil

***Correspondence:**
Yueling Wang
wangyueling88@126.com

Specialty section:
This article was submitted to Antimicrobials, Resistance and Chemotherapy, a section of the journal Frontiers in Microbiology

Received: *06 September 2021*
Accepted: *17 November 2021*
Published: *17 December 2021*

Citation:
Hao Y, Zhao X, Zhang C, Bai Y, Song Z, Lu X, Chen R, Zhu Y and Wang Y (2021) Clonal Dissemination of Clinical Carbapenem-Resistant Klebsiella pneumoniae Isolates Carrying fosA3 and bla_{KPC-2} Coharboring Plasmids in Shandong, China. Front. Microbiol. 12:771170. doi: 10.3389/fmicb.2021.771170

Treatment strategies of infection by carbapenem-resistant *Klebsiella pneumoniae* (CRKP) are limited. Fosfomycin, a broad-spectrum antibiotic, has attracted renewed interest in combination therapy to fight *K. pneumoniae* infections. However, reports on fosfomycin-resistant *K. pneumoniae* are increasing. Among the 57 CRKP strains, 40 (70.2%) were resistant to fosfomycin. Thus, whole-genome sequencing and bioinformatics analysis were conducted to reveal molecular characteristics of fosfomycin-resistant *K. pneumoniae*. Twenty-three isolates coharbored $fosA^{kp}$ and *fosA3*, with *K. pneumoniae* carbapenemase (KPC)-producing ST11-KL64-wzi64-O2 ($n = 13$) and ST11-KL47-wzi209-OL101 ($n = 8$), the predominating clonal groups, while *fosA3* was not detected in isolates carrying class B carbapenemase genes. Twenty-two (out of 26) ST11-KL64 strains were positive for *rmpA2*, of which 12 carried *fosA3*. Four of the 23 *fosA3*-positive isolates could successfully transfer their fosfomycin-resistant determinants to *Escherichia coli* J53Azi^R. All four strains belonged to ST11-KL47 with the same pulsed-field gel electrophoresis profile, and their transconjugants acquired fosfomycin, carbapenem, and aminoglycoside resistance. A 127-kb conjugative pCT-KPC-like hybrid plasmid (pJNKPN52_KPC_fosA) coharboring *fosA3*, bla_{KPC-2}, $bla_{CTX-M-65}$, bla_{SHV-12}, *rmtB*, and bla_{TEM-1} was identified. ST11-KL64 and ST11-KL47 *K. pneumoniae*, with higher resistance and virulence, should be critically monitored to prevent the future dissemination of resistance.

Keywords: ***Klebsiella pneumoniae*, fosfomycin, carbapenem resistant, *fosA3*, bla_{KPC-2}**

INTRODUCTION

Carbapenem-resistant *Klebsiella pneumoniae* (CRKP) poses a serious challenge in clinical medicine (Zhou et al., 2020). CRKP can cause bloodstream infections that are difficult to treat, with dramatically high hospital mortality rates of 55.8% (Xiao et al., 2020). In 2017, the WHO published a list of critical priority pathogens, where CRKP was placed in the Priority 1 group

(Ekwanzala et al., 2019). Drug resistance is spreading rapidly across microbial species; however, new antibiotics are not discovered as frequently. Therefore, reassessing the utility of and the mechanism of drug resistance among microbes against long-established antibiotics is necessary (Vardakas et al., 2016).

Fosfomycin, discovered in 1969, is a broad-spectrum antimicrobial agent targeting peptidoglycan synthesis (Liu et al., 2020). It is effective against carbapenem-resistant Enterobacterales (CRE) and extended-spectrum β-lactamase-producing (ESBL) Enterobacterales and CRE, *in vitro*, and is approved for the management of systemic infections in Spain, Germany, and France (Mączyńska et al., 2021). In China, intravenous fosfomycin has been employed in the treatment of systemic infectious diseases since the 1990s. However, resistance has gradually increased over the past decade; in China, 80% of *K. pneumoniae* carbapenemase-producing *K. pneumoniae* (KPC-KP) strains are resistant to fosfomycin, which is much higher than in other countries (Huang et al., 2021).

Routine susceptibility test for fosfomycin in non-*Escherichia coli* Enterobacterales is not feasible (Elliott et al., 2019; Mączyńska et al., 2021). Clinical and Laboratory Standards Institute (CLSI) recommends glucose-6-phosphate (G6P)-supplemented broth microdilution and agar dilution for accurate susceptibility testing. Even tests like Kirby–Bauer Disk Diffusion (DD) and *E*-tests cannot yield reliable results and screen the fosfomycin resistance phenotype. Moreover, the epidemiology of fosfomycin resistance in clinical CRKP isolates from Shandong, China, is unclear.

Three mechanisms of fosfomycin resistance have been reported (Huang et al., 2021). Mutations in *glpT* and *uhpT* genes affect L-a-glycerophosphate and hexose-6-phosphate uptake, respectively. Mutations in MurA binding site, most notably Asp369Asn and Leu370lle, can also confer fosfomycin resistance. However, the most potent mechanism of resistance is drug hydrolysis by various chromosomal or plasmid-borne fosfomycin hydrolases, including FosA (*fosA2*, *fosA3*, *fosA4*, *foskp96*, $fosA^{kp}$, and *fosA7*), *fosB*, *fosC*, and *fosX* (Liu et al., 2020).

Although the high fosfomycin resistance rate among KPC-KP was considered predominantly caused by clonal dissemination, horizontal transfer of *fosA3*-encoding plasmids among KPC-KP was also documented; in particular, the emergence of conjugative plasmids carrying a combination of the *fosA3* and bla_{KPC-2} genes could accelerate the spread of antibiotic resistance (Jiang et al., 2015; Chen et al., 2019; Zhang et al., 2019). However, little is known regarding the prevalence of plasmid-mediated *fosA3* and bla_{KPC-2} co-dissemination among KPC-KP.

In this study, we aimed to elucidate the molecular epidemiology of fosfomycin resistance among clinical CRKP isolates in China and to determine their genetic lineages. One of the self-transmissible plasmid pJNKPN52_KPC_fosA harboring *fosA3*, bla_{KPC-2}, $bla_{CTX-M-65}$, bla_{SHV-12}, *rmtB*, and bla_{TEM-1} was fully sequenced and characterized. To the best of our knowledge, this is the first report of conjugative pCT-KPC-like plasmid co-carrying *fosA3* and bla_{KPC-2}.

MATERIALS AND METHODS

Bacterial Strains

Fifty seven non-duplicate CRKP clinical isolates from urine ($n = 6$), sputum or bronchoalveolar lavage fluid ($n = 35$), abscess ($n = 2$), blood ($n = 5$), pus ($n = 2$), abdominal fluid ($n = 3$), and other patient samples ($n = 6$) were collected from Shandong Provincial Hospital of China, between January 2017 and June 2020. Matrix-assisted laser desorption/ionization time-of-flight mass spectrometry (MALDI-TOF/MS) (BioMérieux, Marcy-l'Étoile, France) was used to identify the isolates. Carbapenemases were detected using carbapenem inactivation method (CIM) and EDTA-modified CIM (eCIM).

Antibiotic Susceptibility Assay

Antibiotic susceptibility was analyzed with a VITEK-2 compact system (BioMérieux, France) for aztreonam (ATM), cefepime (FEP), ceftriaxone (CRO), ceftazidime (CAZ), ertapenem (ETP), imipenem (IMP), piperacillin-tazobactam (TZP), trimethoprim-sulfamethoxazole (SXT), ciprofloxacin (CIP), levofloxacin (LVX), gentamicin (GEN), and amikacin (AMK); broth microdilution for polymyxin B (POL), tigecycline (TGC); and agar dilution for fosfomycin (FOS), using Mueller–Hinton agar supplemented with 25 μg/ml of G6P (CLSI, 2020). Susceptibility assay results were interpreted by CLSI breakpoints (CLSI, 2020), except for TGC, which were defined by the European Committee on Antimicrobial Susceptibility Testing (EUCAST, 2020) guidelines (EUCAST, 2020). Fosfomycin susceptibility was interpreted according to CLSI breakpoints for *E. coli* urinary isolates. Phenotypic detection of carbapenemases was performed using the CIM and eCIM tests (CLSI, 2020).

Genotyping by Pulsed-Field Gel Electrophoresis

Genomic DNA from clinical strains embedded in gel plugs was digested with QuickCut *Xba*I (Takara, Shiga, Japan), and restriction fragments, ranging from 50 to 500 kb, were separated using CHEF Mapper apparatus (Bio-Rad, Hercules, CA, United States) for 19 h with the pulse time switched from 6 to 36 s. Pulsed-field gel electrophoresis (PFGE) patterns were compared using Gel-J software, version 2.0 (Heras et al., 2015). Pulsotypes were assigned to the clusters with 80% similarity (Chen et al., 2019).

Conjugation Assay

Conjugation experiments were carried out with sodium azide-resistant *E. coli* J53Azi^R being used as the recipient. Transconjugants harboring fosfomycin resistance genes were selected on Mueller–Hinton agar plates containing 64 mg/ml of fosfomycin, 100 mg/ml of sodium azide, and 25 μg/ml of G6P (Xiang et al., 2015). Transconjugants harboring carbapenemase resistance genes were selected on Mueller–Hinton agar plates containing 6 μg/ml of CAZ and 100 mg/ml of sodium azide. Antibiotic susceptibility test and PCR analysis were performed to confirm the *fosA3* and/or carbapenemase gene transfer

(Poirel et al., 2011; Xiang et al., 2015). Furthermore, PCR-based replicon typing (PBRT) was used to characterize the plasmid harbored by the transconjugants (Carattoli et al., 2005).

Whole-Genome Sequencing and Analysis

DNA from clinical isolates was extracted and sequenced using an Illumina Hiseq platform at Novogene Co., Ltd. (Beijing, China). Illumina sequences were assembled *de novo* using the SPAdes v3.10 (Nurk et al., 2013).

For the JNKPN52 and JNKPN30 isolates, genome sequencing was also performed on a PacBio RSII sequencer at Biozeron Biological Technology Co., Ltd. (Shanghai, China). The paired-end short Illumina reads were used to correct the long PacBio reads utilizing *proovread*, and then the corrected PacBio reads were assembled *de novo* utilizing SMARTdenovo.[1] Sequence annotation was conducted using RAST 2.0[2] combined with BLASTP/BLASTN searches against the UniProtKB/Swiss-Prot and RefSeq databases. Annotation of resistance genes and mobile elements was carried out using the online databases, including CARD[3] and ISfinder.[4]

Antimicrobial resistance genes and multilocus sequence typing (MLST) were analyzed *in silico* by using Abricate software[5] (Sherry et al., 2019). Virulence scores, capsular (K) serotypes, and lipopolysaccharide (LPS) O antigen serotype were predicted using Kleborate v0.3.0[6] (Wyres et al., 2020). Single-nucleotide polymorphism (SNP) calling was performed using Snippy 3.1,[7] and recombinant variants were excluded using ClonalFrameML 1.0 (Lu et al., 2019). Maximum likelihood phylogenetic trees were constructed with RAxML,[8] from the recombination-free SNPs.

For our dataset, core-genome MLST (cgMLST) analysis was performed using SeqSphere+ software (8.0.2 version; Ridom, Münster, Germany) according to the "*K. pneumoniae* sensu lato cgMLST" version 1.0 scheme[9] (Weber et al., 2019). A total of 2,358 target genes were used to characterize the gene-by-gene allelic profile of the *K. pneumoniae* strains. The resulting set of target genes was then used for interpreting the clonal relationship displayed in a minimum spanning tree using the "pairwise ignoring missing values" parameter during distance calculations.

Identification of Fosfomycin-Resistant Determinants

The fosfomycin resistance-related proteins MurA, GlpT, and UhpT of the genomes were aligned with *K. pneumoniae* reference strain ATCC 700721 using local BLAST software. Multiple sequence alignments were performed by MAFFT, with the 4-kb $fosA^{kp}$ gene-related fragment of JNKPN10 as a reference.

Analysis of the Plasmid Coharboring *fosA3* and bla_{KPC-2}

The complete sequence of pJNKPN52_KPC_fosA has been deposited in GenBank under accession number MZ709016. Eleven fully sequenced pCT-KPC-like plasmids harboring bla_{KPC-2} were compared with pJNKPN52_KPC_fosA by BLAST Ring Image Generator,[10] including pCT-KPC (GenBank accession no. KT185451), p69-2 (GenBank accession no. CP025458), p1068-KPC (GenBank accession no. MF168402), p20049-KPC (GenBank accession no. MF168404), p675920-1 (GenBank accession no. MF133495), pC2414-2-KPC (GenBank accession no. CP039820), pKP1034 (GenBank accession no. NZ_KP893385), pKSH203-KPC (GenBank accession no. CP034324), p16HN-263_KPC (GenBank accession no. CP045264), pEBSI036-2-KPC (GenBank accession no. MT648513), and pKP19-2029-KPC2 (GenBank accession no. CP047161). More detailed genome alignment between closely related plasmids was conducted by local BLAST and visualized with Easyfig.[11]

Analysis of the Plasmid Harboring bla_{NDM-1}

The complete sequence of pJNKPN30_NDM has been deposited in GenBank under accession number OL389795. Four fully sequenced IncA/C type plasmids harboring bla_{NDM-1} were compared with pJNKPN30_NDM by BLAST Ring Image Generator (see text footnote 10), including pNDM_KN (GenBank accession no. JN157804), pMS6198A (GenBank accession no. CP015835), p1605752AC2 (GenBank accession no. CP022126), and pT1 (GenBank accession no. KX147633).

RESULTS

Antimicrobial Susceptibility

Among the 57 tested CRKP strains, 40 were resistant to fosfomycin. High resistance (> 70%) was observed against β-lactam antibiotics, fosfomycin, and quinolones. The highest resistance (> 98%) was observed against TZP, CRO, FEP, and ETP. All the strains remained 100% susceptible to TGC, and only one isolate showed resistance to POL [minimal inhibitory concentration (MIC) ≥ 64]. The antibiotic susceptibility results are shown in **Table 1** and **Supplementary Table 4**.

Molecular Typing and Phylogenetic Group Genotyping

The 57 *K. pneumoniae* strains had 18 sequence types (STs), with ST11 being the most common (n = 36, 63%) (**Figure 1** and

[1]https://github.com/ruanjue/smartdenovo
[2]https://rast.nmpdr.org/
[3]http://arpcard.mcmaster.ca
[4]https://www-is.biotoul.fr/
[5]https://github.com/tseemann/abricate
[6]https://github.com/katholt/Kleborate
[7]https://github.com/tseemann/snippy
[8]https://github.com/stamatak/standard-RAxML
[9]https://www.cgmlst.org/ncs/schema/2187931/
[10]https://sourceforge.net/projects/brig/
[11]http://mjsull.github.io/Easyfig/files.html

TABLE 1 | Antimicrobial resistance profile of the CRKP strains.

Antimicrobial agents	Resistance rate (%) *n* (%)	MIC_{50} (μg/ml)	MIC_{90} (μg/ml)	MIC range (μg/ml)
TZP	100	≥128	≥128	128–128
CAZ	98.2	≥64	≥64	1–64
CRO	98.2	≥64	≥64	1–64
FEP	98.2	≥64	≥64	2–64
ATM	91.2	≥64	≥64	1–64
ETP	100	≥32	≥32	2–32
IMP	87.7	≥16	≥16	1–16
AMK	57.9	≥64	≥64	2–64
GEN	73.7	≥16	≥16	1–16
CIP	87.7	≥4	≥4	0.25–4
LVX	80.7	≥8	≥8	0.25–8
SXT	54.4	≥16	≥16	1–320
POL	1.8	0.5	1	0.125–128
TGC	0	1	2	0.25–2
FOS	70.2	512	≥1,024	32–1,024

MIC, minimal inhibitory concentrations; TZP, piperacillin/tazobactam; CAZ, ceftazidime; CRO, ceftriaxone; FEP, cefepime; ATM, aztreonam; ETP, ertapenem; IMP, imipenem; AK, amikacin; CEN, gentamicin; CIP, ciprofloxacin; LEV, levofloxacin; STX, trimethoprim/sulfamethoxazole; POL, polymyxin B; TGC, tigecycline; FOS, fosfomycin; CRKP, carbapenem-resistant Klebsiella pneumoniae.

Supplementary Table 2). The others were ST101 ($n = 2$), ST15 ($n = 2$), ST24 ($n = 2$), ST37 ($n = 2$), ST1031, ST133, ST152, ST1537, ST2246, ST25, ST258, ST29, ST323, ST392, ST3924, ST485, and ST528.

Among these strains, we detected 19 different K-loci, the most common being KL64 ($n = 26$, including 25 ST11) and KL47 ($n = 10$), together accounting for 63% of all the strains (**Figure 1**). Seven distinct O antigen encoding loci were detected among the strains, and the most common were O2 ($n = 30$), OL101 ($n = 11$), and O1 ($n = 9$).

According to PFGE profile, seven different clusters as A∼G clone groups and five singletons were identified. The phylogenetic tree revealed that CRKP strains could be broadly clustered into three major clades: clades 1 and clades 2 consisted of ST11 strains alone, while clade 3 consisted of ST11 and the other STs (**Figure 2**). A minimum spanning tree of the 57 *K. pneumoniae* isolates was constructed based on cgMLST allelic profiles, showing the presence of five cluster types (≤ 15 allele differences). ST11-KL64-wzi64-O2 isolates mainly belonged to Cluster 1 ($n = 17$) and Cluster 3 ($n = 6$), while ST11-KL47-OL101 isolates mainly belonged to Cluster 2 ($n = 7$) (**Figure 3** and **Supplementary Table 5**).

Mechanisms of Fosfomycin Resistance

All the 57 strains harbored at least one fosfomycin-modifying enzymes, including *fosA2*, *fosA3*, *foskp96*, and $fosA^{kp}$ (**Figure 2**). $fosA^{kp}$ was the most prevalent chromosomal-encoded enzyme, detected in 52 isolates, followed by *foskp96*, in five isolates. $fosA^{kp}$ and *fosA3* were detected in 23 isolates. *foskp96* was detected among 5 isolates, though only one isolate showed fosfomycin-resistant phenotype *in vitro*.

Among the isolates, 3 isolates had Ser148Asn and Ser209Thr substitutions in MurA, and two isolates had MurA deletion. One variation, Val434Ile, in uhpT was detected in two isolates. Three substitutions in glpT, Ile260Val, Val337Ile, and Ile429Val, were detected in one isolate.

Distribution of Antimicrobial Resistance Genes and Virulence Genes

As illustrated in **Figure 1** and **Supplementary Table 1**, 87.7% of the isolates produced carbapenemase in accordance with the results of CIM test. bla_{KPC-2} was the main type of carbapenemase ($n = 33$). Five strains coharboring bla_{KPC-2} and bla_{NDM-1} were detected. Meanwhile, bla_{NDM-1} ($n = 5$), bla_{NDM-5} ($n = 3$), bla_{NDM-3} ($n = 1$), bla_{IMP-4} ($n = 2$), and $bla_{OXA-232}$ ($n = 1$) also contributed to the carbapenem resistance. Twenty transconjugants harboring carbapenemase genes were acquired. One transconjugant harbored bla_{IMP-4}, ten transconjugants harbored bla_{KPC-2}, and nine transconjugants harbored bla_{NDM}. ESBL resistance genes, such as bla_{TEM}, bla_{CTX-M}, bla_{SHV}, bla_{CMY}, and bla_{SHV}, were also detected, with bla_{TEM}, bla_{CTX-M}, and bla_{SHV} being the most prevalent. The strains coharboring bla_{TEM}, bla_{CTX-M}, and bla_{SHV} made 52.6% of all the CRKP strains (**Figure 4** and **Supplementary Table 1**).

Plasmid-encoded fluoroquinolone resistance genes (QnrS and QnrB) were detected in 18 isolates, while chromosomal *oqxA* and *oqxB* were detected in 33 isolates (**Figure 4** and **Supplementary Table 1**). A high prevalence of specific porin defects was detected, and only 14 isolates were without any mutation in *ompK5* or *ompK36*. It was observed that *ompK35* truncations and *ompK36GD* mutations coexisted in 59.6% of the strains (**Figure 4** and **Supplementary Table 2**).

According to the Katholt criterion, 27 isolates were assigned a virulence score of 4, which were closely related to ST11 ($n = 24$) (**Figure 4**). Analysis of virulence genes showed that 41 isolates possessed yersiniabactin genes located on ICEKp3 ($n = 38$), ICEKp1 ($n = 1$), ICEKp5 ($n = 1$), and ICEKp12 ($n = 1$), with ICEKp3 being the most prevalent carrier. Of 25 ST11-KL64 isolates, 22 (88%) carried *rmpA2* gene, but only three were positive for the string test, suggesting that *rmpA2* was inactive in most isolates. Among 10 ST11-KL47 isolates, only one was positive for *rmpA2* gene (**Supplementary Table 2**).

Genetic Background of *fosA* in Carbapenem-Resistant *Klebsiella pneumoniae*

Four types of genetic environments existed in the 52 $fosA^{kp}$-positive CRKP isolates. The upstream genes of $fosA^{kp}$ among the strains are identical, but those downstream are variable. The intergenic regions between $fosA^{kp}$ and the downstream MocR gene could be DNA helicase-related genes, a Type I restriction–modification system, or a hypothetical Protein. As shown in **Supplementary Figure 1**, the genetic environment of *foskp96* was similar to that of $fosA^{kp}$, with a backbone of *YrkL-LysR-FosA-MocR-YjiS*. The genetic environment of *fosA3* was consistent,

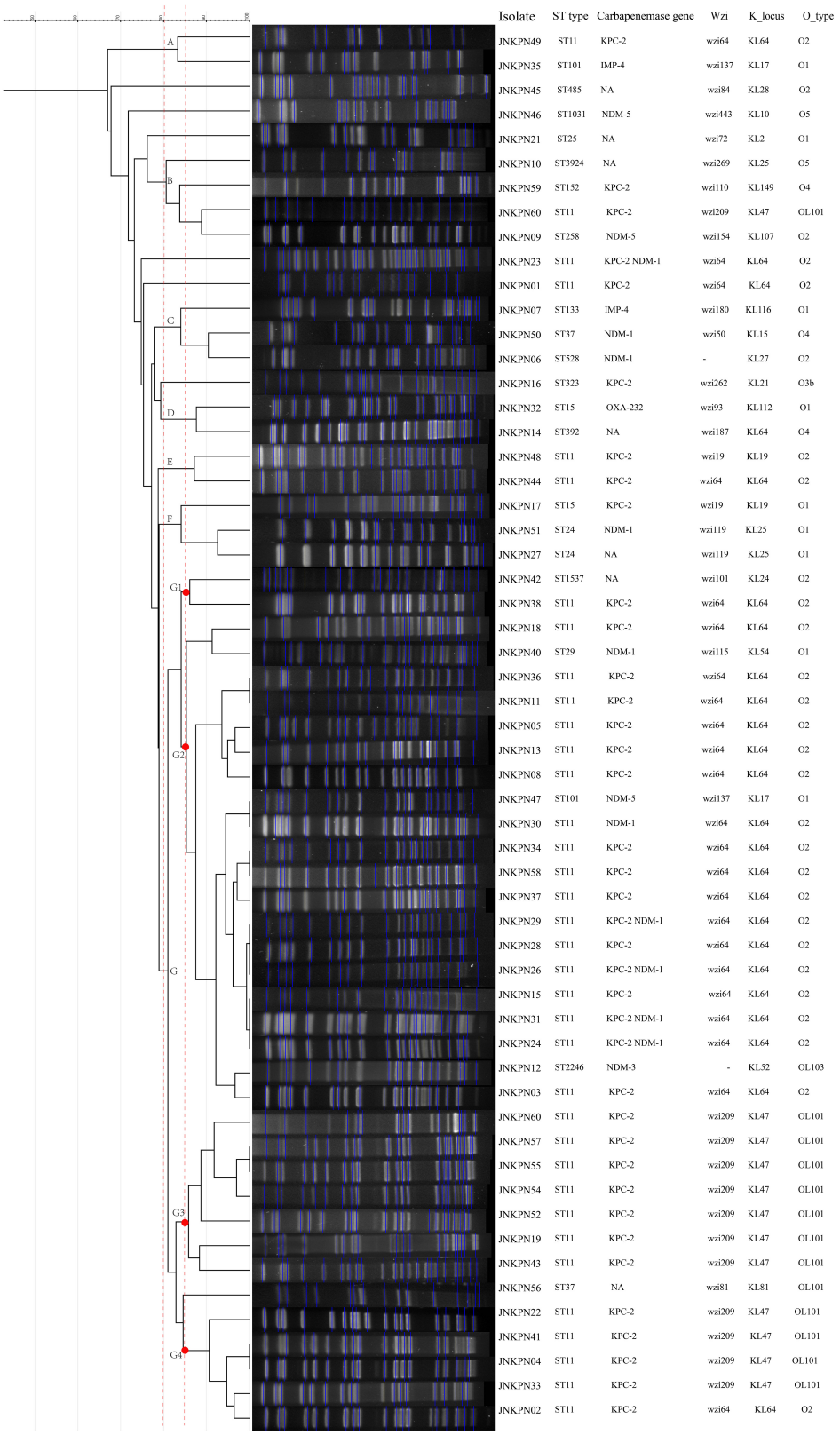

FIGURE 1 | The dendrogram is based on the similarity of pulsed-field gel electrophoresis (PFGE) patterns in the 57 clinical carbapenem-resistant *Klebsiella pneumoniae* (CRKP) isolates. The right panel shows results from isolate name, sequence type, carbapenemase gene, K_locus, and O_type. NA, not available.

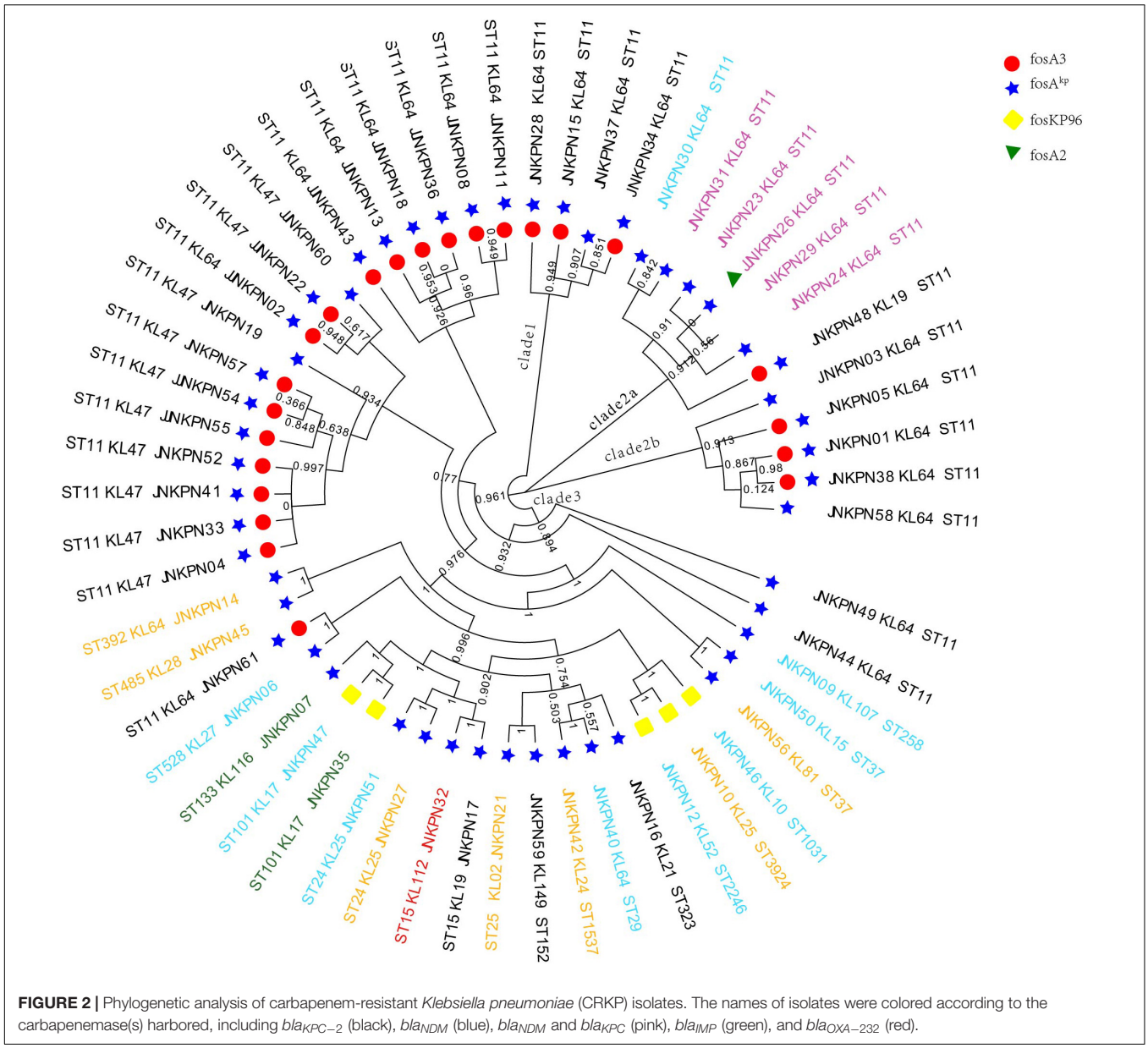

FIGURE 2 | Phylogenetic analysis of carbapenem-resistant *Klebsiella pneumoniae* (CRKP) isolates. The names of isolates were colored according to the carbapenemase(s) harbored, including bla_{KPC-2} (black), bla_{NDM} (blue), bla_{NDM} and bla_{KPC} (pink), bla_{IMP} (green), and $bla_{OXA-232}$ (red).

where *fosA3* is flanked by *IS26* at both ends, in a transposon-like structure.

Phenotypic and Genotypic Characteristics of Plasmids Harboring *fosA3* and bla_{KPC-2}

The plasmids harboring *fosA3* from strains JNKPN52, JNKPN54, JNKPN55, and JNKPN57 were successfully transferred into *E. coli* J53Azi^R by conjugation. All the four transconjugants were resistant to CRO, FEP, CAZ, ATM, TZP, ETP, IMP, AMK, GEN, and FOS but were susceptible to SXT, CIP, LVX, TGC, and POL (**Supplementary Table 3**). JNKPN52 and JNKPN54 were isolated from 2-month-old pediatric patients after cardiac surgery enrolled in the cardiac care unit in December 2019. JNKPN55 and JNKPN57 were isolated from premature babies enrolled in the neonatal intensive care unit in December 2019. A nosocomial outbreak caused by a clone of ST-KL47 KPC-KP strains was considered according to the high similarities of PFGE patterns of group G3 (> 85%) (**Figure 1**) and the high level of correlation within cgMLST Cluster 2 (up to 1 allele difference) (**Figure 3**).

The complete sequence of plasmid pJNKPN52_KPC_fosA from clinical strain JNKPN52 was determined to better characterize the self-transmissible plasmid coharboring *fosA3* and bla_{KPC-2}. pJNKPN52_KPC_fosA is a 127,668-base pair (bp) multireplicon plasmid that belongs to the IncR:IncFII-type and shares a similar structure with pHN7A8/pKPC-LK30 hybrid plasmid pCT-KPC (**Figure 5**).

pJNKPN52_KPC_fosA contains two major accessory resistance regions, including the bla_{KPC-2} region harboring

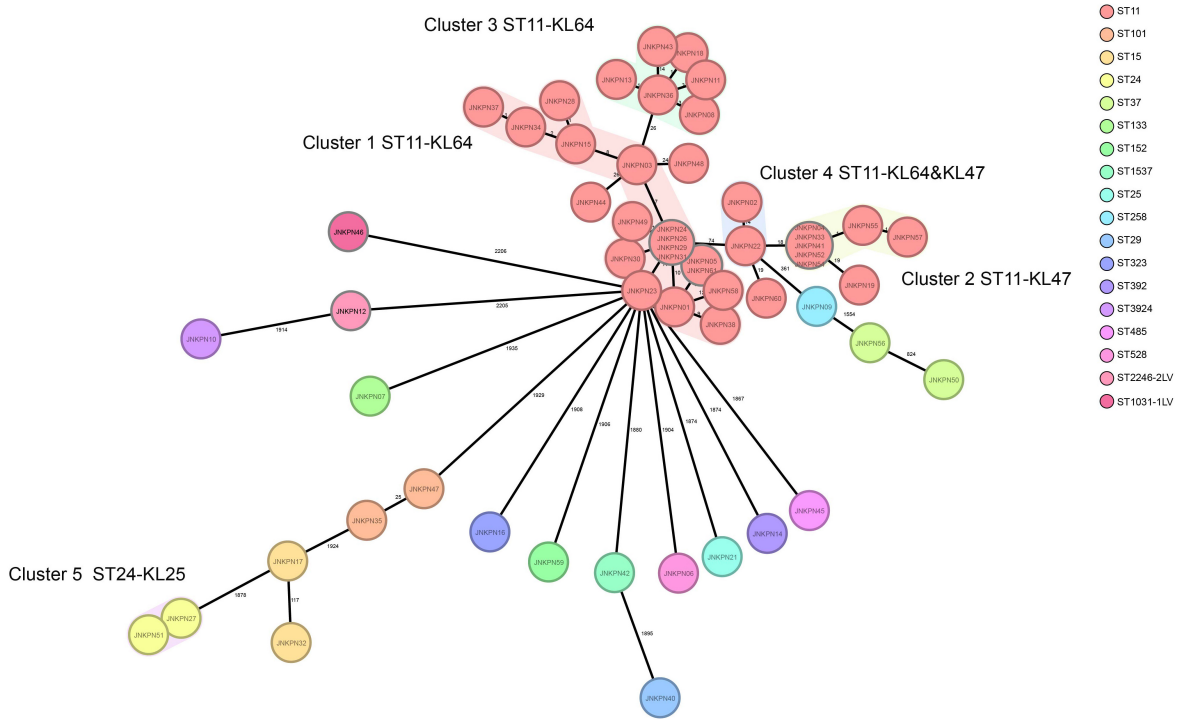

FIGURE 3 | Minimum spanning tree showing core genome multilocus sequence typing (cgMLST) of the 57 carbapenem-resistant *Klebsiella pneumoniae* (CRKP) isolates, showing five cluster types numbered consecutively. Each circle represents an allelic profile. Colors of circles indicate the different sequence types (STs). Cluster types consist of closely related genotypes (≤15 allele differences). The numbers on the connecting lines illustrate the numbers of target genes with different alleles.

bla_{KPC-2} and bla_{SHV-12}, and the multidrug-resistant (MDR) region carrying *rmtB* (aminoglycoside resistance), *fosA3*, bla_{TEM-1}, and $bla_{CTX-M-65}$. The MDR region was generated from the insertion of ΔTn6377–$bla_{CTX-M-65}$, *IS26–fosA3–IS26* unit, ΔTn2-*rmtB* element within *IS1*. The bla_{KPC-2} region was organized in order of a truncated *IS26*–bla_{SHV-12}–*IS26* unit, ΔTn6296, ΔTn21 with insertion of *IS5075*, an *IS903B* remnant, and *ISKpn14* (**Figure 5**).

Comparative Analysis of Plasmids Harboring *fosA3–*bla_{KPC-2}

According to sequence alignment by BRIG, pJNKPN52_KPC_fosA showed 99% nucleotide identity with the previously reported plasmids p16HN-263_KPC and pKP19-2029-KPC2 isolated from China and pEBSI036-2-KPC isolated from Egypt (Ahmed et al., 2021) (**Figure 5**).

The MDR regions of the eleven plasmids were similar, with pJNKPN52_KPC_fosA, p675920-1, p69-2, and p20049-KPC slightly differing from one another. To determine the detailed structural differences between these plasmids, additional linear comparative genomics analysis was performed by BLAST. Compared with pJNKPN52_KPC_fosA, p675920-1 lacked a Δ*IS1294* region, possibly because of recombination of *IS26–fosA3–IS26* region. In p20049-KPC, the deletion of *IS26–fosA3–IS26* region and insertion of partial plasmid backbone genes were observed within the MDR region (**Figure 6**).

The bla_{KPC-2} region of the pJNKPN52_KPC_fosA was similar to that of p20049-KPC and pKP1034, with the inversion of ΔTn6296. Compared with pJNKPN52_KPC_fosA, the deletion of the truncated *IS26*–bla_{SHV-12}–*IS26* unit was observed in p675920-1, probably due to *IS26*-mediated deletion (**Figure 7**).

Genotypic Characteristics of Plasmids Harboring bla_{NDM-1}

The plasmids harboring bla_{NDM} from strains JNKPN23, JNKPN24, JNKPN26, JNKPN29, JNKPN30, JNKPN31, JNKPN46, JNKPN47, and JNKPN51 were successfully transferred into *E. coli* J53Azi^R by conjugation. All the nine transconjugants were resistant to CRO, CAZ, TZP, ETP, and IMP, but were susceptible to FOS, CIP, and LVX (**Supplementary Table 6**). All the plasmids harboring bla_{NDM-1} were shown to belong to IncA/C2 type through plasmid typing (**Supplementary Table 6**).

The complete sequence of plasmid pJNKPN30_NDM from clinical strain JNKPN30 was determined to better characterize the self-transmissible IncA/C2 type plasmid harboring bla_{NDM-1}. pJNKPN30_NDM contains two main accessory resistance regions, including the *IS1380*–bla_{CMY-6} region and the MDR region carrying *Tn6196*, class 1 integron structure bearing *arr-3*, *dfrA1*, *AadA16*, *ErmE*, and *sul1*, and partial of Tn125-bearing bla_{NDM-1} interrupted by the insertion of Δ*ISKpn14*, followed by the 16S rRNA methylase rmtC gene (**Figure 8**).

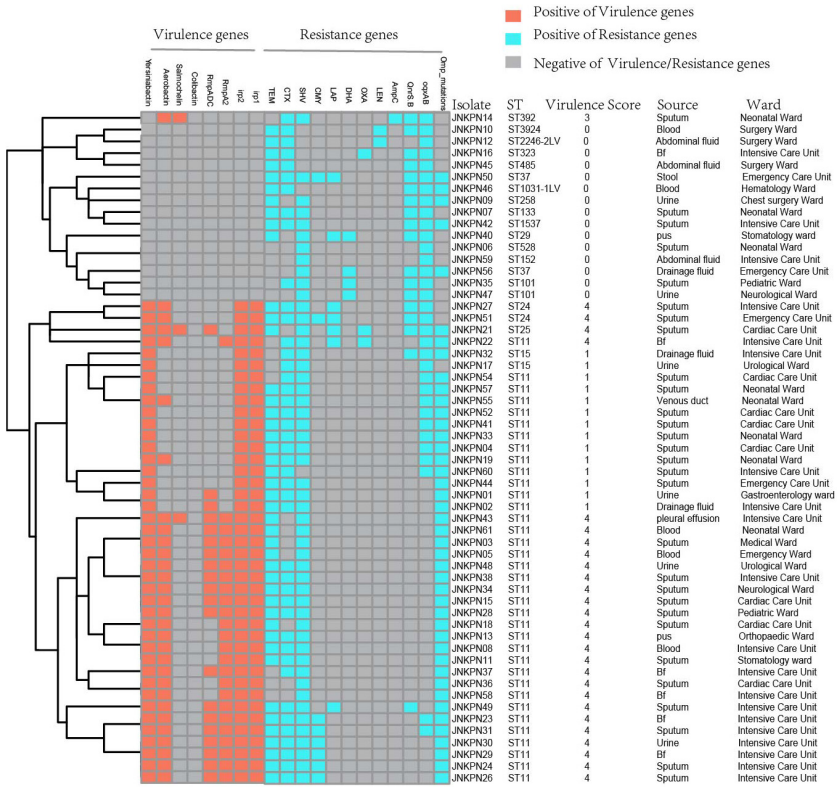

FIGURE 4 | Detection of resistance genes and virulence genes in carbapenem-resistant *Klebsiella pneumoniae* (CRKP) isolates. The sequence type, virulence score, source, and ward of each isolate were marked on the right of the squares. Bf, bronchoalveolar lavage fluids.

According to sequence alignment by BRIG, pJNKPN30_NDM was with a backbone similar to that of other IncA/C2 plasmids (84–99% query coverage, > 99% nucleotide sequence identity). The main regions of discontinuity were within the *Int498* region and the *ISKpn18* region (**Figure 8**).

Nucleotide Sequence Accession Numbers

Raw reads of all 57 isolates have been deposited in GenBank (BioProject PRJNA769451). The complete sequence of pJNKPN52_KPC_fosA and pJNKPN30_NDM has been deposited in GenBank under accession numbers MZ709016 and OL389795, respectively.

DISCUSSION

The emergence of CRKP has become a crucial public health problem, as it limits treatment options and requires novel active agents or combination therapies (Ekwanzala et al., 2019). *K. pneumoniae* isolates have shown susceptibility to fosfomycin; hence, the "old" antibiotic agent is being re-considered as a possible auxiliary drug (Vardakas et al., 2016). Pontikis et al. (2014) reported that intravenous fosfomycin for nosocomial CRKP infections has a good clinical outcome. Intravenous fosfomycin is used in many countries and has completed phase 3 clinical trials for the treatment of urinary tract infection and acute pyelonephritis (Ito et al., 2017). However, information on resistance to fosfomycin among CRKP in China is inadequate. The occurrence of fosfomycin-resistant CRKP in China ranges from 18.7 to 80% (Tseng et al., 2017; Huang et al., 2021). These inconsistent data indicate that resistance of *K. pneumoniae* isolates to fosfomycin, especially to CRKP, requires further evaluation. Our results indicated that 70.2% of CRKP strains were resistant to fosfomycin in Shandong, which is much higher than that in most regions in China.

Fosfomycin resistance may be due to chromosome-encoded *murA*, *glpT*, *uhpT*, *uhpA*, *ptsI*, and *cyaA* mutations, or plasmid-encoded or chromosomal inactivation by fosfomycin-modifying enzymes (Liu et al., 2020). We found that *fosA* homologs were widely distributed among the CRKP strains, and all the strains harbored $fosA^{kp}$ or *foskp96*. Moreover, 40.3% of the strains had both $fosA^{kp}$ and *fosA3*. It was difficult to discriminate *fosA* variants located on plasmids from those on chromosomes because the analysis was based on draft sequences of genomes. $fosA^{kp}$ or *foskp96* is intrinsically distributed on *K. pneumoniae* chromosomes (Ito et al., 2017). According to the previous report, $MIC_{50/90}$ values of fosfomycin for *K. pneumoniae* clinical strains producing KPC-type carbapenemase were 16/64 μg/ml (Ito et al., 2017). In this study, 34 CRKP isolates without *fosA3* had a MIC range of ≤ 32 to ≥ 1,024 μg/ml and $MIC_{50/90}$ values of 256/1,024 μg/ml. Not all the isolates showed

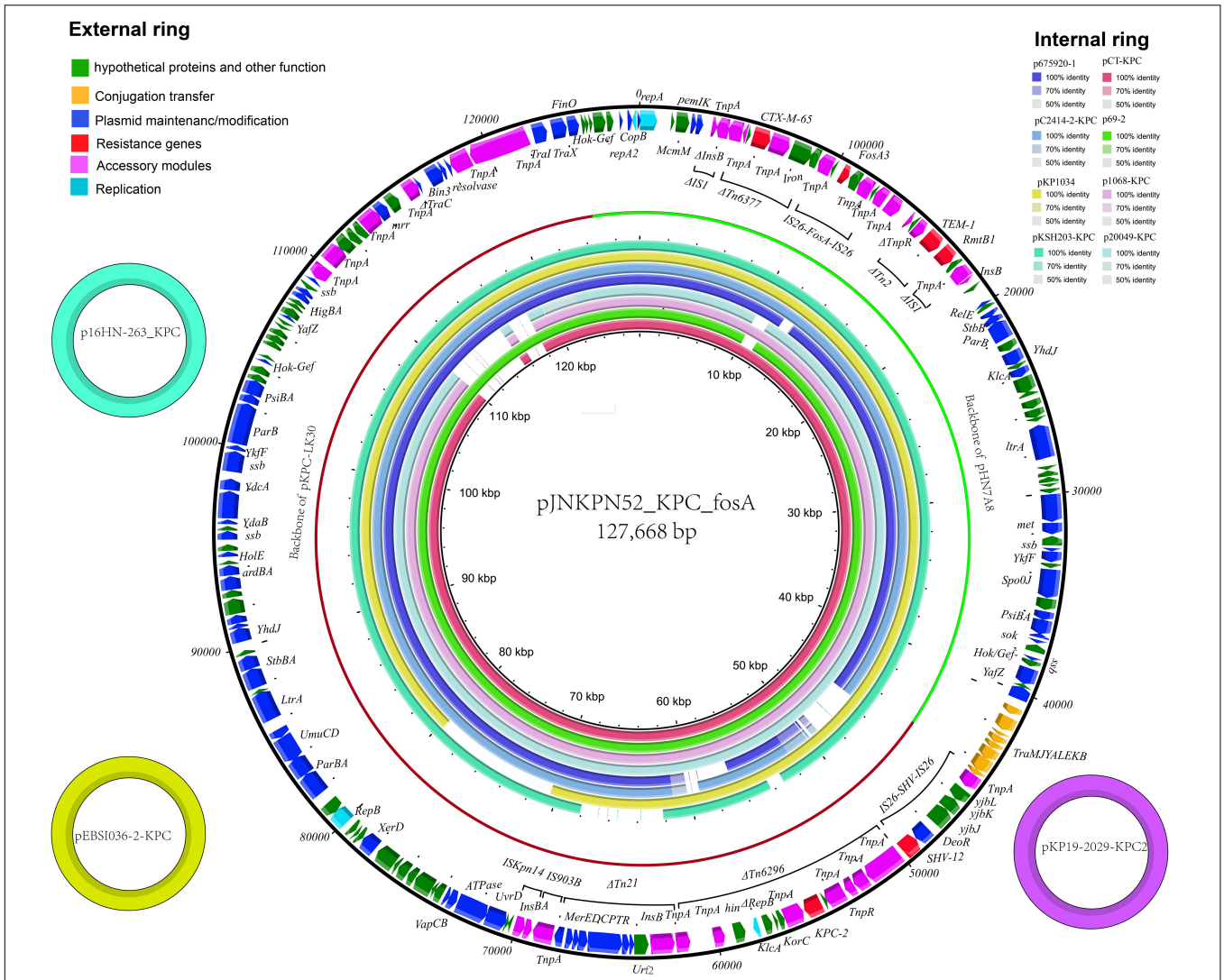

FIGURE 5 | The external ring is the main structural feature of plasmid pJNKPN52_KPC_fosA (GenBank accession no. MZ709016). The three small external rings display plasmids coharboring bla_{KPC-2} and *fosA* with identity > 99%. The internal eight rings showed the comparative analysis of bla_{KPC}-harboring plasmids with pJNKPN52_KPC_fosA (constructed by BRIG).

fosfomycin resistance. We speculated that the dissimilarity between fosfomycin-resistant genotype and phenotype was caused by the expression level of *fosA* gene.

fosA3 is the most common acquired *fosA*, encoded by plasmids (Ito et al., 2017). Apart from *fosA* production, fosfomycin resistance is also related to *MurA*, *glpT*, and *uhpT* mutations, which were rare in our isolates, and only 2, 3, and 1 isolates, respectively, were detected. Therefore, our results strongly suggest that *fosA3* and *fosA* contribute mainly to fosfomycin resistance.

Further, pLVPK-like-positive ST11-KL64 isolates show better survival in the environment (Zhou et al., 2020). Fourteen *fosA3*-positive strains were screened from the ST11-KL64-wzi64-O2 subgroup, and eight *fosA3*-positive strains were screened from the ST11-KL47-wzi209-OL101 subgroup. Twenty-two out of 25 ST11-KL64 strains and only one ST11-KL47 strain contained *rmpA2*. All the seven isolates belonging to cgMLST Cluster 2 and Cluster 6 isolates belonging to cgMLST Cluster 3 coharbored bla_{KPC-2} and *fosA3*. The isolates belonging to cgMLST Cluster 1 and Cluster 3 except JNKPN01 and JNKPN30 were positive for bla_{KPC-2} and *rmpA2*. PFGE profiles and cgMLST confirmed that the clonal relation may predominantly be due to clonal dissemination.

It was noteworthy that bla_{NDM}-producing CRKP isolates were increasingly reported (Qamar et al., 2021). In this study, 24.6% (14/57) of CRKP isolates were positive for bla_{NDM} (including the isolates co-producing bla_{KPC-2} and bla_{NDM}), which were higher than that in the previous research in China (11.5%) (Wang et al., 2018). Plasmids harboring bla_{NDM} from 64.3% (9/14) of bla_{NDM}-carrying isolates could be transferred to the recipients. The conjugative IncA/C2 type plasmids played an important role in the rapid and efficient dissemination of the bla_{NDM-1} gene

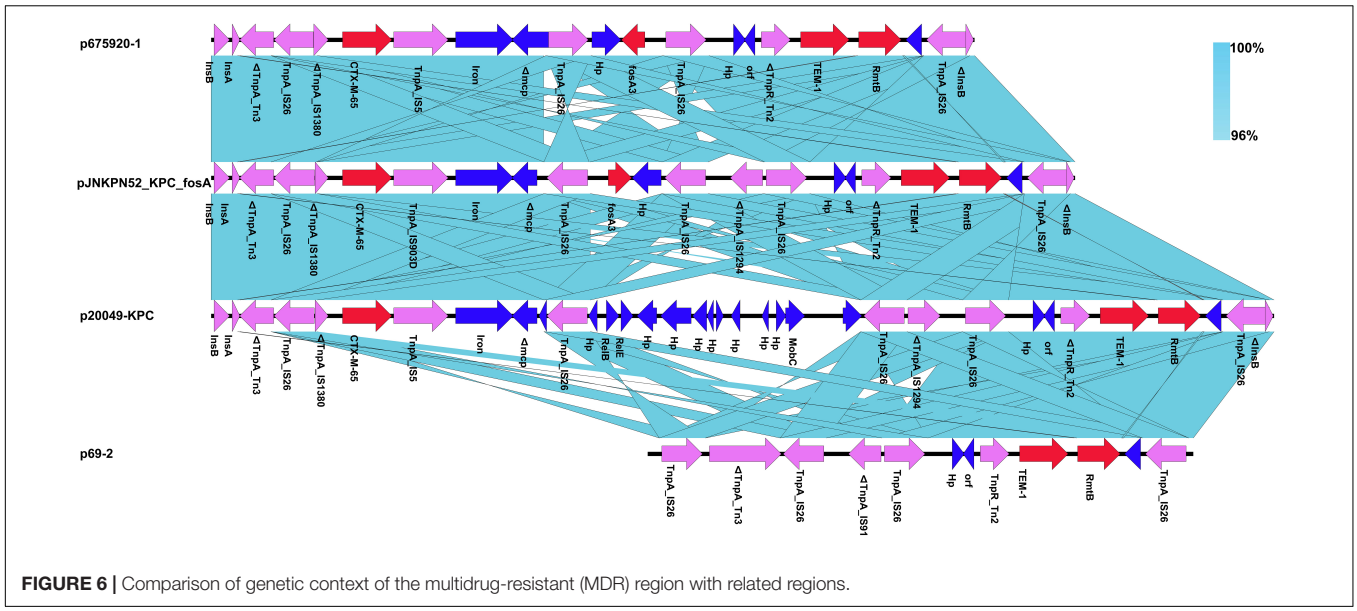

FIGURE 6 | Comparison of genetic context of the multidrug-resistant (MDR) region with related regions.

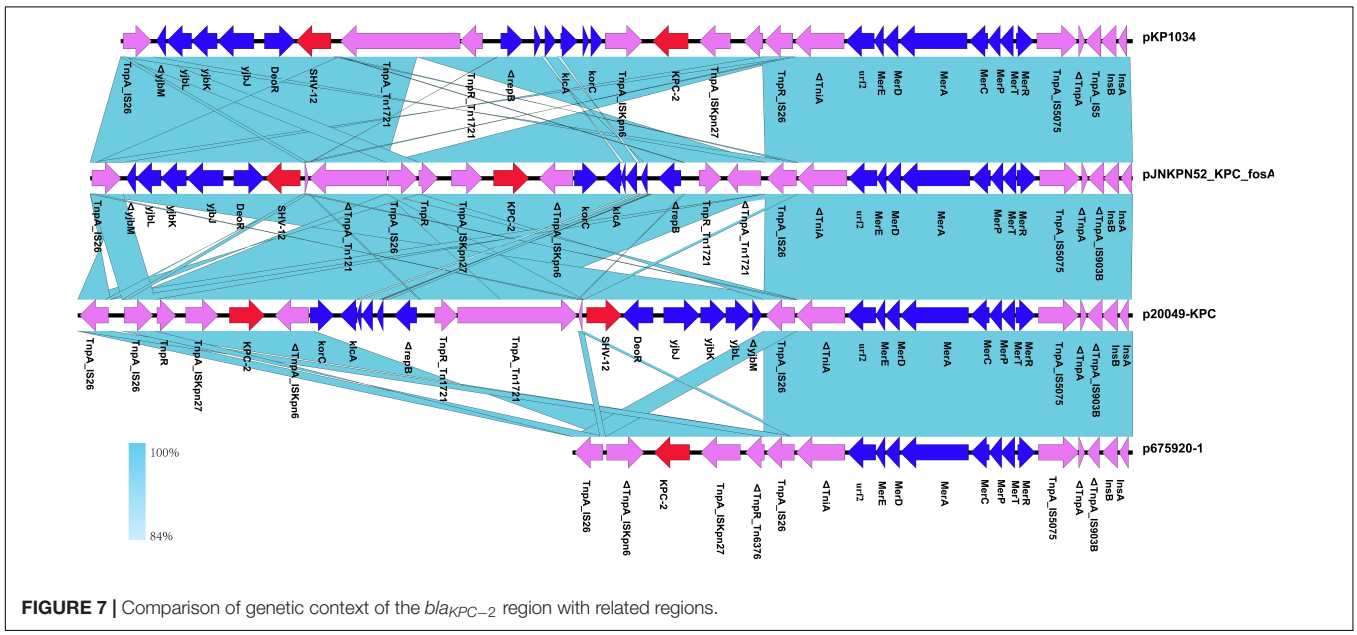

FIGURE 7 | Comparison of genetic context of the bla_{KPC-2} region with related regions.

among CRKP isolates in this study. According to the previous report, IncA/C type plasmids were known to be of broad host range and had been detected in numerous MDR Gram-negative species (Carattoli et al., 2012). Moreover, an outbreak caused by a clone of *Citrobacter freundii* strains bearing bla_{NDM-1} located on IncA/C plasmids and secondary *in vivo* spread of an IncA/C2 plasmid with bla_{NDM-1} to *E. coli*, *K. pneumoniae*, and *Klebsiella oxytoca* from the individual patients was reported in Denmark (Hammerum et al., 2016). Thus, more attention should be paid to monitoring and controlling the horizontal transmission of bla_{NDM} mediated by IncA/C type plasmids among *K. pneumoniae* isolates.

Interestingly, *fosA3* was not detected in any CRKP strains due to class B carbapenemase, including bla_{IMP} or bla_{NDM}. According to the MLST results, KPC-2-producing ST11 was the only clone in our study closely related to *fosA3*. Analysis of the genetic environment confirmed that the mobile element *IS26–fosA3–IS26* played an important role in the dissemination of fosfomycin resistance. Moreover, most of the *fosA3*-positive KPC-2 producing strains (22/23) carried at least two kinds of ESBLs, indicating that ST11 type *K. pneumoniae* might be a good reservoir of resistance genes.

According to previous research, the high prevalence of fosfomycin resistance in KPC-producing isolates from China is associated with plasmids coharboring *fosA3* and bla_{KPC} (Singkham-In et al., 2020). Recently, *fosA3* and bla_{KPC-2} genes located on non-conjugative pCT-KPC-like plasmids have been

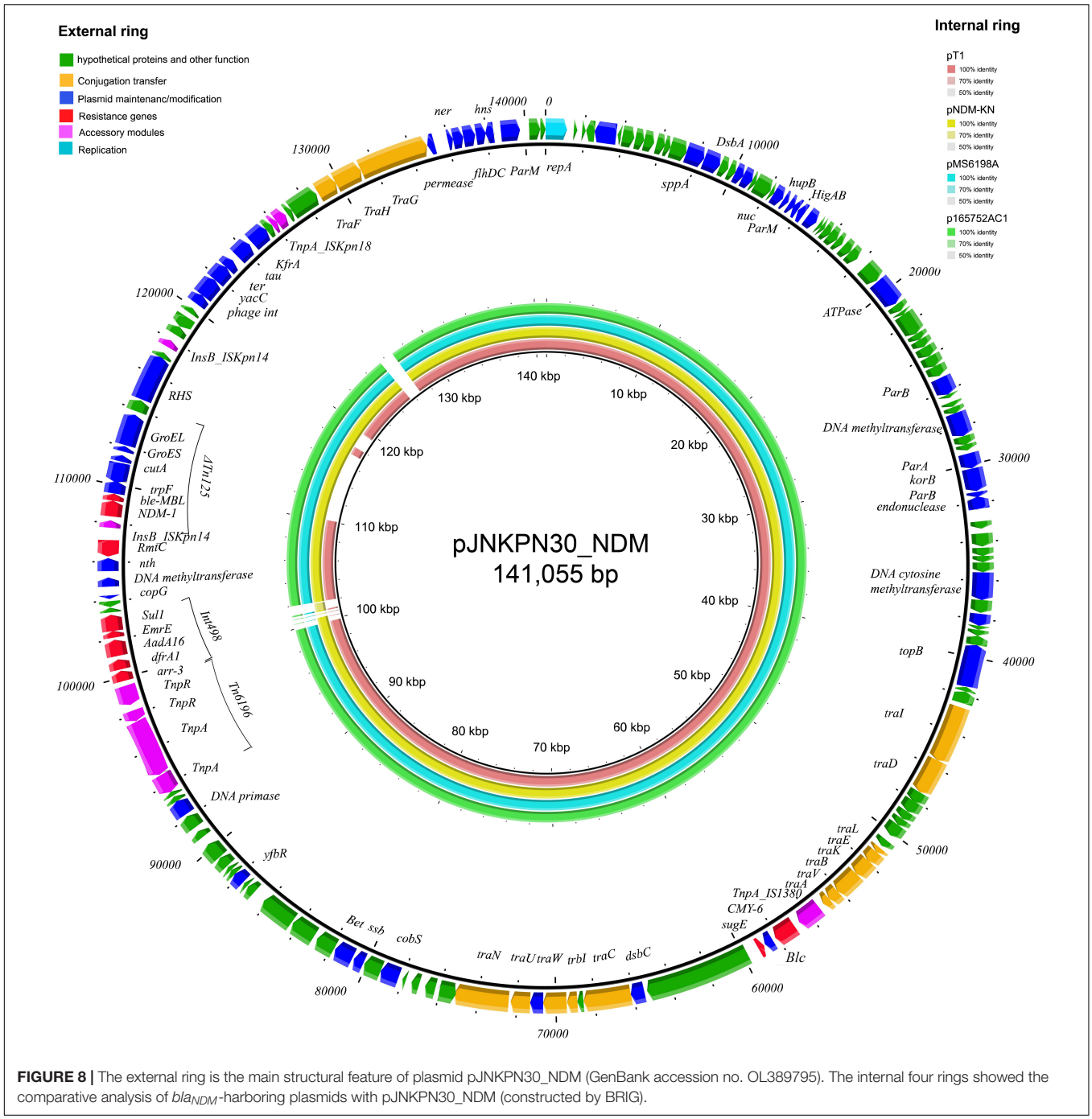

FIGURE 8 | The external ring is the main structural feature of plasmid pJNKPN30_NDM (GenBank accession no. OL389795). The internal four rings showed the comparative analysis of bla_{NDM}-harboring plasmids with pJNKPN30_NDM (constructed by BRIG).

sporadically reported in China (Xiang et al., 2015; Liu et al., 2018; Shi et al., 2018; Zhai et al., 2021). Furthermore, Shi et al. (2018) proved that bla_{KPC-2}- and *rmtB*-carrying pCT-KPC-like plasmids were prevalent among clonal *K. pneumoniae* CG258 strains collected from five different hospitals and were associated with the dissemination of bla_{KPC-2} and *rmtB*. It seemed that the spread of the pCT-KPC-like plasmids was mainly due to the clonal dissemination of ST11 KPC-producing *K. pneumoniae*, as the conjugation tests failed to recover transconjugants in all reports (Zhai et al., 2021).

Recently, a plasmid pEBSI036-2-KPC from a high-risk clone ST11 KL47 serotype of a CR-HvKP strain isolated from an Egyptian hospital was reported. pJNKPN52_KPC_fosA showed 99% identity with pEBSI036-2-KPC. But the transferability of plasmid pEBSI036-2-KPC was not determined (Ahmed et al., 2021). In our study, four ST11-KL47 type *K. pneumoniae* strains, JNKPN52, JNKPN54, JNKPN55, and JNKPN57, could co-transfer *fosA3* and bla_{KPC-2} genes into recipient *E. coli* J53Azi^R by conjugation tests, indicating that the *fosA3* gene could be co-disseminated with bla_{KPC-2}. The four strains

isolated from different patients were identified from the same clone according to the PFGE profiles and cgMLST cluster. Notably, bla_{KPC-2} and *fosA3* genes were confirmed to be located on a plasmid pJNKPN52_KPC_fosA, which shared similar backbones with the previously reported pCT-KPC-like plasmids, including pKP1034, pCT-KPC, pKPC-LK30, p69-2, and p675920-1. For the first time, we confirmed the pCT-KPC-like plasmid-mediated horizontal transmission of bla_{KPC-2} and *fosA3* resistance. We noticed that ten copies of *IS26* were detected in plasmid pJNKPN52_KPC_fosA and would mediate homologous recombination and mobilization of accessory resistance regions within and among different plasmids (Zhai et al., 2021). Therefore, *IS26* may have played a vital role in the generation process of pJNKPN52_KPC_fosA.

CONCLUSION

Our findings indicate that *fosA* is intrinsically distributed in the genome of clinically isolated *K. pneumoniae* and might contribute to fosfomycin resistance. The coexistence of plasmid-mediated *fosA3* and chromosomal-encoded $fosA^{kp}$ was observed commonly among ST11 CRKP strains. The emerging conjugative pCT-KPC-like plasmids coharboring bla_{KPC-2} and *fosA3* would exacerbate the fosfomycin resistance among CRKP strains. ST11-KL64 and ST11-KL47 *K. pneumoniae*, the so-called "super-bug," with higher resistance and virulence, should be monitored by more effective strategies to prevent the future dissemination of resistance.

DATA AVAILABILITY STATEMENT

The datasets presented in this study can be found in online repositories. The names of the repository/repositories and accession number(s) can be found in the article/**Supplementary Material**.

AUTHOR CONTRIBUTIONS

YW contributed to experiment conception and design. YH, YZ, and RC conducted bioinformatics analysis and wrote the manuscript. XZ and YB performed the data analysis. ZS carried out the bacteria identification. XL and CZ prepared the tables and figures. YW is responsible for submitting a competing interest statement on behalf of all authors of the manuscript. All authors contributed to the article and approved the submitted version.

FUNDING

This study was supported by grants from the National Natural Science Foundation of China (81902119) and the Shandong Province Natural Science Foundation (ZR2020MH306).

ACKNOWLEDGMENTS

We thank Mingju Hao of The First Affiliated Hospital of Shandong, First Medical University, and Shandong Provincial Qianfoshan Hospital, for technical assistance.

SUPPLEMENTARY MATERIAL

The Supplementary Material for this article can be found online at: https://www.frontiersin.org/articles/10.3389/fmicb.2021.771170/full#supplementary-material

Supplementary Figure 1 | Comparison of genetic environments of the *fosA*. **(A)** The genetic environment of $fosA^{kp}$ and *foskp96*; **(B)** The genetic environment of *fosA2*; **(C)** The genetic environment of *fosA3*.

REFERENCES

Ahmed, M., Yang, Y., Yang, Y., Yan, B., Chen, G., Hassan, R. M., et al. (2021). Emergence of hypervirulent carbapenem-resistant *Klebsiella pneumoniae* coharboring a bla NDM-1-carrying virulent plasmid and a bla KPC-2-carrying plasmid in an egyptian hospital. *mSphere* 6:e88-21. doi: 10.1128/mSphere.00088-21

Carattoli, A., Bertini, A., Villa, L., Falbo, V., Hopkins, K. L., and Threlfall, E. J. (2005). Identification of plasmids by PCR-based replicon typing. *J. Microbiol. Methods* 63, 219–228. doi: 10.1016/j.mimet.2005.03.018

Carattoli, A., Villa, L., Poirel, L., Bonnin, R. A., and Nordmann, P. (2012). Evolution of IncA/C blaCMY-(2)-carrying plasmids by acquisition of the blaNDM-(1) carbapenemase gene. *Antimicrob. Agents Chemother.* 56, 783–786. doi: 10.1128/AAC.05116-11

Chen, J., Wang, D., Ding, Y., Zhang, L., and Li, X. (2019). Molecular epidemiology of plasmid-mediated fosfomycin resistance gene determinants in *Klebsiella pneumoniae* carbapenemase-producing *Klebsiella pneumoniae* isolates in China. *Microb. Drug Resist.* 25, 251–257. doi: 10.1089/mdr.2018.0137

CLSI (2020). *Performance Standards for Antimicrobial Susceptibility Testing document M100*, 30th Edn. Wayne, PA: Clinical and Laboratory Standards Institute.

Ekwanzala, M. D., Dewar, J. B., Kamika, I., and Momba, M. N. B. (2019). Tracking the environmental dissemination of carbapenem-resistant *Klebsiella pneumoniae* using whole genome sequencing. *Sci. Total Environ.* 691, 80–92. doi: 10.1016/j.scitotenv.2019.06.533

Elliott, Z. S., Barry, K. E., Cox, H. L., Stoesser, N., Carroll, J., Vegesana, K., et al. (2019). The role of fosA in challenges with fosfomycin susceptibility testing of multispecies *Klebsiella pneumoniae* carbapenemase-producing clinical isolates. *J. Clin. Microbiol.* 57:e634-19. doi: 10.1128/JCM.00634-19

EUCAST (2020). *Breakpoints Tables for Interpretation of MICs and Zone Diameters. in Version 10.0*. Växjö: EUCAST.

Hammerum, A. M., Hansen, F., Nielsen, H. L., Jakobsen, L., Stegger, M., Andersen, P. S., et al. (2016). Use of WGS data for investigation of a long-term NDM-1-producing *Citrobacter freundii* outbreak and secondary in vivo spread of blaNDM-1 to *Escherichia coli*, *Klebsiella pneumoniae* and *Klebsiella oxytoca*. *J. Antimicrob. Chemother.* 71, 3117–3124. doi: 10.1093/jac/dkw289

Heras, J., Dominguez, C., Mata, E., Pascual, V., Lozano, C., Torres, C., et al. (2015). GelJ–a tool for analyzing DNA fingerprint gel images. *BMC Bioinformatics* 16:270. doi: 10.1186/s12859-015-0703-0

Huang, L., Cao, M., Hu, Y., Zhang, R., Xiao, Y., and Chen, G. (2021). Prevalence and mechanisms of fosfomycin resistance among KPC-producing *Klebsiella pneumoniae* clinical isolates in China. *Int. J. Antimicrob. Agents* 57:106226. doi: 10.1016/j.ijantimicag.2020.106226

Ito, R., Mustapha, M. M., Tomich, A. D., Callaghan, J. D., McElheny, C. L., Mettus, R. T., et al. (2017). Widespread fosfomycin resistance in gram-negative bacteria

attributable to the chromosomal fosA gene. *mBio* 8:e749-17. doi: 10.1128/mBio.00749-17

Jiang, Y., Shen, P., Wei, Z., Liu, L., He, F., Shi, K., et al. (2015). Dissemination of a clone carrying a fosA3-harbouring plasmid mediates high fosfomycin resistance rate of KPC-producing *Klebsiella pneumoniae* in China. *Int. J. Antimicrob. Agents* 45, 66–70. doi: 10.1016/j.ijantimicag.2014.08.010

Liu, J., Xie, J., Yang, L., Chen, D., Peters, B. M., Xu, Z., et al. (2018). Identification of the KPC plasmid pCT-KPC334: new insights on the evolutionary pathway of epidemic plasmids harboring fosA3-blaKPC-2 genes. *Int. J. Antimicrob. Agents* 52, 510–511. doi: 10.1016/j.ijantimicag.2018.04.013

Liu, P., Chen, S., Wu, Z. Y., Qi, M., Li, X. Y., and Liu, C. X. (2020). Mechanisms of fosfomycin resistance in clinical isolates of carbapenem-resistant *Klebsiella pneumoniae*. *J. Glob. Antimicrob. Resist.* 22, 238–243. doi: 10.1016/j.jgar.2019.12.019

Lu, X., Zeng, M., Xu, J., Zhou, H., Gu, B., Li, Z., et al. (2019). Epidemiologic and genomic insights on mcr-1-harbouring *Salmonella* from diarrhoeal outpatients in Shanghai, China, 2006–2016. *EBioMedicine* 42, 133–144. doi: 10.1016/j.ebiom.2019.03.006

Mączyńska, B., Paleczny, J., Oleksy-Wawrzyniak, M., Choroszy-Król, I., and Bartoszewicz, M. (2021). In vitro susceptibility of multi-drug resistant klebsiellapneumoniae strains causing nosocomial infections to fosfomycin. A comparison of determination methods. *Pathogens* 10:512. doi: 10.3390/pathogens10050512

Nurk, S., Bankevich, A., Antipov, D., Gurevich, A. A., Korobeynikov, A., Lapidus, A., et al. (2013). Assembling single-cell genomes and mini-metagenomes from chimeric MDA products. *J. Comput. Biol.* 20, 714–737. doi: 10.1089/cmb.2013.0084

Poirel, L., Walsh, T. R., Cuvillier, V., and Nordmann, P. (2011). Multiplex PCR for detection of acquired carbapenemase genes. *Diagn. Microbiol. Infect. Dis.* 70, 119–123. doi: 10.1016/j.diagmicrobio.2010.12.002

Pontikis, K., Karaiskos, I., Bastani, S., Dimopoulos, G., Kalogirou, M., Katsiari, M., et al. (2014). Outcomes of critically ill intensive care unit patients treated with fosfomycin for infections due to pandrug-resistant and extensively drug-resistant carbapenemase-producing Gram-negative bacteria. *Int. J. Antimicrob. Agents* 43, 52–59. doi: 10.1016/j.ijantimicag.2013.09.010

Qamar, M. U., Ejaz, H., Walsh, T. R., Shah, A. A., Al, F. D., Alkufeidy, R. M., et al. (2021). Clonal relatedness and plasmid profiling of extensively drug-resistant New Delhi metallo-beta-lactamase-producing *Klebsiella pneumoniae* clinical isolates. *Future Microbiol.* 16, 229–239. doi: 10.2217/fmb-2020-0315

Sherry, N. L., Lane, C. R., Kwong, J. C., Schultz, M., Sait, M., Stevens, K., et al. (2019). Genomics for Molecular Epidemiology and Detecting Transmission of Carbapenemase-Producing Enterobacterales in Victoria, Australia, 2012 to 2016. *J. Clin. Microbiol.* 57:e573-19. doi: 10.1128/JCM.00573-19

Shi, L., Feng, J., Zhan, Z., Zhao, Y., Zhou, H., Mao, H., et al. (2018). Comparative analysis of bla KPC-2- and rmtB-carrying IncFII-family pKPC-LK30/pHN7A8 hybrid plasmids from *Klebsiella pneumoniae* CG258 strains disseminated among multiple Chinese hospitals. *Infect. Drug. Resist* 11, 1783–1793. doi: 10.2147/IDR.S171953

Singkham-In, U., Muhummudaree, N., and Chatsuwan, T. (2020). fosA3 overexpression with transporter mutations mediates high-level of fosfomycin resistance and silence of fosA3 in fosfomycin-susceptible *Klebsiella pneumoniae* producing carbapenemase clinical isolates. *PLoS One* 15:e0237474. doi: 10.1371/journal.pone.0237474

Tseng, S., Wang, S., Ma, L., Wang, T., Yang, T., Siu, L. K., et al. (2017). The plasmid-mediated fosfomycin resistance determinants and synergy of fosfomycin and meropenem in carbapenem-resistant *Klebsiella pneumoniae* isolates in Taiwan. *J. Microbiol. Immunol. Infect.* 50, 653–661. doi: 10.1016/j.jmii.2017.03.003

Vardakas, K. Z., Legakis, N. J., Triarides, N., and Falagas, M. E. (2016). Susceptibility of contemporary isolates to fosfomycin: a systematic review of the literature. *Int. J. Antimicrob. Agents* 47, 269–285. doi: 10.1016/j.ijantimicag.2016.02.001

Wang, Q., Wang, X., Wang, J., Ouyang, P., Jin, C., Wang, R., et al. (2018). Phenotypic and Genotypic Characterization of Carbapenem-resistant *Enterobacteriaceae*: data from a longitudinal large-scale CRE STUDY in China (2012-2016). *Clin. Infect. Dis.* 67, S196–S205. doi: 10.1093/cid/ciy660

Weber, R. E., Pietsch, M., Fruhauf, A., Pfeifer, Y., Martin, M., Luft, D., et al. (2019). IS26-mediated transfer of bla NDM-1 as the main route of resistance transmission during a polyclonal, multispecies outbreak in a german hospital. *Front. Microbiol.* 10:2817. doi: 10.3389/fmicb.2019.02817

Wyres, K. L., Nguyen, T. N. T., Lam, M. M. C., Judd, L. M., van Vinh Chau, N., Dance, D. A. B., et al. (2020). Genomic surveillance for hypervirulence and multi-drug resistance in invasive *Klebsiella pneumoniae* from South and Southeast Asia. *Genome Med.* 12:11. doi: 10.1186/s13073-019-0706-y

Xiang, D. R., Li, J. J., Sheng, Z. K., Yu, H. Y., Deng, M., Bi, S., et al. (2015). Complete sequence of a novel IncR-F33:A-:B- plasmid, pKP1034, harboring fosA3, blaKPC-2, blaCTX-M-65, blaSHV-12, and rmtB from an epidemic *Klebsiella pneumoniae* sequence type 11 strain in China. *Antimicrob. Agents Chemother.* 60, 1343–1348. doi: 10.1128/AAC.01488-15

Xiao, T., Zhu, Y., Zhang, S., Wang, Y., Shen, P., Zhou, Y., et al. (2020). A retrospective analysis of risk factors and outcomes of carbapenem-resistant *Klebsiella pneumoniae* bacteremia in nontransplant patients. *J. Infect. Dis.* 221, S174–S183. doi: 10.1093/infdis/jiz559

Zhai, Y., Li, D., Du, P., Zhang, Z., He, Z., Guo, Y., et al. (2021). Complete sequences of two new KPC-harbouring plasmids in *Klebsiella pneumoniae* ST11 strains in China. *J. Glob. Antimicrob. Resist.* 24, 114–120. doi: 10.1016/j.jgar.2020.11.023

Zhang, W., Zhu, Y., Wang, C., Liu, W., Li, R., Chen, F., et al. (2019). Characterization of a multidrug-resistant porcine *Klebsiella pneumoniae* sequence type 11 strain coharboring bla KPC-2 and fosA3 on two novel hybrid plasmids. *mSphere* 4:e590-19. doi: 10.1128/mSphere.00590-19

Zhou, K., Xiao, T., David, S., Wang, Q., Zhou, Y., Guo, L., et al. (2020). Novel subclone of carbapenem-resistant *Klebsiella pneumoniae* sequence type 11 with enhanced virulence and transmissibility, China. *Emerg. Infect. Dis.* 26, 289–297. doi: 10.3201/eid2602.190594

Conflict of Interest: The authors declare that the research was conducted in the absence of any commercial or financial relationships that could be construed as a potential conflict of interest.

Publisher's Note: All claims expressed in this article are solely those of the authors and do not necessarily represent those of their affiliated organizations, or those of the publisher, the editors and the reviewers. Any product that may be evaluated in this article, or claim that may be made by its manufacturer, is not guaranteed or endorsed by the publisher.

frontiers in Microbiology

ORIGINAL RESEARCH
published: 06 January 2022
doi: 10.3389/fmicb.2021.765492

Temperature-Regulated IncX3 Plasmid Characteristics and the Role of Plasmid-Encoded H-NS in Thermoregulation

*Liu Baomo[1,2†], Shui Lili[3†], Robert A. Moran[4], Willem van Schaik[4]*and Zhuo Chao[1]**

[1]State Key Laboratory of Respiratory Disease, The First Affiliated Hospital of Guangzhou Medical University, Guangzhou, China, [2]Department of Respiratory and Critical Care Medicine, The First Affiliated Hospital of Sun Yat-sen University, Guangzhou, China, [3]Department of Pulmonary and Critical Care Medicine, The First Affiliated Hospital of Chongqing Medical University, Chongqing, China, [4]Institute of Microbiology and Infection, University of Birmingham, Birmingham, United Kingdom

OPEN ACCESS

Edited by:
Fenni Zhang,
Zhejiang University, China

Reviewed by:
Yukihiro Akeda,
Osaka University, Japan
Susu He,
Nanjing University, China

***Correspondence:**
Willem van Schaik
W.vanSchaik@bham.ac.uk
Zhuo Chao
chao_sheep@263.net

†*These authors have contributed equally to this work*

Specialty section:
This article was submitted to Antimicrobials, Resistance and Chemotherapy, a section of the journal Frontiers in Microbiology

Received: *27 August 2021*
Accepted: *17 November 2021*
Published: *06 January 2022*

Citation:
Baomo L, Lili S, Moran RA, van Schaik W and Chao Z (2022) Temperature-Regulated IncX3 Plasmid Characteristics and the Role of Plasmid-Encoded H-NS in Thermoregulation. Front. Microbiol. 12:765492. doi: 10.3389/fmicb.2021.765492

Carbapenem-resistant Enterobacteriaceae (CRE) are a critical public health problem worldwide. Globally, IncX3-type plasmids have emerged as the predominant vehicles carrying the metallo-β-lactamase gene bla_{NDM}. Although bla_{NDM}-bearing IncX3 plasmids have been found in various hosts from diverse environments, whether their transfer and persistence properties vary under different conditions and what factors influence any variation is unknown. By observing the effects of different temperatures on IncX3 plasmid conjugation rates, stability, and effects on host fitness in *Escherichia coli*, we demonstrate that temperature is an important determinant of plasmid phenotypes. The IncX3 plasmid pGZIncX3 transferred at highest frequencies, was most stable and imposed lower fitness costs at 37°C. Temperature-regulated variation in pGZIncX3 properties involved a thermoregulated plasmid-encoded H-NS-like protein, which was produced at higher levels at 30°C and 42°C and inhibited the expression of type IV secretion system genes involved in conjugation. These findings suggest that bla_{NDM}-bearing IncX3 plasmids are adapted to carriage by enterobacteria that colonize mammalian hosts and could explain the rapid dissemination of these plasmids among human-associated species, particularly in hospital settings.

Keywords: IncX3, carbapenem resistance Enterobacteriaceae, temperature, plasmid-encoded hns, fitness

INTRODUCTION

Carbapenem-resistant Enterobacteriaceae (CRE) are a critical public health problem globally, as they can exhibit resistance to almost all available antibiotics and are responsible for extensive morbidity and mortality (Logan and Weinstein, 2017). Bacteremia due to CRE can result in mortality rates higher than 40% in China (Zhang et al., 2018). New Delhi metallo-β-lactamase (NDM)-type carbapenemase is the major mechanism mediating carbapenem resistance in approximately 40% of CRE isolates (Bush and Bradford, 2020). Although the bla_{NDM} gene can be found inserted in the chromosome, the substantial majority of carriage is linked to plasmids, which contribute significantly to the rapid dissemination of carbapenem resistance (Khan et al., 2017).

IncX3 plasmids are emerging as the predominant plasmid type carrying bla_{NDM} worldwide, with approximately one third of bla_{NDM}-carrying plasmids deposited in GenBank containing IncX3-type replicons (Ma et al., 2020). Additionally, IncX3 plasmids appear to function as a platform for the evolution of NDM enzymes, as diverse bla_{NDM} gene variants have been found in plasmids of the same replicon type (Ma et al., 2020). Strains containing bla_{NDM}-bearing IncX3 plasmids have been isolated from clinical settings (Zhou et al., 2020), companion animals (Nigg et al., 2019), agricultural settings (Zhang et al., 2019), and the environment (Zhai et al., 2020), which suggests they can persist in their hosts under various conditions, including different temperatures. The mechanisms that facilitate IncX3 plasmid persistence and dissemination at different temperatures are unknown.

In *Escherichia coli* and other Gram-negative bacteria, the histone-like nucleoid structuring (H-NS) protein has been shown to take part in the regulation of chromosomal transcriptional networks (Dorman and Ni Bhriain, 2020). Many genes encoding different H-NS family proteins have been found in microbial chromosomes as well as in plasmids (Shintani et al., 2015). Our previous work revealed that a H-NS protein homolog encoded by an IncX3-plasmid inhibits plasmid transfer and partitioning (Liu et al., 2020). Plasmid-encoded H-NS-like proteins are also known to play an important role in the regulation of transfer genes in IncH plasmids. The well-studied IncHI1 plasmid R27 exhibits thermosensitive variation in conjugative transfer frequencies modulated by host- and plasmid-encoded H-NS-like proteins (Forns et al., 2005).

In this study, we examined the IncX3 plasmid-encoded H-NS-like protein and characterized its effect on plasmid phenotypes at various temperatures. We show that this protein is essential in linking plasmid phenotypes with temperatures.

TABLE 1 | All test strains in this work.

Strains	Description	Reference
J53	*E. coli* F⁻ *met pro* Azi^r	Matsumura et al., 2018
J330	J53 with pGZIncX3 transferred naturally	Liu et al., 2020
J330(*phns*)	J53 with pACYC184*phns* transferred by electroporation	This work
J330(pACYC184)	J53 with pACYC184 transferred by electroporation	This work
Pkhns	J53 with pGZIncX3Δ*phns* transferred by electroporation	Liu et al., 2020
Pkhns(*phns*)	J330 with pACYC184 *phns* transferred by electroporation	This work
Pkhns(pACYC184)	J330 with pACYC184 transferred by electroporation	This work
Ec600	*E.coli* recipient strains for conjugation experiments	Laboratory stock
Plasmids		
pGZIncX3	blaNDM$^+$, IncX3, sharing 99% similarity with pNDM-HN380	Liu et al., 2020
pGZIncX3Δ*phns*	pGZIncX3 knocking down plasmid-encoded phns gene	Liu et al., 2020
pACYC184	Chl^r, Tet^r, blank vector for gene complementary *hns*::Chl^r, pACYC184	Rose, 1988
pACYC184*phns*	with inserted IncX3 plasmid-encoded *phns* gene	This work

MATERIALS AND METHODS

Bacterial Strains, Plasmids, and Culture Conditions

Bacterial strains and plasmids presented in this study are detailed in **Table 1**.

Strains J330(*phns*), J330(pACYC184), Pkhns(*phns*), and Pkhns(pACYC184) were obtained by transforming the corresponding plasmids into these strains by electrotransformation. Bacteria were stored in 25% glycerol medium at −80°C and recovered and cultured in Luria broth (LB) medium (containing 10 g NaCl, 10 g tryptone, and 5 g yeast per liter) at 37°C unless otherwise mentioned.

Conjugation Experiments

Conjugation assays with pGZIncX3 and its derivatives were conducted as previously reported (Forns et al., 2005; Wang et al., 2017), using rifampin-resistant *E. coli* Ec600 as a recipient strain. Briefly, cultures of donor and recipient strains were grown overnight with shaking at different temperatures (25, 30, 37, or 42°C) in LB medium. The mating mixture, with a 1:2 donor to recipient ratio, was incubated at the corresponding temperature, without shaking overnight and then plated in LB agar supplemented with rifampin (200 μg ml^{-1}) single (for recipients) or with meropenem (2 μg ml^{-1}; for transconjugants). The plates were incubated at 37°C, and the mating frequency was calculated as the number of transconjugants per recipient.

Plasmid Stability Test

Plasmid stability was determined as previously reported with minor modifications (Gao et al., 2020). Briefly, cultures were incubated at 25, 30, 37, or 42°C in a shaking water bath (200 rpm) and were diluted 1,000-fold in antibiotic-free LB broth. After 24 h, cultures were serially diluted and plated on antibiotic-free LB agar and LB agar containing meropenem (0.5 μg ml^{-1} L). The retention rate of the bla_{NDM-1} gene was calculated by dividing the number of colonies that grew on meropenem-containing LB agar by the number of colonies on antibiotic-free LB agar. In addition, 10 colonies were randomly selected and subjected to PCR validation of the bla_{NDM-1} gene. [It is unlikely that the chromosomal integration of *NDM* gene in plasmid stability test occurred. In our previous published work for Inc*X3* plasmid (Liu et al., 2020), we have proved

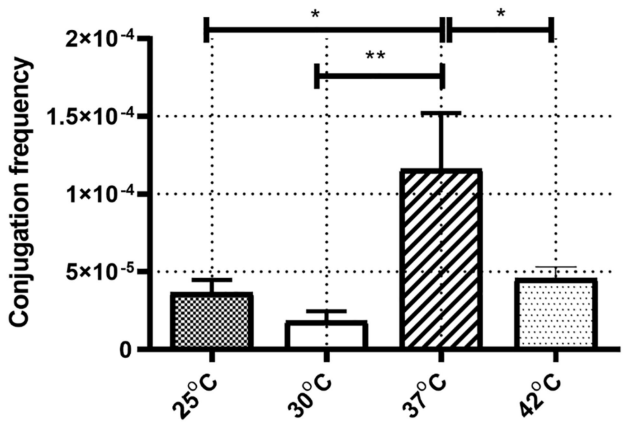

FIGURE 1 | The conjugation frequency of IncX3 at four corresponding temperature. The conjugation frequency was calculated as transconjugants per recipient. Error bars indicate the standard deviations for six triplicate samples. $^{*}p<0.05/^{**}p<0.01$ versus the result for conjugation frequency at 37°C.

that "PCR tests revealed that the blaNDM-1 gene was maintained by transconjugants and wild-type isolates for 1,000 generations. In addition, the location of the blaNDM-1 gene did not change in the decedents, as shown by Southern blotting." The 24 h passage in this plasmid stability test could not lead to *NDM*-1 chromosomal integration].

Competition Experiments

To assess the cost of carriage of bla_{NDM}-bearing plasmid pGZIncX3 in *E. coli* at various temperatures (25, 30, 37, or 42°C), growth competition experiments between *E. coli* J53 and pGZIncX3-carrying derivatives were performed in LB broth using a previously published protocol (Johnson et al., 2015). Briefly, colonies from each strain were initially grown individually in LB broth at 25, 30, 37, or 42°C overnight with shaking. On day 0, bacteria were pelleted and suspended in equal volumes of PBS, and then inoculated at a volume of 25 µl each for competing strains into 5 ml of sterile LB broth. Competitions were performed for 24 h at each temperature, after which the cultures were serially diluted and plated on LB agar without antibiotic for total bacterial counts and on LB agar containing meropenem (0.5 µg ml^{-1}) to select for cells containing pGZIncX3. All competition experiments were performed a minimum of three times. Fitness cost was calculated as follows: $\log2(a/b)/\log2(c/d)$, where a = the number of plasmid-free cells at 24 h, b = the number of plasmid-free cells at 0 h, c = the number of plasmid-containing cells at 24 h, and d = the number of plasmid-containing cells at 0 h (Johnson et al., 2015).

Plasmid Construction

For performing complementation experiments, the plasmid-encoded *phns* gene (positions 28,899–29,354 in GenBank accession JX104760) of IncX3 plasmid pNDM-HN380 (JX104760) was cloned into the pACYC184 vector. After amplifying the *phns* gene using PrimeSTAR® HS DNA Polymerase (Takara), the PCR fragment was purified using TaKaRa MiniBEST DNA Fragment Purification Kit (Takara) and digested with EcoRI and BamHI restriction enzymes (Takara). Ligation was performed in pACYC184 digested with the same restriction enzymes. The resulting plasmid (pACYC184*phns*) was transformed into *E. coli* DH5α and picked in the presence of chloramphenicol. Primers were used for sequencing to confirm correct in-frame insertion of the *phns* gene.

Real-Time Polymerase Chain Reaction

RNA of all samples was isolated using the E.Z.N.A. Bacterial RNA Kit (Omega Bio-tek). The qPCR was conducted with primers targeting the chromosome-encoded *idnT* (reference gene) and the plasmid gene as below. The isolated RNA was then transcribed into cDNA using a PrimeScript™ RT Master Mix (TaKaRa). Real-time polymerase chain reaction (RT-PCR) was used to quantify the expression of genes related to conjugation (*pilX4*, *pliX5*, *pilX9*, and *pilX10*). RT-PCR was conducted using the TB Green™ Premix Ex Taq™ II (TaKaRa) with the standard procedure for two-step PCR amplification (LightCycler96, Roche, Switzerland).

Data Analysis

GraphPad Prism 8.0 was used for statistics analysis and figure drawing. ANOVA was used to analyze the difference between groups.

RESULTS

The Transfer of the IncX3 Plasmid pGZIncX3 to *E. coli* Is Regulated by Temperature

The frequencies of IncX3 plasmid pGZIncX3 conjugative transfer from J330 to *E. coli* Ec600 were determined at different temperatures (**Figure 1**). ANOVA analysis showed a significant difference between conjugation frequencies at different temperatures ($p=0.002$). Conjugation frequency was highest at 37°C (1.2×10^{-4}) while incubation at 25°C, 30°C, and 42°C reduced transfer rates (3.7×10^{-5}, 1.8×10^{-5}, and 4.6×10^{-5}, respectively) with the lowest conjugation frequencies at 25°C or 30°C. There was no significant difference between conjugation frequency at 25°C and 30°C.

H-NS Gene Expression Varied With Differences in Temperature

To study the mechanism of the temperature dependence of plasmid conjugation, stability, and fitness, we focused on the pGZIncX3 gene *phns*, which encodes a H-NS-like protein. We previously showed that this gene is an inhibitor of plasmid transfer and partitioning (Liu et al., 2020). To further characterize the role of *phns,* we first determined the expression of *phns* under different temperatures, which revealed that *phns* was more highly expressed at 30°C and 42°C that at 25°C and 37°C (**Figure 2**). To avoid the impact of plasmid copy numbers

(PCN) at different degree on gene expression, we compared them and found no difference (see **Supplementary data 1, Figure n1**). Moreover, *phns* itself did not affect PCN (**Supplementary data 1, Figure n2**).

Plasmid-Encoded H-NS Affects Thermoregulation of IncX3 Transfer

To confirm the role of *phns* gene in plasmid fitness, we obtained pGZIncX3 derivatives harboring a *phns* deletion and the complemented mutant. *E. coli* strain J53 harboring either wild-type (WT) pGZIncX3 or its *phns* deleted or complemented derivatives were used as the donor in mating assays performed at four different temperatures (**Figure 3**).

At 37°C, conjugation results showed that *phns* deletion derepressed plasmid transfer. Lack of *phns* gene promoted the transfer rates of pGZIncX3 with the *phns* deletion (Pkhns) to Ec600 by 4.2-fold. Complementation of *phns* gene restored the transfer rates of Pkhns. We also found a reduction of conjugation frequencies in J330 complemented with *phns*.

At 25, 30, and 42°C, the plasmid-encoded H-NS-like protein also exerted a negative impact on conjugation. At every temperature, J330 with *phns* complementation exhibited decreased transfer rates relative to the parental strain J330 while *phns*-null strains showed robust transfer ability with high conjugation rates.

Temperature Regulates the Conjugative Transfer of IncX3 Plasmid by Regulating the Expression of H-NS-Like Protein

In order to verify that temperature affects the conjugation frequency of plasmids by regulating the expression of the *phns* gene, we compared the conjugation frequency of pGZIncX3 and pGZIncX3Δhns to the recipient strain EC600 at different temperatures by using a plasmid conjugation experiment. As shown in **Figure 4A**, when the *phns* gene is deleted, there is no difference in the conjugation frequency of plasmid pGZIncX3Δhns at 30 degrees, 37 degrees, and 42 degrees. **Figure 4B** shows the comparison of the conjugation frequency of pGZIncX3 in J330 at 30 degrees, 37 degrees, and 42 degrees with the conjugation frequency of pGZIncX3 in the *phns* gene overexpression strain J330 (*phns*) at 37 degrees. The frequency is significantly reduced at 30 degrees and 42 degrees, which is consistent with the decrease in the conjugation frequency of pGZIncX3 when the *phns* gene is overexpressed at 37 degrees, suggesting that *phns* gene is upregulated at 30 degrees and 42 degrees, further inhibiting plasmid conjugative transfer.

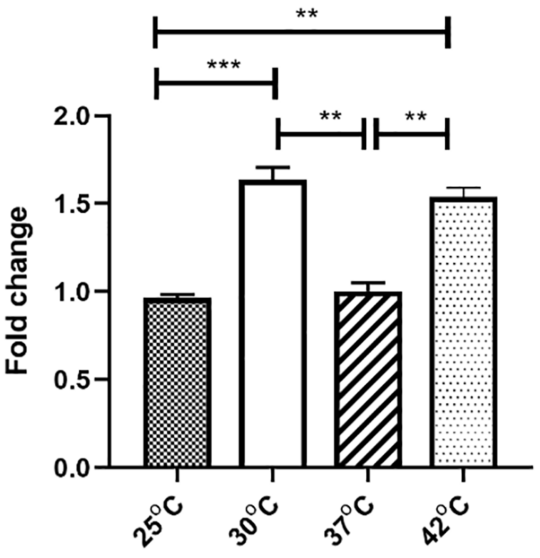

FIGURE 2 | The effect of four temperatures on pGZIncX3 plasmid gene *phns* expression levels. Variances between different temperature groups were shown with *($p < 0.05$), **($p < 0.01$), and ***($p < 0.001$).

Transcription of Several Genes Encoded in pGZIncX3 Is Enhanced in a *phns* Deletion Mutant

We used RT-PCR to test if the plasmid-encoded H-NS-like protein has an impact on the transcription of plasmid genes involved in conjugation. In our previous work (Liu et al., 2020), we have analyzed the transcriptome differences between J330 and Pkhns, which showed that the expressions of all genes from *pilX* operon (including *pilX1,2,3,4,5,6,8,9,10,11*) are elevated in Pkhns. These genes encode constituents of a type IV secretion system (T4SS) and have been shown to be involved in conjugation (Chen et al., 2009). The *pilX4*, *pilX5*, *pilX9,* and *pilX10* genes were chosen to represent expression of the *pilX* operon at different temperatures (**Figure 5**).

We found that the *phns* gene reduces the expression of conjugation genes at various temperature which is corresponding to the results of conjugation test above. At low temperature (25°C or 30°C), the expression of *pilX4,5,9,10* in Pkhns could be more than 50-fold upregulated compared with J330. This experiment demonstrated that although low temperature could inhibit conjugation and the expression of genes involved in conjugation, the deletion of the plasmid gene encoding the H-NS homolog could abolish the impact of temperature.

The Impact of Temperature on Plasmid-Mediated Bacterial Fitness and Plasmid Stability in *E. coli J53*

To explore the impact of temperature on plasmid stability and *E. coli* host fitness, pGZIncX3 was transferred into *E. coli* J53 by conjugation to create J330. The stability of pGZIncX3 in J330 was evaluated after growth in antibiotic-free medium (**Figure 6**). pGZIncX3 was most stable at 37°C, with plasmid retention rate of 6.0%, with significantly lower plasmid retention at 25°C, 30°C, and 42°C (**Figure 6A**).

To evaluate the impact of pGZIncX3 on J330 fitness at different temperatures, growth competition experiments between J330 and plasmid-free J53 were performed at different temperatures. pGZIncX3 had a higher fitness cost at 30°C and 42°C than at 37°C (**Figure 6B**), but no significant difference in fitness cost was observed between 25°C and 37°C.

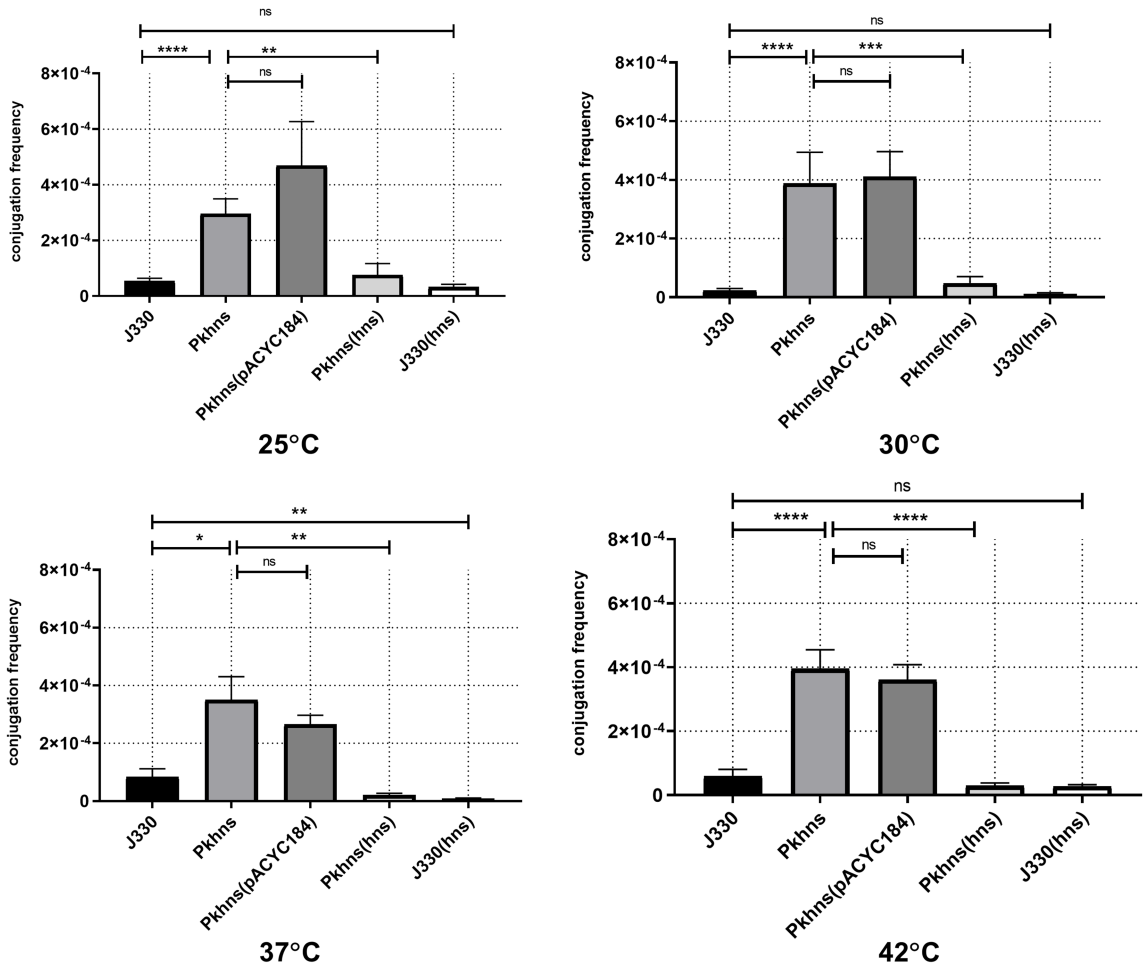

FIGURE 3 | Plasmid-encoded H-NS-like protein represses plasmid transfer at different temperatures. Conjugation frequency at various temperature was evaluated for J330, Pkhns(*phns*-null strains), corresponding *phns* complementary strains Pkhns(hns), J330(hns), and corresponding blank-vector complementary strains J330(pACYC184), Pkhns(pACYC184). Variances between different temperature groups were shown with *($p < 0.05$), **($p < 0.01$), and ***($p < 0.001$), ****($p < 0.0001$).

The Impact of *phns* on Plasmid Stability and Host Fitness Cost at Various Temperature

To test if plasmid stability also changed through regulation of the plasmid-encoded H-NS protein, we compared stability of pGZIncX3 in the *E. coli* host at a range of temperature. Under all temperatures tested, *phns*-null J330 derivate strains showed higher plasmid retention rates versus wild-type strains (**Figure 7A**).

We also tested the effects of *phns* on bacterial fitness. Deletion of *phns* slightly increased the fitness of plasmid-containing *E. coli* fitness at 25 and 30°C, whereas overall fitness at 37 and 42°C did not change significantly (**Figure 7B**).

DISCUSSION

The role of bla_{NDM}-bearing IncX3 plasmids in the spread of carbapenem resistance makes them an important threat to global public health. Our results show that the phenotypes conferred by the IncX3 plasmid pGZIncX3 are affected by environmental temperature and the plasmid-encoded H-NS-like protein is involved in this regulation. In this study, we focused on the effects of four distinct temperatures on IncX3 plasmid phenotypes as they are representative of environmental temperatures in many countries in Asia and the Middle East (25°C and 30°C), the temperature of the human body (37°C), and the body temperature of chickens (42°C; Rozwandowicz et al., 2019).

Here, we demonstrate that the IncX3 plasmid pGZIncX3 could transfer at highest frequencies at 37°C, suggesting that transfer of this important group of plasmids is highest in the guts of humans and other mammals, which is in line with previous work (Liakopoulos et al., 2018; Wang et al., 2018), that showed that the optimal temperature for conjugative transfer of IncX3 plasmids was 37°C. In addition, we have shown that at 37°C, pGZIncX3 was most stable in the absence of antibiotic selective pressure and imposed

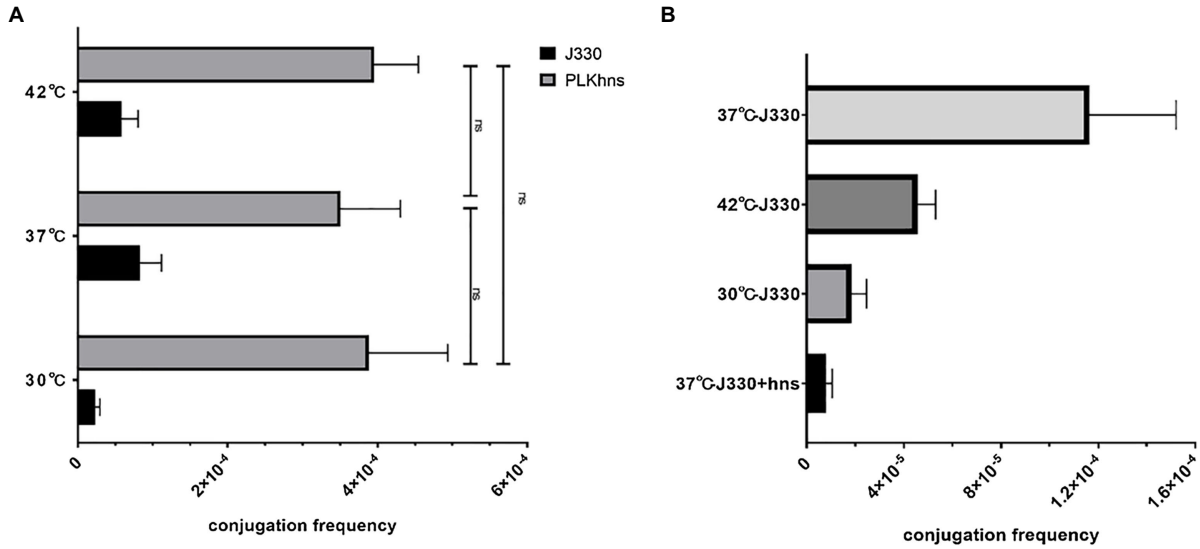

FIGURE 4 | (A) Comparison of the frequency of conjugative transfer between the *phns* gene deletion plasmid and the original plasmid at different temperatures. At different temperatures, the joint frequency of pGZIncX3Δhns and pGZIncX3. **(B)** Comparison of conjugation frequency of pGZIncX3 at three different temperatures and 37 degrees when *phns* gene was overexpressed.

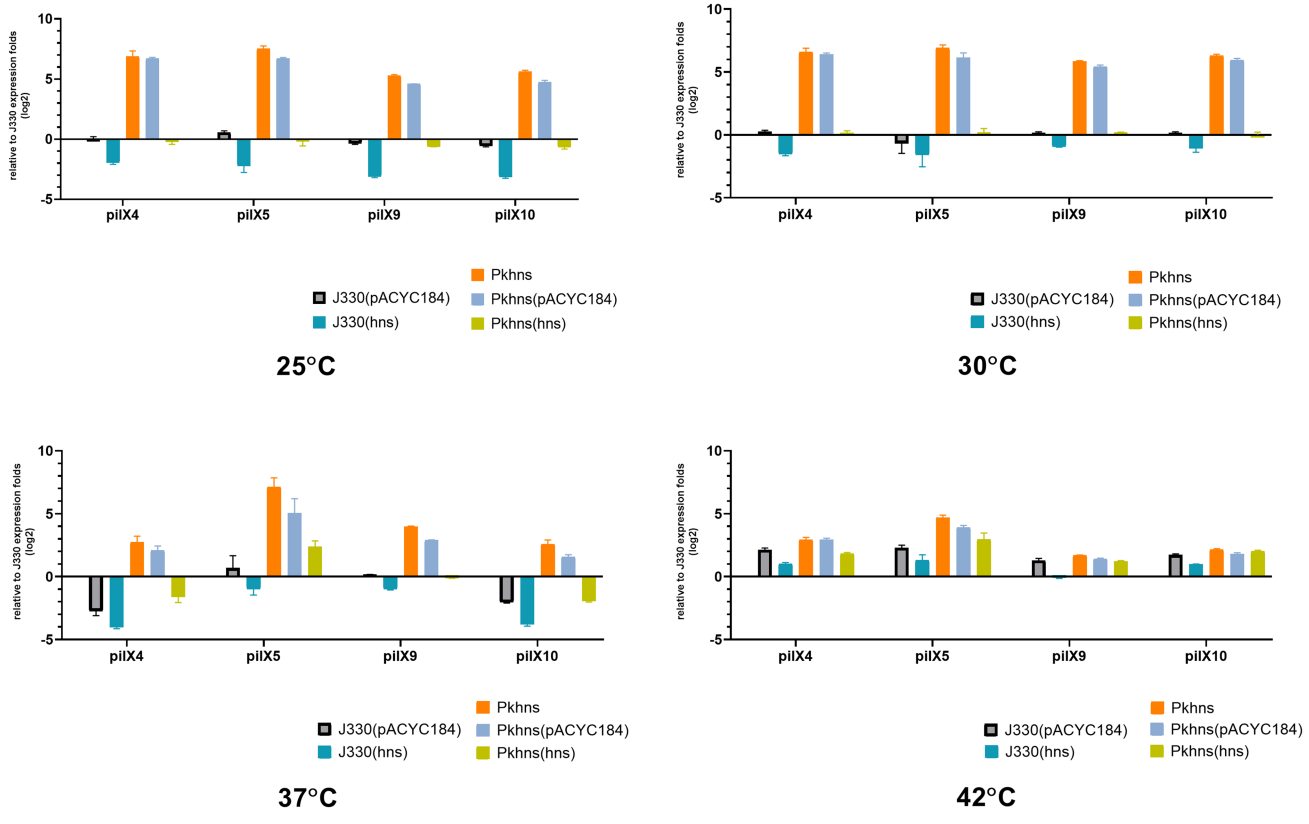

FIGURE 5 | At four different temperatures (25, 30, 37, and 42°C), the mRNA expression of T4SS-related gene pilX4, 5, 9, and 10 of six gene context-related strains: *J330, Pkhns*(*phns*-null strains), corresponding *phns* complementary strains *Pkhns(hns), J330(hns),* and corresponding blank-vector complementary strains *J330(pACYC184), Pkhns(pACYC184)*.

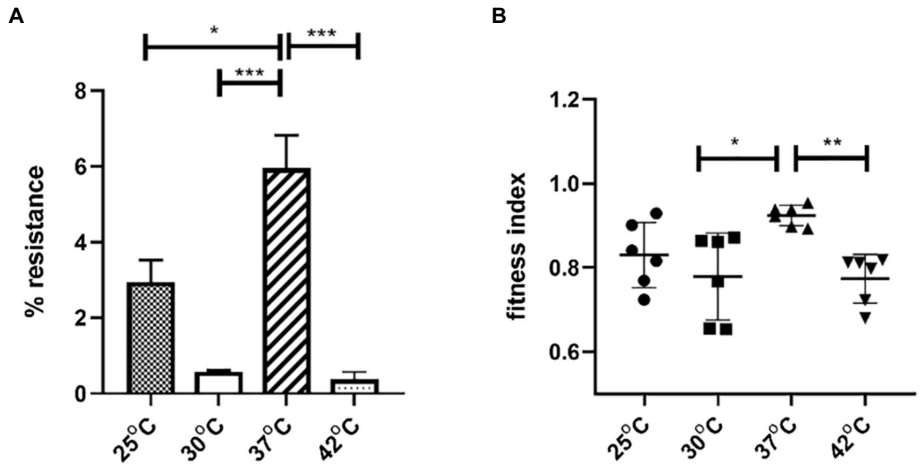

FIGURE 6 | The impact of temperatures on IncX3 plasmid stability **(A)** and fitness cost **(B)** in *Escherichia coli*. **(A)** Plasmid stability is estimated by the percent of plasmid-containing *E. coli* at 24 h as determined by resistance to meropenem. **(B)** Fitness index is calculated by formula described in Section "Materials and Methods." The higher fitness index represents better fitness of plasmid-containing strains. Significant differences between temperatures are indicated with asterisks: $^{*}p<0.05$, $^{**}p<0.01$, and $^{***}p<0.001$.

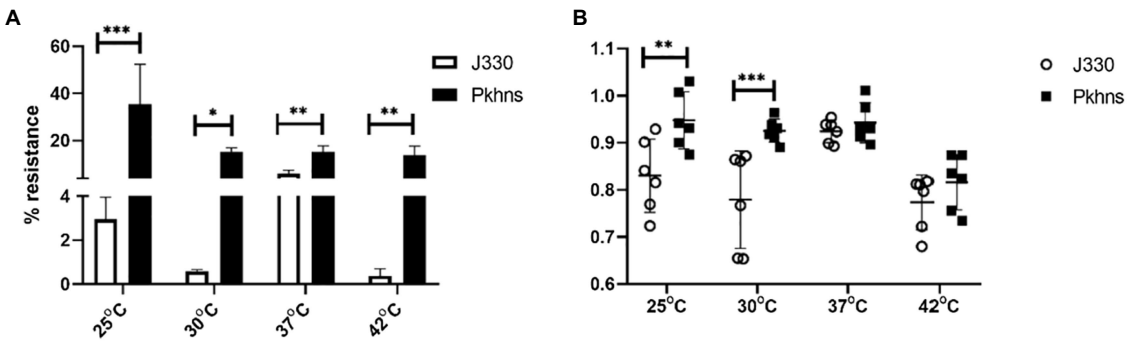

FIGURE 7 | At various temperature, the impact of plasmid-encoded H-NS-like protein on IncX3 plasmid stability **(A)** and fitness cost **(B)** in *E. coli*. **(A)** Plasmid stability is estimated by the percent of plasmid-containing *E. coli* at 24 h (% resistance). **(B)** Fitness index is calculated by formula described in Section "Materials and Methods." The higher fitness index represents better fitness of plasmid-containing strains. Significant differences are indicated with $^{*}(p<0.05)$, $^{**}(p<0.01)$, and $^{***}(p<0.001)$.

the lowest fitness costs. It is not surprising that conjugation rates and stability properties are both optimized at 37°C. As there is an evolutionary selection for small fitness effects of plasmids to ensure long-term persistence of the plasmids in the absence of selective pressures (Wein et al., 2019), these plasmids have adapted to life in gut commensals of mammals.

We found a new mechanism for IncX3 plasmid adaptation to different temperatures. We explored the potential mechanisms that link environmental temperature to plasmid stability, plasmid transfer, and fitness costs of pGZIncX3. Our study showed that growth at 30°C and 42°C caused the elevated expression level of the pGZIncX3 *phns* gene and we confirmed the role of this gene in suppressing conjugation in a temperature-dependent fashion. This phenomenon was linked to *phns*-dependent repression of the genes found in the pilX operon that encodes the IncX3 T4SS, namely, *pilX4*, *pilX5*, *pilX9*, and *pilX10*.

We also found that plasmid stability is repressed by *phns* under all temperatures tested. H-NS inhibition of conjugation leads to lower stability through the mechanisms mentioned above. Results in our study revealed the IncX3 plasmid-encoded H-NS-like protein only slightly affects host fitness, in line with previous work on a different IncX3 plasmid-encoded *hns*-like gene (Ho et al., 2013). But, in previous work, the IncHI1 plasmid-encoded Sfh protein, which is an H-NS homologue, was proposed to promote plasmid transfer to new bacterial hosts with little effects on bacterial fitness (Doyle et al., 2007). The discordant observations between these two plasmid-encoded H-NS homologs could

be due to differences in host species (*Salmonella* spp. vs. *E. coli*), plasmid length (54 vs. 100 kbp), and host adaptive mutations (Takeda et al., 2011). Moreover, discordance of plasmid-encoded *hns* function between *E. coli* and *Salmonella* may be explained by significantly different *hns*-related transcription profiles as shown in the Doyle *et al* study (Doyle et al., 2007) and our previous work (Liu et al., 2020). The current consensus is that an increase in temperature (from 30°C to 37°C) disrupts the binding of H-NS to DNA, resulting in the derepression of gene expression (Shahul Hameed et al., 2019) and this would explain the phenotypes observed in our study. Interestingly, the gene encoding the widely studied H-NS-like protein StpA exhibited higher expression levels at 42°C compared to 37°C which is in line with our findings (Muller et al., 2010). Surprisingly, we saw little difference in plasmid-mediated phenotypes between 25 and 37°C, which suggest that regulatory pathways other than *phns* are important for the regulation of plasmid traits at 25°C. Thus, our results proved that the variation of H-NS expression contributes to the different phenotypes of plasmids at 30°C, 42°C, and 37°C.

The optimal function of IncX3 plasmids at 37°C contrasts with that of IncHI1 plasmids like R27, which exhibit highest transfer frequencies at approximately 25°C. In both cases, thermoregulation is exerted by plasmid-encoded H-NS-like proteins. This suggests that different plasmid families have adapted to certain environmental conditions experienced by their hosts, and it will be interesting to determine whether transfer frequencies are temperature sensitive. It seems possible that the thermoregulation of plasmid functions influences the contributions of certain plasmid types to the dissemination of antibiotic resistance determinants in different environments. For example, IncHI1 plasmids might be expected to play a greater role in the transfer of resistance genes within environmental bacterial populations experiencing ambient temperatures of approximately 25°C, while IncX3 plasmids play a major role in the spread of resistance genes within mammalian enteric populations.

We acknowledge that our study has several limitations. First, our investigation focused on the plasmid-encoded gene *phns* to examine its modulation of plasmid characteristics under different temperatures. However, we could not take the interactions between host and plasmid regulators into consideration. For example, it has been reported that in *E. coli* chromosome-encoded temperature-sensor σ-32 is also involved in thermoregulation of plasmid conjugation (Rozwandowicz et al., 2019). Secondly, although we found that at 30 and 42°C, IncX3 plasmid-bearing *E. coli* exhibits lower transfer ability and stability, various IncX3 plasmids have been isolated from natural environments (Cheng et al., 2019). Therefore, we speculate that IncX3 plasmid-bearing host might require compensatory evolution for long-term adaptation to new environments with temperatures that are different to the mammalian gut (Zwanzig et al., 2019). Further studies of plasmid-host co-evolution need to be conducted to explore the mechanism by which plasmids and hosts reach a fitness optimum at various temperature.

CONCLUSION

In conclusion, this report describes the differential impact of physiological and environmental temperature on IncX3 plasmid phenotypes. The IncX3 plasmid studied here exhibited a higher transfer frequency, was more stable and imposed a lower fitness cost at 37°C than at other temperatures. Temperature-regulated variation involve a plasmid-encoded H-NS-like protein, which acts as a thermosensor and is upregulated at 30 and 42°C. The H-NS-like protein inhibits conjugation genes and appears to decrease plasmid stability and host fitness. Our findings suggest that bla_{NDM}-bearing IncX3 plasmids have evolved to persist and transfer optimally in the mammalian gut, which will complicate the control of the spread of carbapenem-resistant pathogens.

DATA AVAILABILITY STATEMENT

The original contributions presented in the study are included in the article/**Supplementary Material**, and further inquiries can be directed to the corresponding authors.

AUTHOR CONTRIBUTIONS

All authors listed have made a substantial, direct, and intellectual contribution to the work, and approved it for publication.

FUNDING

The research was supported by the National Natural Science Foundation of China (81772238), the Project of International Cooperation and Exchanges NSFC (8181101332), and the Guangzhou Municipal Science and Technology Bureau (project no. 201607020044) and the Medical Research Council (MR/S013660/1).

ACKNOWLEDGMENTS

We acknowledge Prof. Yu Yunsong and Dr. Jiang Yan from Sir Run Shaw Hospital, Zhejiang University School of Medicine for kindly providing strain ATCC 700603. We thank Doctor Zhong LanLan in Sun-Yat University for kindly helping with conjugation experiments.

SUPPLEMENTARY MATERIAL

The Supplementary Material for this article can be found online at: https://www.frontiersin.org/articles/10.3389/fmicb.2021.765492/full#supplementary-material

REFERENCES

Bush, K., and Bradford, P. A. (2020). Epidemiology of beta-lactamase-producing pathogens. *Clin. Microbiol. Rev.* 33:e00047-19. doi: 10.1128/CMR.00047-19

Chen, C.-L., Wang, C.-Y., Chu, C., Su, L.-H., and Chiu, C.-H. (2009). Functional and molecular characterization of pSE34 encoding a type IV secretion system in *Salmonella enterica* serotype Enteritidis phage type 34. *FEMS Immunol. Med. Microbiol.* 57, 274–283. doi: 10.1111/j.1574-695X.2009.00612.x

Cheng, P., Li, F., Liu, R., Yang, Y., Xiao, T., Ishfaq, M., et al. (2019). Prevalence and molecular epidemiology characteristics of carbapenem-resistant *Escherichia coli* in Heilongjiang Province, China. *Infect. Drug Resist.* 12, 2505–2518. doi: 10.2147/IDR.S208122

Dorman, C. J., and Ni Bhriain, N. (2020). CRISPR-Cas, DNA supercoiling, and nucleoid-associated proteins. *Trends Microbiol.* 28, 19–27. doi: 10.1016/j.tim.2019.08.004

Doyle, M., Fookes, M., Ivens, A., Mangan, M. W., Wain, J., and Dorman, C. J. (2007). An H-NS-like stealth protein aids horizontal DNA transmission in bacteria. *Science* 315, 251–252. doi: 10.1126/science.1137550

Forns, N., Banos, R. C., Balsalobre, C., Juarez, A., and Madrid, C. (2005). Temperature-dependent conjugative transfer of R27: role of chromosome- and plasmid-encoded Hha and H-NS proteins. *J. Bacteriol.* 187, 3950–3959. doi: 10.1128/JB.187.12.3950-3959.2005

Gao, H., Liu, Y., Wang, R., Wang, Q., Jin, L., and Wang, H. (2020). The transferability and evolution of NDM-1 and KPC-2 co-producing *Klebsiella pneumoniae* from clinical settings. *EBioMedicine* 51:102599. doi: 10.1016/j.ebiom.2019.102599

Ho, P. L., Cheung, Y. Y., Lo, W. U., Li, Z., Chow, K. H., Lin, C. H., et al. (2013). Molecular characterization of an atypical IncX3 plasmid pKPC-NY79 carrying bla KPC-2 in a *Klebsiella pneumoniae*. *Curr. Microbiol.* 67, 493–498. doi: 10.1007/s00284-013-0398-2

Johnson, T. J., Singer, R. S., Isaacson, R. E., Danzeisen, J. L., Lang, K., Kobluk, K., et al. (2015). In vivo transmission of an IncA/C plasmid in *Escherichia coli* depends on tetracycline concentration, and acquisition of the plasmid results in a variable cost of fitness. *Appl. Environ. Microbiol.* 81, 3561–3570. doi: 10.1128/AEM.04193-14

Khan, A. U., Maryam, L., and Zarrilli, R. (2017). Structure, genetics and worldwide spread of New Delhi Metallo-beta-lactamase (NDM): a threat to public health. *BMC Microbiol.* 17:101. doi: 10.1186/s12866-017-1012-8

Liakopoulos, A., van der Goot, J., Bossers, A., Betts, J., Brouwer, M. S. M., Kant, A., et al. (2018). Genomic and functional characterisation of IncX3 plasmids encoding blaSHV-12 in *Escherichia coli* from human and animal origin. *Sci. Rep.* 8:7674. doi: 10.1038/s41598-018-26073-5

Liu, B., Shui, L., Zhou, K., Jiang, Y., Li, X., Guan, J., et al. (2020). Impact of plasmid-encoded H-NS-like protein on blaNDM-1-bearing IncX3 plasmid in *Escherichia coli*. *J. Infect. Dis.* 221, S229–S236. doi: 10.1093/infdis/jiz567

Logan, L. K., and Weinstein, R. A. (2017). The epidemiology of carbapenem-resistant Enterobacteriaceae: the impact and evolution of a global menace. *J. Infect. Dis.* 215, S28–S36. doi: 10.1093/infdis/jiw282

Ma, T., Fu, J., Xie, N., Ma, S., Lei, L., Zhai, W., et al. (2020). Fitness cost of blaNDM-5-carrying p3R-IncX3 plasmids in wild-type NDM-free Enterobacteriaceae. *Microorganisms* 8:377. doi: 10.3390/microorganisms8030377

Matsumura, Y., Peirano, G., and Pitout, J. D. D. (2018). Complete genome sequence of *Escherichia coli* J53, an azide-resistant laboratory strain used for conjugation experiments. *Genome Announc.* 6:e00433-18. doi: 10.1128/genomeA.00515-18

Muller, C. M., Schneider, G., Dobrindt, U., Emody, L., Hacker, J., and Uhlin, B. E. (2010). Differential effects and interactions of endogenous and horizontally acquired H-NS-like proteins in pathogenic *Escherichia coli*. *Mol. Microbiol.* 75, 280–293. doi: 10.1111/j.1365-2958.2009.06995.x

Nigg, A., Brilhante, M., Dazio, V., Clément, M., Collaud, A., Gobeli Brawand, S., et al. (2019). Shedding of OXA-181 carbapenemase-producing *Escherichia coli* from companion animals after hospitalisation in Switzerland: an outbreak in 2018. *Euro Surveill.* 24:1900071. doi: 10.2807/1560-7917.ES.2019.24.39.1900071

Rose, R. E. (1988). The nucleotide sequence of pACYC184. *Nucleic Acids Res.* 16:355. doi: 10.1093/nar/16.14.7191

Rozwandowicz, M., Brouwer, M. S. M., Mughini-Gras, L., Wagenaar, J. A., Gonzalez-Zorn, B., Mevius, D. J., et al. (2019). Successful host adaptation of IncK2 plasmids. *Front. Microbiol.* 10:2384. doi: 10.3389/fmicb.2019.02384

Shahul Hameed, U. F., Liao, C., Radhakrishnan, A. K., Huser, F., Aljedani, S. S., Zhao, X., et al. (2019). H-NS uses an autoinhibitory conformational switch for environment-controlled gene silencing. *Nucleic Acids Res.* 47, 2666–2680. doi: 10.1093/nar/gky1299

Shintani, M., Suzuki-Minakuchi, C., and Nojiri, H. (2015). Nucleoid-associated proteins encoded on plasmids: occurrence and mode of function. *Plasmid* 80, 32–44. doi: 10.1016/j.plasmid.2015.04.008

Takeda, T., Yun, C. S., Shintani, M., Yamane, H., and Nojiri, H. (2011). Distribution of genes encoding nucleoid-associated protein homologs in plasmids. *Int. J. Evol. Biol.* 2011:685015. doi: 10.4061/2011/685015

Wang, Y., Tian, G. B., Zhang, R., Shen, Y., Tyrrell, J. M., Huang, X., et al. (2017). Prevalence, risk factors, outcomes, and molecular epidemiology of mcr-1-positive Enterobacteriaceae in patients and healthy adults from China: an epidemiological and clinical study. *Lancet Infect. Dis.* 17, 390–399. doi: 10.1016/S1473-3099(16)30527-8

Wang, Y., Tong, M.-K., Chow, K.-H., Cheng, V. C.-C., Tse, C. W.-S., Wu, A. K.-L., et al. (2018). Occurrence of highly conjugative IncX3 epidemic plasmid carrying blaNDM in Enterobacteriaceae isolates in geographically widespread areas. *Front. Microbiol.* 9:2272. doi: 10.3389/fmicb.2018.03354

Wein, T., Hulter, N. F., Mizrahi, I., and Dagan, T. (2019). Emergence of plasmid stability under non-selective conditions maintains antibiotic resistance. *Nat. Commun.* 10:2595. doi: 10.1038/s41467-019-10600-7

Zhai, R., Fu, B., Shi, X., Sun, C., Liu, Z., Wang, S., et al. (2020). Contaminated in-house environment contributes to the persistence and transmission of NDM-producing bacteria in a Chinese poultry farm. *Environ. Int.* 139:105715. doi: 10.1016/j.envint.2020.105715

Zhang, Q., Lv, L., Huang, X., Huang, Y., Zhuang, Z., Lu, J., et al. (2019). Rapid increase in carbapenemase-producing Enterobacteriaceae in retail meat driven by the spread of the bla (NDM-5)-carrying IncX3 plasmid in China from 2016 to 2018. *Antimicrob. Agents Chemother.* 63:e00573-19. doi: 10.1128/AAC.00573-19

Zhang, Y., Wang, Q., Yin, Y., Chen, H., Jin, L., Gu, B., et al. (2018). Epidemiology of carbapenem-resistant Enterobacteriaceae infections: report from the China CRE network. *Antimicrob. Agents Chemother.* 62:e01882-17. doi: 10.1128/AAC.01882-17

Zhou, H., Zhang, K., Chen, W., Chen, J., Zheng, J., Liu, C., et al. (2020). Epidemiological characteristics of carbapenem-resistant Enterobacteriaceae collected from 17 hospitals in Nanjing district of China. *Antimicrob. Agents Chemother.* 9:15. doi: 10.1186/s13756-019-0674-4

Zwanzig, M., Harrison, E., Brockhurst, M. A., Hall, J. P. J., Berendonk, T. U., and Berger, U. (2019). Mobile compensatory mutations promote plasmid survival. *mSystems* 4:e00186-18. doi: 10.1128/mSystems.00186-18

Conflict of Interest: The authors declare that the research was conducted in the absence of any commercial or financial relationships that could be construed as a potential conflict of interest.

frontiers in Microbiology

ORIGINAL RESEARCH
published: 10 February 2022
doi: 10.3389/fmicb.2022.826624

Clinical Impact of Colistin Banning in Food Animal on *mcr-1*-Positive Enterobacteriaceae in Patients From Beijing, China, 2009–2019: A Long-Term Longitudinal Observational Study

Qian Zhao[1†], Yiming Li[2†], Yingxin Tian[1], Yueyun Shen[1], Shaolin Wang[2] and Ying Zhang[1*]*

[1] Department of Laboratory Medicine, The First Medical Center, Chinese PLA General Hospital, Beijing, China, [2] College of Veterinary Medicine, China Agricultural University, Beijing, China

OPEN ACCESS

Edited by:
Guo-bao Tian,
Sun Yat-sen University, China

Reviewed by:
Fupin Hu,
Fudan University, China
Antoine Andremont,
Université Paris Diderot, France

***Correspondence:**
Ying Zhang
cherryzju@aliyun.com
Shaolin Wang
shaolinwang@cau.edu.cn

† These authors have contributed equally to this work and share first authorship

Specialty section:
This article was submitted to Antimicrobials, Resistance and Chemotherapy, a section of the journal Frontiers in Microbiology

Received: 01 December 2021
Accepted: 07 January 2022
Published: 10 February 2022

Citation:
Zhao Q, Li Y, Tian Y, Shen Y, Wang S and Zhang Y (2022) Clinical Impact of Colistin Banning in Food Animal on mcr-1-Positive Enterobacteriaceae in Patients From Beijing, China, 2009–2019: A Long-Term Longitudinal Observational Study. Front. Microbiol. 13:826624. doi: 10.3389/fmicb.2022.826624

The colistin resistance gene *mcr-1* is emerging as a global public health concern, altering the regulation of colistin usage globally since 2017, especially in China. However, few studies have revealed the impact of policy change on the epidemiology of *mcr*-positive Enterobacteriaceae (MCRPE) in patients. Here, we describe a molecular epidemiological study to investigate the MCRPE in patients in China from 2009–2019. During the surveillance period, 26,080 non-duplicated Enterobacteriaceae isolates were collected in Beijing. Colistin-resistant isolates were screened by enrichment culture supplemented with colistin, and the presence of the *mcr* gene was determined by PCR amplification. MCRPE isolates were then analyzed by susceptibility testing, genotyping, and risk factor analysis. Of the 26,080 isolates, *mcr-1* was detected in 171 (1.1%) of 15,742 *Escherichia coli* isolates and 7 (0.1%) of 10,338 *Klebsiella pneumoniae* isolates. The prevalence of *mcr-1*-positive *E. coli* (MCRPEC) showed an increasing trend from 2009 to 2016, while a decreasing trend was observed since 2017. Multi-locus sequence typing analysis showed that MCRPEC isolates had extremely diverse genetic backgrounds, and most of these isolates were non-clonal. The prevalence of MCRPE in China remained at a low level, and even showed a declining trend over the last 3 years after the banning of colistin usage as feed additive in food animal in 2017. However, colistin permission in clinical therapy could still increase the risk of MCRPE transmission and intractable infections, active surveillance and monitoring strategies of MCRPE are recommended to prolong the clinical longevity of colistin.

Keywords: colistin, *mcr-1*, Enterobacteriaceae, longitude study, China

INTRODUCTION

Colistin is regarded as one of the last therapeutic options available to treat infections caused by carbapenem-resistant Enterobacteriaceae (CRE), which pose an increasing risk to public health. Until 2015, resistance to colistin was only associated with mutations and regular changes in chromosomal genes (Wang et al., 2018). Liu et al. (2016) described a plasmid-mediated colistin

resistance gene, *mcr-1*, which encodes a phosphoethanolamine transferase enzyme (MCR-1) and results in the addition of phosphoethanolamine to lipid A in Enterobacteriaceae. The emergence of the mobile colistin resistance gene *mcr-1* could result in bacterial isolates being resistant to all classes of antibiotics, which will compromise the available treatment options for severe infections (Zhong et al., 2018).

Enterobacteriaceae, especially *Escherichia coli* and *Klebsiella pneumoniae*, typically form part of the normal flora in healthy people, yet can induce various infections under certain conditions, such as respiratory, urinary, and bloodstream infections (Paterson, 2006; Seiffert et al., 2013). Although the use of colistin in humans has been very limited in the past, it has been implemented in veterinary medicine since the early 1980s, mainly for the prevention and treatment of Enterobacteriaceae infections (Kempf et al., 2016). In China, colistin sulfate premix has been widely used as animal feed additive since 2009, and the production has reached 30,000 tons in 2015 (Wang et al., 2020). Wang et al. (2017) speculated that the emergence of *mcr-1* probably occurred first in animals, before extending to humans. Liu et al. (2016) identified the plasmid-borne colistin resistance gene, *mcr-1*, in Enterobacteriaceae from hospitalized humans, animals, and raw meat from China in 2015 (Wang et al., 2017). Subsequently, *mcr-1*-positive Enterobacteriaceae (MCRPE) have been found in inpatients, healthy humans, animals, raw meat, vegetables, and a number of environmental settings globally (Quesada et al., 2016). *E. coli* and *K. pneumoniae* are considered key reservoirs and disseminators of *mcr-1*. On April 30, 2017, the Chinese Ministry of Agriculture formally issued the banning of colistin as feed additives for food animals, aiming to reduce the wide spread of colistin resistance and protect the effectiveness of colistin in the clinical setting.

To date, MCRPE have been reported in numerous countries across Asia, Africa, Europe, North America, and South America (Quan et al., 2017; Saavedra et al., 2017; Wang et al., 2018; Clemente et al., 2019), indicating the rapid transfer of *mcr-1* among Enterobacteriaceae (Carattoli, 2013). Colistin has been approved for human medicine by the China Food and Drug Administration since January 2017 (Shen Y. et al., 2018), there is an urgent need to assess the role of MCRPE in the treatment of infections. Herein, we investigated the prevalence, risk factors, and molecular epidemiology of MCRPE carriage among inpatients and outpatients in Beijing, the capital of China, from 2009 to 2019. The aim of our study was to better understand the clinical impact of policy change on the current epidemiological trends and characteristics of MCRPE colonization in patients over this time frame.

MATERIALS AND METHODS

Study Design

The aim of this epidemiological and clinical study was to investigate the prevalence of MCRPE in patients. We conducted a long-term molecular epidemiological surveillance in Beijing from 2009–2019. Beijing, the capital city of China, has a population of 21 million and widely accepts patients from throughout the country. MCRPE strains were isolated from different specimen types in patients, including blood, urine, sputum, fecal, and tissue. At least 1,000 samples were collected annually.

All samples were taken from non-duplicate patients and we screen MCRPE isolates from samples by culturing in enrichment media supplemented with 2 mg/L colistin. The isolates before 2017 were identified from the retrospective collection. Pure colonies of *E. coli* and *K. pneumoniae* were selected according to their morphology and color on an SS agar plate supplemented with 2 mg/L colistin. The surviving bacteria were identified by matrix-assisted laser desorption/ionization time of flight mass spectrometry (MALDI-TOF MS) (Bruker Daltonik GmbH, Bremen, Germany), and further confirmed by 16S rDNA sequence analysis. Ethics approval was granted by the Chinese PLA General Hospital. Individual consent forms obtained from all patients before sampling. All participants held the right to quit the study at any stage.

Genetic Screening and Sequence Type Analysis

The presence of the colistin-resistance genes (*mcr*) was confirmed by Sanger sequencing (Seiffert et al., 2013). All *mcr*-positive strains were subjected to whole-genome sequencing (WGS). Genomic DNA extraction of isolates was performed using the Wizard Genomic DNA Purification Kit (Promega, Beijing, China) following a standard protocol, and then sequenced on the Illumina HiSeq 2500 platform (Annoroad Biotec Co.) with a 150-bp paired-end strategy. All procedures were carried out according to the manufacturer's instructions. The sequencing data were analyzed using multiple programs. The draft assembly of the sequences was generated using SPAdes version 3.11.1. Colistin resistance gene *mcr* and multi-locus sequence typing (MLST) were confirmed using standalone BLAST analysis SRST2 (Shen Z. et al., 2018).

Antimicrobial Susceptibility Testing

We calculated minimum inhibitory concentrations (MICs) for all MCRPE isolates against commonly used antibiotics *via* the broth microdilution method in accordance with the Clinical and Laboratory Standards Institute (CLSI) guidelines. Breakpoints for aminoglycosides (amikacin, gentamicin, and tobramycin), β-lactams (ampicillin and piperacillin), β-lactam/β-lactamase inhibitor combination (amoxicillin-clavulanate, ampicillin-sulbactam, and piperacillin-tazobactam), carbapenems (ertapenem, imipenem, and meropenem), cephems (cefazolin, cefepime, ceftazidime, cefotetan, and ceftriaxone), fluoroquinolones (ciprofloxacin and levofloxacin), trimethoprim-sulfamethoxazole, and nitrofurantoin were interpreted according to the annual CLSI-M100-S28[1] [Clinical and Laboratory Standards Institute (CLSI), 2018], while the results of antimicrobial susceptibility for colistin was interpreted in accordance with the European Committee on Antimicrobial Susceptibility Testing (EUCAST) criteria[2] [European Committee on Antimicrobial Susceptibility Testing [ECAST], 2020]. The

[1]http://www.clsi.org/

[2]https://www.eucast.org/

reference strains *E. coli* ATCC 25922 and *K. pneumoniae* ATCC 13883 (carbapenem-susceptible) were used as controls.

Classification of Variants and Statistical Analysis

We collected clinical data from patients with or without *mcr*-positive isolates between 2009 and 2019. Multiple risk factors were assessed, including sex (male and female), age (<15, 15–24, 25–34, 35–44, 45–54, 55–64, and ≥ 65 years), living conditions (city or village), specimen types (blood, sputum, and urine), patient types (inpatient or outpatient), comorbidities (diabetes, hypertension, and malignant tumor), and other risk factors (operation history, mechanical ventilation, urinary catheter, drainage tube, venous catheterization, and antibiotic use in the past 3 months). Variants were collated into specifically designed databases using Microsoft Excel 2016 (Microsoft, Redmond, WA, United States). Univariate analysis was performed using the Statistical Package for the Social Sciences version 23.0 (SPSS, Chicago, IL, United States). A chi-square test was used to examine the difference in the resistance levels of the different groups, and variables with a p-value < 0.2 were considered statistically significant. Significant variables with $P < 0.2$ were taken into multivariable analysis. A multivariable logistic regression model using a backward stepwise process was adopted to estimate the odds ratios (ORs) and 95% confidence intervals (CIs) of the risk factors related to *mcr*-positive *E. coli*. Variables with a p-value < 0.05 were considered significant risk factors. Pooled prevalence was estimated using a metaphor package with 95% CIs to represent the resistance rates of bacteria from 2010 to 2019 (Zou et al., 2019).

RESULTS

Overview of MCRPE Strains

For the prevalence study, a total of 26,080 non-duplicated isolates from inpatients and outpatients were collected in Beijing from 2009 to 2019, which included 15,742 *E. coli* and 10,338 *K. pneumoniae* isolates. We detected the *mcr-1* in 171 (1.09, 95 CI, 0.93–1.26) *E. coli* (MCRPEC) and 7 (0.07, 95 CI, 0.03–0.14) *K. pneumoniae* (MCRPKP) isolates (**Supplementary Table 1**). The age, specimen type, and sex information about the MCRPEC cases and the study population are shown in **Figures 1A–C**, and the information of the 7 MCRPKP cases is shown in **Supplementary Table 2**. The majority of the patients were over 65 (41.4%), and most isolates were obtained from urine (71.1%). The distribution of age, sex, and specimen information was similar among the MCRPEC cases and total cases. During the study period, the overall percentage of *mcr-1*-positive isolates remained low, especially for *K. pneumoniae*, and we found diverse trends in the prevalence of MCRPEC (**Figure 1A** and **Supplementary Table 1**). The proportion of MCRPEC increased from 2009 (0.0%) to 2016 (1.8%) ($p < 0.001$), except in 2013 (0.3%), while a decreasing trend was observed since 2017 (1.6%) (**Figure 1A**).

Antimicrobial Resistance Patterns of MCRPE

Overall, 150/171 (87.72%) MCRPEC and all 7 MCRPKP strains exhibited resistance to colistin (**Supplementary Tables 3, 4**). Antimicrobial susceptibility profiles of the 171 MCRPEC strains are shown in **Supplementary Table 3**. Among the 171 MCRPEC isolates, the MICs for colistin ranged from 0.25 to 16 μg/mL. Most MCRPEC remained susceptible to amikacin (85.4%), ertapenem (95.9%), imipenem (98.2%), piperacillin-tazobactam (91.0%), and cefotetan (96.2%). Among the 171 MCRPEC isolates, 3 (1.8%) were carbapenem-resistant, 132 (77.2%) were extended-spectrum β-lactamases (ESBL), and the proportion of ESBL strains increased from 50.0% in 2010 to 82.4% in 2019 (data not shown). We classified the MCRPEC isolates from 2010 to 2019 into inpatient and outpatient groups. The MIC_{50} values were similar between clinical *E. coli* isolates from inpatients ($n = 127$) and outpatients ($n = 44$), except for gentamicin and amikacin, which were both more than 16-fold higher in the inpatient group (**Supplementary Table 5**).

Risk Factors and Associated Outcomes of MCRPEC Infection

We collected clinical data from 171 *mcr-1*-positive clinical *E. coli* isolates and randomly selected 734 *mcr-1*-negative clinical *E. coli* isolates (62 isolates were excluded because of incomplete data, leaving 672) from 15,571 *mcr-1*-negative *E. coli* infection cases. Multiple variables were assessed to determine the risk factors associated with MCRPEC by OR analysis (**Tables 1**, **2**). Age and living conditions were not associated with MRCPEC infection. We determined that *E. coli* isolated from male were more likely to be *mcr-1* positive compared to those from outpatients (OR = 1.6, $p < 0.02$). Specimen types of *E. coli* were significantly associated with *mcr-1* positivity; *E. coli* isolates from bile and drainage fluid samples had a higher proportion of MCRPEC than those from other samples. Furthermore, MCRPEC was far more prevalent among *E. coli* isolated from patients with malignant tumors ($R = 2.3$, $p < 0.001$).

In addition, we analyzed the outcome of patients in 28 days with MRCPEC or *mcr-1*-negative *E. coli* (**Table 3**). Significant differences were observed between the two groups; in particular, patients with MRCPEC infections were more likely to result in treatment failure.

Molecular Epidemiology of MCRPEC

We further evaluated the molecular characteristics of MRCPEC strains as minimum spanning trees, phylogenetic tree and heatmaps (**Figures 2**, **3** and **Supplementary Figures 1, 2**). There were 66 distinct sequence types (STs) in the 171 isolates, suggesting extreme divergence of MRCPEC strains. Molecular epidemiological analysis revealed that none of these STs were predominant, but ST410 ($n = 10$), ST648 ($n = 9$), ST156 ($n = 7$), and ST224 ($n = 7$) were more prevalent than the other STs. These four STs have been recognized as common clades of *E. coli* carrying *mcr-1* in a previous study (Wang et al., 2017). Our results suggest that horizontal dissemination of *mcr-1* in *E. coli* was discovered between 2014 and 2019. In addition, an ST617 *E. coli*

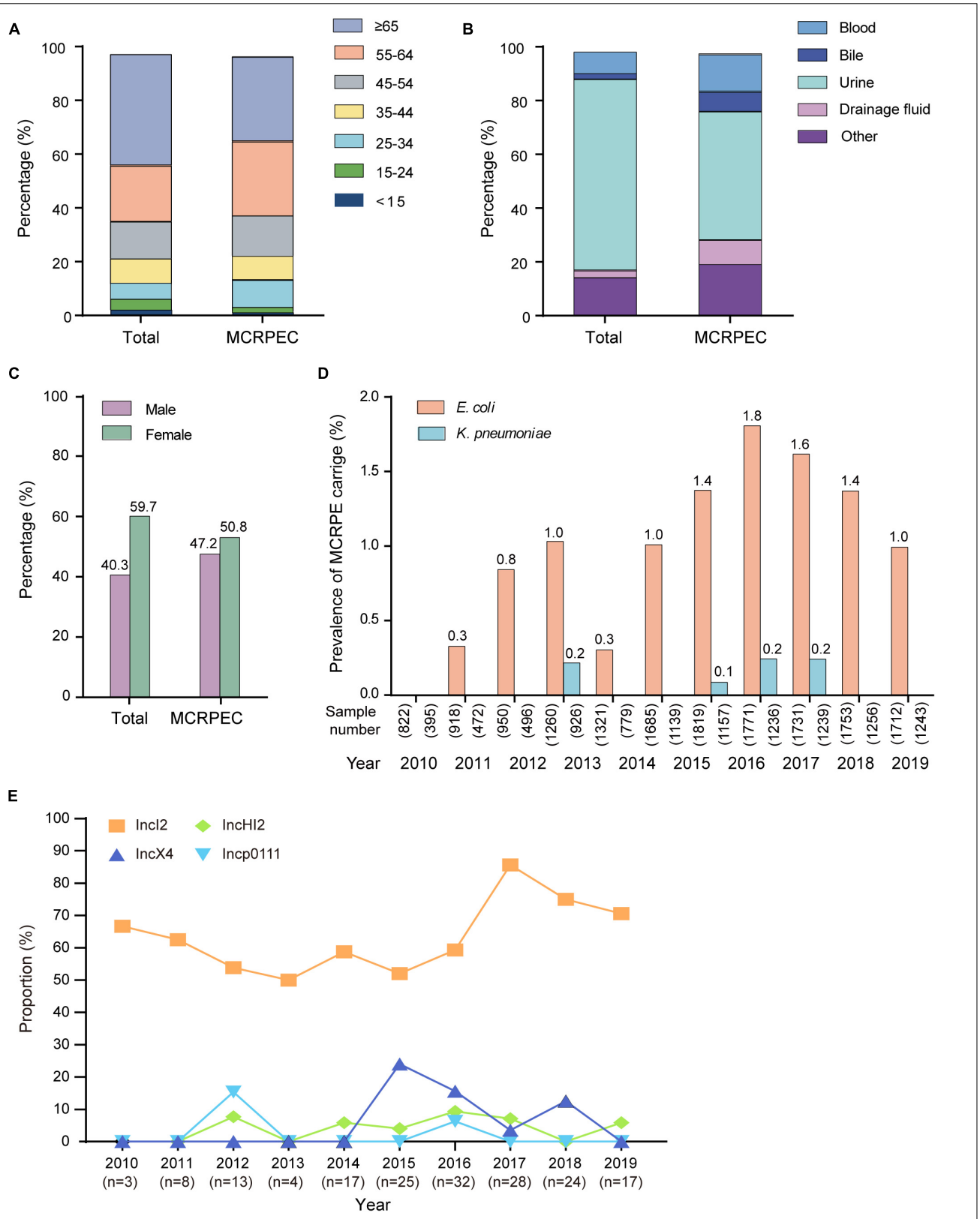

FIGURE 1 | Summary of information. **(A)** The age distribution of the total sample population and *mcr-1*-positive *E. coli* (MCRPEC). **(B)** The specimen type distribution of the total sample population and MCRPEC. **(C)** The sex distribution of the total sample population and MCRPEC. **(D)** The prevalence of *mcr-1*-positive Enterobacteriaceae (MCRPE) during 2009–2019. **(E)** The prevalence of main plasmids types in all MCRPEC during 2010–2019.

TABLE 1 | Analysis of risk factors associated with *mcr-1*-positive *E. coli* (*n* = 843).

Variables	*mcr-1*-positive *E. coli* (*n* = 171)		*mcr-1*-negative *E. coli* (*n* = 672)		OR (95% CI) [a]	*P*[b]
Sex						0.051
Female	89	52.0%	405	60.3%	1.0	
Male	82	48.0%	266	39.6%	1.4 (1.0–2.0)	
Age						
<15	1	0.6%	19	2.8%	0.2 (0.0–1.5)	**0.150**
15–24	4	2.3%	27	4.0%	0.6 (0.2–1.7)	0.298
25–34	18	10.5%	42	6.3%	1.8 (1.0–3.2)	0.052
35–44	17	9.9%	65	9.7%	1.0 (0.6–1.8)	0.916
45–54	27	15.8%	95	14.1%	1.1 (0.7–1.8)	0.583
55–64	49	28.7%	145	21.6%	1.5 (1.0–2.1)	0.05
≥65	55	32.1%	279	41.5%	0.7 (0.5–1.0)	**0.026**
Living condition						0.683
City	141	82.5%	566	84.2%	1.0	
Village	29	17.0%	106	15.7%	1.7 (0.7–1.7)	
Treatment						**0.029**
Outpatient	41	24.0%	219	32.6%	1.0	
Inpatient	130	76.0%	453	67.4%	1.5 (1.0–2.3)	
Specimen type						
Blood	23	13.3%	105	15.6%	1.0	0.429
Urine	79	46.4%	373	55.5%	1.0 (0.6–1.6)	**0.003**
Bile	8	4.4%	12	1.8%	5.0 (2.2–11.1)	**<0.001**
Drainage fluid	11	6.6%	11	1.7%	6.7 (3.0–14.6)	**<0.001**
Comorbidities and risk factors						
Diabetes	17	9.9%	123	18.3%	1.0	**0.009**
Hypertension	37	21.6%	193	28.7%	1.4 (0.8–2.6)	0.063
Malignant tumor	46	26.9%	92	13.7%	3.6 (2.0–6.7)	**<0.001**
Operation history	70	40.9%	216	32.1%	2.3 (1.3–4.2)	**0.030**
Mechanical ventilation	9	5.3%	52	7.7%	1.3 (0.5–3.0)	0.265
Urinary catheter	35	20.5%	179	26.6%	1.4 (0.8–2.6)	0.098
Drainage tube	36	121.1%	160	23.8%	1.6 (0.9–3.0)	0.446
Venous catheterization	25	14.6%	104	15.5%	1.7 (0.9–3.4)	0.781
Antibiotic use in the past 3 months	65	38.0%	158	23.5%	3.0 (1.7–5.3)	**<0.001**

[a] *CI, confidence interval; OR, odds ratio.* [b] *$P < 0.05$ are shown in boldface.*

isolate in 2014 and an ST3224 *E. coli* isolate in 2015 carried both *mcr-1* and the carbapenem resistance gene $bla_{\mathrm{NDM-1}}$.

In order to investigate the correlation between human MCRPEC and animal MCRPEC, the whole genomes of 150 animal MCRPEC, 122 animal *mcr-1* negative *E. coli* (MCRNEC), and 137 human MCRNEC were downloaded from the published data in the National Center for Biotechnology Information (NCBI) database. All the MCRPEC and MCRNEC isolates were allocated to 142 STs, and the diversity of clinical origin was greater than isolates of animal origin (**Supplementary Figure 1**). Of these *mcr-1*-positive clades, most sequence-types were common to both animal and human origin, such as ST156, ST101, ST354, and ST48 (**Figure 4** and **Supplementary Figure 1**). Interestingly, several ST branches were discovery only in human carriage, such as ST131 and ST95 (**Supplementary Figure 1**).

A total of 139 *mcr-1* positive plasmids were identified and assigned to known Inc types, among which the most prevalence was IncI2 (*n* = 111, 64.9%), followed by IncX4 (*n* = 15, 8.8%), IncHI2 (*n* = 9, 5.3%), and Incp0111 (*n* = 4, 2.3%). IncI2 remains the dominant Inc type in MCRPEC prevalence during 2010 to 2019, while a decreasing trend was observed in the proportion of IncI2 plasmids from 2017 to 2019 (**Figure 1E**). The genetic environment of *mcr-1* depends on its backbone structure plasmids, which vary greatly between different Inc types (**Figure 2**). The genetic context of *mcr-1* within each plasmid type (IncI2, IncX4, IncHI2, and Incp0111) was similar to the four reported *mcr-1*-carrying plasmid (pHNSHP45, KX254343, MF774186, and MF455226, respectively) from four pig-derived *E. coli* isolates (**Supplementary Figures 3–6**). Notably, the ancestral mobile element, ISApl1, which previously thought to be responsible for *mcr-1* transmission, was only detected in 42 (24.6%) isolates.

Antibiotic resistance genes (ARGs), heavy metal genes, and virulence-associated genes (VAGs) in the 171 MCRPEC isolates were determined by WGS. The percentages of ARGs, heavy metal genes, and VAGs for each year are shown in **Figure 3**. The *mcr-1* gene co-existed with *strA/B* (aminoglycoside resistance), *ampC1* (β-lactam ARG), $bla_{\mathrm{CTX-M-1}}$ and $bla_{\mathrm{TEM-1D}}$

TABLE 2 | Multivariable logistic regression analysis of factors associated with *mcr-1*-positive *E. coli*.

Variables	OR (95% CI) [a]	*P*[b]
Sex		**0.023**
Female	1	
Male	1.6 (1.1–2.4)	
Specimen type		
Blood	1.0	NA
Urine	2.0 (1.1–3.4)	**0.020**
Bile	4.2 (1.5–12.0)	0.007
Drainage fluid	6.0 (2.2–16.0)	**<0.001**
Comorbidities and risk factors		
Diabetes	0.5 (0.3–0.8)	**0.007**
Malignant tumor	2.3 (1.5–3.6)	**<0.001**
Urinary catheter	0.5 (0.3–0.7)	**0.001**

[a]*CI, confidence interval; OR, odds ratio.* [b]*P < 0.05 are shown in boldface.*

(ESBL-encoding genes), *floR* (florfenicol resistance), and *tetA* (tetracycline resistance gene) (**Figure 3**). *espL/R/X* (type III secretion system), *csgB* (which encodes the curli nucleator protein of *E. coli*), *ompA* (outer membrane protein A), *fdec* (intimin-like protein), and *fimH* (type I fimbriae) were more strongly associated with *mcr-1* carriage than other VAGs (**Figure 3**). Furthermore, WGS showed that *mcr-1* was mostly located on 3 Inc (incompatible) type plasmids, IncX4-type (n = 21, 12.3%), IncI2-type (n = 115, 67.3%), and IncHI2-type (n = 28, 16.4%), which is similar to a previous report (Jiang et al., 2020).

DISCUSSION

In 2009–2016, we noted a significant increase in the prevalence of MCRPEC from 2009 to 2016 (0.0% ∼ 1.8%), except in 2013, while a decreasing trend was noted after 2016 (**Figure 1D**). Notably, the Ministry of Agriculture of China (Article number 2428) withdrew colistin as a feed additive and growth promoter in November 2016, and this was officially enforced in April 2017 (Walsh and Wu, 2016). Colistin produced before Apr, 2017 was still allowed to use according to the data from Ministry of Agricultural. The overall production of colistin sulfate reached over 50,000 tons in 2015–2016, we believed the rising of colistin resistance may be later comparing with the sales and usage of colistin, and several studies also indicated colistin resistance reached peak around later 2016-mid 2017 (Shen et al., 2016; Wang et al., 2020). In Tu et al.'s study, the prevalence of *mcr-1* (5.6%) was significantly lower than before the ban (86.4%, $p < 0.01$) in a large scale swine farm (Tu et al., 2021). According to previous study, the banning had a significant effect on reducing colistin resistance in both animal and humans by comparing 2016–2017 and 2018–2019 (Shen et al., 2020; Wang et al., 2020). Furthermore, the human carriage of MCRPEC also decreased from 14.3% in 2016 to 6.3% in 2019 ($p < 0.0001$) in hospital across 24 provincial capital cities and municipalities in China (Wang et al., 2020). In a prevalence dynamics analysis of human *mcr-1* colonization from April 2011 to December 2019, a dramatic decline in human *mcr-1* colonization prevalence was observed, consisting with the complete ban of colistin in animal feed (Shen et al., 2021). Above all, we suggest that the withdrawal of colistin as an animal growth promoter in China had a positive impact on MCRPEC infections in both animals and humans. However, we believed the overall colistin resistance will remain declining as long as the banning in effective. It might take a few extra years for the resistance reduced to the stage before colistin usage. In this study, the prevalence of *mcr-1* decreased from 32 (1.8%) of 1,771 in 2016, to 24 (1.6%) of 1,731 ($p = 0.3$) in 2018 and 17 (1.0%) of 1,712 ($p < 0.05$) in 2019. However, the extended longitude study was necessary to further evaluate the effective of banning.

In the analysis of different factors associated with MCRPEC carriage, we observed that *E. coli* from inpatients were more likely to carry the colistin resistance gene *mcr-1* (OR = 1.5, $p < 0.05$), suggesting that hospitalization may be a risk factor for colonization of *mcr-1*. Among the different specimen types, we observed that *E. coli* isolates from bile and drainage fluid were much more likely to be *mcr-1* positive than from urine and blood. In addition, we observed a significant association between MCRPEC infection and comorbidities, such as diabetes, malignant tumors, and operation history ($p < 0.05$). Unsurprisingly, antibiotic use in the past 3 months was strongly associated with high MCRPEC occurrence.

Our MLST analysis showed that the 171 MRCPEC isolates had extremely diverse genetic backgrounds, and many were non-clonal. In this study, ST410 (n = 9) was the most prevalent sequence type among inpatients, while ST648 (n = 4) and ST117 (n = 4) were more prevalent than other types among outpatients. *E. coli* ST410 has been reported worldwide as an extraintestinal pathogen associated with multidrug resistance and is capable of patient-to-patient transmission, causing hospital outbreaks (Roer et al., 2018). *E. coli* ST648 is a predominant multidrug-resistant clone observed worldwide and is frequently associated with various β-lactamases, including ESBLs, NDM, and KPC (Mushtaq et al., 2011; Kim et al., 2012). *E. coli* ST117 is a highly virulent pathogenic lineage associated with extraintestinal infections in humans and poultry (Cummins et al., 2019). These findings indicate that *mcr-1* has wide host adaptability in *E. coli* and different virulence potentials. Of all *mcr-1*-positive isolates,

TABLE 3 | Patient outcomes with *mcr-1*-positive *E. coli* and *mcr-1*-negative *E. coli* infections.

Variables	*mcr-1*-positive *E. coli* (n = 120)	*mcr-1*-negative *E. coli* (n = 504)	OR (95% CI) [a]	*p* [b]
Cure	5 (4.2%)	76 (15.1%)	0.2 (0.1–0.6)	**0.001**
Improve	103 (85.8%)	405 (80.4%)	1.5 (0.8–2.6)	0.166
Treatment failure	12 (10.0%)	23 (4.6%)	2.3 (1.1–4.8)	**0.020**

[a]*CI, confidence interval; OR, odds ratio.* [b]*P < 0.05 are shown in boldface.*

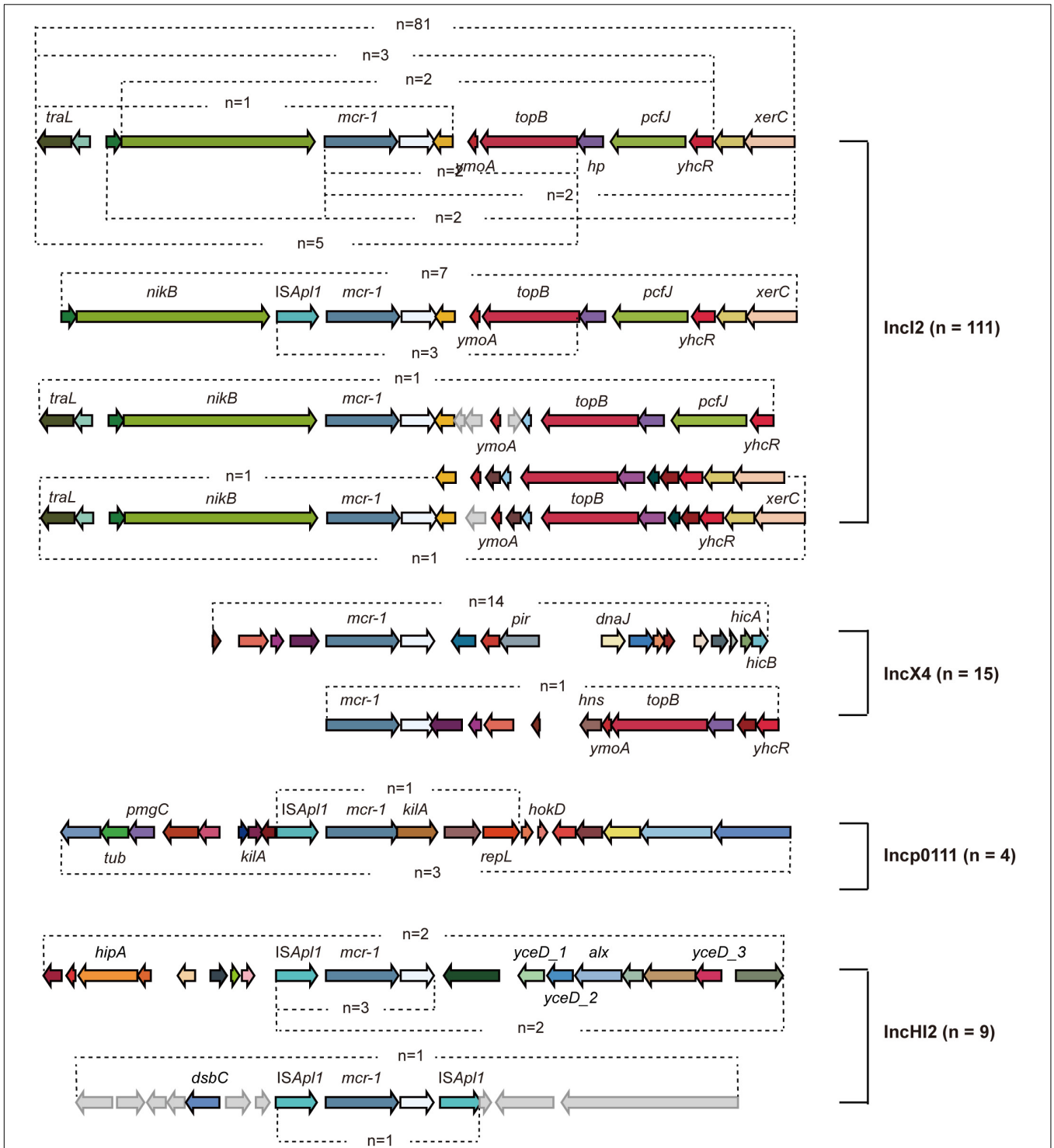

FIGURE 2 | Genetic analysis *of mcr-1*- carrying plasmids. Different arrows represent particular genes having a name written underneath of each arrow. The arrows without names represent hypothetical proteins.

most sequence-types were common in both human and animal origin, and nucleotide sequences of four main plasmid Inc-types (IncI2, IncX4, IncHI2, and Incp0111) were similar to reported plasmids from animal origins in China, which reminds us the speculation that *mcr-1* probably occurred first in animals and extended to humans (Wang et al., 2017).

The plasmid-mediated gene *mcr-1* has disseminated globally and could pose severe threats to human health when

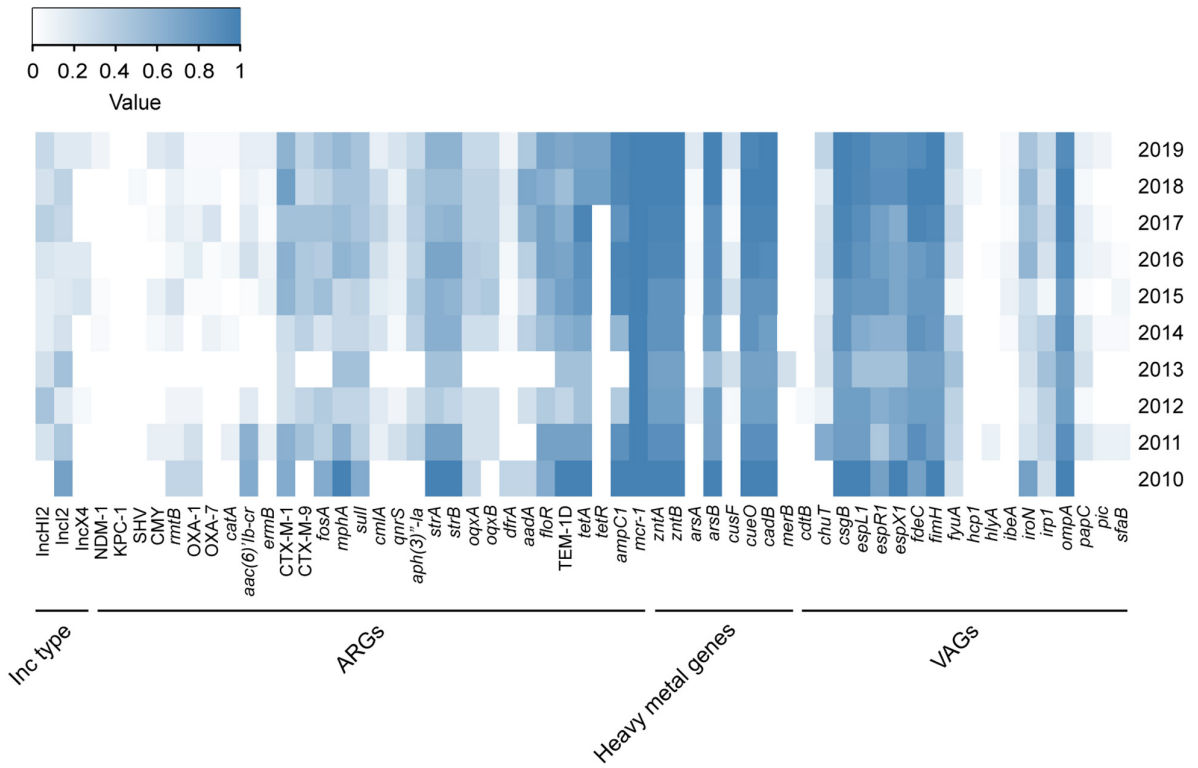

FIGURE 3 | Distribution of Inc type, ARGs, heavy metal genes, and VAGs among MCRPEC isolates. The color of each box represents the percentage of the corresponding item among sequenced isolates in the corresponding year. ARGs, antibiotic resistance genes; HMGs, heavy metal genes; VAGs, virulence-associated genes.

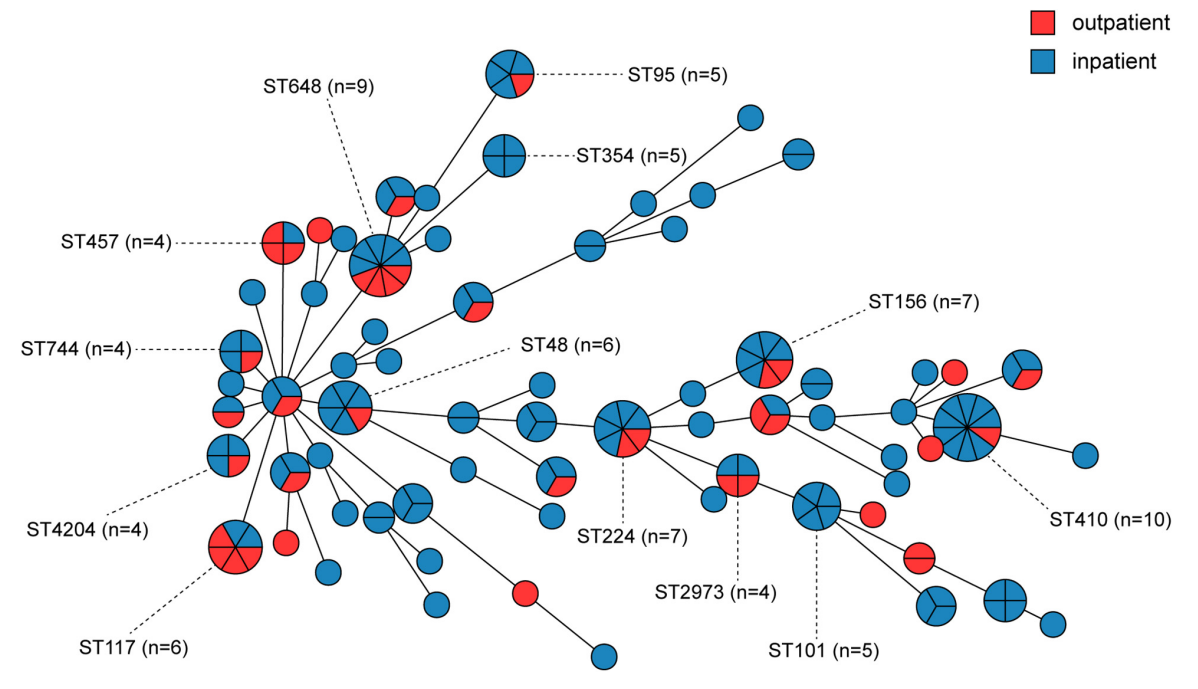

FIGURE 4 | Minimum spanning tree of *mcr-1*-positive *E. coli* by MLST type and gene allele from inpatients and outpatients. Each node in the tree represents an ST, and the size of a node is proportional to the number of isolates it represents. The length of the branch is equal to the number of different alleles (calculated using seven MLST genes) between two linked nodes.

transferred into CRE and extended-spectrum beta-lactamase Enterobacteriaceae (ESBL-E), leaving fewer treatment options for infections caused by multi-drug resistant strains. Among 178 *mcr-1* positive Enterobacteriaceae, 161 (90.5%) isolates harbored ESBL-encoding genes (such as $bla_{\mathrm{CTX-M}}$ and bla_{TEM}) and 35 (19.7%) isolates were carbapenemases (such as NDM-1, KPC-2, and OXA-48) producer. To date, a few reports showed that 0.1–4.6% CRE strains were *mcr-1* positive in clinical settings (Huang et al., 2018; Chen et al., 2019; Xiaomin et al., 2020), and one study showed that 2.40% ESBL-E strains also harbored *mcr-1* (Jørgensen et al., 2017). The coexistence of transferable colistin and carbapenem resistance has become an alarming concern, calling for global monitoring and surveillance. Although mobile colistin resistance poses great difficulties in the treatment of severe infectious diseases, in this study, most *mcr-1* positive isolates remained susceptible to many other antibiotics, such as carbapenems, piperacillin-tazobactam, amikacin, and cefotetan. Therefore, antimicrobials should be used in combination to defend against colistin-resistant bacteria in clinical therapy.

Our study has several limitations. One limitation was that the colistin resistance gene *mcr-1* was screened in Enterobacteriaceae isolates collected retrospectively. It is possible to lose *mcr-1* carrying plasmids during preservation, which may result in an underestimation of the prevalence of *mcr-1*. Another limitation is the partial collection of patient information. Since the colossal groups surveyed in this study, we only included 672 (4.3%) of 15,571 *mcr-1* negative *E. coli* isolates for multivariable analysis. Even though, our data were large-scale and combined across different periods each year. For further studies, analysis of more isolates should be included to reduce bias in identifying the risk factors related to *mcr-1* in patients.

In conclusion, this survey revealed a decreasing prevalence from 2016 to 2019, which is opposite to the increasing trend observed between 2009 and 2016. MCPREC isolates possessed extremely diverse genetic backgrounds in patients in the clinical setting from Beijing, China, and our findings provide evidence of the transmission of *mcr-1* among patients. Moreover, the coexistence of transferable colistin resistance and carbapenem resistance poses a great threat, and effective monitoring and surveillance are necessary to control and prevent the dissemination of MCRPE.

DATA AVAILABILITY STATEMENT

Whole-genome sequencing data that support the findings of this study have been deposited in the NCBI database under BioProject accession number PRJNA78361.

AUTHOR CONTRIBUTIONS

QZ contributed significantly to perform the experiments. YL contributed significantly to perform the data analyses and wrote the manuscript. YT and YS helped to perform the experiments and manuscript preparation. SW and YZ contributed significantly to the conception of the study. All authors contributed to the article and approved the submitted version.

FUNDING

This work was supported by National Key Research and Development Program is supported by Ministry of Science and Technology of the People's Republic of China (2017YFC1601502).

SUPPLEMENTARY MATERIAL

The Supplementary Material for this article can be found online at: https://www.frontiersin.org/articles/10.3389/fmicb.2022.826624/full#supplementary-material

REFERENCES

Carattoli, A. (2013). Plasmids and the spread of resistance. *Int. J. Med. Microbiol.* 303, 298–304. doi: 10.1016/j.ijmm.2013.02.001

Chen, C. W., Tang, H. J., Chen, C. C., Lu, Y. C., Chen, H. J., Su, B. A., et al. (2019). The microbiological characteristics of carbapenem-resistant *Enterobacteriaceae* carrying the mcr-1 gene. *J. Clin. Med.* 8:261. doi: 10.3390/jcm8020261

Clemente, L., Manageiro, V., Correia, I., Amaro, A., Albuquerque, T., Themudo, P., et al. (2019). Revealing mcr-1-positive ESBL-producing *Escherichia coli* strains among *Enterobacteriaceae* from food-producing animals (bovine, swine and poultry) and meat (bovine and swine), Portugal, 2010–2015. *Int. J. Food Microbiol.* 296, 37–42. doi: 10.1016/j.ijfoodmicro.2019.02.006

Clinical and Laboratory Standards Institute [CLSI] (2018). *Performance Standards for Antimicrobial Testing: twenty-eighth Informational Supplement M100-S28*. Available online at: https://community.clsi.org/media/1930/m100ed28_sample.pdf. [Accessed January 2018].

Cummins, M. L., Chowdhury, P. R., Marenda, M. S., Browning, G. F., and Djordjevic, S. P. (2019). *Salmonella* genomic island 1B variant found in a sequence type 117 avian pathogenic *Escherichia coli* isolate. *Msphere* 4, e00169–19. doi: 10.1128/mSphere.00169-19

European Committee on Antimicrobial Susceptibility Testing [ECAST] (2020). *Breakpoint Tables for Interpretation of MICs and Zone Diameters*. Available online at: http://www.eucast.org. [Accessed 1 January 2020]

Huang, B., He, Y., Ma, X., Cai, R., Zeng, J., Lu, Y., et al. (2018). Promoter variation and gene expression of mcr-1-harboring plasmids in clinical isolates of *Escherichia coli* and *Klebsiella pneumoniae* from a Chinese hospital. *Antimicrob. Agents Chemother.* 62, e00018–e18. doi: 10.1128/AAC.00018-18

Jiang, Y., Zhang, Y., Lu, J., Wang, Q., Cui, Y., Wang, Y., et al. (2020). Clinical relevance and plasmid dynamics of mcr-1-positive *Escherichia coli* in China: a multicentre case-control and molecular epidemiological study. *Lancet Microbe.* 1, e24–e33. doi: 10.1016/S2666-5247(20)30001-X

Jørgensen, S. B., Søraas, A., Arnesen, L. S., Leegaard, T., Sundsfjord, A., and Jenum, P. A. (2017). First environmental sample containing plasmid-mediated colistin-resistant ESBL-producing *Escherichia coli* detected in Norway. *APMIS* 125, 822–825. doi: 10.1111/apm.12720

Kempf, I., Jouy, E., and Chauvin, C. (2016). Colistin use and colistin resistance in bacteria from animals. *Int. J. Antimicrob. Agents* 48, 598–606. doi: 10.1016/j.ijantimicag.2016.09.016

Kim, Y. A., Qureshi, Z. A., Adams-Haduch, J. M., Park, Y. S., Shutt, K. A., and Doi, Y. (2012). Features of Infections Due to *Klebsiella pneumoniae* Carbapenemase–Producing *Escherichia coli*: emergence of Sequence Type 131. *Clin. Infect. Dis.* 55, 224–231. doi: 10.1093/cid/cis387

Liu, Y. Y., Wang, Y., Walsh, T. R., Yi, L. X., Zhang, R., Spencer, J., et al. (2016). Emergence of plasmid-mediated colistin resistance mechanism MCR-1 in animals and human beings in China: a microbiological and molecular biological study. *Lancet Infect. Dis.* 16, 161–168. doi: 10.1016/S1473-3099(15)00424-7

Mushtaq, S., Irfan, S., Sarma, J., Doumith, M., Pike, R., Pitout, J., et al. (2011). Phylogenetic diversity of *Escherichia coli* strains producing NDM-type carbapenemases. *J. Antimicrob. Chemother.* 66, 2002–2005. doi: 10.1371/journal.pone.0147740

Paterson, D. L. (2006). Resistance in gram-negative bacteria: *enterobacteriaceae*. *Am. J. Infect. Control.* 34, S20–S28. doi: 10.1016/j.amjmed.2006.03.013

Quan, J., Li, X., Chen, Y., Jiang, Y., Zhou, Z., Zhang, H., et al. (2017). Prevalence of mcr-1 in *Escherichia coli* and *Klebsiella pneumoniae* recovered from bloodstream infections in China: a multicentre longitudinal study. *Lancet Infect. Dis.* 17, 400–410. doi: 10.1016/S1473-3099(16)30528-X

Quesada, A., Ugarte-Ruiz, M., Iglesias, M. R., Porrero, M. C., Martínez, R., Florez-Cuadrado, D., et al. (2016). Detection of plasmid mediated colistin resistance (MCR-1) in *Escherichia coli* and *Salmonella enterica* isolated from poultry and swine in Spain. *Res. Vet. Sci.* 105, 134–135. doi: 10.1016/j.rvsc.2016.02.003

Roer, L., Overballe-Petersen, S., Hansen, F., Schønning, K., Wang, M., Røder, B. L., et al. (2018). *Escherichia coli* sequence type 410 is causing new international high-risk clones. *Msphere* 3, e337–18. doi: 10.1128/mSphere.00337-18

Saavedra, S. Y., Diaz, L., Wiesner, M., Correa, A., Arévalo, S. A., Reyes, J., et al. (2017). Genomic and molecular characterization of clinical isolates of *Enterobacteriaceae* harboring mcr-1 in Colombia, 2002 to 2016. *Antimicrob. Agents Chemother.* 61, e841–e17. doi: 10.1128/AAC.00841-17

Seiffert, S. N., Hilty, M., Perreten, V., and Endimiani, A. (2013). Extended-spectrum cephalosporin-resistant Gram-negative organisms in livestock: an emerging problem for human health. *Drug Resist. Updates.* 16, 22–45. doi: 10.1016/j.drup.2012.12.001

Shen, C., Zhong, L., Yang, Y., Doi, Y., Paterson, D., Stoesser, N., et al. (2020). Dynamics of mcr-1 prevalence and mcr-1-positive *Escherichia coli* after the cessation of colistin use as a feed additive for animals in China: a prospective cross-sectional and whole genome sequencing-based molecular epidemiological study. *Lancet Microbe.* 1, e34–e43. doi: 10.1016/S2666-5247(20)30005-7

Shen, C., Zhong, L. L., Zhong, Z., Doi, Y., Shen, J., Wang, Y., et al. (2021). Prevalence of mcr-1 in Colonized Inpatients. China, 2011-2019. *Emerg. Infect. Dis.* 27, 2502–2504. doi: 10.3201/eid2709.203642

Shen, Y., Zhou, H., Xu, J., Wang, Y., Zhang, Q., Walsh, T. R., et al. (2018). Anthropogenic and environmental factors associated with high incidence of mcr-1 carriage in humans across China. *Nat. Microbiol.* 3, 1054–1062. doi: 10.1038/s41564-018-0205-8

Shen, Z., Hu, Y., Sun, Q., Hu, F., Zhou, H., Shu, L., et al. (2018). Emerging Carriage of NDM-5 and MCR-1 in *Escherichia coli* From Healthy People in Multiple Regions in China: a Cross Sectional Observational Study. *EClin. Med.* 6, 11–20. doi: 10.1016/j.eclinm.2018.11.003

Shen, Z., Wang, Y., Shen, Y., Shen, J., and Wu, C. (2016). Early emergence of mcr-1 in *Escherichia coli* from food-producing animals. *Lancet Infect. Dis.* 16:293. doi: 10.1016/S1473-3099(16)00061-X

Xiaomin, S., Yiming, L., Yang, Y., Shen, Z., Yongning, W., and Shaolin, W. (2020). Global impact of mcr-1-positive *Enterobacteriaceae* bacteria on "one health". *Crit. Rev. Microbiol.* 46, 565–577. doi: 10.1080/1040841X.2020.1812510

Tu, Z., Gu, J., Zhang, H., Liu, J., Shui, J., and Zhang, A. (2021). Withdrawal of colistin reduces incidence of mcr-1-harboring IncX4-type plasmids but has limited effects on unrelated antibiotic resistance. *Pathogens* 10:1019. doi: 10.3390/pathogens10081019

Walsh, T. R., and Wu, Y. (2016). China bans colistin as a feed additive for animals. *Lancet Infect. Dis.* 16:1102. doi: 10.1016/S1473-3099(16)30329-2

Wang, R., Van, D. L., Shaw, L. P., Bradley, P., Wang, Q., Wang, X., et al. (2018). The global distribution and spread of the mobilized colistin resistance gene mcr-1. *Nat. Commun.* 9, 1–9. doi: 10.1038/s41467-018-03205-z

Wang, Y., Tian, G. B., Zhang, R., Shen, Y., Tyrrell, J. M., Huang, X., et al. (2017). Prevalence, risk factors, outcomes, and molecular epidemiology of mcr-1-positive *Enterobacteriaceae* in patients and healthy adults from China: an epidemiological and clinical study. *Lancet Infect. Dis.* 17, 390–399. doi: 10.1016/S1473-3099(16)30527-8

Wang, Y., Xu, C., Zhang, R., Chen, Y., Shen, Y., Hu, F., et al. (2020). Changes in colistin resistance and mcr-1 abundance in *Escherichia coli* of animal and human origins following the ban of colistin-positive additives in China: an epidemiological comparative study. *Lancet Infect. Dis.* 20, 1161–1171. doi: 10.1016/S1473-3099(20)30149-3

Zhong, L. L., Phan, H. T., Shen, C., Vihta, K. D., Sheppard, A. E., Huang, X., et al. (2018). High rates of human fecal carriage of mcr-1–positive multidrug-resistant *Enterobacteriaceae* emerge in China in association with successful plasmid families. *Clin. Infect. Dis.* 66, 676–685. doi: 10.1093/cid/cix885

Zou, Z. Y., Lei, L., Chen, Q. Y., Wang, Y. Q., Cai, C., Li, W. Q., et al. (2019). Prevalence and dissemination risk of antimicrobial-resistant *Enterobacteriaceae* from shared bikes in Beijing. China. *Environ. Int.* 132:105119. doi: 10.1016/j.envint.2019.105119

Conflict of Interest: The authors declare that the research was conducted in the absence of any commercial or financial relationships that could be construed as a potential conflict of interest.

Publisher's Note: All claims expressed in this article are solely those of the authors and do not necessarily represent those of their affiliated organizations, or those of the publisher, the editors and the reviewers. Any product that may be evaluated in this article, or claim that may be made by its manufacturer, is not guaranteed or endorsed by the publisher.

frontiers in Microbiology

ORIGINAL RESEARCH
published: 10 March 2022
doi: 10.3389/fmicb.2022.820577

Epidemiology and Drug Resistance of Neonatal Bloodstream Infection Pathogens in East China Children's Medical Center From 2016 to 2020

Xin Zhang, Yang Li, Yunzhen Tao, Yu Ding, Xuejun Shao† and Wei Li*†*

Department of Clinical Laboratory, Children's Hospital of Soochow University, Suzhou, China

OPEN ACCESS

Edited by:
Fang He,
Zhejiang Provincial People's Hospital, China

Reviewed by:
Soojin Jang,
Korea Pasteur Institute, South Korea
Anusak Kerdsin,
Kasetsart University, Thailand

***Correspondence:**
Xuejun Shao
xjshao@suda.edu.cn
Wei Li
2248797907@qq.com

†These authors have contributed equally to this work

Specialty section:
This article was submitted to Antimicrobials, Resistance and Chemotherapy, a section of the journal Frontiers in Microbiology

Received: *23 November 2021*
Accepted: *24 January 2022*
Published: *10 March 2022*

Citation:
Zhang X, Li Y, Tao Y, Ding Y, Shao X and Li W (2022) Epidemiology and Drug Resistance of Neonatal Bloodstream Infection Pathogens in East China Children's Medical Center From 2016 to 2020. Front. Microbiol. 13:820577. doi: 10.3389/fmicb.2022.820577

Introduction: To analyze the pathogen distribution and drug resistance of newborns with bloodstream infection (BSI) to help clinicians choose the appropriate empirical antibiotic therapy for clinical infection control.

Methods: A total of 707 neonatal BSI cases were retrospectively analyzed. The bacteria in blood culture-positive samples were cultured, identified, and analyzed for drug sensitivity by routine methods. Statistical software was used to compare and analyze the basic data, pathogenic information, and drug resistance of the main bacteria.

Results: The 5-year average positive rate of neonatal blood culture was 2.50%. The number of specimens submitted for inspection in 2020 significantly decreased. The top five infectious pathogens with the highest proportion were coagulase-negative *Staphylococcus* (67.35%), of which *Staphylococcus epidermidis* had the highest proportion (31.26%), followed by *Escherichia coli* (12.87%), *Klebsiella pneumoniae* (9.05%), *Streptococcus agalactiae* (8.63%), and *Staphylococcus aureus* (3.25%). Gram-positive (G^+) bacteria were dominant, accounting for 69.45%. The main G^+ bacteria had a higher rate of resistance to erythromycin and penicillin G. The main Gram-negative (G^-) bacteria had a high resistance rate to a variety of antibacterial drugs, especially cephalosporin antibiotics. The overall resistance of *K. pneumoniae* was higher than that of *E. coli*. The top two fungi detected were *Candida parapsilosis* and *Candida albicans*. *C. parapsilosis* did not appear to be resistant to antibiotics, while *C. albicans* was resistant to multiple antibiotics. The type of microbial infection had a statistically significant difference in the positive rate among the age at delivery and wards ($p < 0.05$). There were significant differences in the detection of fungi among these groups ($p < 0.05$). The positive rate of G^+ bacteria in the term newborns was significantly higher than that in the preterm newborns ($p < 0.05$). Preterm newborns are more susceptible to pneumonia.

Conclusion: G^+ bacteria are the main pathogens of neonatal BSI. Preterm newborns are more likely to be infected with G^- bacteria. *E. coli* and *K. pneumoniae* are the most common G^- bacteria, and both have a high resistance rate to a variety of antibacterial drugs. According to the distribution characteristics and drug resistance, it is very important to select antibiotics reasonably.

Keywords: newborns, bloodstream infection, resistance, antibacterial drugs, epidemiology

INTRODUCTION

Infection is the main cause of morbidity in infancy, accounting for 15% of global neonatal deaths (Lucia Hug and You, 2017). Among them, bloodstream infection (BSI) is a common nosocomial type of neonatal death (Yuan et al., 2015). In 2017, the National Bacterial Drug Resistance Monitoring Network reported that 15.2% of bacterial infections in China came from blood samples (Hu et al., 2018). The immune function of newborns is underdeveloped, and resistance is poor. It is very easy to cause sepsis when blood flow infection occurs. The incidence rate of neonatal septicemia among the surviving newborns was 4.5–9.7% (FLeischmann-Struzek et al., 2018). However, due to the clinical use of unilateral blood culture for examination, fewer bacteria, and the use of antibiotics during delivery, blood culture results are often false negative (Klingenberg et al., 2018). The treatment and survival of newborns, especially premature babies, often rely on effective antibiotics, but due to the delay in laboratory tests, empirical medication is often given before the results are available (Puopolo et al., 2018). For neonates, especially premature infants, the use of antibiotics for more than 5 days in infants with negative blood cultures will increase the risk of necrotizing enterocolitis, bronchopulmonary dysplasia, and invasive fungal infections (Ting et al., 2016; Esaiassen et al., 2017). Therefore, the use of big data analysis to explore the results of neonatal drug susceptibility is very important to guide the clinical selection of appropriate antibiotics. At present, there have been research reports on BSI (Spaulding et al., 2019; Johnson et al., 2020; Liu et al., 2020), but due to the influence of factors such as different subjects and regions, the infection characteristics are also different. There are few research papers and comments on the correlation of neonatal BSI in East China. Grasping the distribution characteristics of BSI pathogens in a certain area and performing empirical treatment for the first time are of great significance to saving the lives of newborns. Therefore, a retrospective study of 707 clinical cases of neonatal BSI in East China was performed to understand the composition of pathogenic bacteria and bacterial resistance. The report is as follows.

MATERIALS AND METHODS

General Information

During January 1, 2016, to December 31, 2020, 28,287 blood culture specimens were collected from the Children's Hospital of Soochow University. A total of 707 newborns with BSI were selected as the research subjects. The inclusion criteria were as follows: (1) newborns; (2) positive blood culture; and (3) increased inflammatory indexes with fever and other blood flow infection symptoms. Among them, 16,040 were male newborns, and 12,244 were female newborns, with a male–female ratio of 1.31:1. According to the age at delivery, the term newborns (11,822 cases) have gestational ages of $\geq$ 37 weeks, and the preterm newborns (16,465 cases) have gestational ages of $<$ 37 weeks. According to the different admission wards, newborns who have been assessed by the doctor in serious condition will be admitted to the neonatal intensive care unit (NICU) (6,628 cases), and other newborns will be admitted to the general neonatology unit (21,659 cases).

Instruments and Reagents

The blood culture instrument was purchased from BD (BACTEC FX, United States). The carbon dioxide incubator was purchased from Panasonic (MCO-18AC, Japan). Mass spectrometry was purchased from Bruker (Microflex LT/SH, Germany). The automatic bacterial detection and analysis system was purchased from BioMerieux (VITEK2® compact, France). Drug-sensitive paper was purchased from Oxoid (Basingstoke, Britain). All kinds of culture plates were purchased from Antu (Zhenzhou, China).

Strain Identification and Drug Sensitivity Test

Blood culture bottles were placed into the instrument for incubation. The positive samples were transferred to the culture plate and incubated at 37°C for 18–24 h (5% CO_2). The colonies were identified by using a mass spectrometer. The automatic bacterial detection and analysis system and Kirby–Bauer (KB) method were used for the drug sensitivity test. The results were judged according to the latest standards of the Clinical Laboratory Standardization Association (Clinical and Laboratory Standards Institute, 2020). Extended-spectrum β-lactamases (ESBLs) were determined by the automatic bacterial detection and analysis system. The judgment results were obtained according to its own expert system. The quality control strains were *Escherichia coli* (*ATCC 25922*), *Pseudomonas aeruginosa* (*ATCC 27853*), *Staphylococcus aureus* (*ATCC 25923* and *ATCC 29213*), *Enterococcus faecalis* (*ATCC 29212*), and *Streptococcus pneumoniae* (49619), which were purchased from the clinical testing center of the National Health Commission.

Statistical Analysis

SPSS 20.0 and WHONET 5.6 were used to analyze data. The counting data were expressed as the number of cases (n) and rate

(%). The χ^2-test was used in univariate analysis. The comparison between groups was carried out by the χ^2-test, with $p < 0.05$ as the difference, which was statistically significant.

RESULTS

Annual Distribution of Pathogenic Bacteria [*n* (%)]

The positive rates in the 5 years from 2016 to 2020 were 3.89, 2.49, 2.18, 1.53, and 2.45%, respectively. In 707 cases of neonatal BSI, 491 strains of Gram-positive (G^+) bacteria were isolated, accounting for 69.45%, and among them were *Staphylococcus epidermidis* (31.26%), *Streptococcus agalactiae* (8.63%), and *Staphylococcus hominis* (8.20%). Strains of Gram-negative (G^-) bacteria (182) were isolated, accounting for 25.74%, and among them were *E. coli* (12.87%) and *Klebsiella pneumoniae* (9.05%). Strains of fungi (Akbarian-Rad et al., 2020) were isolated, accounting for 4.24% (see **Figure 1** and **Table 1** for details).

Resistance Rate of the Main G^+ Bacteria to Common Antibiotics (%)

Coagulase-negative *Staphylococcus* (CNS), *S. agalactiae*, *S. aureus*, and *Enterococcus* are the main G^+ bacteria. **Table 2** shows that the above bacteria are resistant to various antibiotics to varying degrees. They have a higher rate of resistance to erythromycin. *Staphylococcus* has over 80% resistance to penicillin G, and *S. agalactiae* is 100% sensitive to penicillin G (see **Table 2** for details).

Resistance Rate of the Main G^- Bacteria to Common Antibiotics (%)

E. coli and *K. pneumoniae* are the main G^- bacteria. *K. pneumoniae* produces ESBLs, accounting for up to 55.73%. The overall resistance of *K. pneumoniae* is higher than that of *E. coli* (see **Table 3** for details). Subsequently, the multidrug resistances of *K. pneumoniae* and *E. coli* were analyzed. The results are shown in **Figure 2**.

Comparison of Positive Rates of Bloodstream Infection in Newborns of Different Groups [*n* (%)]

The type of microbial infection had a statistically significant difference in the positive rate among the age at delivery and the ward ($p < 0.05$). There were significant differences in the detection of fungi among these groups ($p < 0.05$). Details are shown in **Table 4**.

Clinical Diagnoses

Among the clinical diagnoses, pneumonia, jaundice, purulent meningitis, newborn enteritis, and newborn intestinal obstruction accounted for the top five, of which pneumonia accounted for 53.18%, followed by jaundice, accounting for 24.75% (see more in **Table 5**). Pathogens detected in the different groups are further analyzed in **Table 6**.

DISCUSSION

BSI has a high incidence and accounts for a high proportion of nosocomial infections, and its incidence has been increasing in recent years. It is complicated and poorly effective. According to reports, the in-hospital mortality rate of sepsis is as high as 30–60% (Bouza et al., 2015), exceeding the sum of mortalities due to acquired immune deficiency syndrome, breast cancer, and prostate cancer. For every hour of delay in treatment, the patient's mortality rate will increase by 7.6% (Kumar et al., 2006). International guidelines recommend that effective antibiotics should be used intravenously within 1 h after sepsis is diagnosed (Dellinger et al., 2013).

In this study, the 5-year average positive rate of neonatal blood culture was 2.50%. As shown in **Figure 1**, the positive rates of blood culture from 2016 to 2020 were 3.89, 2.49, 2.18, 1.53, and 2.45%, respectively. Even during the COVID-19 pandemic, the total number of specimens submitted for clinical examination decreased, but it did not affect the detection of positive specimens. The 5-year average distribution of pathogens was mainly G^+ bacteria (69.45%), which is consistent with previous similar research results (Jing and Big, 2019). However, a survey of pathogens of neonatal sepsis from Nigeria showed that the infection was mainly G^- bacteria (Pius et al., 2016). The above differences suggest that the distribution of common pathogens of neonatal BSI may have differences in research time, research locations, or research objects, which only represent the situation of the research institution at a certain time. CNS is the main pathogen of neonatal blood flow infection in the hospital, accounting for 50.77%, but the CNS isolated from a single blood culture may also be contaminated (García-Gudiño et al., 2017). Therefore, blood collection personnel should pay special attention to aseptic operation and hand hygiene. Nevertheless, the positive rate of CNS is still very high in neonatal blood culture, as reported by Siti et al. (2020). The detection of *Streptococcus* is very important for perinatal pregnant women, especially those with premature rupture of membranes. Previous studies have found that the colonization rate of *S. agalactiae* in pregnant women is 19% (Lixiang et al., 2018). *S. agalactiae* was the second most susceptible G^+ bacteria to neonatal BSI in this study, accounting for 8.63%, which is consistent with the results reported in other literature (Lili et al., 2017). It is worth noting that the ratio of *S. agalactiae* among the detected G^+ bacteria was quite different in 2020 (∼25%) compared with other years (7–14%). Recent studies have shown that *S. agalactiae* is closely related to COVID-19 (Soto et al., 2021; Xiong et al., 2021). The high ratio of *S. agalactiae* among the detected G^+ bacteria in 2020 may be related to the environment of COVID-19 infection, but further studies are needed. There are relatively few cases of neonatal BSI caused by *S. aureus*. Only 23 strains were found in this study, of which 8 strains were methicillin-resistant *S. aureus* (MRSA). The positive rate of MRSA is significantly lower in neonates than that in older children (Seas et al., 2018; Fang et al., 2020). The drug sensitivity results showed that the drug resistance rates of the main G^+ bacteria to erythromycin and penicillin G were high, while they were 100% sensitive to vancomycin and linezolid. The resistance rates of CNS represented by

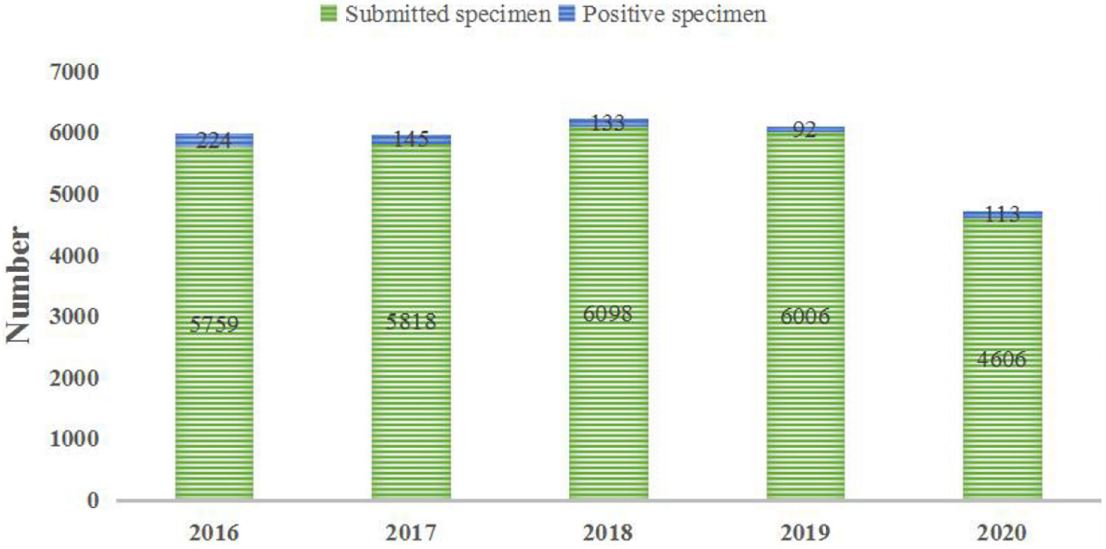

FIGURE 1 | Analysis of bacterial detection in 2016–2020.

S. epidermidis to penicillin G, erythromycin, and oxacillin were 89.76, 72.20, and 68.78%, respectively, and it is 100% sensitive to quinuptin/dafopudin, linezolid, and vancomycin. The resistance rate to moxifloxacin was 3.41% based on the overall antimicrobial susceptibility testing profile. It should be noted that the resistance rates of *Staphylococcus epidermidis* to moxifloxacin from 2016 to 2020 were 3.7, 7.69, 2.94%, 0, and 0, respectively. This suggests that in the case of poor efficacy of conventional drugs, moxifloxacin can be selected according to the situation of patients. In this study, *Staphylococcus haemolyticus* had high resistance to most antibiotics. There were 16 strains of methicillin-resistant *S. haemolyticus*. According to Takeuchi et al. (2005) *S. haemolyticus* has the maximum level of antimicrobial resistance among all CNS species. In recent years, linezolid-resistant *S. haemolyticus* has been reported (Rajan et al., 2017; Ahmed et al., 2019), and no quinuptin/ dafopudin-, linezolid-, or vancomycin-resistant *S. haemolyticus* were reported in the present study. *S. agalactiae* has different degrees of resistance to common antibiotics, and the rate of resistance to erythromycin is the highest, up to 91.11%. However, it is 100% sensitive to penicillin G, so penicillin G is also the first choice for the treatment of neonatal *S. agalactiae* infection. The resistance rate of *S. aureus* to penicillin G was as high as 85%, but to macrolide antibiotics represented by erythromycin, it was 50%. Therefore, macrolides have been widely used in neonatal and perinatal diseases in recent years (Wang et al., 2015). *Enterococcus faecium* has a high resistance rate to a variety of antibiotics, such as 100% resistance to rifampicin and penicillin G, 81.82% resistance to levofloxacin, and 72.72% resistance to minocycline. However, it was 100% sensitive to tigecycline and linezolid. There were no vancomycin-resistant *E. faecium* strains. See **Supplementary Material 1** for more antimicrobial susceptibility testing results of pathogen.

In the present research, 182 G^- bacterial strains were detected, accounting for 25.74%. The proportion of the positive rate of G^- bacteria was lower than that in previous similar literature reports (Pius et al., 2016; Akbarian-Rad et al., 2020). This may be related to the high positive rate of CNS (accounting for 50.77%) in the study. The main G^- bacteria in neonatal BSI were *E. coli* and *K. pneumoniae*, which is consistent with the study by other developing countries (Dat et al., 2017). The detected proportions of *E. coli* and *K. pneumoniae* were 12.87 and 9.05%, respectively. Interestingly, there was a little difference in the rate of *E. coli* and *K. pneumoniae* among the detected G^- bacteria from 2016 to 2017. However, after 2018, the proportion of *E. coli* significantly increased and was nearly twice that of *K. pneumoniae*. Nevertheless, due to the small number of positive specimens every year, it is necessary to continue to track the changes in detected bacteria in follow-up studies. Both *K. pneumoniae* and *E. coli* have high resistance to ampicillin, trimethoprim, and cefotaxime, which is similar to the results of Michael et al. (2017). However, the resistance rate to piperacillin/tazobactam, ciprofloxacin, aztreonam, and so on is low. As shown in **Table 3**, *K. pneumoniae* was 100% resistant to ampicillin, and the resistance rate to ampicillin/sulbactam reached 83.93%. The resistance rate to second- and third-generation cephalosporins is very high, and the resistance rate to some antibiotics is as high as 50%. The resistance rate of *E. coli* to cefuroxime was 25%, the resistance rate to ceftriaxone was 33.33%, and the resistance rate to fourth-generation cefotaxime was as high as 40.90%. The above results indicate that the resistance rate of *K. pneumoniae* to multiple antibacterial drugs is significantly higher than that of *E. coli*. The high resistance of bacteria to a variety of cephalosporin antibiotics indicates that the proportion of bacteria producing ESBLs is relatively high. In this study, the

TABLE 1 | Annual distribution of pathogenic bacteria [*n* (%)].

Type	2016	2017	2018	2019	2020	Total	Percentage (%)
Gram-positive bacteria	**154**	**104**	**86**	**62**	**85**	**491**	**69.45**
Staphylococcus epidermidis	83	39	33	30	36	221	31.26
Staphylococcus hominis	27	9	10	5	7	58	8.2
Staphylococcus capitis	7	16	8	6	8	45	6.36
Staphylococcus haemolyticus	8	4	4	2	0	18	2.55
Staphylococcus warneri	1	1	5	0	4	11	1.56
Staphylococcus caprae	0	0	0	0	3	3	0.42
Staphylococcus lugdunensis	0	0	1	0	2	3	0.42
Streptococcus agalactiae	11	12	12	5	21	61	8.63
Staphylococcus aureus	6	8	0	7	2	23	3.25
Listeria monocytogenes	5	0	9	3	0	17	2.4
Enterococcus faecium	2	4	2	2	2	12	1.70
Enterococcus faecalis	1	0	0	0	0	1	0.14
Streptococcus pallidus	2	6	1	0	0	9	1.27
Other *Streptococcus*	1	5	1	2	0	9	1.27
Gram-negative bacteria	**56**	**37**	**41**	**26**	**22**	**182**	**25.74**
Escherichia coli	26	12	24	15	14	91	12.87
Klebsiella pneumoniae	25	15	9	7	8	64	9.05
Enterobacter cloacae	2	4	1	2	0	9	1.27
Enterobacter aerogenes	0	3	1	0	0	4	0.57
Enterobacter asheri	0	0	0	2	0	2	0.28
Klebsiella oxytoca	0	0	2	0	0	2	0.28
Citrobacter Klebsiella	0	0	2	0	0	2	0.28
Serratia marcescens	0	1	0	0	0	1	0.14
Salmonella Typhimurium	0	0	1	0	0	1	0.14
Pseudomonas stephensi	0	0	1	0	0	1	0.14
Acinetobacter baumannii	1	0	0	0	0	1	0.14
Elizabetha meningealis	1	0	0	0	0	1	0.14
Acinetobacter yoelii	0	1	0	0	0	1	0.14
Hospital *Acinetobacter*	1	0	0	0	0	1	0.14
Acinetobacter pittii	0	1	0	0	0	1	0.14
Fungi	**14**	**4**	**6**	**3**	**3**	**30**	**4.24**
Candida parapsilosis	11	1	4	0	0	16	2.26
Candida albicans	3	3	2	3	1	12	1.7
Candida jiyemeng	0	0	0	0	2	2	0.28
Mix-infection	**0**	**0**	**0**	**1**	**3**	**4**	**0.57**
Total	**224**	**145**	**133**	**92**	**113**	**707**	**100**

positive rates of ESBLs-producing *K. pneumoniae* and *E. coli* were 55.73 and 27.16%, respectively, which are lower than the results reported in previous studies (Wang et al., 2020). In recent years, the clinical isolation rate of carbapenem-resistant *Enterobacter* (CRE), especially carbapenem-resistant *K. pneumoniae* (CRKP), has increased (Stein et al., 2019). According to data from the China Antibiotic Resistance Surveillance Network, the isolation rate of CRKP among Chinese children rose from 3.0 to 20.9% from 2005 to 2017, which was significantly higher than that of adults (Wang et al., 2020). As shown in **Figure 2**, there were 12 strains of CRKP and 4 strains of carbapenem-resistant *E. coli*, which accounted for 18.75 and 4.40% of their respective strains. Carbapenem-resistant strains are resistant to most antibacterial drugs, and clinical treatment measures are limited. Therefore, it is difficult to control infection, and the mortality rate is high (Gu et al., 2018). Special attention should be given to the abovementioned carbapenem-resistant strains to actively prevent infection.

In recent years, BSI caused by fungi has increased significantly, and *Candida* is the most common fungi (Dilhari et al., 2016). Previous studies reported that the neonatal BSI caused by fungi was mainly by *Candida albicans* (Ting et al., 2018), which is somewhat different from the results of this study. In this study, a total of 30 strains of fungi were detected, including 16 strains of *Candida parapsilosis* and 12 strains of *C. albicans*. This may be related to the low number of fungi detected in this study. *C. parapsilosis* is 100% sensitive to 5-fluorocytosine, voriconazole, fluconazol, itraconazole, and amphotericin B, which is also consistent with the conclusion reported by

TABLE 2 | Resistance rate of the main G^+ bacteria to common antibiotics (%).

Antibiotics	*Staphylococcus epidermidis* (*n* = 205)	*Staphylococcus haemolyticus* (*n* = 18)	*Streptococcus agalactiae* (*n* = 45)	*Staphylococcus aureus* (*n* = 20)	*Enterococcus faecium* (*n* = 11)
Oxacillin	68.78	88.89	–	35.00	–
Sulfamethoxazole	34.15	33.33	–	5.00	–
Erythromycin	72.20	94.44	91.11	50.00	–
Ciprofloxacin	25.85	77.78	–	0.00	–
Quinuptin/Dafopudin	0.00	0.00	6.67	0.00	0.00
Linezolid	0.00	0.00	0.00	0.00	0.00
Rifampicin	8.78	22.22	–	0.00	100
Clindamycin	28.78	44.44	80.00	50.00	–
Moxifloxacin	3.41	55.56	–	0.00	–
Penicillin G	89.76	88.89	0.00	85.00	100
Gentamicin	14.15	72.22	–	5.00	–
Tetracycline	13.17	38.89	73.33	5.00	–
Tigecycline	0.00	72.22	–	0.00	0.00
Cefoxitin	38.89	88.89	–	65.00	–
Vancomycin	0.00	0.00	0.00	0.00	0.00
Levofloxacin	27.80	77.78	33.33	0.00	81.82
Minocycline	–	–	–	–	72.72

"–": This means it is not detected.

TABLE 3 | Resistance rate of the main G^- bacteria to common antibiotics (%).

Antibiotics	*Escherichia coli* (*n* = 75)	*Klebsiella pneumoniae* (*n* = 56)
ESBLs	27.16	55.73
Ampicillin	73.33	100
Ampicillin/Sulbactam	32	83.93
Aztreonam	17.33	21.43
Amikacin	0	1.96
Sulfamethoxazole	50.67	55.36
Ciprofloxacin	33.33	10.71
Levofloxacin	32	0
Piperacillin	41.93	83.33
Piperacillin/Tazobactam	4.50	5.36
Gentamicin	30.67	7.14
Tobramycin	9.33	10.71
Cefotetan	4.05	23.21
Ceftazidime	13.33	55.36
Cefatriaxone	33.33	75
Cefepime	8.21	50
Cefazolin	33.33	80.36
Cefoxitin	8.21	35.71
Cefazoxime	18.67	50
Cefuroxime	25	76.78
Cefotaxime	40.90	69.23
Cefoperazone/Sulbactam	8.21	30.36
Imipenem	7.24	21.43
Meropenem	6.81	32

Van Asbeck et al. (2009). Drug resistance was concentrated on *C. albicans*, and two strains of resistant *C. albicans* were obtained. One strain was only resistant to 5-fluorocytosine, and the other was only sensitive to amphotericin B. The low resistance rate to amphotericin B may be related to the greater side effects of the drug.

The differences in pathogen detection between genders, age at delivery, and ward were further analyzed. In **Table 4**, fungi

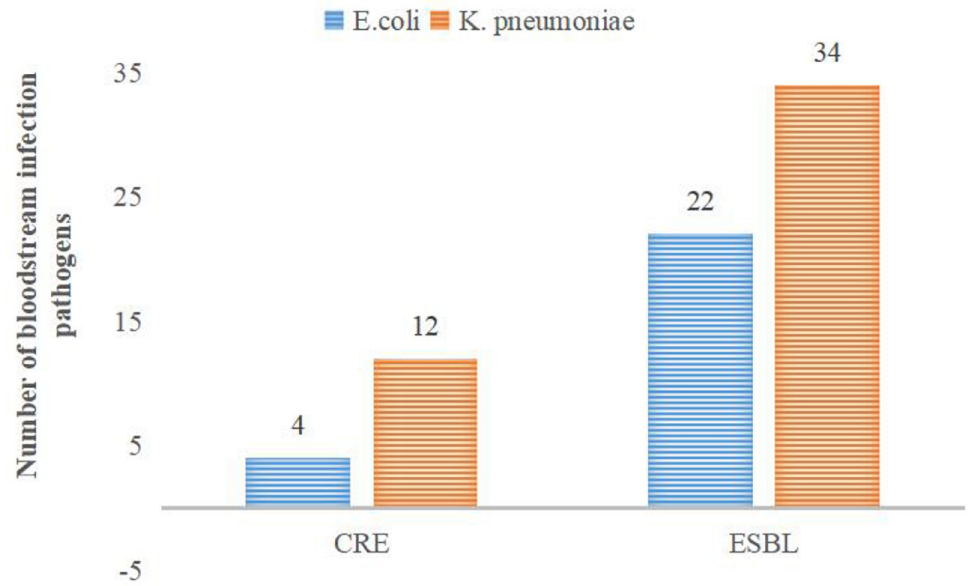

FIGURE 2 | Distribution of the main drug-resistant bacteria.

TABLE 4 | Comparison of the positive rate of BSI in newborns of different groups (*n*).

Index		Total	Positive number	G^+ bacteria	G^- bacteria	fungi	Mix-infection
Gender	Male	16,040	404	283	110	10	1
	Female	12,244	303	208	72	20	3
	χ^2	–	0.055	0.175	1.038	6.685	1.639
	p	–	0.814	0.676	0.308	**0.01**	0.201
	OR	–	1.018	1.039	1.167	0.381	0.254
	95% CI	–	0.876–1.184	0.868–1.245	0.866–1.573	0.178–0.815	0.026–2.446
Age at delivery	Term newborns	11,822	316	249	63	1	3
	Preterm newborns	16,465	391	242	119	29	1
	χ^2	–	2.512	16.342	3.879	18.261	1.813
	p	–	0.113	**<0.001**	**0.049**	**<0.001**	0.178
	OR	–	1.129	1.442	0.736	0.048	4.179
	95% CI	–	0.972–1.312	1.207–1.724	0.542–1.000	0.007–0.352	0.435–40.180
Ward	NICU	6,628	255	135	89	30	1
	Neonatology	21,659	452	356	93	0	3
	χ^2	–	64.54	4.599	66.234	98.138	0.005
	p	–	**<0.001**	**0.032**	**<0.001**	**<0.001**	0.941
	OR	–	1.877	1.244	3.156	1.005	1.089
	95% CI	–	1.606–2.194	1.019–1.520	2.357–4.226	1.003–1.006	0.113–10.474

OR, the odds ratio; 95% CI, the 95% confidence interval.

were a risk factor for BSI in female newborns. The positive rate of G^+ bacteria in term newborns was 2.11% (249/11,822), which was higher than the 1.47% (242/11,465) of preterm newborns, while the positive rate of G^- bacteria was the opposite. The above differences were statistically significant ($p < 0.05$). These results are consistent with the finding that preterm newborns are more susceptible to G^- bacteria (Zhang, 2020). The study also found that 30 patients with fungal infections were all preterm newborns, and the difference in fungal detection between preterm newborns and term newborns was statistically significant ($\chi^2 = 18.261$, $p < 0.001$). Studies have shown that the immune function of preterm newborns is relatively weak, and they are more prone to fungal infections (Manzoni et al., 2015). Most of the newborns admitted to the NICU have more serious underlying diseases, may undergo more invasive procedures, and have a significantly increased risk of infection. Statistics found that the positive rates of $G^{\pm}$ bacteria and fungi in newborns in the NICU were significantly higher than those in neonatology, and the difference was statistically significant ($p < 0.05$). Therefore, the ICU should

TABLE 5 | Comparison of clinical diagnoses of different groups (*n*).

Index		Pneumonia	Jaundice	Purulent meningitis	Enteritis	Intestinal obstruction	Respiratory distress syndrome	Urinary tract infection	Vomiting	Hyperbilirubinemia	Other infections	Other symptoms
Gender	Male	218	102	17	11	9	4	8	4	6	5	20
	Female	158	73	21	10	8	13	3	5	0	7	5
	χ^2	0.25	0.178	2.222	0.165	0.098	7.629	1.15	0.552	4.581	1.107	5.528
	p	0.617	0.673	0.136	0.685	0.754	0.006	0.284	0.458	**0.032**	0.293	0.019
	OR	1.054	1.067	0.618	0.837	0.859	0.235	2.036	0.611	1	0.545	3.056
	95% CI	0.858–1.295	0.789–1.442	0.326–1.171	0.356–1.973	0.331–2.226	0.077–0.720	0.540–7.676	0.164–2.274	1.000–1.001	0.173–1.718	1.147–8.145
Age at delivery	Term newborns	144	106	19	7	9	4	3	3	2	8	11
	Preterm newborns	232	69	19	14	8	13	8	6	4	4	14
	χ^2	1.914	25.525	1.054	0.618	0.869	2.332	0.954	0.265	0.177	3.053	0.050
	p	0.167	**<0.001**	0.305	0.432	0.351	0.127	0.329	0.607	0.674	0.081	0.823
	OR	0.863	2.150	1.393	0.696	1.567	0.428	0.522	0.696	0.696	2.787	1.094
	95% CI	0.700–1.064	1.586–2.914	0.737–2.633	0.281–1.725	0.605–4.063	0.140–1.314	0.138–1.969	0.174–2.785	0.128–3.802	0.839–9.256	0.497–2.411
Ward	NICU	177	7	16	8	10	16	1	4	6	2	8
	Neonatology	199	168	22	13	7	1	10	5	0	10	17
	χ^2	118.731	37.059	7.396	2.519	11.876	47.373	1.261	2.216	19.611	0.306	1.024
	P	**<0.001**	**<0.001**	**0.007**	0.112	**0.001**	**<0.001**	0.261	0.137	**< 0.001**	0.58	0.132
	OR	2.959	0.135	2.38	2.012	4.674	52.409	0.327	2.615	1.001	0.653	1.538
	95% CI	2.412–3.630	0.063–0.288	1.249–4.534	0.834–4.857	1.778–12.283	6.949–395.262	0.042–2.552	0.702–9.742	1.000–1.002	0.143–2.983	0.664–3.566
Infection	G + bacteria	246	147	27	13	11	5	4	9	0	10	19
	G^- bacteria	109	28	10	8	5	1	7	0	6	2	6
	fungi	17	0	1	0	1	11	0	0	0	0	0
	Mix-Infection	4	0	0	0	0	0	0	0	0	0	0
Total		376	175	38	21	17	17	11	9	6	12	25

OR, the odds ratio; 95% CI, the 95% confidence interval.

TABLE 6 | Analysis of bacterial species of different groups (*n*).

Group		G^+ bacteria						G^- bacteria				Fungi	Mix-infection	Total
		Staphylococcus epidermidis	Other CNS	*Streptococcus agalactiae*	*Staphylococcus aureus*	*Listeria monocytogenes*	*Enterococcus*	Other *Streptococcus*	*Escherichia coli*	*Klebsiella pneumoniae*	*Enterobacter cloacae*	*Enterobacter aerogenes*	Other G^- bacteria			
Gender	Male	123	71	43	11	9	8	10	62	38	8	3	7	10	1	404
	Female	98	67	18	12	8	5	8	29	26	1	1	7	20	3	303
Age at delivery	Term newborns	125	60	38	11	5	5	5	43	10	7	1	2	1	3	316
	Preterm newborns	96	78	23	12	12	8	13	48	54	2	3	12	29	1	391
Ward	NICU	35	38	27	7	15	9	4	23	53	5	3	5	30	1	255
	Neonatology	186	100	34	16	2	4	14	68	11	4	1	9	0	3	452
Clinical diagnoses	Pneumonia	98	72	37	9	13	7	10	42	51	4	3	9	17	4	376
	Jaundice	91	46	2	3	0	1	4	20	6	0	1	1	0	0	175
	Purulent meningitis	2	2	15	4	4	0	0	8	0	0	0	2	1	0	38
	Enteritis	7	2	0	2	0	1	1	1	5	0	0	2	0	0	21
	Intestinal Obstruction	4	2	2	1	0	2	0	2	2	1	0	0	1	0	17
	Respiratory distress syndrome	1	2	1	0	0	0	1	1	0	0	0	0	11	0	17
	Urinary tract infection	2	2	0	0	0	0	0	7	0	0	0	0	0	0	11
	Vomiting	3	3	0	0	0	2	1	0	0	0	0	0	0	0	9
	Hyperbilirubinemia	0	0	0	0	0	0	0	6	0	0	0	0	0	0	6
	Other infections	4	2	0	4	0	0	0	0	0	2	0	0	0	0	12
	Other symptoms	9	5	4	0	0	0	1	4	0	2	0	0	0	0	25
Total		221	138	61	23	17	13	18	91	64	9	4	14	30	4	707

pay special attention to aseptic operation and hand hygiene and reduce cross-infection among newborns. In the main clinical diagnosis, the top five diseases were pneumonia (53.18%), jaundice (24.75%), purulent meningitis (5.37%), and neonatal enteritis (2.97%), the intestinal obstruction and respiratory distress syndrome ranked fifth (2.40%). Statistical analysis of the prevalence of pneumonia and jaundice found that compared with term newborns, preterm newborns are more susceptible to pneumonia and have a lower risk of jaundice, which is consistent with the results reported by Chen et al. (2017). The above results may be related to premature newborns due to immature lung development and more mechanical ventilation, so they are prone to respiratory tract infections which induce severe pneumonia. The study also found that the positive rate of pneumonia among newborns in the NICU was 2.67%, which was significantly higher than that of newborns in neonatology (0.92%), and the difference in detection was statistically significant ($\chi^2 = 118.731$, $p < 0.001$). Among the 255 patients with BSI in the NICU, there were 181 preterm newborns, of which 141 were clinically diagnosed with pneumonia, accounting for 77.91%. Therefore, it is necessary to pay special attention to the correlation between bloodstream infection and pneumonia in premature infants to be vigilant and take preventive measures as early as possible.

Subsequently, the types and quantities of bacteria among different genders, age at delivery, wards, and clinical diagnoses were determined. As shown in **Table 6**, many clinical diagnoses were closely related to the detection of G^+ bacteria, except urinary tract infection and hyperbilirubinemia. It is worth noting that 17 strains of *Listeria monocytogenes* were detected in the present study. Among them, 6 strains of *L. monocytogenes* entered the cerebrospinal fluid and caused meningitis. *L. monocytogenes* is a pathogen of sepsis and meningitis in children. A study on *L. monocytogenes* infection shows that infection in children is common in newborns, especially in preterm newborns, which easily causes suppurative meningitis (Cai et al., 2020). The detection of *L. monocytogenes* is closely related to preterm newborns admitted to the NICU with purulent meningitis and pneumonia in this study. Therefore, the neonatal ward should attach great importance to the spread of bacterial infection and do a good job in the prevention and control measures of cross infection.

In summary, regular monitoring of bacterial resistance and understanding of changes in pathogen spectrum and antimicrobial resistance patterns will help clinicians use drugs rationally and better prevent and control the occurrence of infectious diseases. Corresponding wards should pay attention to the inspection rate of blood cultures, consider the trend of drug resistance in the hospital, adjust medications, and reduce infection mortality. However, there are some limitations in this study. The overall positive rate and drug resistance of pathogens in the last 5 years were analyzed. There is a lack of further exploration of the resistance changes of various antimicrobials. It is also significant to analyze the change in the positive rate and drug resistance rate of each pathogen during the epidemic period of COVID-19. Therefore, we will pay more attention to the above limitations in a follow-up study.

DATA AVAILABILITY STATEMENT

The raw data supporting the conclusions of this article will be made available by the authors, without undue reservation.

ETHICS STATEMENT

The studies involving human participants were reviewed and approved by the Medical Ethics Committee of the Children's Hospital of Soochow University (ethics batch number: 2021CS158). Written informed consent to participate in this study was provided by the participants' legal guardian/next of kin. Written informed consent was obtained from the individual(s) for the publication of any potentially identifiable images or data included in this article.

AUTHOR CONTRIBUTIONS

XZ and WL conceived the study and designed the experiments. YL and XS provided financial support. XS, YD, and YT collected, analyzed the data, and interpreted the results. XZ drafted the manuscript. All authors critically revised the manuscript for intellectual content and read and approved the final manuscript.

FUNDING

This study was supported by grants from the Special Foundation for National Science and Technology Basic Research Program of China (2019FY101200), the High-level Innovative and Entrepreneurial Talents Introduction Program of Jiangsu Province (2020-30191), the Natural Science Foundation of the Jiangsu Higher Education Institutions of China (20KJB310012), the Medical Research Project of Jiangsu Commission of Health (M2020027), the Science and Technology Program of Suzhou (SYS2020163 and SYSD2019120), and the Science and Technology Program of Suzhou (SLC201904).

ACKNOWLEDGMENTS

We thank the staff from the Department of Clinical Laboratory, Children's Hospital of Soochow University, who took part in the study. We thank YT for the great help offered in manuscript revision.

SUPPLEMENTARY MATERIAL

The Supplementary Material for this article can be found online at: https://www.frontiersin.org/articles/10.3389/fmicb.2022.820577/full#supplementary-material

REFERENCES

Ahmed, A., Satti, L., Zaman, G., Gardezi, A., Sabir, N., and Khadim, M. T., (2019). Catheter related recurrent blood stream infection caused by linezolid-resistant, methicillin resistant *Staphylococcus haemolyticus*; an emerging super bug. *J. Pak. Med. Assoc.* 69, 261–263.

Akbarian-Rad, Z., Riahi, S. M., Abdollahi, A., Sabbagh, P., Ebrahimpour, S., Javanian, M., et al. (2020). Neonatal sepsis in iran: a systematic review and meta-analysis on national prevalence and causative pathogens. *PLoS One* 15:e0227570. doi: 10.1371/journal.pone.0227570

Bouza, C., Cuadrado, T. L., Parkinson, Z. S., and Amate-Blanco, J. M. (2015). Epidemiology and recent trends of severe sepsis in Spain: a nationwide population-based analysis 2006∼2011. *BMC Infect. Dis.* 14:717. doi: 10.1186/s12879-014-0717-7

Cai, Z. Q., Yang, J. Y., Jiang, X. Y., Huang, Y. C., Lin, T. Y., and Chiu, C. H. (2020). Clinical characteristics of *Listeria monocytogenes* infection. *Chin. J. Infect. Control* 19, 900–903.

Chen, D. X., Wang, X. J., Lu, H. R., Zhang, Q., and Chen, F. N. (2017). Comparative study on the clinical characteristics of sepsis in preterm infants and term infants. *J. Shanxi Med. Univ.* 48, 1291–1294.

Clinical and Laboratory Standards Institute (2020). *Performance Standards for Antimicrobial Susceptibility Testing* . Wayne, PA: Clinical And Laboratory Standards Institute.

Dat, V. Q., Vu, H. N., Nguyen, T. H., Nguyen, H. T., Hoang, L. B., Vu Tien Viet, D., et al. (2017). Bacterial bloodstream infections in a tertiary infectious diseases hospital in Northern Vietnam: aetiology, drug resistance, and treatment outcome. *BMC Infect. Dis.* 17:493. doi: 10.1186/s12879-017-2582-7

Dellinger, R. P., Levy, M. M., Rhodes, A., Annane, D., Gerlach, H., Opal, S. M., et al. (2013). Surviving sepsis campaign: international guidelines for the treatment of severe sepsis and septic shock 2012. *Crit. Care Med.* 41:580.

Dilhari, A., Weerasekera, M. M., Siriwardhana, A., Maheshika, O., Gunasekara, C., Karunathilaka, S., et al. (2016). *Candida* infection in oral leukoplakia:an unprceived public health problem. *Acta. Odontol. Scand.* 74, 565–569.

Esaiassen, E., Fjalstad, J. W., Juvet, L. K., van den Anker, J. N., and Klingenberg, C. (2017). Antibiotic exposure in neonates and early adverse outcomes:a systematic review and meta-analysis. *J Antimicrob. Chemother.* 72, 1858–1870.

Fang, P. P., Yang, J. W., Gao, K. J., Yang, J. M., Sun, H. Q., and Wang, Y. Y. (2020). Distribution and drug resistance analysis of pathogenic bacteria from bloodstream infection in a children's hospital in Zhengzhou from 2014 to 2019. *China Pharm.* 31, 98–103.

FLeischmann-Struzek, C., GoLdfarb, D. M., SchLattmann, P., Schlapbach, L. J., Reinhart, K., and Kissoon, N. (2018). The global burden of paediatric and neonataL sepsis: a systematic review. *Lancet Respir. Med.* 6, 223–230.

García-Gudiño, I., Yllescas-Medrano, E., Maida-Claros, R., Soriano-Becerril, D., Díaz, N. F., García-López, G., et al. (2017). Microbiological comparison of blood culture and amplification of 16S rDNA methods in combination with DGGE for detection of neonatal sepsis in blood samples. *Eur. J. Pediatr.* 177, 85–93. doi: 10.1007/s00431-017-3036-3

Gu, D., Dong, N., Zheng, Z., Lin, D., Huang, M., Wang, L., et al. (2018). A fatal outbreak of ST11 carbapenem-resistant hyper virulent *Klebsiella pneumoniaeina* Chinese hospital: a molecular epidemiological study. *Lancet Infect. Dis.* 18, 37–46. doi: 10.1016/s1473-3099(17)30489-9

Hu, F. P., Guo, Y., Zhu, D. M., Wang, F., Jiang, X. F., Xu, Y. C., et al. (2018). 2017 China bacterial drug resistance monitoring. *Chin. J. Infect. Chemother.* 18, 241–251.

Jing, Z., and Big, L. (2019). Analysis on the applicability of neonatal blood flow infection and antimicrobial regimen in a third class hospital. *Chin. Med. Rec.* 20, 96–101.

Johnson, A., Watson, D., Dreyfus, J., Heaton, P., Lampland, A., and Spaulding, A. B. (2020). Epidemiology of serratia bloodstream infections among hospitalized children in the united states, 2009-2016. *Pediatr. Infect. Dis. J.* 39, e71–e73. doi: 10.1097/INF.0000000000002618

Klingenberg, C., Kornelisse, R. F., Buonocore, G., Maier, R. F., and Stocker, M. (2018). Culture-negative early onset neonatal sepsis:at the crossroad between efficient sepsis care and antimicrobial stewardship. *Front. Pediatr.* 6:285. doi: 10.3389/fped.2018.00285

Kumar, A., Roberts, D., Wood, K. E., Light, B., Parrillo, J. E., Sharma, S., et al. (2006). Duration of hypotension before initiation of effective antimicrobial therapy is the critical determinant of survival in human septic shock. *Crit. Care Med.* 34, 1589–1596. doi: 10.1097/01.CCM.0000217961.75225.E9

Lili, L., Da, W., and Lifan, D. (2017). Correlation analysis between colonization of Streptococcus agalactiae in the birth canal of pregnant women with premature rupture of membranes and neonatal infection in the third trimester. *Chin. J. Microecol.* 29, 1330–1332.

Liu, M. X., Huang, L. Y., Liang, J. H., Wang, S. J., Cen, Z. J., Zeng, S. J., et al. (2020). Analysis of pathogen distribution and drug resistance of blood flow infection in children in Nanning from 2017 to 2018. *J. Pract. Med.* 36, 527–531.

Lixiang, Y., Huimin, L., and Xiaoqiong, Z. (2018). Clinical characteristics and drug sensitivity analysis of *Streptococcus agalactiae* infection in pregnant women and neonatal patients in Heyuan area. *Mod. Med. Health* 34, 710–712.

Lucia Hug, D. S., and You, D. (2017). *Levels &Trends in Child Mortality*. New York, NY: UNICEF.

Manzoni, P., Mostert, M., and Castagnola, E. (2015). Update on the management of *Candida* infections in preterm neonates. *Arch. Dis. Child Fetal Neonatal Ed.* 100, 454–459.

Michael, G. B., Kaspar, H., Siqueira, A. K., de Freitas Costa, E., Corbellini, L. G., Kadlec, K., et al. (2017). Extendedspectrum β-lactamase (ESBL)-producing *Escherichia coli* isolates collected from diseased food-producing animals in the GERM-Vet monitoring program 2008-2014. *Vet. Microbiol.* 200, 142–150. doi: 10.1016/j.vetmic.2016.08.023

Pius, S., Bello, M., Galadima, G. B., Ibrahim, H. A., Yerima, S. T., and Ambe, J. P. (2016). Neonatal septicaemia, bacterial isolates and antibiogram sensitivity in Maiduguri North-Eastern Nigeria. *Niger. Postgrad. Med. J.* 23, 146–151. doi: 10.4103/1117-1936.190340

Puopolo, K. M., Benitz, W. E., Zaoutis, T. E., and Committee On Fetus And Newborn; Committee On Infectious Diseases. (2018). Management of neonates born at ≤34 6/7 weeks' gestation with suspected or proven early-on set bacterial sepsis. *Pediatrics* 142:e20182896.

Rajan, V., Haleebedo, P., and Gopal, S. (2017). Occurrence of linezolid-resistant *Staphylococcus haemolyticus* in two tertiary care hospitals in Mysuru, South India. *J. Glob. Antimicrob. Resist.* 8, 140–141. doi: 10.1016/j.jgar.2016.12.005

Seas, C., Garcia, C., Salles, M. J., Labarca, J., Luna, C., Alvarez-Moreno, C., et al. (2018). *Staphylococcus aureus* bloodstream infections in Latin America:results of a multinational prospective cohort study. *J. Antimicrob. Chemother.* 73, 212–222. doi: 10.1093/jac/dkx350

Siti, N. M., Wan Nazirah, W. A. B., Rosni, I., Mohamed, A. N., and Salbiah, N. (2020). Species distribution and clinical profiles of coagulase-negative staphylococci (CoNS) isolated from blood cultures among paediatric patients in Hospital Kuala Lumpur. *Med. J. Malaysia* 75, 266–273.

Soto, A., Quiñones-Laveriano, D. M., Valdivia, F., Juscamayta-López, E., Azañero-Haro, J., Chambi, L., et al. (2021). Detection of viral and bacterial respiratory pathogens identified by molecular methods in COVID-19 hospitalized patients and its impact on mortality and unfavorable outcomes. *Infect. Drug Resist.* 21, 2795–2807. doi: 10.2147/IDR.S306439

Spaulding, A. B., Watson, D., Dreyfus, J., Heaton, P., Grapentine, S., Bendel-Stenzel, E., et al. (2019). Epidemiology of bloodstream infections in hospitalized children in the United States, 2009-2016. *Clin. Infect. Dis.* 69, 995–1002.

Stein, C., Vincze, S., Kipp, F., Makarewicz, O., Al Dahouk, S., and Pletz, M. W. (2019). Carbapenem-resistant *Klebsiella pneumoniae* with low chlorhexidine susceptibility. *Lancet Infect. Dis.* 19, 932–933. doi: 10.1016/S1473-3099(19)30427-X

Takeuchi, F., Watanabe, S., Baba, T., Yuzawa, H., Ito, T., Morimoto, Y., et al. (2005). Whole-genome sequencing of *Staphylococcus haemolyticus* uncovers the extreme plasticity of its genome and the evolution of humancolonizing staphylococcal species. *J. Bacteriol.* 187, 7292–7308. doi: 10.1128/JB.187.21.7292-7308.2005

Ting, J. Y., Roberts, A., Synnes, A., Canning, R., Bodani, J., Monterossa, L., et al. (2018). Canadian neonatal network investigators. invasive fungal infections in neonates in Canada: epidemiology and outcomes. *Pediatr. Infect. Dis. J.* 37, 1154–1159. doi: 10.1097/INF.0000000000001968

Ting, J. Y., Synnes, A., Roberts, A., Deshpandey, A., Dow, K., Yoon, E. W., et al. (2016). Association between antibiotic use and neonatal mortality and morbidities in very low-birth-weight infants without culture-proven sepsis or necrotizing enterocolitis. *JAMA Pediatr.* 70, 1181–1187. doi: 10.1001/jamapediatrics.2016.2132

Van Asbeck, E. C., Clemons, K. V., and Stevens, D. A. (2009). *Candida parapsilosis*: a review of its epidemiology, pathogenesis, clinical aspects, typing and antimicrobial susceptibility. *Crit. Rev. Microbiol.* 35, 283–309. doi: 10.3109/10408410903213393

Wang, B., Pan, F., Wang, C., Zhao, W., Sun, Y., Zhang, T., et al. (2020). Molecular epidemiology of carbapenem-resistant *Klebsiella pneumoniae* in a paediatric hospital in China. *Int. J. Infect. Dis.* 93, 311–319. doi: 10.1016/j.ijid.2020.02.009

Wang, H. M., Jiang, Y. Q., Huang, B. X., Zhao, R. Z., Cheng, H. Y., and Ma, D. L. (2015). Analysis of pathogen distribution and drug resistance of neonatal infectious pneumonia from 2010 to 2013. *Chin. J. Infect. Control* 13, 411–412.

Xiong, D., Muema, C., Zhang, X., Pan, X., Xiong, J., Yang, H., et al. (2021). Enriched opportunistic pathogens revealed by metagenomic sequencing hint potential linkages between pharyngeal microbiota and COVID-19. *Virol. Sin.* 36, 924–933. doi: 10.1007/s12250-021-00391-x

Yuan, Y., Zhou, W., Rong, X., Lu, W. N., and Zhang, Z. (2015). Incidence and factors associated with nosocomial infections in a neonatal intensive care unit (NICU) of an urban children' s hospital in China. *Clin. Exp. Obstet. Gynecol.* 42, 619–628.

Zhang, W. D. (2020). Comparison of clinical characteristics of neonatal sepsis in preterm and term infants. *China Health Stand. Manag.* 11, 36–38.

Author Disclaimer: The views, opinions, assumptions, or any other information set out in this article are solely those of the authors and should not be attributed to the funders or any other person connected with the funders.

Conflict of Interest: The authors declare that the research was conducted in the absence of any commercial or financial relationships that could be construed as a potential conflict of interest.

Publisher's Note: All claims expressed in this article are solely those of the authors and do not necessarily represent those of their affiliated organizations, or those of the publisher, the editors and the reviewers. Any product that may be evaluated in this article, or claim that may be made by its manufacturer, is not guaranteed or endorsed by the publisher.

frontiers | Frontiers in Microbiology

ORIGINAL RESEARCH
published: 17 June 2022
doi: 10.3389/fmicb.2022.865254

Epidemiology of *bla*$_{CTX-M}$-Positive *Salmonella* Typhimurium From Diarrhoeal Outpatients in Guangdong, China, 2010–2017

*Qi Jiang[1,2], Bi-xia Ke[3], De-shu Wu[1,2], Dong Wang[1,2], Liang-xing Fang[1,2], Ruan-yang Sun[1,2], Min-ge Wang[1,2], Jing-er Lei[1,2], Zheng Shao[1,2] and Xiao-ping Liao[1,2,4]**

[1]National Risk Assessment Laboratory for Antimicrobial Resistance of Animal Original Bacteria, South China Agricultural University, Guangzhou, China, [2]Laboratory of Veterinary Pharmacology, College of Veterinary Medicine, South China Agricultural University, Guangzhou, China, [3]Guangdong Provincial Center for Disease Control and Prevention, Guangzhou, China, [4]Guangdong Laboratory for Lingnan Modern Agriculture, Guangzhou, China

OPEN ACCESS

Edited by:
Guo-bao Tian,
Sun Yat-sen University, China

Reviewed by:
Hong-Ning Wang,
Sichuan University, China
Manal Mohammed,
University of Westminster,
United Kingdom

***Correspondence:**
Xiao-ping Liao
xpliao@scau.edu.cn

Specialty section:
This article was submitted to Antimicrobials, Resistance and Chemotherapy, a section of the journal Frontiers in Microbiology

Received: 29 January 2022
Accepted: 12 May 2022
Published: 17 June 2022

Citation:
Jiang Q, Ke B-x, Wu D-s, Wang D, Fang L-x, Sun R-y, Wang M-g, Lei J-e, Shao Z and Liao X-p (2022) Epidemiology of bla$_{CTX-M}$-Positive Salmonella Typhimurium From Diarrhoeal Outpatients in Guangdong, China, 2010–2017. Front. Microbiol. 13:865254. doi: 10.3389/fmicb.2022.865254

Salmonella enterica can lead to intestinal diarrhea, and the emergence and spread of cephalosporin-resistant *Salmonella* have brought great challenges to clinical treatment. Therefore, this study investigated the prevalence and transmission of *bla*$_{CTX-M}$ genes among *S.* Typhimurium from diarrhoeal outpatients in Guangdong, China, from 2010 to 2017. A total of 221 *bla*$_{CTX-M}$-positive isolates were recovered from 1,263 *S.* Typhimurium isolates from the facal samples of diarrhoea patients in 45 general hospitals from 11 cities. The most popular CTX-M gene was *bla*$_{CTX-M-55}$ (39.6%, 72/182) in the CTX-M-1 group, followed by *bla*$_{CTX-M-14}$ (22.5%, 41/182) and *bla*$_{CTX-M-65}$ (19.2%, 35/182) in the CTX-M-9 group. The isolates that carried *bla*$_{CTX-M-9G}$ had significantly higher resistance rates to multiple antibacterials compared with *bla*$_{CTX-M-1G}$ ($p < 0.01$). Meanwhile, PFGE analysis not only showed the clonal transmission of *bla*$_{CTX-M-55/14/65}$-positve isolates of diarrhoeal outpatients' origins from different hospitals in Guangdong province, but also the characteristic of *bla*$_{CTX-M-55/14/65}$-positve isolates' bacterial persistence. Multilocus sequence typing (MLST) analysis indicated that these *S.* Typhimurium isolates possessed ST34 and ST19. Furthermore, genomic Beast phylogenomic analysis provided the evidence of a close relationship of *bla*$_{CTX-M}$-positive *S.* Typhimurium isolates between the outpatients and pork. Most *bla*$_{CTX-M-55/14/65}$ genes were transmitted by non-typeable or IncI1/IncFII/IncHI2 plasmids with the size of ranging from ~80 to ~280 kb. Moreover, whole-genome sequencing (WGS) analysis further revealed that *bla*$_{CTX-M-55/14/65}$ coexisted with other 25 types of ARGs, of which 11 ARGs were highly prevalent with the detection rates >50%, and it first reported the emergence of *bla*$_{TEM-141}$ in *S.* Typhimurium. This study underscores the importance of surveillance for *bla*$_{CTX-M}$-positive microbes in diarrhea patients.

Keywords: *Salmonella* Typhimurium, *bla*$_{CTX-M}$, diarrhoeal outpatients, Guangdong, bacterial persistence

INTRODUCTION

Salmonella enterica is a zoonotic pathogen of substantial concern to human and animal health (Yin and Zhou, 2018). What's more, it is a leading cause of morbidity and mortality in people worldwide, with approximately 90 million cases of gastroenteritis and 150,000 associated deaths (Xu et al., 2021). So far, more than 2,610 *Salmonella* serovars have been identified, while salmonellosis is caused mainly by *S. enterica* serovars Typhimurium, Enteritidis and Dublin (Shi, 2015; Mohammed et al., 2017). Nontyphoidal *S.* Typhimurium is a dominant factor of human gastroenteritis, and improper handling and digestion of inadequately looked food primarily result in the infection. Invasive complications, including meningitis, sepsis and bacteraemia, are very common in infants, the elderly and immunocompromised patients. The disease of *S.* Typhimurium is usually related to contaminated foods, such as pork and fruits, unpasteurized milk and dairy products, and undercooked eggs (Wegener et al., 2003).

In these potentially life-threatening *S.* Typhimurium cases, the antibiotics of choice are fluoroquinolones and extended-spectrum cephalosporins (Diard and Hardt, 2017). Third-generation cephalosporins (3GCs) are used across the world to threat infections caused by *Salmonella*, and subsequently the emergence of resistance attracts particular attention (Whichard et al., 2007). Multidrug-resistant (MDR) *Salmonella* spp. potentially arising for the selective pressure from sustained antimicrobial exposure are more likely to be the causative agents of invasive disease (Okoro et al., 2015). Moreover, the ESBL-producing strains of *Salmonella* have been reported in many regions in China, including Beijing, Shanghai, Guangdong, and Shandong (Cao C. et al., 2021). Worse, ESBL-producing *S.* Typhimurium have increasingly been detected from food animals, even environmental water and human patients (Fu et al., 2020; Ma et al., 2020). Hence, the number of ESBL-*Salmon* has increased worldwide.

TEM, SHV, and CTX-M were the most prevalent ESBL types. It has commonly been found that ESBL-CTX-M is located on plasmids and considered as the most prevalent type of ESBLs in many European countries (Paterson and Bonomo, 2005). At the same time, there is tremendous diversity of bla_{CTX-M} genotypes isolated from food animals and human populations. Usually, among the reported bacteria with $bla_{CTX-M-55}$-positive or $bla_{CTX-M-14}$-positive or $bla_{CTX-M-65}$-positive, most are isolated from food and animal sources (Xiang et al., 2015; Zhang et al., 2015; Nadimpalli et al., 2019). A practice was selected for antibiotic resistant *S. enterica* that can spread to human through contaminated foods. However, this practice is not currently monitored or regulated in Guangdong Province.

Therefore, in this study, ESBL-producing *S.* Typhimurium isolates, mainly from diarrheal patients, isolated from Guangdong province, and collected at the Guangdong Provincial CDC during the period of 2010–2017, were investigated to gain insight into their public health impacts.

MATERIALS AND METHODS

Bacterial Isolates, Detection of ESBL/*pAmpC* Genes, and Antimicrobial Susceptibility Testing

A total of 1263 *S.* Typhimuriums were recovered from facal samples of diarrhoea patients in 45 general hospitals from 11 cities of Guangdong province between 2010 and 2017. These isolates were collected by the Guangdong Provincial Center for Disease Control and Prevention (CDC) in a clinic-based *Salmonella* infection surveillance of outpatients with diarrhea, as described previously (Zhang et al., 2013). All 1263 *S.* Typhimurium isolates were incubated on MacConkey agar plates, containing 4 mg/L cefotaxime. The cefotaxime-resistant *S.* Typhimurium isolates were subjected to screening for CTX-M, CTX-M-1G, CTX-M-9G, CMY-2G, SHV, and DHA genes (**Supplementary Table S1**; Liu et al., 2007), and $bla_{CTX-M-1G/9G}$-positive isolates were further subjected to determine the subtypes of ESBL-encoding genes, as previously reported (Zhao and Hu, 2013). The DNA sequences and deduced amino acid sequences were compared with the reported sequences from GenBank. Antimicrobial susceptibility testing was performed on all the CTX-M-producing isolates by the agar dilution method, except for colistin with the broth dilution method. The following antimicrobials were tested: cefotaxime, ceftriaxone, ceftazidime, ceftiofur, meropenem, ciprofloxacin, nalidixic acid, sulfamethoxazole/trimethoprim, gentamicin, amikacin, florfenicol, fosfomycin, azithromycin, doxycycline, olaquindox, tigecycline, and colistin. The results were interpreted according to the Clinical and Laboratory Standards Institute (CLSI, 2018: M100-S25), and veterinary CLSI (VET01-A4/VET01-S2) guidelines (Humphries et al., 2019), and the resistance breakpoints for colistin were interpreted based on EUCAST (>2 mg/L) criteria, respectively. *Escherichia coli* ATCC25922 was used as the quality control strain.

Molecular Typing

The genetic relatedness of bla_{CTX-M}-positive *S.* Typhimurium isolates was analyzed by PFGE with the *Xba*I digestion of genomic DNA (Palhares et al., 2014). PFGE patterns were analyzed using BioNumerics software (Applied Maths, Sint-Martens-Latem, Belgium) with the Dice similarity coefficient, and a cut-off value of 85% of the similarity values was chosen to indicate identical or similar PFGE types.

WGS and Phylogenetic Analysis

Based on the results of PFGE types and resistance profiles analysis, representative bla_{CTX-M}-positive *S.* Typhimurium isolates ($n = 57$) were selected and their genomic DNA were subjected to 250-bp paired-end whole-genome sequencing (WGS), which at a depth of 100X, using the Illumina MiSeq system (Illumina, San Diego, CA, United States), using default parameters, followed by assembling the 150 bp paired-end Illumina reads using SPAdes v3.6.2 (Humphries et al., 2019). Multi locus sequence typing (MLST), antibiotic resistance genes (ARGs), and plasmid

replicon types were analyzed using the CGE server.[1] Phylogenetic tree for CTX-M-producing isolates was structured on the basis of the core genome using Harvest version 1.1.2 (Treangen et al., 2014), and the corresponding characteristics of each isolate were visualized using online tool iTOL version 4 (Letunic and Bork, 2019). The population structure of each phylogenetic tree was defined using hierBAPS v6.0 (Cheng et al., 2013).

Conjugation Assay, Gene Location, and Plasmids Analysis

To test the transferability of *bla*$_{CTX-M}$ genes, conjugation experiment was carried out by the liquid mating-out assay, with the streptomycin-resistant *E. coli* C600 as the recipient. Transconjugants were selected on MacConkey agar plates that were supplemented with cefotaxime (2 mg/L) and streptomycin (1,500 mg/L). Antimicrobial susceptibility testing was conducted on transconjugants and the *bla*$_{CTX-M}$ gene was confirmed by PCR, as described above. PCR-based replicon typing was performed for transconjugants, as previously described (Bankevich et al., 2012). To determine the location of *bla*$_{CTX-M}$, plasmids from the selected transconjugants were linearized using S1 nuclease and subjected to PFGE, followed by Southern blot hybridization using a digoxigenin-labeled probe specific for *bla*$_{CTX-M-1G/9G}$, as previously described (Liu et al., 2007).

Data Availability

All genome assemblies of the 57 *bla*$_{CTX-M}$-positive strains were deposited in GenBank and are registered under BioProject accession number PRJNA797940 and PRJNA629650.

RESULTS

Prevalence of CTX-M Genes

A total of 221 (17.5%) isolates displayed resistance to cefotaxime among the 1,263 *S.* Typhimurium isolates collected in 45 hospitals across 11 cities from Guangdong, China. Of which, 82.4% (182/221) carried one or two *bla*$_{CTX-M}$ variants. In addition, 20.8% (46) isolates contained *bla*$_{CMY-2G}$ gene and 16 (7.2%) isolates harbored *bla*$_{DHA}$ gene, and no *bla*$_{SHV}$ gene was detected among these isolates. A total of nine *bla*$_{CTX-M}$ variants (*bla*$_{CTX-M-55}$, *bla*$_{CTX-M-14}$, *bla*$_{CTX-M-65}$, *bla*$_{CTX-M-64}$, *bla*$_{CTX-M-130}$, *bla*$_{CTX-M-27}$, *bla*$_{CTX-M-15}$, *bla*$_{CTX-M-104}$, and *bla*$_{CTX-M-123}$) were detected in 182 *bla*$_{CTX-M}$-producing isolates, and the most predominant was *bla*$_{CTX-M-55}$ (39.6%, 72/182), followed by *bla*$_{CTX-M-14}$ (22.5%, 41/182) and *bla*$_{CTX-M-65}$ (19.2%, 35/182; **Figure 1B**). Furthermore, one isolate harbored both *bla*$_{CTX-M-55}$ and *bla*$_{CTX-M-14}$.

The percentages of cefotaxime-resistant isolates and *bla*$_{CTX-M}$-positive isolates had been shifted significantly from 11.5% and 6.1% in 2010 to 24.7% and 17.2% in 2015, but decreased to 15.1% and 13.4% in 2017, respectively (**Figure 1A**). The *bla*$_{CTX-M}$-positive isolates were identified in 35 hospitals among 11 cities. Of which, Shaoguan had the highest detection power of 25.0%. The mean positive prevalence of *bla*$_{CTX-M}$ carriages was 13.5% among the 12 cities (**Figure 1C**). Among the patients who were found to be positive for *bla*$_{CTX-M}$-positive *S.* Typhimurium isolates, the median age of patients with *bla*$_{CTX-M}$-producing isolates was 1 year (range 0–90 years), and 90% of patients were <5 years of age. In addition, 70.3% patients were male (**Table 1**).

Antimicrobial Susceptibility

Antimicrobial susceptibility was tested among the 182 *bla*$_{CTX-M}$-positive *S.* Typhimurium isolates, and most of the isolates showed resistance to sulfamethoxazole/trimethoprim (81.3%), and florfenicol (70.9%), followed by gentamicin (48.4%) and ciprofloxacin (31.3%). Relatively low resistance rates were observed for colistin (14.8%), fosfomycin (14.3%), and amikacin (1.7%). All the 182 isolates were susceptible to meropenem. Of note, the isolates that carried *bla*$_{CTX-M-9G}$ had significantly higher resistance rates to nine antibacterials compared with *bla*$_{CTX-M-1G}$ ($p < 0.01$), including florfenicol, amikacin, gentamicin, ciprofloxacin, nalidixic acid, polymyxin, fosfomycin, azithromycin, and sulfamethoxazole/trimethoprim (**Figure 2A**). The same scenario was also observed in *bla*$_{CTX-M-55}$, *bla*$_{CTX-M-14}$, and *bla*$_{CTX-M-65}$ positive isolates. However, the isolates that carried *bla*$_{CTX-M-1G}$, including *bla*$_{CTX-M-55}$, had remarkably higher rates of resistance to ceftazidime compared with *bla*$_{CTX-M-9G}$ including *bla*$_{CTX-M-14}$ and *bla*$_{CTX-M-65}$ ($p < 0.001$).

Furthermore, to determine the association between the dominant *bla*$_{CTX-M}$ genes and the 3GCs susceptibility, MICs of cefotaxime, ceftriaxone and ceftazidime were grouped into three levels, namely low resistance level (≤8 mg/ml), medium resistance level (16–64 mg/ml), and high resistance level (≥128 mg/ml; **Figure 2C**). The majority of *bla*$_{CTX-M-55}$, *bla*$_{CTX-M-14}$, and *bla*$_{CTX-M-65}$-positive *S.* Typhimurium isolates showed moderate and high levels resistance to cefotaxime and ceftriaxone. However, the proportion of high levels of resistance to cefotaxime and ceftriaxone in *bla*$_{CTX-M-55}$-positive *S.* Typhimurium isolates was higher than that of *bla*$_{CTX-M-14/65}$-positive *S.* Typhimurium. It was obvious that most *bla*$_{CTX-M-55}$-positive isolates are resistant to ceftazidime at high levels. In contrast, most isolates *bla*$_{CTX-M-14}$-positive or *bla*$_{CTX-M-65}$-positive were presented low-level resistant to ceftazidime.

Molecular Typing

The genetic relatedness of *bla*$_{CTX-M-55}$-positive, *bla*$_{CTX-M-14}$-positive and *bla*$_{CTX-M-65}$-positive *S.* Typhimurium isolates were analyzed by PFGE, respectively. PFGE was successfully performed in 71 *bla*$_{CTX-M-55}$-positive isolates and distributed into 26 pulsotypes. The 22 isolates in Type III were obtained in nine hospitals across four cities during 2014–2016. Similarly, the 17 isolates in Type VII were originated in six hospitals from four cities during 2010–2015 (**Supplementary Figures S1A**, **S2**). The clonal transmission of *bla*$_{CTX-M-55}$-positive strains was observed at different hospitals in the same city between 2014 and 2016. A total of 21 different pulsotypes were detected among 41 *bla*$_{CTX-M-14}$-positve isolates, and Type I was predominant ($n = 9$, 21.95%; **Supplementary Figures S1B**, **S2**). The clonal transmission of *bla*$_{CTX-M-14}$-positive strains was observed at the same hospitals

[1]https://cge.cbs.dtu.dk/services/

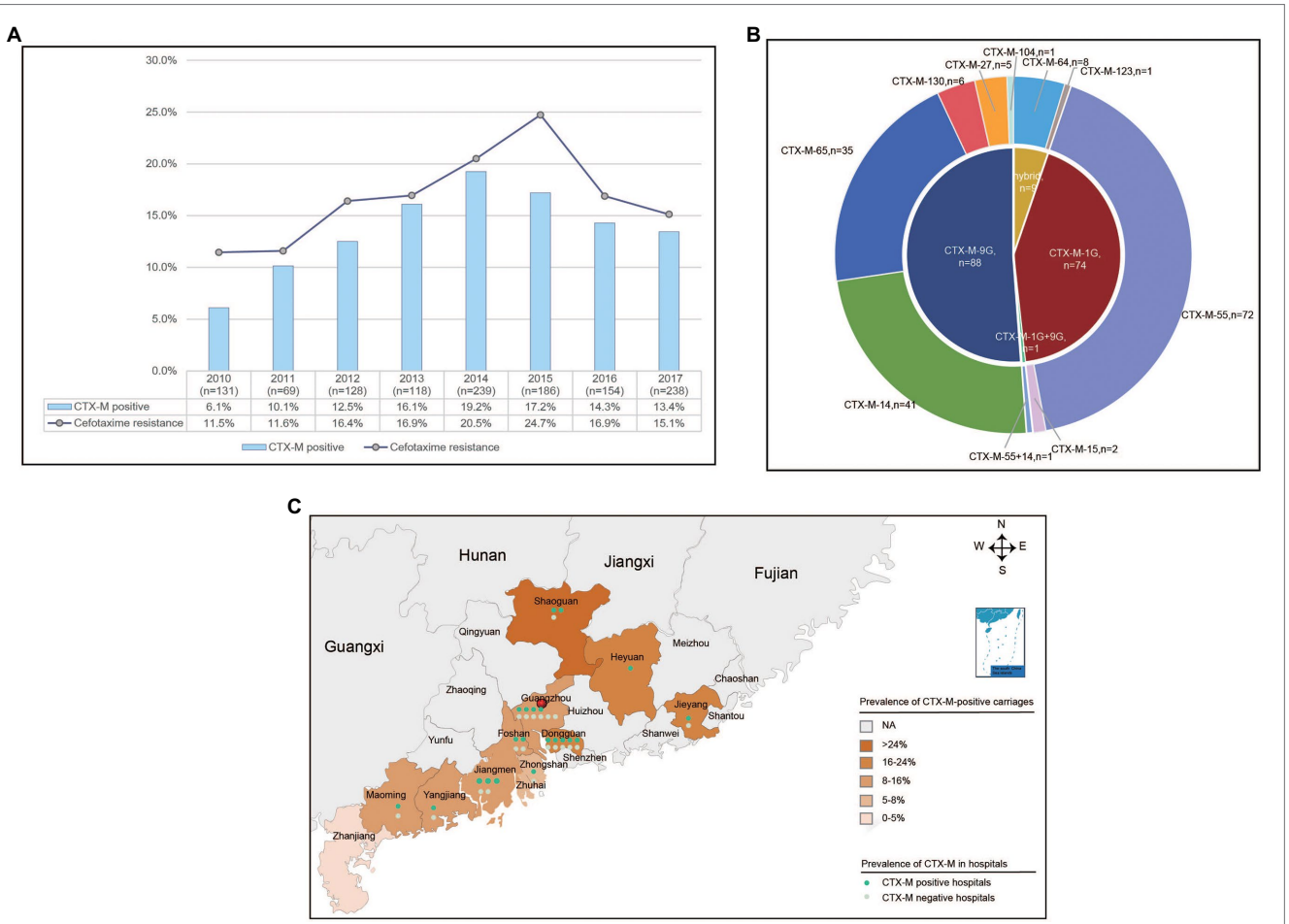

FIGURE 1 | The prevalence of *bla*$_{CTX-M}$-positive *Salmonella* Typhimurium isolates from diarrhoeal patients in 11 hospitals in Guangdong Province, China from 2010 to 2017. **(A)** The rate of resistance to cefotaxime and detection rate of *bla*$_{CTX-M}$-positive *S.* Typhimurium isolates in Guangdong Province from 2010 to 2017. **(B)** The subtypes and numbers of variants in CTX-M. **(C)** The detection rate of *bla*$_{CTX-M}$-positive *S.* Typhimurium isolates in 11 cities in Guangdong Province.

TABLE 1 | *bla*$_{CTX-M}$-Positive *S.* Typhimurium isolates collected from patient demographics characteristics, Guangdong, 2010–2017 (*N* = 182).

Characteristics	Value
Sex	
M	128
F	53
Unknown	1
Age, y, median (range)	1, (0–90)
Age group, y	
≤5	165
>5	15
Unknown	2

in the same city in 2012. Most importantly, all 35 *bla*$_{CTX-M-65}$-positve isolates were distributed into 15 pulsotypes, and the most predominant Type VIII contained 19 isolates (54.3%) and was originated from nine hospitals in seven cities during 2013–2017 (**Supplementary Figures S1C**, **S4**). The spread of *bla*$_{CTX-M-65}$-positve isolates' clones from Guangzhou and Jieyang was observed.

According to PFGE typing and resistance phenotype, 57 (27 *bla*$_{CTX-M-55}$, 14 *bla*$_{CTX-M-14}$, 15 *bla*$_{CTX-M-65}$, and 1 *bla*$_{CTX-M-55/14}$) *S.* Typhimurium isolates were selected for WGS. *In silico* MLST analysis revealed that these isolates belong to ST34 (*n* = 40) and ST19 (*n* = 17; **Figure 3**). Among them, most ST34 (3.8%, 15/40) and ST19 (4.1%, 7/17) belong to cluster 1 from Guangzhou and cluster 2/3/4 from Dongguan, respectively.

Phylogenetic Analysis of *bla*$_{CTX-M-55/14/65}$-Positive *Salmonella* Typhimurium

The population structure was further analyzed by constructing phylogenetic trees based on the core genomes of the 57 *bla*$_{CTX-M}$-positive isolates. Bayesian analysis displayed that all isolates were classified into four different lineages. The major Lineage I belong to ST34 and Lineage II-IV belong to ST19.

To explore the genetic relationships of *bla*$_{CTX-M-55/14/65}$-positive *S.* Typhimurium isolates in this study and other resources in China, 84 *bla*$_{CTX-M}$-positive *S.* Typhimurium isolates (including 36 *bla*$_{CTX-M-55}$, 33 *bla*$_{CTX-M-14}$, and 15 *bla*$_{CTX-M-65}$) were selected from GenBank. A maximum likelihood phylogenetic tree was constructed

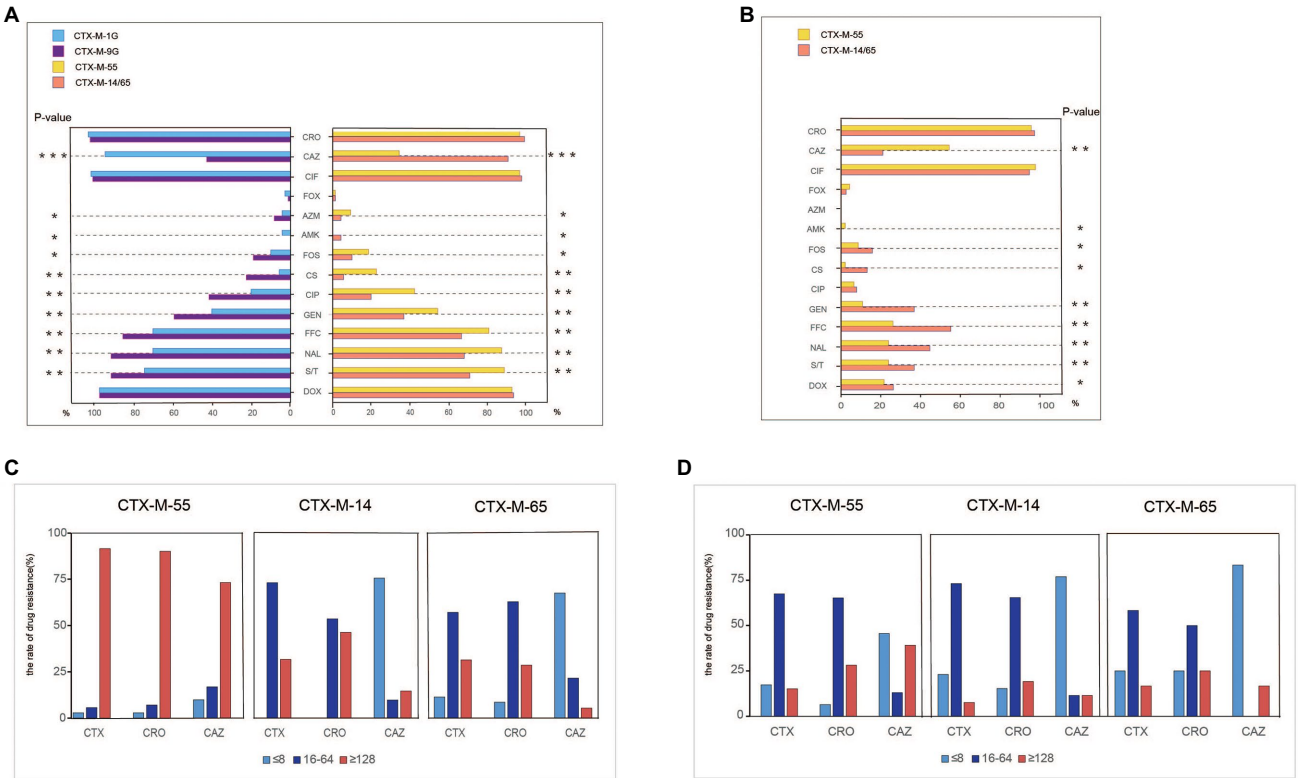

FIGURE 2 | Antimicrobial-resistant phenotypes analysis of *bla*$_{CTX-M}$-positive *S.* Typhimurium isolates and transconjugants isolates. **(A)** Antimicrobial-resistant phenotypes analysis of *bla*$_{CTX-M-1G/9G/55/14/65}$-positive *S.* Typhimurium isolates. **(B)** Antimicrobial-resistant phenotypes analysis of *bla*$_{CTX-M-1G/9G/55/14/65}$-positive *S.* Typhimurium' transconjugants. **(C)** Anslysis of resistant to CTX, CRO, and CAZ in *bla*$_{CTX-M-55/14/65}$-positive *S.* Typhimurium isolates. **(D)** Anslysis of resistant to CTX, CRO, and CAZ in *bla*$_{CTX-M-55/14/65}$ *S.* Typhimurium' transconjugants. CTX, cefotaxime; CRO, ceftriaxone; CAZ, ceftazidime; CIF, ceftiofur; FOX, cefoxitin; AZM, azithromycin; AMK, amikacin; FOS, fosfomycin; CS, polymyxin; CIP, ciprofloxacin; GEN, gentamicin; FFC, florfenicol; NAL, nalidixic acid; S/T, sulfamethoxazole/trimethoprium; and DOX, doxycycline. *means statistically different ($p < 0.05$), **means the difference is more significant ($p < 0.01$), ***means the difference is particularly significant ($p < 0.001$).

on the basis of 32,165 core genome single nucleotide polymorphisms (cgSNPs) among 138 isolates (**Figure 4**). These 138 isolates were mainly distributed in Guangdong province ($n = 134$) and other provinces ($n = 4$), such as Shanghai, Hebei, Jiangxi, and Zhejiang. Notably, these 138 isolates were primarily ST34 and ST19 members and originated from diverse sample types, including humans (patients, synviol fluid and blood culture), food (beef, chicken, feces, pork) and the environments (stool). It should be noted that four *bla*$_{CTX-M-14}$-positive ST34 *S.* Typhimurium isolates from patient samples in three cities, Guangdong (own isolate' number: 17E74), shared only 64 SNPs with a *bla*$_{CTX-M-14}$-positive ST34 *S.* Typhimurium isolate from a blood culture sample in Jiangxi (accession number SAMN10914546). In addition, a *bla*$_{CTX-M-55}$-positive ST34 *S.* Typhimurium isolate from a patient in Dongguan, Guangdong, in this study (own isolate' number: L-S2816) shared only six SNPs with a *bla*$_{CTX-M-55}$-positive ST34 *S.* Typhimurium isolates from pork in Shenzhen, Guangdong (accession number SAMN16986615). Finally, one *bla*$_{CTX-M-65}$-positive ST19 *S.* Typhimurium isolate from a patient sample in Zhongshan, Guangdong, in this study (own isolate' number: 17E594) shared only 28 SNPs with a *bla*$_{CTX-M-65}$-positive ST19 *S.* Typhimurium isolate from pork sample in Shenzhen, Guangdong (accession number SAMN16986937). These data may demonstrate that *bla*$_{CTX-M}$-positive *S.* Typhimurium isolates from human were likely to be closely related to food and environment in China, and the environment and food chain may play an important role in the transmission of *bla*$_{CTX-M}$-positive *S.* Typhimurium isolates.

Plasmid Analysis

Conjugation experimental results proved that 84 *bla*$_{CTX-M}$-positive plasmids were successfully transferred to *E. coil* C600 recipient strains among 148 *bla*$_{CTX-M-55/14/65}$ positive *S.* Typhimurium isolates. The transconjugants *bla*$_{CTX-M-55/14/65}$-positive mainly showed moderate levels resistance to cefotaxime and low levels resistance to ceftazidime. Notably, the proportion of *bla*$_{CTX-M-55}$-positive transconjugants with high levels of resistance to ceftazidime was higher than that of *bla*$_{CTX-M-14/65}$-positive transconjugants (**Figure 2B**). Meanwhile, the *bla*$_{CTX-M-55}$-positive transconjugants had significantly higher resistance rates to ceftazidime compared with *bla*$_{CTX-M-14/65}$-positive transconjugants ($p < 0.001$; **Figure 2B**).

In addition to cephalosporins, partial transconjugants displayed resistance to florfenicol ($n = 33$), doxycline ($n = 29$), sulfamethoxazole/trimethoprim ($n = 28$), gentamicin ($n = 25$),

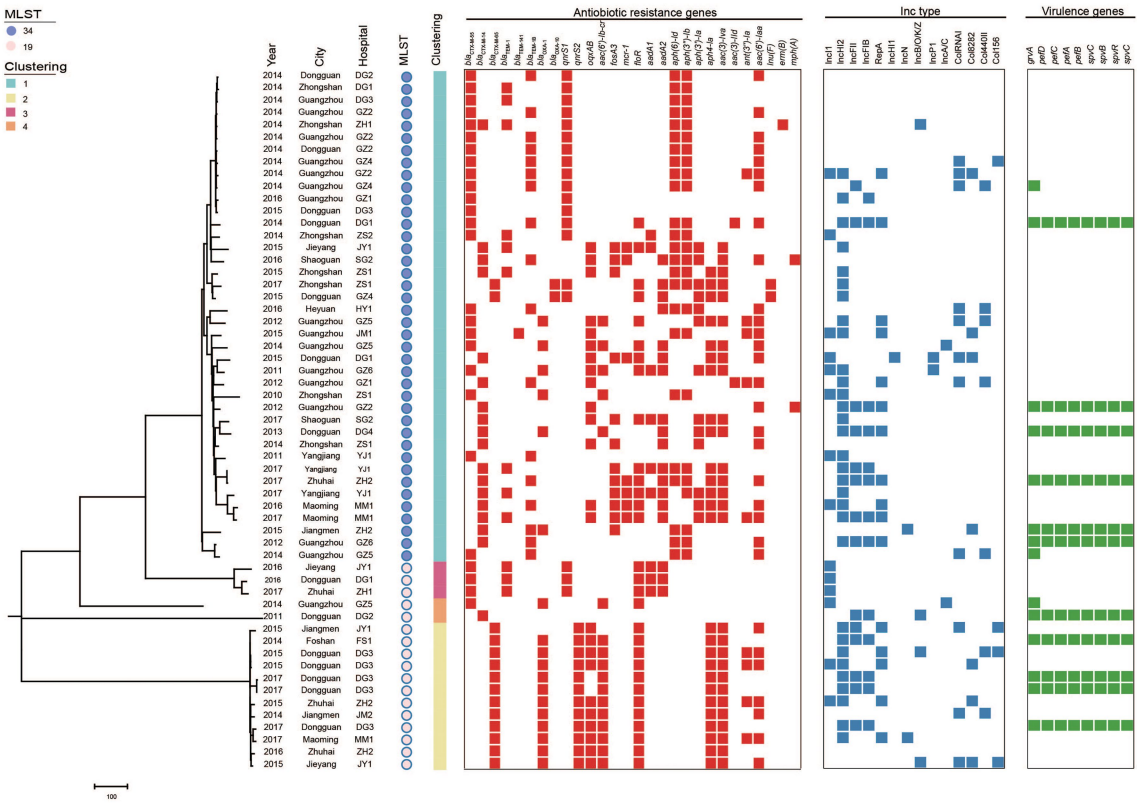

FIGURE 3 | Phylogenetic analysis of *bla*$_{CTX-M}$-positive *S.* Typhimurium isolates in this study ($n = 57$). Bayesian evolutionary tree was constructed using core-genome SNPs. Each isolate is labeled with the city of isolation year, hospital, ST and cluster. The red-filled squares indicate the possession of the indicated antimicrobial resistance genes (ARGs), the blue-filled squares indicate plasmid (Inc type), and the green-filled squares indicate virulence genes.

fosfomycin ($n = 17$), and azithromycin ($n = 17$). Obviously, the transconjugants that carried *bla*$_{CTX-M-9G}$ had significantly higher resistance rate to seven antibiotics compared with *bla*$_{CTX-M-1G}$ ($p < 0.01$), including amikacin, fosfomycin, gentamicin, polymyxin, florfenicol, sulfamethoxazole/trimethoprim, nalidixic, acid and doxycycline (**Figure 2D**).

Through conjugation assay and gene location methods, replicon analysis was performed on the *bla*$_{CTX-M-55/14/65}$-positive transconjugants, mainly IncI1($n = 49$), followed by IncHI2($n = 23$) and IncFII ($n = 8$; **Supplementary Figure S7**). Based on PFGE profiles, one isolate from each clonal lineage was selected for *S1*-PFGE and hybridization. For the *bla*$_{CTX-M-55/14/65}$-positive isolates ($n = 12$, 8, and 6, respectively), S1-PFGE and hybridization analyses confirmed that *bla*$_{CTX-M-55}$-positive genes ($n = 10$) from 12 isolates were mainly located on ~76.8 kb plasmids, *bla*$_{CTX-M-14}$-positive genes ($n = 4$) from eight isolates were mainly located on 54.7–80 kb plasmids, and *bla*$_{CTX-M-65}$-positive genes ($n = 4$) were from six isolates mainly located on 216.9–244.4 kb plasmids (**Supplementary Figures S5**, **S6**). Primers connecting contigs containing the backbone of different plasmids and *bla*$_{CTX-M}$ genes were used. The results illustrated that IncI1 (65.3%, 32/49), IncFII (50.0%, 4/8) and IncHI2 (30.4%, 7/23) plasmids may be major vectors for the wide dissemination of *bla*$_{CTX-M-55}$, *bla*$_{CTX-M-14}$, and *bla*$_{CTX-M-65}$ genes in *S.* Typhimurium isolates. In addition, WGS analysis revealed that sequenced strains also carry other plasmids, such as IncFIB-type, IncHI1-type, IncN-type and other different kinds of plasmids.

Resistance Profiles

WGS analysis demonstrated that 57 *bla*$_{CTX-M}$-producing isolates possessed 47 distinct ARGs. Several clinically important ARGs were identified to co-carry with *bla*$_{CTX-M}$, including *mcr-1*, *fosA3*, *oqxAB*, *qnrS1*, *qnrS2*, *aac-(6′)-Ib-cr*, and *floR*, with a prevalence rate from 12.3% to 52.6%. Moreover, *bla*$_{TEM-141}$ ($n = 1$) was first detected in *S.* Typhimurium isolates.

Notably, some ARGs were co-existence with a specific *bla*$_{CTX-M}$ variant. For example, *mcr-1* and *fosA3* were unique to *bla*$_{CTX-M-14}$-positive isolates. *qnrS2*, *aac(6′)-Ib-cr*, and *bla*$_{OXA-1}$ were primarily found in *bla*$_{CTX-M-65}$-positive isolates. In contrast, *qnrS1* and *bla*$_{TEM-1B}$ were largely present in *bla*$_{CTX-M-55}$-positive isolates. Additionally, both *oqxAB* and *floR* mostly presented in *bla*$_{CTX-M-65}$- and *bla*$_{CTX-M-14}$-positive isolates.

DISCUSSION

In this study, the detection rate of *bla*$_{CTX-M}$-positive *S.* Typhimurium from diarrhoeal outpatients increased from 2010 to 2015 in Guangdong Province, China. It was speculated that *bla*$_{CTX-M}$-positive *S.* Typhimurium outbreaks are linked to

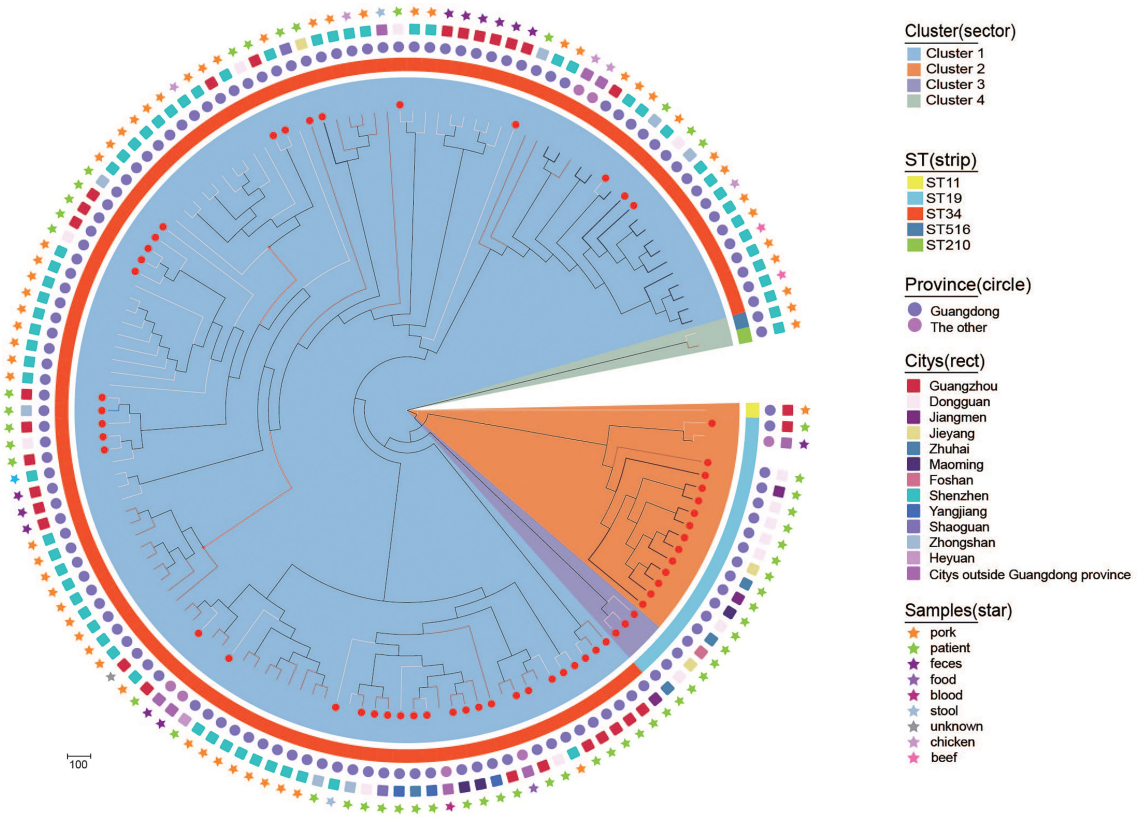

FIGURE 4 | Phylogenetic structures of the *bla*$_{CTX-M}$-positive *S.* Typhimurium isolates from this study and the GenBank database. The Bayesian evolutionary tree shows the relationships among the 141 *bla*$_{CTX-M-55/14/65}$-positive *S.* Typhimurium isolates. Sample source, city, province and ST from which isolates obtained are indicated as star, rect, circle, and strip. *bla*$_{CTX-M-55}$-positive, *bla*$_{CTX-M-14}$-positive, and *bla*$_{CTX-M-65}$-positive *S.* Typhimurium are indicated with a white, black, and red line, respectively. The red dots on the branches represent the bacteria that belong to this study.

the consumption of food animal or raw meat, particularly pork. Firstly, previous studies showed that the swine is one of the major reservoirs for *Salmonella* (Wang et al., 2007; Jackson et al., 2013). Secondly, the data from China's National Nutrition Survey also displayed that the total pork intake of Chinese residents increased by 73% from 1992 to 2012 (He et al., 2015). It's worth noting that the overall percentage of cephalosporin use had an upward trend from 2012 to 2017 in hospitals (Branch, 2020), which can give us some hints that the transmission of *bla*$_{CTX-M}$ may be relevant to the selective pressure of cephalosporin antibiotics. Then, it was obvious that the detection rate of cefotaxime-resistant *S.* Typhimurium in Guangdong province steadily decreased from 2016 to 2017. Meanwhile, according to CHINET bacterial resistance monitoring, the detection rate of cefotaxime-resistant *Enterobacter* decreased gradually from 2015 to 2017. Therefore, the long-term monitoring of cephalosporin usage and the prevalence of the *bla*$_{CTX-M}$-positive *Salmonella* are necessary for public health.

In this study, nine *bla*$_{CTX-M}$ variants were detected in 182 *bla*$_{CTX-M}$-producing isolates, and the most predominant was *bla*$_{CTX-M-55}$, followed by *bla*$_{CTX-M-14}$ and *bla*$_{CTX-M-65}$, which is consistent with previous studies (Zhang et al., 2018). Currently, *bla*$_{CTX-M-55}$-positive *Salmonella* has been reported as the dominant genotype in other countries, including Germany, Cambodia, Korea and Vietnam, and was frequently detected in food animals, especially in poultry and pork (Nguyen et al., 2016; Kim et al., 2017; Lay et al., 2021; Pietsch et al., 2021); *bla*$_{CTX-M-14}$-positive *Enterobacteriaceae* has been reported as the dominant genotype in some countries, including China, South Korea, Japan, and Spain, and was frequently detected in food, especially in retail chicken meat and pork (Bai et al., 2016; Shigemura et al., 2020; Wang et al., 2021); *bla*$_{CTX-M-65}$-positive *Salmonella* has been found in China, the United States, and Germany, and was commonly found in food animal sources, especially in chicken (Brown et al., 2018; Martínez-Puchol et al., 2021; Pietsch et al., 2021).

The *bla*$_{CTX-M-65}$-positive *S.* Typhimurium isolates with the same profile were found in the three hospitals (GZ5, JY1, and DG3), which indicated that the clonal dissemination of *bla*$_{CTX-M-65}$-positive *S.* Typhimurium occurred in hospital. Furthermore, a few *bla*$_{CTX-M-55/14/65}$-positive *S.* Typhimurium isolates from 2010 to 2017 showed 100% homology by PFGE analysis, which suggested that the possible long-term outbreaks were caused by clonal transfer of *bla*$_{CTX-M-55/14/65}$-positive *S.* Typhimurium strains within the hospital. WGS demonstrated that these *S.* Typhimurium isolates belonged to ST34 and ST19. In fact,

it has been shown that ST34 and ST19 are common *S.* Typhimurium STs responsible for infections worldwide, especially in China (Woh et al., 2021). It has been proved previously that the ST34 *S.* Typhimurium isolates with the highest percentage of MDR are mainly recovered from diarrhea patients (Biswas et al., 2019; Jiu et al., 2020; Luo et al., 2020; Sun et al., 2020). Furthermore, ST19 has been found mostly in human clinical *Salmonella* isolates, but also in animals and the environment, and successful in South African and China. ST19 was only occasionally found in United States and Mexico and coexists with quinolone resistance genes *qnrS* (Kariuki and Onsare, 2015; Gómez-Baltazar et al., 2019; Monte et al., 2020; Yao et al., 2020; Xiaoting et al., 2021).

Our genomic Beast tree analysis provided evidence for the closer relationship among *bla*$_{CTX-M}$-positive strains from the outpatients in this study and pork. Pig has been singled out as the most likely reservoir for the amplification and spread of Enterobacteriaceae that are resistant to ESBL and other antibiotics (Nordmann and Poirel, 2016), The same major *bla*$_{CTX-M}$, as presented in this study, was also detected in isolates from a pig farm in China (Zhang et al., 2019). Therefore, our study provides strong genome epidemiology-based evidence that the consumption of pork is the likely contamination source of *bla*$_{CTX-M}$-positive *S.* Typhimurium.

In the current study, most *bla*$_{CTX-M-55/14/65}$ genes identified were carried by IncI1, IncHI2, and IncFII plasmids, which indicated that plasmids belonged to *bla*$_{CTX-M-55/14/65}$-positive isolates and were diverse. Among them, IncI1 has become one of the most common plasmid families in contemporary Enterobacteriaceae from both human and animal sources. In clinical epidemiology, IncI1 ranks first as the confirmed vehicle of the transmission of extended spectrum beta-lactamase and *AmpC* genes in isolates from food-producing animals (Carattoli et al., 2021). The second, HI2, followed by FII plasmid, was found to be associated with the transfer of the *mcr-1* and ESBL encoding genes all over the world, especially in European and African countries. The coexistence of *mcr-1* and ESBL encoding genes in HI2 plasmids was less reported in China in recent years (Biswas et al., 2019; Wang et al., 2020). Worryingly, as the vector of drug resistance gene, FII plasmid not only carries *mcr-1*, but also is one of the common carriers of NDM gene (Wu et al., 2019).

WGS analysis further revealed that *bla*$_{CTX-M-55/14/65}$ coexisted with other 25 types of ARGs, of which 11 ARGs were highly prevalent with detection rates >50%. Of note, *mcr-1*, conferring resistance to the last-resort antibiotic colistin, was detected in seven *bla*$_{CTX-M}$-positive *S.* Typhimurium isolates. To begin with, the coexistence of *mcr-1* and *bla*$_{CTX-M-55}$ was first reported in the literature from colistin-resistant clinical source *E. coli* isolates in Ecuador in 2016 (Ortega-Paredes et al., 2016). Next, the coexistence of *mcr-1* and ESBL encoding genes (including *bla*$_{CTX-M-55/14}$) has been found in Tunisian from chicken, in China from food animal (including pigs, cattle and chickens) and in France from human *E. coli* (Birgy et al., 2018; Hassen et al., 2020; Shafiq et al., 2021). The coexistence of *mcr-1* and *bla*$_{CTX-M}$ in *Salmonella* isolates was mostly reported from food animal sources and found in Asian countries, including China, Cambodia and Laos (Ma et al., 2017; Lay et al., 2021). Last but not least, the coexistence of *mcr-1*, *bla*$_{NDM-5}$, and *bla*$_{CTX-M-55}$ in *Klebsiella pneumoniae* ST485 Clinical Isolates appeared in China (Cao X. et al., 2021), which further alerted us to the dangers of multidrug-resistant strains.

CONCLUSION

In summary, our study investigated the epidemiology of *S.* Typhimurium in Guangdong province, China. which could supplement important local epidemiological data. Among them, ST34 *S.* Typhimurium dominated the cefotaxime-resistant strains and the major resistance mechanism of cefotaxime-resistant *Salmonella* produced the CTX-M-type ESBLs, in which *bla*$_{CTX-M-55}$ was most prevalent. Obviously, the prevalence of *bla*$_{CTX-M}$-positive *S.* Typhimurium carried multiple resistance genes, which indicated the potential risk of *Salmonella* infections. In the current study, *bla*$_{CTX-M-55/65}$-positive *S.* Typhimurium isolates were found from different outpatients with community acquired diarrhoea at same hospital, which suggested the nosocomial cloning transmission. This study underscored the importance of surveillance for *bla*$_{CTX-M}$-positive microbes in patients and indicated a high likelihood for the spread of cephalosporin resistance from pig chain to humans.

DATA AVAILABILITY STATEMENT

The datasets presented in this study can be found in online repositories. The names of the repository/repositories and accession number(s) can be found in the article/**Supplementary Material**.

ETHICS STATEMENT

Ethical review and approval was not required for the study on human participants in accordance with the local legislation and institutional requirements. Written informed consent for participation was not required for this study in accordance with the national legislation and the institutional requirements.

AUTHOR CONTRIBUTIONS

QJ wrote the first draft of the manuscript. QJ and L-xF contributed to conception and design of the study. B-xK, D-sW, DW, M-gW, R-yS, J-eL, and ZS performed the statistical analysis. All authors contributed to manuscript revision, read, and approved the submitted version.

FUNDING

This work was jointly supported by the International Cooperation and Exchange of the National Natural Science Foundation of China (grant no. 31520103918), the Program for Changjiang

Scholars and Innovative Research Team in University of Ministry of Education of China IRT_17R39, the National Natural Science Fund of China (grant no. 31802244), and the National Science and Technology Major Project (2018ZX10714002).

SUPPLEMENTARY MATERIAL

The Supplementary Material for this article can be found online at: https://www.frontiersin.org/articles/10.3389/fmicb.2022.865254/full#supplementary-material

Supplementary Figure S1 | Genetic relatedness, year, city and hospital of the *bla*$_{CTX-M}$-positive *Salmonella* Typhimurium isolates in Guangdong from 2010 to 2017. **(A,B)** Genetic relatedness, year, city, hospital and pulsotype of the *bla*$_{CTX-M-55}$-positive *S*. Typhimurium isolates **(C)** genetic relatedness, year, city, hospital and pulsotype of the *bla*$_{CTX-M-14}$-positive *S*. Typhimurium isolates **(D)** genetic relatedness, year, city, hospital and pulsotype of the *bla*$_{CTX-M-65}$-positive *S*. Typhimurium isolates.

Supplementary Figure S2 | Genetic relatedness, year, city and hospital of the *bla*$_{CTX-M-55}$-positive *S*. Typhimurium isolates in Guangdong from 2010 to 2017.

Supplementary Figure S3 | Genetic relatedness, year, city and hospital of the *bla*$_{CTX-M-14}$-positive *S*. Typhimurium isolates in Guangdong from 2010 to 2017.

Supplementary Figure S4 | Genetic relatedness, year, city and hospital of the *bla*$_{CTX-M-65}$-positive *S*. Typhimurium isolates in Guangdong from 2010 to 2017.

Supplementary Figure S5 | S1 endonuclease pulsed-field gel electrophoresis analysis of plasmids from the *bla*$_{CTX-M-1G}$-positive *S*. Typhimurium isolates.

Supplementary Figure S6 | S1 endonuclease pulsed-field gel electrophoresis analysis of plasmids from the *bla*$_{CTX-M-9G}$-positive *S*. Typhimurium isolates.

Supplementary Figure S7 | PBRT types that *bla*$_{CTX-M}$-positive *S*. Typhimurium isolates **(A)** all PBRT types that *bla*$_{CTX-M}$-positive *S*. Typhimurium isolates **(B)** PBRT types that *bla*$_{CTX-M-55}$-positive *S*. Typhimurium isolates. **(C)** PBRT types that *bla*$_{CTX-M-14}$-positive *S*. Typhimurium isolates. **(D)** PBRT types that *bla*$_{CTX-M-65}$-positive *S*. Typhimurium isolates.

REFERENCES

Bai, L., Zhao, J., Gan, X., Wang, J., Zhang, X., Cui, S., et al. (2016). Emergence and diversity of *Salmonella enterica* serovar Indiana isolates with concurrent resistance to ciprofloxacin and cefotaxime from patients and food-producing animals in China. *Antimicrob. Agents Chemother.* 60, 3365–3371. doi: 10.1128/aac.02849-15

Bankevich, A., Nurk, S., Antipov, D., Gurevich, A. A., Dvorkin, M., Kulikov, A. S., et al. (2012). SPAdes: a new genome assembly algorithm and its applications to single-cell sequencing. *J. Comput. Biol.* 19, 455–477. doi: 10.1089/cmb.2012.0021

Birgy, A., Madhi, F., Hogan, J., Doit, C., Gaschignard, J., Caseris, M., et al. (2018). CTX-M-55-, MCR-1-, and FosA-producing multidrug-resistant *Escherichia coli* infection in a child in France. *Antimicrob. Agents Chemother.* 62, 00127–18. doi: 10.1128/aac.00127-18

Biswas, S., Li, Y., Elbediwi, M., and Yue, M. (2019). Emergence and dissemination of mcr-carrying clinically relevant *Salmonella* Typhimurium monophasic clone ST34. *Microorganisms* 7:298. doi: 10.3390/microorganisms7090298

Branch, I. C. (2020). Summary report on antimicrobial resistance in public hospitals, China.

Brown, A. C., Chen, J. C., Watkins, L. K. F., Campbell, D., Folster, J. P., Tate, H., et al. (2018). CTX-M-65 extended-spectrum β-lactamase-producing *Salmonella enterica* serotype infantis, United States(1). *Emerg. Infect. Dis.* 24, 2284–2291. doi: 10.3201/eid2412.180500

Cao, C., Niu, Q., Chen, J., Xu, X., Sheng, H., Cui, S., et al. (2021). Epidemiology and characterization of CTX-M-55-type extended-spectrum β-lactamase-producing *Salmonella enterica* serovar enteritidis isolated from patients in Shanghai, China. *Microorganisms* 9:260. doi: 10.3390/microorganisms9020260

Cao, X., Zhong, Q., Guo, Y., Hang, Y., Chen, Y., Fang, X., et al. (2021). Emergence of the coexistence of mcr-1, bla (NDM-5), and bla (CTX-M-55) in *Klebsiella pneumoniae* ST485 clinical isolates in China. *Infect. Drug Resist.* 14, 3449–3458. doi: 10.2147/idr.s311808

Carattoli, A., Villa, L., Fortini, D., and García-Fernández, A. (2021). Contemporary IncI1 plasmids involved in the transmission and spread of antimicrobial resistance in Enterobacteriaceae. *Plasmid* 118:102392. doi: 10.1016/j.plasmid.2018.12.001

Cheng, L., Connor, T. R., Siren, J., Aanensen, D. M., and Corander, J. (2013). Hierarchical and spatially explicit clustering of DNA sequences with BAPS software. *Mol. Biol. Evol.* 30, 1224–1228. doi: 10.1093/molbev/mst028

CLSI (2018). Performance Standards for Antimicrobial Susceptibility Testing—Twenty-Eighth Edition: M100.

Diard, M., and Hardt, W. D. (2017). Basic processes in *Salmonella*-host interactions: within-host evolution and the transmission of the virulent genotype. *Microbiol. Spectr.* 5:5. doi: 10.1128/microbiolspec.MTBP-0012-2016

Fu, Y., Xu, X., Zhang, L., Xiong, Z., Ma, Y., Wei, Y., et al. (2020). Fourth generation cephalosporin resistance among *Salmonella enterica* serovar enteritidis isolates in Shanghai, China conferred by bla (CTX-M-55) harboring plasmids. *Front. Microbiol.* 11:910. doi: 10.3389/fmicb.2020.00910

Gómez-Baltazar, A., Vázquez-Garcidueñas, M. S., Larsen, J., Kuk-Soberanis, M. E., and Vázquez-Marrufo, G. (2019). Comparative stress response to food preservation conditions of ST19 and ST213 genotypes of *Salmonella enterica* serotype Typhimurium. *Food Microbiol.* 82, 303–315. doi: 10.1016/j.fm.2019.03.010

Hassen, B., Abbassi, M. S., Ruiz-Ripa, L., Mama, O. M., Hassen, A., Torres, C., et al. (2020). High prevalence of mcr-1 encoding colistin resistance and first identification of bla(CTX-M-55) in ESBL/CMY-2-producing *Escherichia coli* isolated from chicken faeces and retail meat in Tunisia. *Int. J. Food Microbiol.* 318:108478. doi: 10.1016/j.ijfoodmicro.2019.108478

He, Y., Yang, X., Xia, J., Zhao, L., and Yang, Y. (2015). Consumption of meat and dairy products in China: a review. *Proc. Nutr. Soc.* 75, 385–391. doi: 10.1017/S0029665116000641

Humphries, R. M., Abbott, A. N., and Hindler, J. A. (2019). Understanding and addressing CLSI breakpoint revisions: a primer for clinical laboratories. *J. Clin. Microbiol.* 57, 00203–19. doi: 10.1128/JCM.00203-19

Jackson, B. R., Griffin, P. M., Cole, D., Walsh, K. A., and Chai, S. J. (2013). Outbreak-associated *Salmonella enterica* serotypes and food commodities, United States, 1998–2008. *Emerg. Infect. Dis.* 19, 1239–1244. doi: 10.3201/eid1908.121511

Jiu, Y., Meng, X., Hong, X., Huang, Q., Wang, C., Chen, Z., et al. (2020). Prevalence and characterization of *Salmonella* in three typical commercial pig abattoirs in Wuhan, China. *Foodborne Pathog. Dis.* 17, 620–627. doi: 10.1089/fpd.2019.2737

Kariuki, S., and Onsare, R. S. (2015). Epidemiology and genomics of invasive nontyphoidal *Salmonella* infections in Kenya. *Clin. Infect. Dis.* 61(Suppl. 4), S317–S324. doi: 10.1093/cid/civ711

Kim, J. S., Kim, S., Park, J., Shin, E., Yun, Y. S., Lee, D. Y., et al. (2017). Plasmid-mediated transfer of CTX-M-55 extended-spectrum beta-lactamase among different strains of *Salmonella* and *Shigella* spp. in the Republic of Korea. *Diagn. Microbiol. Infect. Dis.* 89, 86–88. doi: 10.1016/j.diagmicrobio.2017.03.014

Lay, K. K., Jeamsripong, S., Sunn, K. P., Angkititrakul, S., Prathan, R., Srisanga, S., et al. (2021). Colistin resistance and ESBL production in *Salmonella* and *Escherichia coli* from pigs and pork in the Thailand, Cambodia, Lao PDR, and Myanmar border area. *Antibiotics* 10:657. doi: 10.3390/antibiotics10060657

Letunic, I., and Bork, P. (2019). Interactive tree of life (iTOL) v4: recent updates and new developments. *Nucleic Acids Res.* 47, W256–W259. doi: 10.1093/nar/gkz239

Liu, J. H., Wei, S.-Y., Ma, J.-Y., Zeng, Z.-L., Lü, D.-H., Yang, G.-X., et al. (2007). Detection and characterisation of CTX-M and CMY-2 β-lactamases among *Escherichia coli* isolates from farm animals in Guangdong Province of China. *Int. J. Antimicrob. Agents* 29, 576–581. doi: 10.1016/j.ijantimicag.2006.12.015

Luo, Q., Wan, F., Yu, X., Zheng, B., Chen, Y., Gong, C., et al. (2020). MDR *Salmonella enterica* serovar Typhimurium ST34 carrying mcr-1 isolated from

cases of bloodstream and intestinal infection in children in China. *J. Antimicrob. Chemother.* 75, 92–95. doi: 10.1093/jac/dkz415

Ma, S., Lei, C., Kong, L., Jiang, W., Liu, B., Men, S., et al. (2017). Prevalence, antimicrobial resistance, and relatedness of *Salmonella* isolated from chickens and pigs on farms, abattoirs, and markets in Sichuan Province, China. *Foodborne Pathog. Dis.* 14, 667–677. doi: 10.1089/fpd.2016.2264

Ma, Y., Xu, X., Gao, Y., Zhan, Z., Xu, C., Qu, X., et al. (2020). Antimicrobial resistance and molecular characterization of *Salmonella enterica* serovar corvallis isolated from human patients and animal source foods in China. *Int. J. Food Microbiol.* 335:108859. doi: 10.1016/j.ijfoodmicro.2020.108859

Martínez-Puchol, S., Riveros, M., Ruidias, K., Granda, A., Ruiz-Roldán, L., Zapata-Cachay, C., et al. (2021). Dissemination of a multidrug resistant CTX-M-65 producer *Salmonella enterica* serovar infantis clone between marketed chicken meat and children. *Int. J. Food Microbiol.* 344:109109. doi: 10.1016/j.ijfoodmicro.2021.109109

Mohammed, M., Le Hello, S., Leekitcharoenphon, P., and Hendriksen, R. (2017). The invasome of *Salmonella* Dublin as revealed by whole genome sequencing. *BMC Infect. Dis.* 17:544. doi: 10.1186/s12879-017-2628-x

Monte, D. F. M., Sellera, F. P., Lopes, R., Keelara, S., Landgraf, M., Greene, S., et al. (2020). Class 1 integron-borne cassettes harboring blaCARB-2 gene in multidrug-resistant and virulent *Salmonella* Typhimurium ST19 strains recovered from clinical human stool samples, United States. *PLoS One* 15:e0240978. doi: 10.1371/journal.pone.0240978

Nadimpalli, M., Fabre, L., Yith, V., Sem, N., Gouali, M., Delarocque-Astagneau, E., et al. (2019). CTX-M-55-type ESBL-producing *Salmonella enterica* are emerging among retail meats in Phnom Penh, Cambodia. *J. Antimicrob. Chemother.* 74, 342–348. doi: 10.1093/jac/dky451

Nguyen, D. T., Kanki, M., Nguyen, P. D., Le, H. T., Ngo, P. T., Tran, D. N., et al. (2016). Prevalence, antibiotic resistance, and extended-spectrum and AmpC β-lactamase productivity of *Salmonella* isolates from raw meat and seafood samples in Ho Chi Minh City, Vietnam. *Int. J. Food Microbiol.* 236, 115–122. doi: 10.1016/j.ijfoodmicro.2016.07.017

Nordmann, P., and Poirel, L. (2016). Plasmid-mediated colistin resistance: an additional antibiotic resistance menace. *Clin. Microbiol. Infect.* 22, 398–400. doi: 10.1016/j.cmi.2016.03.009

Okoro, C. K., Barquist, L., Connor, T. R., Harris, S. R., Clare, S., Stevens, M. P., et al. (2015). Signatures of adaptation in human invasive *Salmonella* Typhimurium ST313 populations from sub-Saharan Africa. *PLoS Negl. Trop. Dis.* 9:e0003611. doi: 10.1371/journal.pntd.0003611

Ortega-Paredes, D., Barba, P., and Zurita, J. (2016). Colistin-resistant *Escherichia coli* clinical isolate harbouring the mcr-1 gene in Ecuador. *Epidemiol. Infect.* 144, 2967–2970. doi: 10.1017/s0950268816001369

Palhares, J. C., Kich, J. D., Bessa, M. C., Biesus, L. L., Berno, L. G., and Triques, N. J. (2014). *Salmonella* and antimicrobial resistance in an animal-based agriculture river system. *Sci. Total Environ.* 472, 654–661. doi: 10.1016/j.scitotenv.2013.11.052

Paterson, D. L., and Bonomo, R. A. (2005). Extended-spectrum beta-lactamases: a clinical update. *Clin. Microbiol. Rev.* 18, 657–686. doi: 10.1128/CMR.18.4.657-686.2005

Pietsch, M., Simon, S., Meinen, A., Trost, E., Banerji, S., Pfeifer, Y., et al. (2021). Third generation cephalosporin resistance in clinical non-typhoidal *Salmonella enterica* in Germany and emergence of bla (CTX-M)-harbouring pESI plasmids. *Microb. Genom.* 7:000698. doi: 10.1099/mgen.0.000698

Shafiq, M., Huang, J., Shah, J. M., Wang, X., Rahman, S. U., Ali, I., et al. (2021). Characterization and virulence factors distribution of bla(CTX-M) and mcr-1carrying *Escherichia coli* isolates from bovine mastitis. *J. Appl. Microbiol.* 131, 634–646. doi: 10.1111/jam.14994

Shi, C. (2015). Molecular methods for serovar determination of *Salmonella*. *Crit. Rev. Microbiol.* 41, 309–325. doi: 10.3109/1040841x.2013.837862

Shigemura, H., Sakatsume, E., Sekizuka, T., Yokoyama, H., Hamada, K., Etoh, Y., et al. (2020). Food workers as a reservoir of extended-spectrum-cephalosporin-resistant *Salmonella* strains in Japan. *Appl. Environ. Microbiol.* 86, 00072–20. doi: 10.1128/aem.00072-20

Sun, R. Y., Ke, B. X., Fang, L. X., Guo, W. Y., Li, X. P., Yu, Y., et al. (2020). Global clonal spread of mcr-3-carrying MDR ST34 *Salmonella enterica* serotype Typhimurium and monophasic 1,4,[5],12:i:- variants from clinical isolates. *J. Antimicrob. Chemother.* 75, 1756–1765. doi: 10.1093/jac/dkaa115

Treangen, T. J., Ondov, B. D., Koren, S., and Phillippy, A. M. (2014). The harvest suite for rapid core-genome alignment and visualization of thousands of intraspecific microbial genomes. *Genome Biol.* 15:524. doi: 10.1186/s13059-014-0524-x

Wang, S., Duan, H., Zhang, W., and Li, J. W. (2007). Analysis of bacterial foodborne disease outbreaks in China between 1994 and 2005. *FEMS Immunol. Med. Microbiol.* 51, 8–13. doi: 10.1111/j.1574-695X.2007.00305.x

Wang, J., Jiang, Y., Ji, R. Y., Wang, Z. Y., Lu, M. J., Wu, H., et al. (2021). Colistin- and tigecycline-resistant CTX-M-14-producing *Salmonella enterica* serovar Kentucky ST198 from retail chicken meat, China. *Int. J. Antimicrob. Agents* 59:106504. doi: 10.1016/j.ijantimicag.2021.106504

Wang, Z., Xu, H., Tang, Y., Li, Q., and Jiao, X. (2020). A multidrug-resistant monophasic *Salmonella* Typhimurium co-harboring mcr-1, fosA3, Bla (CTX-M-14) in a transferable IncHI2 plasmid from a healthy catering worker in China. *Infect. Drug Resist.* 13, 3569–3574. doi: 10.2147/idr.s272272

Wegener, H. C., Hald, T., Lo Fo Wong, D., Madsen, M., Korsgaard, H., and Bager, F. (2003). Salmonella control programs in Denmark. *Emerg. Infect. Dis.* 9, 774–780. doi: 10.3201/eid0907.030024

Whichard, J. M., Gay, K., Stevenson, J. E., Joyce, K. J., Cooper, K. L., Omondi, M., et al. (2007). Human *Salmonella* and concurrent decreased susceptibility to quinolones and extended-spectrum cephalosporins. *Emerg. Infect. Dis.* 13, 1681–1688. doi: 10.3201/eid1311.061438

Woh, P. Y., Yeung, M. P. S., Goggins, W. B. 3rd, Lo, N., Wong, K. T., Chow, V., et al. (2021). Genomic epidemiology of multidrug-resistant nontyphoidal *Salmonella* in young children hospitalized for gastroenteritis. *Microbiol. Spectr.* 9:e0024821. doi: 10.1128/Spectrum.00248-21

Wu, W., Feng, Y., Tang, G., Qiao, F., McNally, A., and Zong, Z. (2019). NDM metallo-β-lactamases and their bacterial producers in health care settings. *Clin. Microbiol. Rev.* 32, 00115–18. doi: 10.1128/cmr.00115-18

Xiang, D. R., Li, J. J., Sheng, Z. K., Yu, H. Y., Deng, M., Bi, S., et al. (2015). Complete sequence of a novel IncR-F33:A-:B- plasmid, pKP1034, harboring fosA3, blaKPC-2, blaCTX-M-65, blaSHV-12, and rmtB from an epidemic *Klebsiella pneumoniae* sequence type 11 strain in China. *Antimicrob. Agents Chemother.* 60, 1343–1348. doi: 10.1128/aac.01488-15

Xiaoting, W., Chengcheng, N., Chunhui, J., Yan, L., Jing, L., Qingling, M., et al. (2021). Antimicrobial resistance profiling and molecular typing of ruminant-borne isolates of *Clostridium perfringens* from Xinjiang, China. *J. Glob. Antimicrob. Resist.* 27, 41–45. doi: 10.1016/j.jgar.2021.08.003

Xu, Z., Wang, M., Wang, C., Zhou, C., Liang, J., Gu, G., et al. (2021). The emergence of extended-spectrum β-lactamase (ESBL)-producing *Salmonella* London isolates from human patients, retail meats and chickens in southern China and the evaluation of the potential risk factors of *Salmonella* London. *Food Control* 128:108187. doi: 10.1016/j.foodcont.2021.108187

Yao, Z., Jiayin, W., Xinyi, Z., Ling, C., Mingyuan, H., Simin, M., et al. (2020). Identification of group B *Streptococcus* serotypes and genotypes in late pregnant women and neonates that are associated with neonatal early-onset infection in a South China population. *Front. Pediatr.* 8:265. doi: 10.3389/fped.2020.00265

Yin, Y., and Zhou, D. (2018). Organoid and enteroid modeling of *Salmonella* infection. *Front. Cell. Infect. Microbiol.* 8:102. doi: 10.3389/fcimb.2018.00102

Zhang, C. Z., Ding, X. M., Lin, X. L., Sun, R. Y., Lu, Y. W., Cai, R. M., et al. (2019). The emergence of chromosomally located Bla (CTX-M-55) in *Salmonella* from foodborne animals in China. *Front. Microbiol.* 10:1268. doi: 10.3389/fmicb.2019.01268

Zhang, L., Fu, Y., Xiong, Z., Ma, Y., Wei, Y., Qu, X., et al. (2018). Highly prevalent multidrug-resistant *Salmonella* from chicken and pork meat at retail markets in Guangdong, China. *Front. Microbiol.* 9:2104. doi: 10.3389/fmicb.2018.02104

Zhang, L., Lü, X., and Zong, Z. (2013). The emergence of blaCTX-M-15-carrying *Escherichia coli* of ST131 and new sequence types in Western China. *Ann. Clin. Microbiol. Antimicrob.* 12:35. doi: 10.1186/1476-0711-12-35

Zhang, W. H., Ren, S. Q., Gu, X. X., Li, W., Yang, L., Zeng, Z. L., et al. (2015). High frequency of virulence genes among *Escherichia coli* with the blaCTX-M genotype from diarrheic piglets in China. *Vet. Microbiol.* 180, 260–267. doi: 10.1016/j.vetmic.2015.08.017

Zhao, W. H., and Hu, Z. Q. (2013). Epidemiology and genetics of CTX-M extended-spectrum beta-lactamases in Gram-negative bacteria. *Crit. Rev. Microbiol.* 39, 79–101. doi: 10.3109/1040841X.2012.691460

Conflict of Interest: The authors declare that the research was conducted in the absence of any commercial or financial relationships that could be construed as a potential conflict of interest.

be evaluated in this article, or claim that may be made by its manufacturer, is not guaranteed or endorsed by the publisher.

Advantages of publishing in Frontiers

OPEN ACCESS
Articles are free to read for greatest visibility and readership

FAST PUBLICATION
Around 90 days from submission to decision

HIGH QUALITY PEER-REVIEW
Rigorous, collaborative, and constructive peer-review

TRANSPARENT PEER-REVIEW
Editors and reviewers acknowledged by name on published articles

Frontiers
Avenue du Tribunal-Fédéral 34
1005 Lausanne | Switzerland

Visit us: www.frontiersin.org
Contact us: frontiersin.org/about/contact

REPRODUCIBILITY OF RESEARCH
Support open data and methods to enhance research reproducibility

DIGITAL PUBLISHING
Articles designed for optimal readership across devices

FOLLOW US
@frontiersin

IMPACT METRICS
Advanced article metrics track visibility across digital media

EXTENSIVE PROMOTION
Marketing and promotion of impactful research

LOOP RESEARCH NETWORK
Our network increases your article's readership